UNIVERSITY OF
LIVERPOOL

Heparan sulfate-protein interactions: Evidence for Sulfate Group-Dependent Selectivity

Thesis submitted in accordance with the requirements of the University of Liverpool for the degree of

Doctor in Philosophy

By

Yassir Ahmed Mohmed Ali Ahmed

October 2010

Table of contents

Abstract

Heparan sulfates (HS) are a family of structurally diverse, sulfated polysaccharides located at the cell surface and in the extracellular matrix. They are distributed widely in virtually all metazoan organisms. The structural diversity occurs via variability in the positions of sulfation along the HS chain and in α L-iduronic acid and D-glucuronic acid substitutions. There is now strong evidence that these molecules perform diverse functions *in vivo* through their ability to regulate the activity of different proteins. A wide variety of proteins have been found to be ligands for HS, including growth factors, cytokines, receptors, adhesion and matrix molecules, enzymes, coagulation factors and a variety of bacterial and viral coat proteins. Hence, there is a very significant need to determine the molecular basis of HS activity and HS-protein interactions, addressing important issues such as the degree of molecular selectivity.

In this study, two model protein systems were selected to test the hypothesis that selective saccharide sequence and sulfation patterns regulate protein binding and activity.

In the first model, heparin and chemically modified heparin saccharides were screened for Slit and Robo binding and activity, as signalling by Slit requires two receptors, Robo transmembrane proteins and HS. How HS controls Slit-Robo signalling is unclear. Competition and direct enzyme linked immunoassay (ELISA) data showed that heparin derivatives enhance the affinity of Slit-Robo binary and ternary complexes. Analytical gel filtration chromatography demonstrated that Slit associates with a soluble Robo fragment and heparin derivatives to form a ternary complex. Furthermore, retinal growth cone collapse triggered by Slit requires cell surface HS or exogenously added heparin derivatives. The data indicate a complex relationship between HS binding and Slit-Robo proteins, which support selectivity in regulation of signalling responses, but do not suggest requirement for strictly defined sequence.

In the second model, HS saccharides were prepared by heparinase treatment of porcine mucosal HS and purified by size-exclusion and SAX-HPLC chromatography. Purified or semi-purified complex sulfated HS 6-mer and 8-mer sequences were prepared. This library was screened for binding to FGF-1 and FGF-2 using a competition ELISA, and for corresponding bioactivity (regulation of FGF-1 and FGF-2 signalling using a BaF3 cell assay with defined FGF receptors). This screen identified fractions that bound and activated these ligands, and ones that did not. Selected structures were subjected to activity analysis after further separation using ion-pairing reverse phase (IPRP-HPLC). Structures with similar or identical size and sulfation content, but distinct sulfation sequences, differed widely in their bioactivity, though binding data alone did not necessarily predict activity. The results provided information that supports the view that a significant degree of specificity for activation of FGF biological activity is encoded in the complex sulfation sequences observed in HS chains. However, is not simply related to sulfation pattern.

Overall, the results from these two model protein systems suggest that the degree of selectivity or specificity of HS structures for regulation of biological activity is complex, and varies according to the proteins involved. Nevertheless, they provide the basis for HS to act as an important modulator of protein function in a wide variety of biological systems.

Dedicated to my late father and to my family

Acknowledgements

First and foremost, my utmost gratitude to my supervisors Prof. Jerry Turnbull and Dr. Andrew Powell for their time, help, support and the insightful comments, suggestions and advice throughout the PhD project.

Special thanks to Dr. Edwin Yates, for his supply of the chemically modified heparins and his endless time and patience in explaining heparin/ HS chemistry and proofreading the thesis draft.

I also wish to thank Dr. Scott Guimond for showing me the BaF3 assay and helping me with all my computer problems.

I would like also to thank all members of Lab B in the Institute of Integrative Biology, particularly the molecular glycobiology group, past and present. I would like to express my gratitude to Dr. Sophie Thompson, Dr. Nicola Wells, Dr. Tim Rudd, Dr. Tarja Kinnunen, Dr. Mark Skidmore, Ms. Elizabeth Edwards, Miss Chloe Williams, Mr Joseph Holman, Dr. Tania Puvirajesinghe, Dr. Urszula Polanska and Miss Alexandra Holme, for their support and useful discussion and ideas during lab meetings and tea. In addition, special thanks to Dr. Abdel Atrih and Miss Rebecca Miller for useful discussion and the mass spectrometry help.

I would like to thank Dr. Diana Moss for giving me space in her lab and teaching me how to dissect and culture the chick retina. I also thank Dr. Christine McNamee for providing me with all my experiment needs.

I would like to thanks Prof. Erhard Hohenester, Dr. Noemi Fukuhara, and Miss Sadaf-Ahmahni Hussain for providing me with the Slit and Robo proteins.

I am similarly grateful to Prof. David Fernig for training me on the IASys and useful, insightful discussions throughout the project.

Most especially, I would like to thank my parents and my wife, Wala and my son Ahmed and daughter Lujain, and all my family and friends for all their constant support and encouragement.

List of figures

Chapter 1

Chapter 3

Chapter 4

Chapter 5

Appendices

List of tables

Chapter 1

Chapter 2

Chapter 3

Chapter 4

Chapter 5

Appendices

List of abbreviations

ACE	Affinity co-electrophoresis
AP	ammonium persulphate
APS	adenosine 5' phosphosulphate
AT III	antithrombin III
AUC	Analytical ultracentrifugation
BLH	bovine lung heparin
BNP	brain natriuretic peptide
BSA	bovine serum albumin
CAD	collision activated dissociation
CAR	conformation activity relationship
CC0-3	conserved cytoplasmic motifs
CID	collision induced dissociation
CNS	central nervous system
hSlit-2-CM	hSlit-2 conditioned medium
CS	chondroitin sulfate
CSRs	composite sulfated regions
2-de	2-de-O-sulfate N sulfate heparin
6-de	6-de-O-sulfate N sulfate heparin
2,6-de	2,6-de-O-sulfate N sulfate heparin
2-de NAc	2-de-O-sulfate N acetyl heparin
6-de NAc	2-de-O-sulfate N acetyl heparin
2,6-de NAc	2-de-O-sulfate N acetyl heparin
DRG	dorsal root ganglion
DPI	dual polarization interferometry
EC_{50}	half maximal response concentration
ECM	extracellular matrix

ECL	enhanced chemiluminescence
EGF	epidermal growth factor
ELISA	enzyme-linked immunosorbant assay
EM	electromagnetic
ER	endoplasmic reticulum
ES	endostatin
ESI	Electro-spray ionization
EXT	exostosin family of genes encodes glycosyltransferases
EXTL3	Exostosin tumour-like-3 gene
Fc	constant region domain of human Ig G1
FCS	foetal calf serum
FGF	fibroblast growth factor
FGFR	fibroblast growth factor receptor (IIIc isoform unless stated otherwise)
GAG	glycosaminoglycans
Gal	galactose
GalT	galactosyltransferase
GalNAc	N-acetylgalactosamine
Glc	glucosamine
GlcA	glucuronic acid
GlcA2S	glucuronic acid 2-sulfate
GlcAT	glucuronyltransferase
GlcNAc	N-acetyl glucosamine
GlcNS	N-sulfated glucosamine
GlcNS6S	N-sulfated glucosamine 6-sulfate
GlcNS6S, 3S	N-sulfated glucosamine 6-sulfate, 3-sulfate
GFLs	GDNF family ligands
GDNF	glial cell line-derived growth factor

GPC	glypican
GPI	glycosylphosphatidylinositol
HA	hyaluronan
HBDs	heparin-binding domains
HB-EGF	Heparin-binding epidermal growth factor
HBPs	heparin-binding proteins
HBS	Hepes-buffered saline
HEPES	4-(2-Hydroxyethyl)piperazine-1-ethanesulfonic acid
HGF	hepatocyte growth factor
Hh	hedgehog
HMBC	heteronuclear multiple bond spectroscopy
HPLC	high performance liquid chromatography
HRP	horseradish peroxidase
HS	heparan sulfate
HSPG	heparan sulfate proteoglycan
HSV-1	herpes simplex virus type 1
IC_{50}	half maximal inhibition concentration
IdoA	iduronic acid
IdoA2S	iduronic acid 2-sulfate
IFT	isothermal fluorescence titrations
Ig	immunoglobulin
IL-8	Interleukin-8
IL-3	Interleukin-3
INFγ	interferon gamma
IPRP-HPLC	ion pairing reverse phase -HPLC
IPTG	isopropyl-β-thiogalactopyranoside
IR	infrared
ITC	isothermal calorimetry

Kd	equilibrium dissociation constant
kDa	kilodalton
KS	keratan sulfate
K18K	K 18 amino acid sequence of FGFR1 proposed as primary heparin interaction site
LC-MS	liquid chromatography MS
LN	laminin
LRR	leucine rich repeats
M	molar
MALDI- TOF	Matrix-assisted laser desorption/ ionization time-of-flight
µg	microgram
µl	microlitre
µM	micromolar
ml	millilitre
MIP1α	macrophage inflammatory protein 1α
mM	millimolar
MPS	mucopolysaccharidoses
MS	mass spectrometry
mU	milliunit
MTT	3-[4,5-Dimethylthiazol-2-yl]-2,5-diphenyl tetrazolium bromide
NA-domain	N-acetylated domain
nm	nanometre
NDST	N-deacetylase/N-sulphotransferase
NHS	N-hydroxysuccimide
NMR	Nuclear magnetic resonance
NS/NA-domain	N-sulfated/N-acetylated domain
NS-domain	N-sulfated domain
OB	olfactory bulb

OPD	orthophenylenediamine
OST	O-sulfotransferase
PAGE	polyacrylamide gel electrophoresis
PAPS	3'-phosphoadenosine 5'-phosphosulphate
PBS	phosphate-buffered saline
PBST	phosphate-buffered saline, Tween-20
PDGF	platelet-derived growth factor
PerS heparin	Over sulfated heparin
PF-4	platelet factor 4
PG	proteoglycan
Phe	phenylalanine
PMH	porcine mucosal heparin
PMHS	porcine mucosal heparan sulfate
PNPS	p-nitrophenol sulfate
PSC	phenylsemicarbazide tag
PTB	phosphotyrosine binding
QCM-D	Quartz crystal-microbalance-dissipation
RNAi	RNA interference
SAM	self-assembled monolayer
SAX	strong anion exchange
S-domain	sulfated domain
SDC	syndecan
SDS	sodium dodecyl sulphate
SDT	substrate deprivation therapy
SEC	size-exclusion chromatography
SH2	Src homology 2
shRNA	small hairpin RNA
SPR	surface plasmon resonance

SULF	Endo-6-O sulfatase
TEMED	N, N, N', N'-tetramethylenediamine
TGF-β	transforming growth factor beta
THAP	2', 4', 6'- trihydroxyacetophenone
TOF	time-of-flight
Tris	Tris (hydroxymethyl) aminomethane
Trp	Tryptophan
UDP	uridine diphosphate
UV	ultraviolet
V	volt
VEGF	vascular endothelial growth factor
v/v	volume/ volume
w/v	weight/ volume
Xyl	xylose
XylT	xylosyltransferase

1 Chapter one: Introduction

1.1 Background

Glycans are the most abundant bio-molecule in cells (Varki *et al.*, 2009). They play many roles in the living organisms, such as the storage and transport of energy (e.g. starch, glycogen) and structural molecules (e.g. cellulose, chitin). They also occupy the extracellular matrix and are a component of metabolic intermediates (e.g. ATP, NAD) and presentation of functional groups (e.g. DNA, RNA). Glycans with their diverse chemical structures also play a vital role in transmitting important biochemical signals into and between cells. In this way, they guide the cellular communication that is essential for normal cell and tissue development and physiological function.

The science of the biosynthesis, structure and function of glycans is referred to as "glycobiology" (Rademacher *et al.*, 1988). The term glycome is also emerging now to describe the characteristics of the whole set of saccharides produced by an organism, tissue or cell. From glycome came the phrase "glycomics" which is the discipline that deals with the comprehensive study of the structure and function of the entire saccharide repertoire of an organism, tissue or cell (Turnbull and Field, 2007; Varki *et al.*, 2009).

1.2 Proteoglycans (PGs)

PGs are found in all metazoan organisms (e.g. mammals, flies, worms, sponges). They are major components of the extracellular matrix (ECM), cell surface and are also found in the intracellular vesicles (Bernfield *et al.*, 1999). PGs have various functions, ranging from mechanical maintenance and structural organization of most tissues, binding cytokines, chemokines, growth factors, and morphogens and protecting proteins against proteolysis (Kjellen and Lindahl, 1991). In addition, they assist in the arrangement of the basement membranes, thus providing a scaffold for epithelial cell migration, proliferation, and differentiation (Iozzo, 2005). PGs are thought to concentrate positively charged proteases and histamine within the storage granules, and regulate coagulation, host defence, and wound repair (Kjellen and Lindahl, 1991).

PGs are glycoproteins consisting of a core protein to which are covalently attached polysaccharide chains that belong to the glycosaminoglycan (GAG) family (Kjellen and Lindahl, 1991). A GAG chain is composed of repeating disaccharide units consisting of a hexosamine and a hexuronic acid (Esko and Selleck, 2002) (Figure 1.1). The two main types of GAGs are the galactosaminoglycans and glucosaminoglycans. The galactosaminoglycans include chondroitin sulfate (CS) and dermatan sulfate (DS). The glucosaminoglycans include heparan sulfate (HS) and heparin.

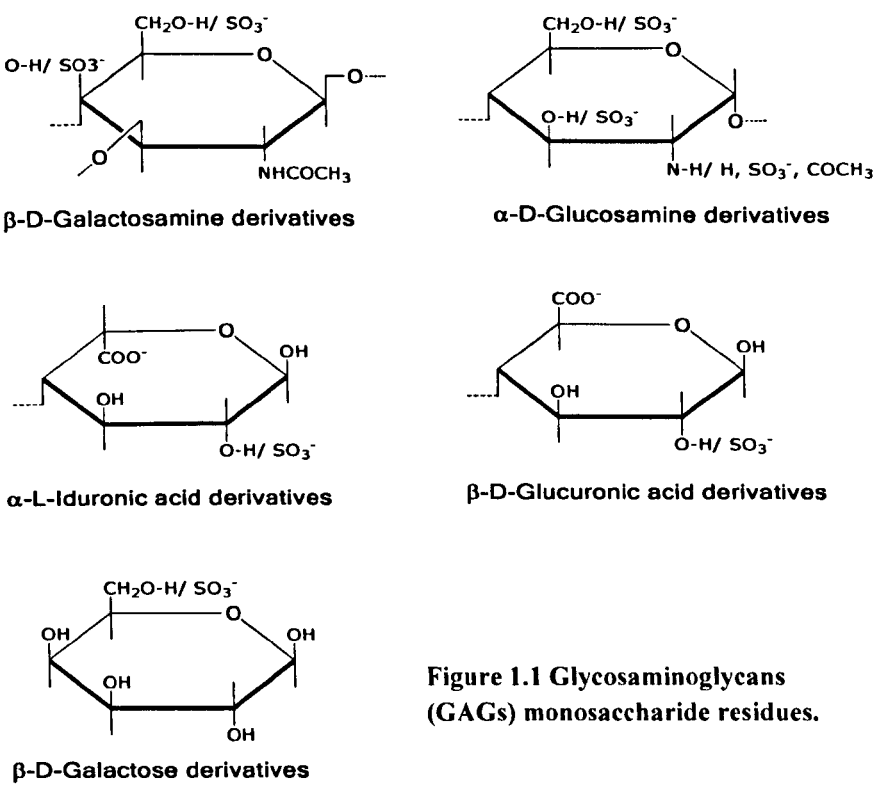

Figure 1.1 Glycosaminoglycans (GAGs) monosaccharide residues.

Both GAGs have the same hexuronic acid subunits, either glucuronic acid (GlcA) or iduronic acid (IdoA), while they are different in their aminosugar, galactosamine in the case of galactosaminoglycans or glucosamine in the case of glucosaminoglycan (Campbell *et al.*, 1994; Sugahara *et al.*, 2003). Keratan sulfate is a member of the glucosaminoglycan family but has galactose (Gal) derivatives instead of hexuronic acid (Funderburgh, 2000). Hyaluronan is a protein-free glucosaminoglycan; it is composed of glucosamine and GlcA (Evanko *et al.*, 2007). All GAGs, except hyaluronan, are sulfated making the chains strongly anionic (Lind *et al.*, 1998) (Figure 1.2).

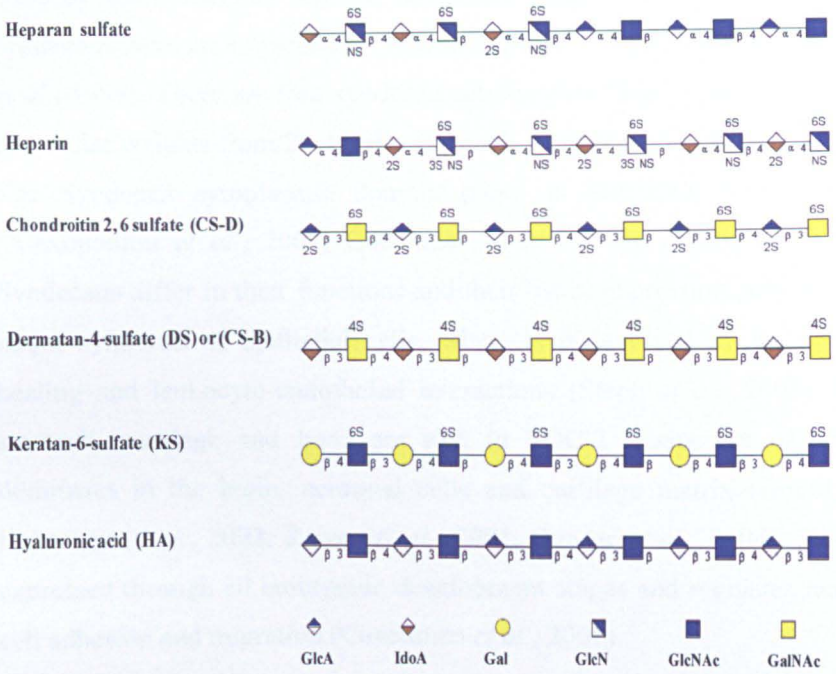

Figure 1.2 Glycosaminoglycan (GAG) structures. GAGs consist of repeating disaccharide units composed of an N-acetylated or N-sulfated hexosamine and either uronic acid (glucuronic acid or iduronic acid) or galactose. Hyaluronan lacks sulfate groups and keratan sulfates lack uronic acids. Monosaccharide is represented according to the guidelines of the Nomenclature Committee of the Consortium for Functional Glycomics (http://glycomics.scripps.edu/CFGnomenclature.pdf).

1.3 Heparan sulfate proteoglycans (HSPGs)

Heparan sulfate proteoglycans (HSPGs) are PGs carrying HS or heparin polysaccharide chains. They may also contain one or more CS chains. Each of these HSPGs have a number of important biological functions, ranging from maintenance of basement membrane homeostasis to effects on angiogenesis and neuromuscular junctions (Bezakova and Ruegg, 2003; Iozzo, 2005; Lin, 2004) (Table 1.1). They are divided into four main families, categorized by their various core proteins (Figure 1.3).

Two of these families are the membrane-bound syndecans and glypicans. The syndecans have an extracellular, transmembrane and cytoplasmic domain (Bernfield *et al.*, 1999). There are four syndecan sub-families (SDC-1-SDC-4), ranging in their molecular weights from 22-45 kDa (Bonneh-Barkay *et al.*, 1997; Adam *et al.*, 2004). The Syndecan cytoplasmic domain plays an important role in their function (Alexopoulou *et al.*, 2007; Couchman *et al.*, 2001; Zimmermann *et al.*, 2005). Syndecans differ in their functions and their tissue expression patterns. SDC-1 is the major syndecan of epithelial cells, where it is involved in angiogenesis, wound healing and leukocyte-endothelial interactions (Stepp *et al.*, 2002). Kidney, lung, stomach, cartilage and bone are rich in SDC-2 (Essner *et al.*, 2006). SDC-3 dominates in the brain, neuronal cells and cartilage matrix (Gould *et al.*, 1992; Kaksonen *et al.*, 2002; Reizes *et al.*, 2001; Strader *et al.*, 2004). SDC-4 is widely expressed through all embryonic development stages and regulates matrix structure, cell adhesion and migration (Couchman *et al.*, 2001).

Glypicans are HSPGs that possess a glycosylphosphatidyl inositol (GPI) linkage (Bernfield *et al.*, 1999). There are six glypicans (GPC-1-GPC-6) found in mammals; their molecular weights are about 60 kDa (Carmeliet *et al.*, 1990). GPCs are found in most tissues especially during development; embryonic central nervous system and the skeletal system are rich in GPC-1 (Litwack *et al.*, 1998; Fransson *et al.*, 2004). The axon and growth cone of the developing brain contain GPC-2 (Ivins *et al.*, 1997). GPC-3 to GPC-6 are highly expressed during embryonic development with a lower level in the adult tissues (Fransson *et al.*, 2004).

The third HSPG family comprises of various secreted forms (ECM-HSPGs), including perlecan, collagen XVIII and agrin (Iozzo, 2005). Perlecan is a multi-domain HSPG found in the extracellular matrix and has a molecular weight of more than 400 kDa (Knox and Whitelock, 2006). It is found in the kidney, lung and connective tissues and has a vital role in development and homeostatic processes (Handler *et al.*, 1997; Mongiat *et al.*, 2000).

Agrin is one of the major ECM-HSPGs, it is also a multi-domain similar to perlecan, and has a molecular weight of about 220 kDa (Hoch *et al.*, 1994). Agrin is considered a neuronal HSPG, but is also widely expressed during development (Kroger and Schroder, 2002; Bezakova and Ruegg, 2003).

Collagen type XVIII is a PG that has several collagenous triple-helical domains interrupted by non-collagenous parts carrying a total of three HS chains. It occurs in the basement membrane of various tissues (Marneros and Olsen, 2005).

Lastly, serglycin is a member of the intracellular HSPG family. It is found mainly in the storage granules of connective tissue type mast cells. It has a small core protein, heavily substituted with heparin chains. Heparin chains bind to histamine and to proteases, thereby helping to retain these inflammatory mediators in the granules (Kolset *et al.*, 2004; Kolset and Tveit, 2008).

Proteoglycan	Core protein (kDa)	Number of GAG chains	Tissue distribution
Perlecan	400	1-3 HS	secreted; basement membranes; cartilage
Agrin	200	1-3 HS	secreted; neuromuscular junctions
Collagen type XVIII	147	2-3 HS	secreted; basement membranes
Syndecans 1–4	31-45	1-3 CS 1-2 HS	membrane bound epithelial cells and fibroblasts
Glypicans 1–6	~60	1-3 HS	membrane bound; epithelial cells and fibroblasts
Serglycin	10-19	10-15 heparin/ CS	intracellular granules; mast cells

Table 1.1 Maior HSPG families. Adopted from (Varki *et al.*, 2009)

1.4 Biosynthesis of HS

Heparin and HS chains are synthesized by number of enzymes located predominantly in the Golgi apparatus. Biosynthesis employs chain initiation, elongation and modification, utilizing about eleven different enzymes, many of which have multiple isoforms. These enzymes do not act to completion; hence, the final product is a heterogeneous polysaccharide chain (Bernfield *et al.*, 1999; Aikawa *et al.*, 2001; Esko and Selleck, 2002).

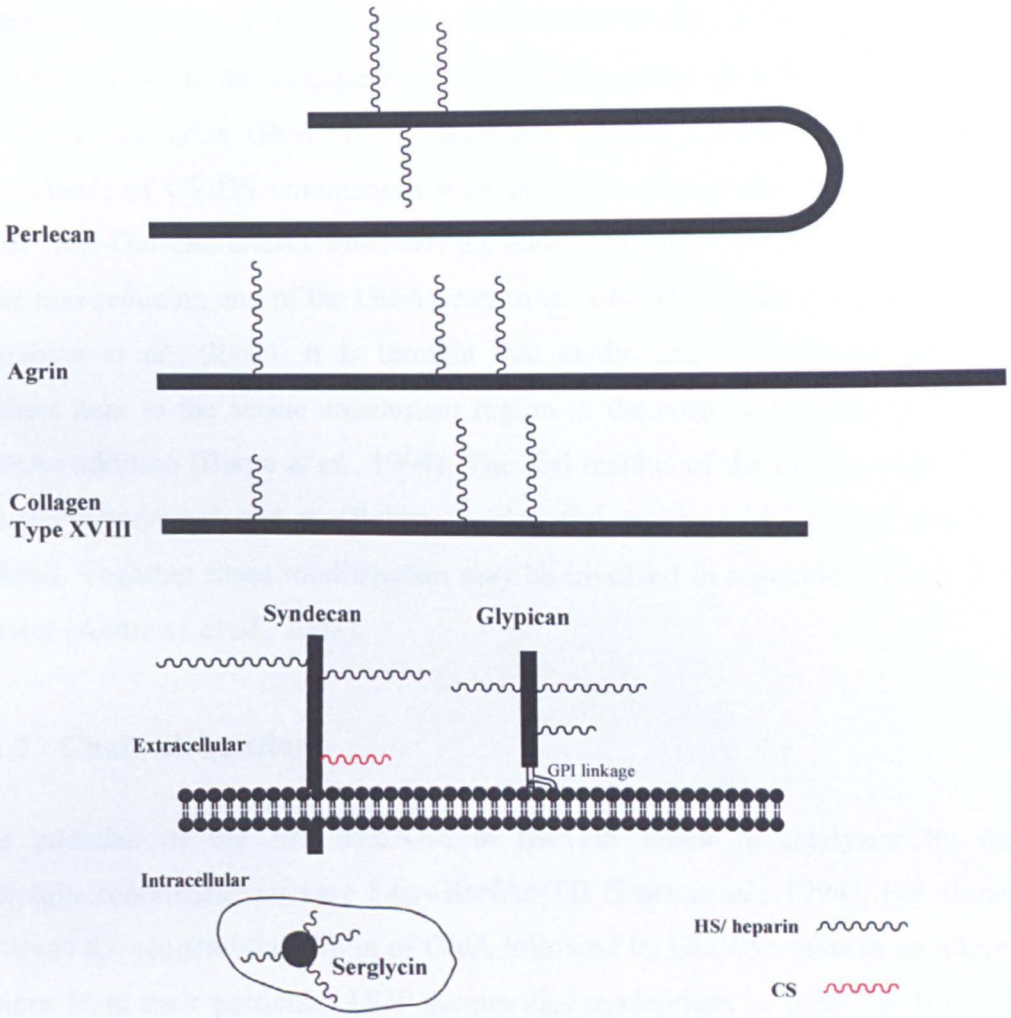

Figure 1.3 Schematic representations of the six main HSPG subtypes. These include syndecans, glypicans, and one each of perlecan, agrin, and collagen type XVIII, also heparin PG serglycin. The core protein size is roughly proportional to the number of amino acid residues (the bold line used in for simplicity).

1.4.1 Chain initiation

The initiation step starts with the action of the xylosyltransferase (XylT) which uses uridine-5'-diphosphate (UDP)-Xyl as a xylose donor and a serine residue in the PG core protein as an acceptor. There are two XylT isoforms in mammals, which both have a role in PG biosynthesis (Ponighaus *et al.*, 2007).

The successive addition of two galactose residues is catalyzed by galactosyltransferases I (GalT-I) and galactosyltransferases II (GalT-II) respectively. The completion of the linkage region is by the action of glucuronyltransferase I (GlcAT-I) that adds GlcA to the galactose residue (Bhakta *et al.*, 2000). The biosynthesis of CS/DS commences with the same tetrasaccharide 'linkage region' (serine-Xyl-Gal-Gal-GlcA), however, the addition of α1-4 GlcNAc or β1-4 GalNAc to the non-reducing end of the GlcA determines whether the end product is HS or CS (Sugahara *et al.*, 2003). It is thought that acidic and hydrophobic amino acids residues near to the serine attachment region in the core protein appear to endorse GlcNAc addition (Bame *et al.*, 1994). The Xyl residue of the linkage region may be 2-O phosphorylated and the linkage region Gal residues in CS/ DS may be 6-O sulfated. Together these modification may be involved in regulation of the GlcAT-I activity (Andrews *et al.*, 2008).

1.4.2 Chain elongation

The addition of the first GlcNAc in the HS chain is catalyzed by the N-acetylglucosaminyltransferase I (α-GlcNAc-TI) (Fritz *et al.*, 1994). HS elongation involves the sequential addition of GlcA followed by GlcNAc units in an alternating pattern from their particular UDP-saccharides nucleotides to form the HS chain of about 50-150 disaccharides long.

These reactions are catalyzed by the action of HS co-polymerases. This enzyme is composed of two gene products, the exostosis related enzymes EXT-1 and EXT-2 (Jeong *et al.*, 2001; Kim *et al.*, 2001; Deepa *et al.*, 2002). Mutations in the genes encoding these enzymes lead to serious bone formation disorders termed hereditary multiple exostoses (HME) (Zak *et al.*, 2002). While the HS polysaccharide is being synthesised it is subjected to a series of consecutive enzymatic modification reactions in which the product of one reaction is the substrate for the next (Figure 1.4).

1.4.3 Chain modification

Generally, the diversity of HS structure is generated through the modification steps. The first modification is the substitution of the N-acetyl group of GlcNAc residues with a sulfate group forming N-sulfated glucosamine (GlcNS). This is catalysed by the N-deacetylase/ N-sulfotranferases (NDSTs). The NDSTs have four isoenzymes in vertebrates; NDST-1 and NDST-2 are found in most tissues (Kjellen, 2003). NDST-3 is present through embryogenesis and in the brain, testis and kidney of adult mammals (Pallerla *et al.*, 2008). NDST-4 is also found during embryogenesis and in adult brain (Aikawa and Esko, 1999; Aikawa *et al.*, 2001). Owing to the specific actions of these enzymes, HS chains exhibit regions with high sulfation levels and other with low or no sulfates (Figure 1.4) (Aikawa *et al.*, 2001; Gallagher, 2001; Turnbull and Gallagher, 1990; Turnbull and Gallagher, 1991). The NDSTs enzymes have a vital role in HS synthesis, as most of the subsequent modifications require the presence of GlcNS (Crawford *et al.*, 2010; Merry *et al.*, 2001; Pinhal *et al.*, 2001; Spillmann *et al.*, 1998). The HS C5-epimerase is a single enzyme in mammals (Adam *et al.*, 2003). It acts on the C5 of the GlcA residues next to Glc-NS residues to create an IdoA (Li *et al.*, 1997). The presence of a GlcNS at the C4 position of the GlcA is crucial for C5-epimerase function (Jacobsson *et al.*, 1984). Also, if the GlcA is 2-O sulfated or next to a 6-O sulfated GlcNS the C5-epimerase will not function, however, the presence of a 2-O sulfate sequences will not stop the GlcNS from being 6-O sulfated (Figure 1.5a and b) (Hagner-Mcwhirter *et al.*, 2000; Hagner-McWhirter *et al.*, 2004). The 2-O sulfotransferase (2-OST) adds a sulfate to the C2 of an IdoA or GlcA, this enzyme has a single isoform and it favours the IdoA over GlcA, as a result, GlcA2S is a rare modification (Fisher *et al.*, 2001).

Following the 2-OST, a number of GlcNS and a small number of GlcNAc residues are O-sulfated at the C6 by 6-O sulfotransferases (6-OSTs); there are three isoforms of this enzyme (6-OST-1-3) (Habuchi *et al.*, 2000). Although, the GlcNS and GlcNAc can be modified indiscriminately, the GlcNAc 6-O sulfation favours the presence of adjacent GlcNS saccharide (Gong *et al.*, 2003; Holmborn *et al.*, 2004).

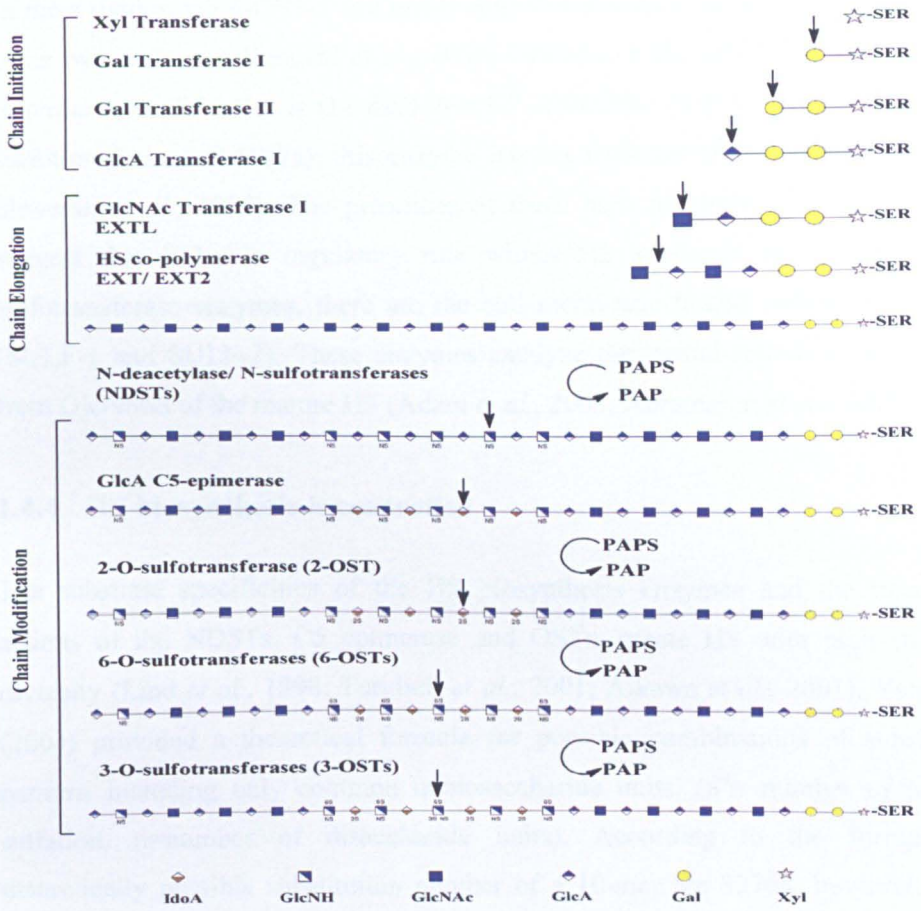

Figure 1.4 HS biosynthesis. Starts with formation of a tetrasaccharide linker (Xyl-Gal-Gal-GlcA) attached to a serine residue on the core protein, onto which GlcA and Glc NAc residues are sequentially added. The HS chain is then modified successively by N-deacetylase/ N-sulfotransferase, epimerase and (2, 6, 3-sulfotransferase); sulfotransferases utilize PAPS as sulfate donor. Monosaccharide is represented according to the guidelines of the Nomenclature Committee of the Consortium for Functional Glycomics (http://glycomics.scripps.edu/CFGnomenclature.pdf).

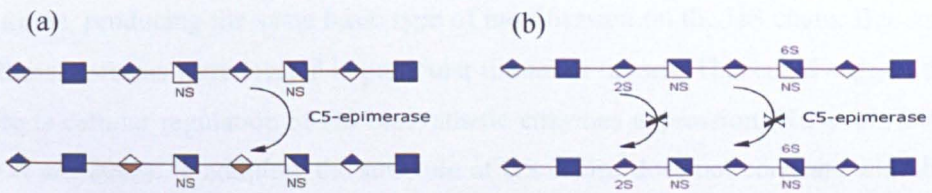

Figure 1.5. Showing substrate specificity of C5-epimerase. A) Common enzyme mode of action on HS chain. B) If the GlcA is 2-O sulfated or next to a 6-O sulfated GlcNS the C5-epimerase will not function,

In most tissues, the 6-OST-1 is a major contributor to 6-O-sulfation compared to the other two isoforms (Habuchi *et al.*, 2000; Habuchi *et al.*, 2007). The final, if most infrequent, modification is O-sulfation at C3 of GlcNS, GlcNAc or $GlcNH^+$ by 3-O-sulfotransferases (3-OSTs); this enzyme has six isoforms (Kobayashi *et al.*, 1999; Shworak *et al.*, 1999). The presences of these high numbers of 3-OST isoforms suggest that it has a regulatory role within HS synthesis. In addition to the sulfotransferase enzymes, there are the cell membrane linked endo-6-O sulfatases (SULF-1 and SULF-2). These enzymes catalyze the partial release of 6-O sulfate from GlcNS6S of the mature HS (Adam *et al.*, 2003; Abramsson *et al.*, 2007).

1.4.4 HS biosynthesis is controlled

The substrate specificities of the HS biosynthesis enzymes and the incomplete actions of the NDSTs, C5 epimerase and OSTs, create HS with high structural diversity (Lind *et al.*, 1998; Turnbull *et al.*, 2001; Aikawa *et al.*, 2001). Yates et al (2004) provided a theoretical formula for possible combinations of substitution patterns including only common monosaccharide units, (8^n= number of possible sulfation, n=number of disaccharide units). According to the formula the theoretically possible substitution number of a 10-mer are 32768, however, tissue derived 10-mer HS saccharides have been demonstrated to have more like several hundred species (Guimond and Turnbull, 1999). Therefore, there is some sort of controlled biosynthesis. This may be due to the restricted substrate specificity of the biosynthesis enzymes, as the product of one enzyme is the substrate for the other in a sequential manner. In addition, most of the HS biosynthesis enzymes have multiple isoforms, producing the same basic type of modification on the HS chain. But some of these isoforms were located in particular tissues or organs. This could suggest that there is cellular regulation of HS biosynthetic enzymes expression (Xu *et al.*, 2005; Xu *et al.*, 2008). In addition, the structure of HS chains does not correlate with their core proteins, but on the cell type of origin, this could be due to the controlled expression of the biosynthetic enzymes (Kato *et al.*, 1994).

Furthermore, Esko and Selleck (2002) have pioneered the idea that the HS biosynthesis enzymes do work in close proximity of each other and are grouped in a complex called a GAGosome (Esko and Selleck, 2002). Different GAGosome assemblages may result in different modification patterns of the HS chain.

There is evidence that there are interactions between pairs of enzymes such as that between the EXT-1 and EXT-2, and between the C5-epimerase and 2-OST (Kobayashi *et al.*, 2000; Pinhal *et al.*, 2001). It has been suggested that NDST-1 is regulated by the concentrations of EXT-1 and EXT-2, which subsequently influence the sulfation pattern of HS chain (Abramsson *et al.*, 2007; Presto *et al.*, 2008).

Structure of oligosaccharides purified from different animal species showed wide structural heterogeneity indicating that there is controlled biosynthesis (Warda *et al.*, 2006). Furthermore, disaccharide compositional analysis of HS from different organs across species revealed that there is organ specificity within species (Guimond *et al.*, 2009a). Moreover, HS isolated from different mice organs showed similar structural composition indicating specificity within species (Ledin *et al.*, 2004). In addition, phage display anti-HS antibody staining of different tissues showed selective expression of multiple HS epitopes, which could be a proof of diverse structures (Asundi *et al.*, 2003; van Kuppevelt *et al.*, 1998). As well, post-biosynthetic extracellular enzymes sulfatase (SULF) continually edits and processes the HS structure by removing the 6-O sulfate from the NS domains. Gene knock-out experiments showed that disruption of these enzymes affects the fine structure of the HS, by accumulation of the 6-O-sulfates and subsequently altered HS function, and the interruption of the non-substrate sulfate groups (Ai *et al.*, 2003; Ai *et al.*, 2006; Ai *et al.*, 2007;; Lamanna *et al.*, 2007; Lamanna *et al.*, 2008).

These findings indicate that HS is highly regulated. Despite that, there are many questions remaining unanswered. For example: why does 2-O sulfation take place only on the NS domains, whilst 6-O sulfation occurs on both NS and NA/ NS domains (Gallagher, 2001)? In addition, why the 6-O sulfation was found in HS chains that lacking the N-sulfate groups and contains N un-substituted glucosamine units (Holmborn *et al.*, 2004)? Moreover, why do some uncommon monosaccharide units such as $GlcNH^+$ exist in the HS chain (Westling and Lindahl, 2002)? Is this due to the regulated or the incomplete action of the NDSTs?

1.5 HS structure

Owing to the regulated actions of the biosynthetic enzymes, about 40-50 % of the GlcNAc would be converted into GlcNS in the final HS chain (Gallagher, 2001). The GlcNAc units are clustered in regions that have no sulfates termed NA-domains. In addition, the GlcNS units are grouped in regions of 2-8 disaccharides in length termed NS or S-domains. In between these two domains, there are transition zones consisting of N-acetylated and N-sulfated units termed NA/ NS domain (Figure 1.6) (Gallagher, 2001; Lindahl *et al.*, 1998; Turnbull and Gallagher, 1990; Turnbull and Gallagher, 1991). The NA domains are composed mainly of GlcNAc-GlcA; however, most of the GlcA in the NS domain is converted into IdoA. In addition, the O sulfations occur on the IdoA2S and on the GlcNS6S, but the 6-O sulfation may occur also on the GlcNAc in the NA/ NS domain. In addition, NS domains with GlcNS lacking the 6-O-sulfate groups are relatively common (Maccarana *et al.*, 1996; Merry *et al.*, 1999; Safaiyan *et al.*, 2000). Furthermore, the majority of the IdoA residues in the NS domain are converted to IdoA2S, and therefore the disaccharide of IdoA2S-GlcNS are the common feature of these regions (Merry *et al.*, 1999). In addition, the rare chain modifications such as the GlcNS3S and the $GlcNH^+$ also take place with low frequency in the NS and NA/ NS domains (Liu *et al.*, 1999; van den Born *et al.*, 1995).

This molecular design of spatially distinct domains is a unique characteristic of HS and may confer distinctive physical and chemical properties on the saccharide chain such as the conformational flexibility and the presence of unusual chemical structures. There are some exceptions to this arrangement found in the HS from the rat liver, in which the NS domains are located in close proximity in the distal portion of the polysaccharide (Lyon *et al.*, 1994; Powell *et al.*, 2004; Stringer *et al.*, 1999).

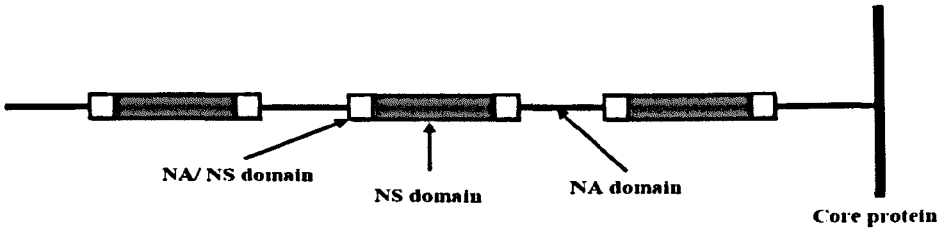

Figure 1.6 Domain structure of HS polysaccharide. The action of HS modifying enzymes to generate diverse domain organization. There are three recognized regions, highly sulfated also known as NS domains, mixed region termed NA/NS domains and unmodified regions known as NA domain. It has been anticipated that the majority of HS binding sequences are within NS and NA/NS regions.

1.5.1 HS conformation

There have been few analyses of the physical properties of HS. Nevertheless, the chemically related heparin has been thoroughly studied. Heparin initially was thought to adopt the conformation of a relatively stiff helix (Mulloy *et al.*, 1993). This can be understood in terms of the charge density imparted by the high level of sulfation found in heparin and the transient H-bond that can be formed between the N-sulfate and the C-3 hydroxyl of the adjacent IdoA residue. However, later work on a series of modified heparins utilizing advanced NMR analysis showed that heparin is a more flexible polymer that previously considered (Hricovini *et al.*, 1995). The IdoA2S residues in heparin exhibit a remarkable conformational plasticity in comparison with other hexopyranose rings, oscillating between $^{2}S_{0}$, $^{4}C_{1}$ and $^{1}C_{4}$ forms with minimal change in linkage geometries to adjacent sugars, while both GlcA and GlcNS6S are stable in the $^{4}C_{1}$ conformation (Figure 1.7) (Casu, 1990; Yates *et al.*, 1996; Mulloy and Forster, 2000).

The importance of the IdoA2S ring plasticity in molecular recognition is revealed by X-ray crystallography of a heparin 6-mer complex with the FGF-2 in which the two internal IdoA2S residues were locked in different conformations that increase the area of contact with the protein surface (Faham *et al.*, 1996).

In contrast, IdoA residues exist mostly in the $^4C_1$ or $^1C_4$ chair form in aqueous solution and more recent studies showed that the internal IdoA residues has a restricted motion (Ferro *et al.*, 1990; Angulo *et al.*, 2005). A study on the K5 polysaccharide found in the *Escherichia coli*, composed of GlcA-GlcNAc repeats established that it is has limited internal motions compared to heparin due to the lack of IdoA residues (Hricovini *et al.*, 1997).

HS conformation has been poorly studied, largely due to the lack of sufficiently homogeneous samples in the amounts needed for NMR analysis. In addition, the number of potential sulfation sequences increases dramatically with chain length. In HS, both the NA and NS domains are thought to contribute to its structural flexibility (Mobli *et al.*, 2008; Murphy *et al.*, 2008). Moreover, the work on heparin conformation indicates that NA domains in HS will have very flexible glycosidic linkages, since there is no H-bond across the linkage and only a single carboxylic acid contributing to negative charge per disaccharide. The sugar rings in these domains will be fairly rigid. In contrast, the glycosidic linkage of NS domains will be more rigid, due to the H-bond across the linkage and to the much higher negative charge density, but the conformational versatility of the IdoA ring will make an important contribution to the flexibility of the NS domain.

Recent studies on the conformation of IdoA have shown that replacement of the N-sulfate group to the reducing side of IdoA by an N-acetyl group has little effect on the IdoA conformational equilibrium. In addition, the presence of the 6-O-sulfate group on the GlcNS at the reducing side alters the balance of the IdoA2S to toward the $^2S_0$ conformation (Murphy *et al.*, 2008). This suggested that the flexibility of the linkage region would enable the NS domains in the HS to explore a variety of orientations as they combine with different proteins.

The motional properties of the NA domains were shown to improve HS-protein interaction and function (Mobli *et al.*, 2008). This idea could explain the interaction of macrophage inflammatory protein 1α (MIP1α) with HS, where it has been proposed that HS saccharides containing two NS domains and a middle NA domain wrap around the MIP1α dimer in a "horseshoe" shape (Stringer *et al.*, 2002). The importance of the NA domain has also been established for many other proteins, such as interferon-gamma (IFN-γ), transforming growth factor beta (TGF-β), and interleukin-8 (IL-8), which have separate binding sites on each subunit (Lortat-Jacob *et al.*, 1995; Lyon *et al.*, 1997; Spillmann *et al.*, 1998). In these instances, the flexibility of the glycosidic bond of the NA domain is likely to allow the sugar chain to adopt the necessarily sharp curve required for such interactions.

Another issue regarding HS conformation is the effect of the cations as the replacement of Na^+ with K^+, Mg^{2+}, Ca^{2+} or Cu^{2+} could influence the overall molecular shape of the heparin oligosaccharides through changes in the IdoA conformation. This has been confirmed by the differential effect of counterions in the activities of the FGF/FGFR signalling complex (Guimond *et al.*, 2009; Rudd *et al.*, 2008).

Recent structural data have suggested that the glycosidic linkages variation due to IdoA2S and GlcNS are crucial in HS conformation, however, the 6-O-sulfation has a less dramatic effect compared to the NS and 2-O-sulfation (Rudd and Yates, 2010). Ultimately, HS displays a highly accommodating polymer structure that is able to adopt various binding configurations on the large and small scale to meet the needs of protein recognition.

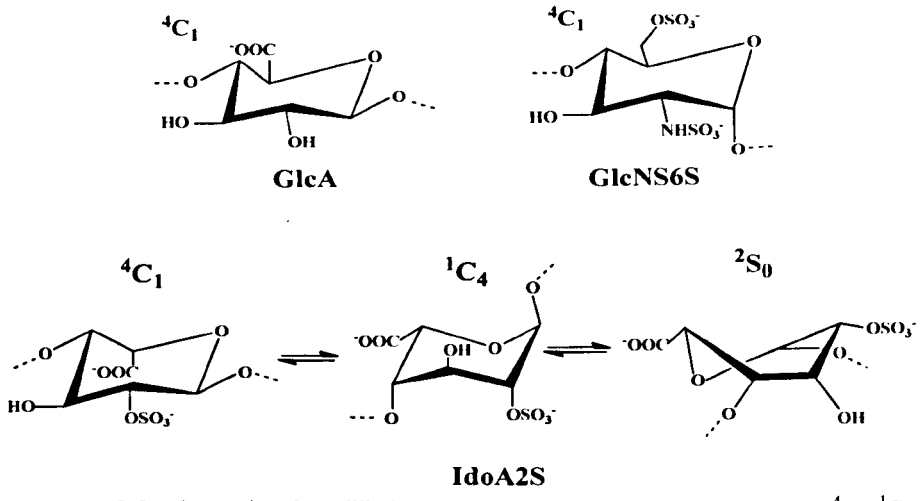

Figure 1.7 Conformational equilibrium of IdoA2S, which exists in three forms $^4C_1$, $^1C_4$ and $^2S_0$; this contrast with predominant $^4C_1$ conformations found in the GlcNS6S and GlcA.

1.5.2 Heparin

Heparin has been known as blood anti-coagulant since 1916, as it was first described by McLean (Dinis da Gama, 2008; Jorpes, 1959). Heparin and its derivatives are regularly used in medical practice during and after operations to prevent blood clotting. Heparin is found *in vivo* in the granules of connective tissue mast cells in vertebrates, hence differs from HS, which is present on the surface of almost all cells, and in the extracellular matrix (Forsberg *et al.*, 1999; Gallagher and Walker, 1985). The heparin chain is attached to a unique core protein, serglycin, found only in the mast cells and some hematopoietic cells (Gallagher and Walker, 1985; Kolset and Tveit, 2008; Rabenstein, 2002).

Heparin chains are shorter than HS chains, but they share the same saccharide backbone and the same biosynthetic route, in which incomplete modifications are made to the chains resulting in sequence diversity. However, heparin is more structurally homogeneous than HS, due to more extensive epimerization of GlcA units and 2-O and 6-O-sulfation of IdoA and GlcNS units, respectively (Salmivirta *et al.*, 1996). Heparin has the highest negative charge density of any known biological macromolecule, a characteristic that could lead to nonspecific electrostatic binding with large numbers of positively charged proteins.

Furthermore, owing to its commercial availability and broad structural similarity heparin has been used as a proxy for HS in many experiments. Nevertheless, the information acquired by these experiments should not be over-interpreted. Furthermore, the co-crystal structure of heparin with fibroblast growth factors (FGFs) have shown that only some of the sulfate groups in heparin contribute to protein interactions, and also that a variable set of sulfate groups mediate these interactions depending on the orientation of the heparin chain (see Chapter 5 for detailed discussion on HS-FGFs studies). Importantly, HS has a lower degree of sulfation, but it is present in almost all cells and is thought to be more important in regulation of protein function than heparin. In addition, the unique HS structure found in the NA and NA/ NS domains cannot be accessed using heparin, and heparin is extensively modified and characterized by a high IdoA/ GlcA ratio. HS on the contrary is subjected to substantially fewer modifications (Lindahl *et al.*, 1994) (Table 1.2).

Characteristics	Heparan sulfate	heparin
Soluble in 2 M potassium acetate (pH 5.7, 4°C)	Yes	no
Size	10-70 kDa	7-20 kDa
Sulfate/ hexosamine ratio	0.8-1.8	1.8-2.6
GlcNS	40-60 %	≥80 %
IdoA	30-50 %	≥70 %
Binding to anti-thrombin III	0-0.3%	~30 %
Site of synthesis	virtually all cells	connective-tissue-type mast cells

Table 1.2 comparing characteristic features of HS vs. heparin.

1.5.3 Chemically modified heparins

Semi-synthetic chemically modified heparins are commercially available and have been generated by various groups (Figure 1.8).

The methods of production of these saccharides involve a single or multiple modifications carried out on the authentic heparin polysaccharide chain. The common modifications (N-acetamido, N-sulfonamido, and O-sulfoxy) are carefully removed or added by chemical treatment to produce a near homogeneous polysaccharide, compared to the heterogeneous HS (Powell *et al.*, 2004; Yates *et al.*, 1996). In addition, the availability of these modified heparins facilitates in depth investigation of the HS domains.

Modified heparins are normally characterised by nuclear magnetic resonance (NMR), however, other techniques are also used such as mass spectrometry (MS), compositional analysis and infrared (IR) spectroscopy (Grant *et al.*, 1989; Linhardt *et al.*, 1990; Yates *et al.*, 1996). After characterization, chemically modified heparins were used as markers for the existence or the absence of a particular group that may be involved in HS structure-activity relationship. There were many examples that showed that there is a link between a change in activity or interaction and the type of modification (Chen *et al.*, 2009; Guimond *et al.*, 1993; Guimond *et al.*, 2006; Irie *et al.*, 2002; Maccarana *et al.*, 1993; Powell *et al.*, 2002; Yates *et al.*, 2004). In addition, modified heparin was found to block L and P-selectin-mediated cell adhesion and prevent tumour metastasis in human ovarian and colon carcinoma respectively (Chen *et al.*, 2009; Wei *et al.*, 2004). Moreover, Skidmore et al (2008) have used modified heparin to disrupt the rosetting of the red blood cells caused by *Plasmodium falciparum* in severe and cerebral malaria (Skidmore *et al.*, 2008).

The data generated from using these modified heparins should not be over interpreted and it should be remembered they are modified heparins and not natural HS. In addition, removing one or more types of sulfate from heparin could have a radical effect on the conformation of the chain. It should also be noted that any heterogeneity found in these modified heparins could have a significant impact on their actions, as protein interactions and activities with HS have been suggested to only need subtle changes in the structure.

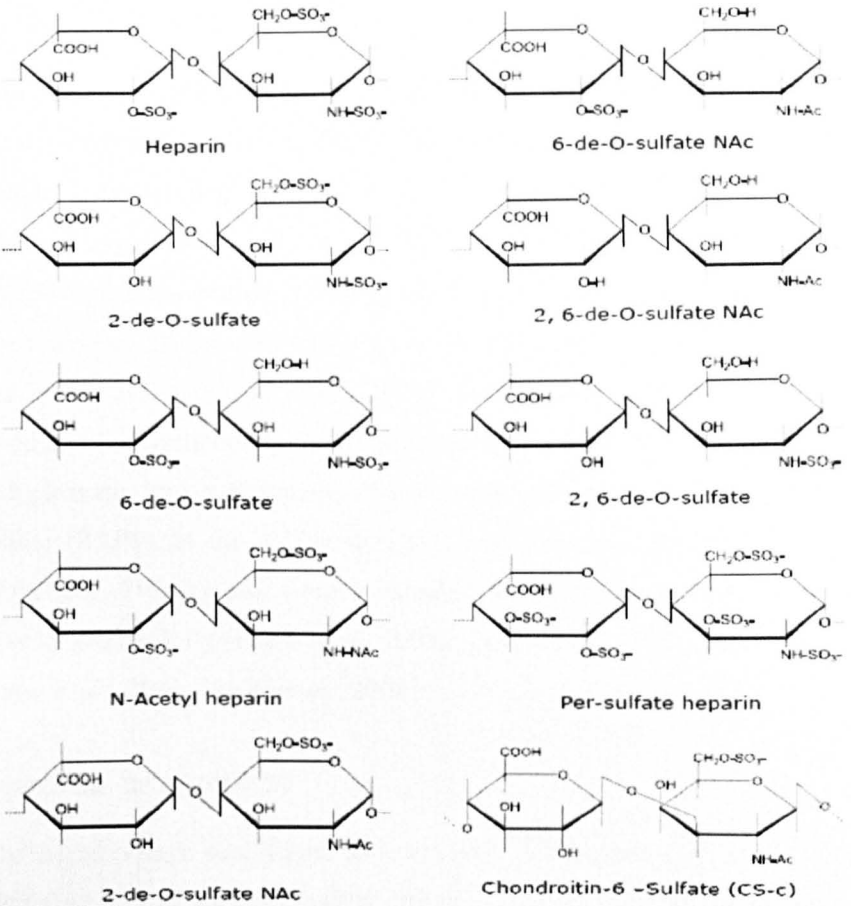

Figure 1.8 Predominant disaccharides structure of the chemically modified heparin polysaccharides. The chemically modified heparins were prepared from porcine intestinal mucosal heparin (Celsus), as described Yates *et al* (1996).

1.5.4 Oligosaccharide library production for HS-protein interactions studies

In order to study the high number of protein interactions with HS (Capila and Linhardt, 2002; Zmojdzian *et al.*, 2008) tools are needed to unravel the extensive structural complexity of HS polysaccharides (Merry *et al.*, 2001). Chemical synthesis has been achieved for a limited number of oligosaccharides (Xie *et al.*, 2006; Vorup-Jensen *et al.*, 2007; Peterson *et al.*, 2009). Furthermore, enzymatic synthesis of oligosaccharide up to 8-mer is also possible (Copeland *et al.*, 2008; Peterson *et al.*, 2009). However, generating a larger HS oligosaccharide with heterogeneous arrangements resembling naturally occurring HS has proved to be a difficult and prolonged process.

This difficulty is due to the chemistry of HS, which provides serious challenges such as structural isomerism and anomerism, which are common within its oligosaccharide structure and also the presence of sulfates and carboxylic acid groups which are highly acidic (Yates *et al.*, 2004). Furthermore, the sensitivity of HS to pH (de-N-sulfation occurs at low pH and epoxide formation occurs at high pH) and their insolubility in common organic solvents presents further limitations (Drummond *et al.*, 2001; Powell *et al.*, 2004). The Lindahl group have generated tissue-derived and biosynthetically modified heparins oligosaccharide libraries using nitrous acid cleavage and sulfotransferases together with 3′-phosphoadenosine 5′-phosphosulfate (PAPS) as the sulfate donor. These libraries have shown a wide range of structural diversity and were a valuable tool in the investigation of HS-proteins structural selectivity (Feyzi *et al.*, 1997a; Feyzi *et al.*, 1997b; Kreuger *et al.*, 1999; Kreuger *et al.*, 2001; Jemth *et al.*, 2002).

1.6 HS-protein interactions

Hundreds of proteins have been found to intact with HS/ heparin (Ori *et al.*, 2008). These proteins are termed heparin-binding proteins (HBPs). They are greatly diverse in their nature, as they comprise enzymes, enzymes inhibitors, growth factors, cytokines, morphogens, matrix proteins and lipoproteins (Kjellen and Lindahl, 1991; Conard, 1998; Bernfield *et al.*, 1999; Capila and Linhardt, 2002; Bishop *et al.*, 2007; Ori *et al.*, 2008). However, the biological importance of the interactions for most of them has yet to be discovered.

Heparin is used as a proxy for HS in studying proteins interactions due to its commercial availability. However, most of the functionally significant interactions involve HS rather than heparin. The HS chains, rather than core proteins, are involved in most of these interactions. However, the core protein may also have a role in these interactions as was observed in the extracellular domain of SDC-1, which can regulate cell adhesion in an integrin dependent manner (Beauvais *et al.*, 2004; McQuade *et al.*, 2006), and in the role of SDC-1 and SDC-4 in wound healing (Gallo *et al.*, 1996).

For reviews on the structure and function of syndecan core proteins see (Rapraeger and Ott, 1998; Couchman *et al.*, 2001; Alexopoulou *et al.*, 2007).

Initial HS/ heparin interactions with proteins are thought to be predominantly ionic binding between the anionic sulfates and carboxylic acid groups on the HS/ heparin chains and the cationic ammonium, guanidinium and imidazolium groups on the proteins (Rabenstein, 2002). Both amino acids arginine and lysine contribute to the binding. Arginine occurs more often in the heparin binding sites of proteins and binds more tightly to heparin than lysine, a difference thought to arise from the intrinsic properties of arginine and lysine side chains (Fromm *et al.*, 1995). Non-ionic interactions such as van der Waal's forces and hydrogen bonds also contribute to HS binding to proteins; earlier work by Thompson et al (1994) on FGF-2 with heparin oligosaccharides indicated that only 30 % of the binding free energy is purely electrostatic (Thompson *et al.*, 1994a). Hydrophobic amino acids such as phenylalanine (Phe 122 and 121) play a significant role in heparin binding and its conformational activation of anti-thrombin III by arranging an extensive network of ionic and non-ionic interactions between positively charged heparin binding site amino acids and negatively charged heparin (Jairajpuri *et al.*, 2003). In addition, Hillman et al (1998) found that hydrogen bonding between the polar residues of brain natriuretic peptide (BNP) and heparin is the major factor contributing to the free energy of BNP binding to heparin, despite BNP having a high frequency of basic amino acid residues (lysine and arginine) (Hileman *et al.*, 1998b). The non-ionic and ionic interactions are thought to be linked, and it is likely that sulfation and the charge distribution of the saccharide might influence the three-dimensional structure and conformation of the bound protein ligand.

Different researchers in the field have predicted the topologies of heparin binding sites. By comparing proteins that bind to heparin and those that do not, Cardin and Weintraub (1989) proposed a "consensus sequence" in proteins for heparin binding. The sequence is XBBXBX or XBBBXXBX, where B is lysine or arginine and X is a hydropathic amino acid (Cardin and Weintraub, 1989).

Furthermore, Sobel et al (1992) anticipated a third consensus sequence, XBBBXXBBBXXBBX, for the von Willebrand factor (Sobel *et al.*, 1992). The structural analysis of the heparin binding sites in FGF-1, FGF-2 and TGF β-1 implicated a TXXBXXTBXXXTBB motif where T defines a turn (Hileman *et al.*, 1998a). These sequences are true if the sequence was contained in β-strand and α-helical conformations. However, this assumption is misleading if other protein structural conformations are to be considered.

Margalit et al (1993) investigated the presence of a common spatial motif in heparin binding sequences. They proposed that the arrangements of the two local basic amino acids on heparin binding proteins are located at about 20 Angstrom (Å) apart and facing opposite directions on the alpha helix forming an amphipathic structure with their polar groups towards the outside and their hydrophobic chains towards the inside. This spatial distribution of the basic residues suggests that heparin and protein are twisted together and a possible wrapping of heparin around the peptide backbone forming a coil-like structure. In addition, the conserved space of about 20 Å gaps would be enough to accommodate 5-mer heparin, this distance is enough for several heparin-protein interaction (Margalit *et al.*, 1993). This work was focused on the contribution of local heparin binding sequences; however, other sequences from neighbouring regions were not investigated.

Spillmann and Lindahl (1994) have suggested that amino acids involved in heparin binding may be located in distinct juxtaposition loops within the heparin binding proteins. Due to the helical conformation of heparin chains, residues on the chain facing toward the protein can interact directly with its amino acids. Those on the other side of the helix might be free to interact with a different protein such as a protein receptor. Alternatively, amino acids in juxtaposed loops could interact with both sides of the helix. In addition, only small saccharide sections of the HS/ heparin chains are involved in protein binding, therefore a single heparin chain can bind multiple protein ligands (Spillmann and Lindahl, 1994), leading to complex multivalency effects.

HS-protein binding regions may range in size from a few disaccharide residues to 12-mer or sometimes-larger saccharides (Spillmann *et al.*, 1998; Gallagher, 2001). However, the existence of NS domains larger than eight saccharides is uncommon in HS chains. As a result, Kreuger et al (2002) have proposed a mixed domain for saccharides larger than 8-mer with two NS(S) regions separated by at least one NA (A) glucosamine unit (SAS-domain), this was true in the case of endostatin (ES) binding to HS as removing the N-acetylated domain disrupted ES binding to HS (Kreuger *et al.*, 2002). HS serves as a multifunctional regulator of protein activities. The next sections illustrate some examples of HS binding to model proteins.

1.6.1 HS functions

1.6.1.1 HS as co-receptor

HS chains could directly contribute to biological activities or signalling processes. The mechanism by which HS regulates the formation of signalling complexes with different growth factors have been under intense investigation. HS could variously serve to sustain morphogen gradients, deliver the signalling protein to the receptors or directly participate in formation of signalling complexes (Turnbull *et al.*, 2001). However, the specific nature of HS participation remains undecided. In the case of Wnt signalling, Ai et al (2003) have proposed a two-state "catch or present" model for SULF-1regulation of Wnt signalling in which SULF-1 removes 6-O sulfates from HS chains to promote the formation of low affinity HS-Wnt complexes that can functionally interact with Frizzled receptors to initiate Wnt signal transduction (Adam *et al.*, 2003).

1.6.1.2 HS and protein transport

HS on the cell surface or in the extracellular matrix may interact with proteins and help in presenting and positioning of proteins at a given site and time during development and homeostasis.

HS on the cell surface or extracellular matrix play an important role in lipid physiology by acting as a carrier for lipases (Mahley and Ji, 1999). In inflammatory processes, chemokines need HS for correct positioning (Mei *et al.*, 2005). Growth factors require HSPGs for angiogenesis (Abramsson *et al.*, 2007). It has been suggested that HSPG interactions with growth factors or morphogens help stabilizing the protein gradient, control signalling and protect proteins against degradation (Gonzalez-Martinez *et al.*, 2004; Koziel *et al.*, 2004).

1.6.2 The inhibition of blood coagulation by HS/ heparin

The binding of heparin/ HS to antithrombin III (ATIII) is the best-studied example for HS-protein interactions (Marcum and Rosenberg, 1987; Princivalle *et al.*, 2001). ATIII is a member of the serine protease inhibitors (serpin) family, which is able to inhibit factor Xa, and other proteases of the coagulation cascade. Factor Xa converts prothrombin to thrombin (factor IIa), which subsequently converts soluble fibrinogen into fibrin monomers and become cross-linked (Bourin and Lindahl, 1993; Linhardt, 2003). The high-affinity binding of HS/ heparin to ATIII is mediated through a pentasaccharide sequence present predominantly in HS/ heparin. This pentasaccharide sequence (GlcNAc/ NS (6S)-GlcA-GlcNS3S6S-IdoA2S-GlcNS6S) has several uncommon features, most evidently a 3-O-sulfated glucosamine unit that is adjacent to GlcA and located to the non-reducing side of a fully modified disaccharide (Figure 1.9a) (Choay *et al.*, 1983; Petitou *et al.*, 1986).

The interaction of HS/ heparin with ATIII has a dual effect; it causes a conformational change in the tertiary structure of ATIII resulting in a dramatic enhancement (~1000-fold) in the rate at which ATIII inactivates factor Xa; and through a "template" mechanism binding thrombin (Factor IIa) in close proximity to ATIII for inhibition. Binding of HS/ heparin to thrombin requires a sulfated 6-mer of no particular specific sequence (Petitou *et al.*, 1999; Petitou *et al.*, 2001).

Thus, HS/ heparin 18-mer or more, at the non-reducing end of the ATIII specific pentasaccharide binding sequence, enhances the juxtapositioning of ATIII and inactivation of thrombin. HS/ heparin operate as an allosteric activator in these reactions by improving the rate of the reaction through conformational change of ATIII and approximation of its substrate, thrombin (Figure 1.9b) (Li *et al.*, 2004). The inactivation of thrombin by ATIII is initiated by interacting with a specific reactive bond within the ATIII, which is associated with a conformational change of the ATIII, forming a kinetically stable, possibly covalently linked, ATIII-thrombin complex (Bjork *et al.*, 1993; Olson and Bjork, 1992). Once the inactivation of thrombin by ATIII occurs, the ATIII-thrombin complex loses its attraction to HS and they separate. HS may participate in a new inhibition cycle. The physical separation of the binding sites imparts a bell-shaped response curve for inactivation since a high concentration of heparin essentially competes for thrombin (Esko and Selleck, 2002).

(a)

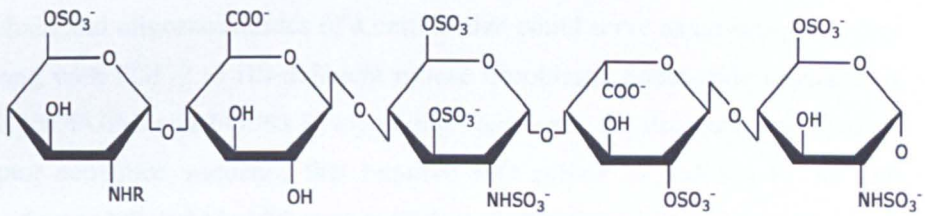

(b)

Figure 1.9 The pentasaccharides sequence for antithrombin activation and the co-crystal structure of antithrombin ternary complex. a) showing the structure of heparin pentasaccharide sequence. b) The pdb file of the tenary complex of the antithrombin-thrombin-heparin ternary complex (PDB file: 1TB6); left view showing the oligosaccharides in ball and sticks form, the protein in cartoon form and the water molecules in white (Li *et al.*, 2004).

1.6.3 Regulation of various growth factors by HS/ heparin

Growth factors are a large family of proteins that are involved in stimulating cellular growth, proliferation and differentiation. HS is found to interact with most growth factors, thereby playing an essential role in the regulation of many physiological processes. Here are examples of some growth factors and their interactions and regulations by HS.

The role of HS in fibroblast growth factors (FGF) signalling has been under investigation for many years. There are 22 FGFs member to date, 15 of them have shown strong affinities to HS i.e. needing between 1-1.5 M sodium chloride to be eluted from heparin-sepharose affinity columns (Asada *et al.*, 2009; Ornitz, 2000). FGFs transmit their signalling through tyrosine kinase receptors (FGFRs) (Eswarakumar *et al.*, 2005). FGF-2 was the first growth factor shown to be reliant on HS for interactions with its receptors (Avivi *et al.*, 1993; Rapraeger *et al.*, 1991). HS/ heparin chain and oligosaccharides of a certain size could serve as co-receptor when added along with FGF-2 to HS-deficient mouse fibroblasts. Saccharide interactions with both the FGF-2 and FGFRs in signalling complexes are dependent on finding the receptor activation sequence that required 6-O sulfate in addition to NS and IdoA2S, whereas NS and IdoA2S were sufficient for binding of FGF-2 alone without the receptor (Guimond *et al.*, 1993).

Vascular endothelial growth factor (VEGF) is also known as angiogenic growth factor. A single *vegf* gene gives rise to a number of VEGF isoforms through alternate mRNA splicing. The VEGF isoforms differ by the presence or absence of short C-terminal heparin-binding domains (HBDs) (Ruhrberg, 2003). VEGF plays a key role in most aspects of vascular development and function. It is also thought to have functions in a number of pathological processes such as cancer, diabetic retinopathy, rheumatoid arthritis, wound healing and vascular diseases. The flexibility of VEGF as a patterning molecule is linked to its association with various signalling receptor complexes, but also its expression in several isoforms with a differential affinity to HS.

$VEGF_{165}$ is the most potent and widely expressed isoform, and it is secreted as a disulfide-linked homodimer with two identical heparin-binding sites. Its interaction with HS regulates the diffusion, half-life, and affinity of $VEGF_{165}$ for its signalling receptors (Robinson *et al.*, 2006). Some features of HS have been found to contribute to the strength of the $VEGF_{165}$ interactions with HS, such as carboxylate groups and 2-O, 6-O, and N-sulfation, with emphasis on the 6-O sulfates. In addition, it has been found that an oligosaccharide of six or seven monosaccharide residues was sufficient to fully, occupy the heparin-binding site of a $VEGF_{165}$ monomer (Robinson *et al.*, 2006).

The hepatocyte growth factor (HGF), also known as Scatter Factor, is a powerful stimulator of epithelial cell migration. HGF is a tumour suppressor, morphogen, and angiogenic factor (Bussolino *et al.*, 1992; Naka *et al.*, 1993). It has been shown to interact with HS on cell surfaces, as well as free HS and DS via interactions between the sulfate groups and certain charged residues in the N-terminus of the growth factor. Sequences of HS that contain 6-O-sulfated, NS glucosamine and IdoA residues are particularly significant for HGF interactions and the minimal binding sequence must be at least 10-12-mer in length (Lyon and Gallagher, 1994).

Transforming growth factor beta (TGF-β) is a family of 25-kDa disulfide-linked dimeric proteins. It has three members in mammals (TGF-β_1, TGF-β_2, and TGF-β_3), TGF-β exhibits bi-functional growth regulation; it inhibits growth of most epithelial cell types and stimulates proliferation of mesenchymal cells such as fibroblasts. The growth regulatory activity of TGF-β has been implicated in many physiological and pathological processes (McCarthy *et al.*, 1989; Palladino *et al.*, 1990; Chen *et al.*, 2006). Heparin and high sulfated HS binds to TGF-β_1 and TGF-β_2, but not TGF-β_3. This interaction improves the biological activity of TGF-β_1 (but not the other isoforms). The improvement is thought to be due to reduced binding and inactivation of TGF-β_1 by α-2-macroglobulin. TGF-β_2-α-2-macroglobulin complexes are not dependent on HS/ heparin, and those involving TGF-β_3 cannot be affected.

Interaction with heparin and liver HS may be most effective because of the ability of the dimer to co-operative engage two specific sulfated binding sequences, separated by a distance of approximately seven disaccharides, within the same chain (McCaffrey *et al.*, 1989; Lyon *et al.*, 1997).

Other members of TGF-β family such as glial cell line-derived growth factor (GDNF) are also found to interact with HS/ heparin. GDNF is a disulfide-linked homodimer of 18-22 kDa N-glycosylated polypeptides (Baloh *et al.*, 2000). It is the prototypic member of a subfamily of four cytokines, the GDNF family ligands (GFLs), which also include artemin, neurturin, and persephin. GDNF, neurturin and artemin were found to bind HS/ heparin with high affinity (Barnett *et al.*, 2002; Rider, 2006; Alfano *et al.*, 2007). However, heparin does not inhibit nor potentiate the GDNF-GDNF receptor (GFR-α-1) interaction (Alfano *et al.*, 2007). GDNF has various functions, as a potent regulator of neuron growth and survival in the enteric sensory and central nervous systems. GDNF has a significant role in controlling kidney morphogenesis; however, to perform this role it requires IdoA2S rich HS within kidney progenitor tissues (Rickard *et al.*, 2003; Rider, 2003).

Platelet-derived growth factors (PDGFs) are dimeric polypeptides that regulate the proliferation and differentiation of smooth muscle cells, fibroblasts, and other cells of mesenchymal origin (Heldin and Westermark, 1990; Westermark *et al.*, 1990). The homo or hetero-dimers of the PDGFs are known as A and B chains. The A chain exists as two splice variants due to the alternative usage of exons 6 (PDGF-$_L$, longer) and 7 (PDGF-$_S$, shorter). Exon 6 encodes an 18 amino acid sequence rich in basic amino acid residues, which has been implicated as a cell retention signal. Several lines of evidence indicate that the retention is due to binding of PDGF-$_L$ to glycosaminoglycans, especially to HS. The shortest PDGF-$_L$ binding domain consists of 6–8 monosaccharide units.

Studies using selectively de-sulfated heparins and heparin fragments suggest that N, 2-O, and 6-O-sulfate groups all contribute to the interaction. Structural comparison of HS oligosaccharides separated by affinity chromatography on immobilized PDGF-$_L$ showed that the bound pool was enriched in IdoA2S-GlcNS6S disaccharide units. Furthermore, analogous separation of a partially O-de-sulfated heparin using a nitrocellulose filter-trapping system yielded a PDGF-$_L$-bound fraction in which more than half of the disaccharide units had the structure (IdoA2S-GlcNS6S) (Feyzi *et al.*, 1997a).

Heparin-binding epidermal growth factor (HB–EGF) is a heparin-binding member of the EGF family that was initially identified as a product of macrophages and macrophage-like cells. Soluble mature HB–EGF is a potent (as PDGF) mitogen for fibroblasts, smooth muscle cells and keratinocytes (Raab and Klagsbrun, 1997). HB-EGF activates two EGF receptor subtypes, HER-1 and HER-4 and binds to cell surface HS (Higashiyama *et al.*, 1993; Thompson *et al.*, 1994b; Feyzi *et al.*, 1997a).

Proteins	*Function*	*Selectivity*
Antithrombin III (ATIII)	Serine protease inhibitors (serpin) family.	Pentasaccharide sequence with a 3-O-sulfated glucosamine unit (Choay *et al.*, 1983; Petitou *et al.*, 1986).
Thrombin	Converts soluble fibrinogen into fibrin monomers and become cross-linked (Bourin and Lindahl, 1993; Linhardt, 2003).	18-mer or more at the non-reducing end of the containing the specific pentasaccharide; no selective sequence.
Growth factors:		
Fibroblast growth factors (FGFs) FGF-1 and FGF-2	Multifunctional proteins, critical during normal development, cell differentiation and proliferation, angiogenesis and important in wound healing (Rapraeger *et al.*, 1991; Avivi *et al.*, 1993; Ornitz and Itoh, 2001).	6-O sulfate and NS and IdoA2S, whereas NS and IdoA2S were sufficient for binding of FGF-2 alone without the receptor (Guimond *et al.*, 1993).
Vascular endothelial growth factor (VEGF)	Angiogenic growth factor plays a key role in vascular development and function.	2-O, 6-O, and N-sulfation, with emphasis on the 6-Osulfates (Robinson *et al.*, 2006), no selective sequence.
The hepatocyte growth factor (HGF) also known as Scatter Factor	HGF is a tumour suppressor, morphogen, and angiogenic factor and a powerful stimulator of epithelial cell migration	6-O-sulfated, NS glucosamine and IdoA, the minimal binding sequence 10-12-mer in length (Lyon and Gallagher, 1994), no selective sequence.
Transforming growth factor beta (TGF-β) (TGF-β_1 and TGF-β_2)	Inhibits growth of most cell types and stimulates proliferation of mesenchymal cells such as fibroblasts (McCarthy *et al.*, 1989; Palladino *et al.*, 1990; Chen *et al.*, 2006).	Heparin and high sulfated HS (McCaffrey *et al.*, 1989; Lyon *et al.*, 1997; Zhao *et al.*, 2006), no selective sequence.
Glial cell line-derived growth factor (GDNF), a member of TGF-β family	Various functions, as a potent regulator of neuron growth and survival in the enteric sensory and central nervous systems and also, a significant role in controlling kidney morphogenesis (Barnett *et al.*, 2002; Rider, 2006; Alfano *et al.*, 2007)	IdoA2S rich HS/ heparin (Rickard *et al.*, 2003; Rider, 2003), no selective sequence.
Platelet-derived growth factors (PDGFs)	Regulate the proliferation and differentiation of smooth muscle cells, fibroblasts, and other cells of mesenchymal origin (Heldin and Westermark, 1990; Westermark *et al.*, 1990)	Six–eight monosaccharide units with N, 2-O, and 6-O-sulfate groups all contribute to the interaction (Feyzi *et al.*, 1997a), no selective sequence.
Heparin-binding epidermal growth factor (HB–EGF)	Potent mitogen for fibroblasts, smooth muscle cells and keratinocytes (Raab and Klagsbrun, 1997).	Heparin/ HS (Higashiyama *et al.*, 1993; Thompson *et al.*, 1994b), no selective sequence.

Table1.3 Summary of the function and the HS selectivity for antithrombin, thrombin and selected growth factors.

1.6.4 Techniques used to study HS-protein interactions

The increasing numbers of HS/ heparin binding proteins to be studied has led to the development of various biochemical and biophysical techniques for analysing their interactions. Some of these methods are easy and low cost while others are more sophisticated and need specialized equipment and expertise to operate and analyse data. Furthermore, the readout of these techniques may also vary from direct measurement of affinity in term of K_d values, to detailed thermodynamic data, kinetic and high resolution structural data on atomic contacts. One issue that should be taken in consideration is that the *in vitro* binding measurements may differ from *in vivo* since the surface density of protein, or receptor, and other interacting factors varies greatly. In addition, using various techniques, that tackle different HS-protein interactions issues, may provide a better overall picture than just using a single technique. Here are some of the available biochemical and biophysical methods for HS-protein interaction studies.

Affinity chromatography is a frequently used biochemical method for the determination of relative affinity of proteins for HS/ heparin. This can be achieved by quantifying the amount of salt needed for elution of the protein from a heparin sepharose affinity column (Kreuger *et al.*, 1999; Kreuger *et al.*, 2002). This method is rapid, inexpensive and uses relatively small amounts of protein. However, it is not a true measure of affinity; because salt is used for elution, hence, the results may be biased toward identifying a highly charged amino acid as binding epitope.

In equilibrium competition binding heparin is immobilized on Sepharose beads and incubated with radioactively labelled proteins of interest which are then competed off by increasing the concentrations of HS/ heparin (Kuschert *et al.*, 1999; Johnson *et al.*, 2004). A difficulty of this method is the use of radioactively labelled material, which is costly and needs a specifically designated working space. However, it is fast and very reliable, and IC_{50} and K_d determinations are possible with this method.

In the affinity co-electrophoresis (ACE) technique, HS/ heparin are mixed with a protein or antibody and the mixture is electrophoretically separated by PAGE (Lee and Lander, 1991; Watson *et al.*, 1997). This method is particularly useful in defining the apparent K_d of the interaction and allows for identification of groups of HS saccharides that differentially interact with the protein.

Analytical ultracentrifugation (AUC) sedimentation equilibrium is used for determining the mass of a protein or protein complex in solution and can be used to characterize associating systems including subunit stoichiometries and equilibrium constants for the assembly process. A sample is subject to high centrifugal force in an analytical ultracentrifuge (Mach *et al.*, 1993; Handel *et al.*, 2008). The drawback of this technique is that it is lengthy and the data can be difficult to handle particularly when there are issues with non-equilibrium aggregation or precipitation, which often occurs in the presence of larger HS saccharides (6-mer and larger).

Enzyme-linked immunosorbent assay (ELISA) has been developed using BD™ heparin binding plate (formally known as Plasso EpranExP™P plates). These plates provide a surface onto which HS/ heparin can be immobilized. The assay needs moderate amounts of protein and HS and it is easy to perform, with no specialized equipment required (Barth *et al.*, 2006; Yates *et al.*, 2006; Mitsi *et al.*, 2008). The downside of this assay is that it allows the determination of relative affinities rather than the true affinities. The kinetics of the interactions (K_d) are difficult to obtain due to the lack of information with regard to the exact amount and orientation of immobilized HS/ heparin saccharide.

Competition ELISA assays using conventional ELISA plates (e.g. Maxisorp™) have been developed to probe the binding site of a protein or an antibody (more details in chapter 4) (Foxall *et al.*, 1995; Najjam *et al.*, 1997; Powell *et al.*, 2002; Rickard *et al.*, 2003).

The advantages of this approach are that it is relatively easy, it has a high throughput capability and can be used in an automated way by robotic handling; it can also provide relative binding affinity and K_d value if the protein concentration is varied appropriately over a large range and the binding curve is saturated. In addition, it has the ability to compare the binding activity of a panel of saccharides. Difficulty arises from the fact that it does not provide direct information about affinity constants, and it regularly requires chemical derivatization of the saccharides for immobilization.

The emerging glyco-microarray technology facilitates the detection and quantification of hundreds of HS/ heparin protein interactions in a high-throughput manner (Noti *et al.*, 2006; Powell *et al.*, 2009). A number of microarray surfaces have been developed and different saccharide immobilisation methods have been exploited. One of these surfaces is commercially available aminosaline slides, which uses a condensation reaction between the amines present on the slide surface and the reducing end of the sugar, forming an imine (or Schiff's base) (Powell *et al.*, 2009; Yates *et al.*, 2003). Recently, a gold surface has been developed using hydrazide-derivatized self-assembled monolayer (SAM) for oriented capture of saccharides. The gold surface has the capacity for diverse interrogations using fluorescent-labelled proteins, but also via other biophysical detection techniques such as MALDI-MS, surface plasmon resonance (SPR) and Quartz crystal-microbalance-dissipation (QCM-D) (Zhi *et al.*, 2008). HS arrays are expected to provide fundamental new insights into structure activity relationships because they assist in the screening and comparison of a wide range of saccharides for their interaction with proteins (Powell *et al.*, 2009; Zhi *et al.*, 2006). However, since the saccharides are immobilized on the surface, this could affect the interacting protein, and this technique is still under-developed for routine use.

One of the biophysical methods is the optical biosensor, using for example, the surface plasmon resonance (SPR) and resonant mirror instruments. These techniques are based on the phenomenon that enables detection of unlabeled binding components in real time and depend on the refractive index of the sample within the evanescent field above the sensor surface (Capila *et al.*, 1999; Cochran *et al.*, 2009;

Schuck, 1997). A schematic for an optical biosensor experiment procedure is shown in Figure 1.10a and b. HS is readily immobilized on a streptavidin sensor chip surface by biotinylation (Delehedde *et al.*, 2002a; Osmond *et al.*, 2002). This method uses relatively small amounts of material and protein labelling is not required, and it gives a direct measurement of association and dissociation rate constants. The drawback for this technique is the cost of the equipment and the immobilisation of the saccharide on the sensor surface.

Another biosensor related technique is dual polarization interferometry (DPI), a surface-based technique that allows the concurrent measurement of the changes in thickness, refractive index and the immediate conformational change in the mass of saccharides bound to the surface. This could describe the geometry of the bound proteins, which is also termed conformation activity relationship (CAR) (Delehedde *et al.*, 2002a; Delehedde *et al.*, 2002bCross, 2003 #2892; Swann *et al.*, 2004).

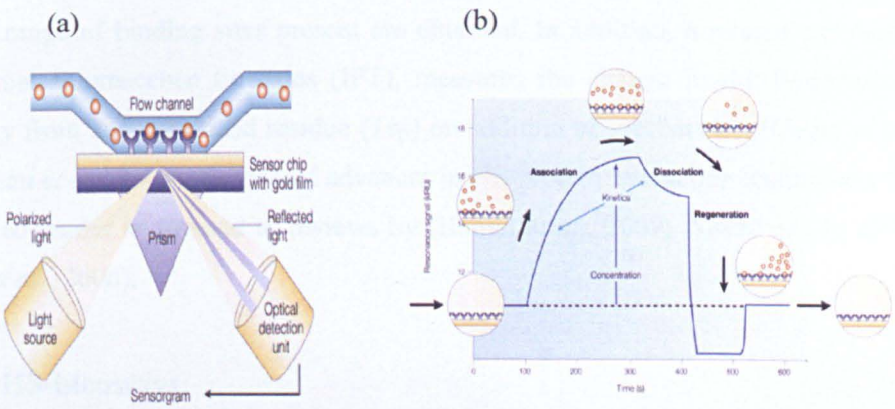

Figure 1.10 Principles of the SPR optical biosensor. a) Schematic represents SPR experiment. SPR detects changes in the refractive index in the immediate surrounding area of the surface layer of a sensor chip. SPR is observed as a sharp shadow in the reflected light from the surface at an angle that is dependent on the mass of material at the surface. The SPR angle shifts (from I to II in the lower left-hand diagram) when bio-molecules bind to the surface and change the mass of the surface layer. This change in resonant angle can be monitored non-invasively in real time as a plot of resonance signal (proportional to mass change) versus time. b) Typical binding cycle observed with an optical biosensor. Adopted from (Cooper, 2002).

It is more advanced than the basic optical biosensor, as absolute measurements are possible. An advance in DPI surfaces are needed and newly developed surfaces are promising (Popplewell *et al.*, 2005; Terry *et al.*, 2006; Popplewell *et al.*, 2009). In addition, this method could be used to resolve key questions relating to the binding of proteins to saccharides and add to the understanding the geometry of complexes of the HS/ heparin-protein interactions. Ternary complexes could also be characterized by this method. Nevertheless, this technique may suffer from limitations caused by immobilizing saccharides.

One of the older biophysical techniques used is isothermal titration calorimetry (ITC) which determines the thermodynamic parameters of the interactions. The binding of HS and protein is measured as a change in enthalpy through isothermal titration microcalorimetry using a commercial microcalorimeter (Pantoliano *et al.*, 1994; Thompson *et al.*, 1994a). This method is able to provide direct thermodynamic information about the binding of HS saccharide to protein. However, a relatively large amount of protein is required and if pure saccharides not used average values for the range of binding sites present are obtained. In addition, a related technique, isothermal fluorescence titrations (IFT), measures the change in the fluorescence intensity from an amino acid residue (Trp) on addition of saccharides. (Goger *et al.*, 2002; Lau *et al.*, 2004). For recent advances in HS-protein interaction techniques, the interested reader is directed to reviews by (Hamel *et al.*, 2009; Powell *et al.*, 2004; Yates *et al.*, 2006).

1.6.5 HS-bioassays

Bioactivity assays are used to determine the physiological relevance of the biochemical interactions. The interaction alone is not enough to forecast the biological activity, as it has been reported that a subtle difference can alter such activity (Rahmoune *et al.*, 1998). There are a number of cell lines utilized in HS/ heparin bioassays studies, such as BaF3 cells, which are naturally deficient in HS (Ornitz *et al.*, 1996; Ornitz *et al.*, 1992) and hence, need an exogenous source of HS to restore activity. In addition, some cell lines which have been made HS deficient by mutation have been developed, for example CHO cells (Zhang *et al.*, 2006).

Both systems provide an efficient approach for activity studies; however, the number of signalling systems currently covered is limited.

It is difficult to study the bioactivity of exogenous HS/ heparin saccharides in other cell systems, as most cells have endogenous HS. Hence, the effects of exogenous HS/ heparin saccharides would compete with the endogenous HS. Therefore, there is a need to remove of endogenous HS. This is made possible by using two approaches. The first approach is by treating the cells with sodium chlorate, to inhibit the enzyme that makes the (universal) sulfate donor (PAPS) (Rapraeger *et al.*, 1994). Hence, the new HS will be biosynthesised without any sulfate modifications, which usually abolishes its protein binding properties (Rapraeger *et al.*, 1991). However, sodium chlorate will inhibit the entire cell sulfation reactions, and may have other side effects on the cells. In addition, the use of sodium chlorate may cause undesired effects on proteins themselves, as it is known for it is oxidizing activity. The second approach for removing endogenous HS is by using a combination of heparinase (I, II and III) enzymes. The advantage of using heparinases is that they only act on HS, and they do not have any recorded side effects. Nevertheless, these enzymes act on mature HS that has been transported to the surface and extracellular matrix. Hence, there is need for the presence of these enzymes for the whole duration of the experiment, which is expensive. Furthermore, heparinases may not fully digest the HS, as any small fraction remaining could preserve HS activity.

A newly developed approach for removing HS from cells is by RNA interference (RNAi). This method involves transfecting the cells with small hairpin RNA (shRNA) to silence the Exostosin tumour-like-3 (*EXTL3*) gene that encodes for α-1, 4-N-acetylglucosaminyl-transferase, the enzyme responsible for triggering HS biosynthesis. This method has been examined in substrate deprivation therapy (SDT) for HS storage, mucopolysaccharidoses (MPS) diseases (Kaidonis *et al.*, 2010). Furthermore, it was used in regulation of normal insulin secretion by HS (Takahashi *et al.*, 2009). A concern for using this method is that some other off-target genes might be silenced by shRNA; so careful controls are required.

1.7 Tools for HS structure analysis and characterization

The structural analysis of HS is of fundamental importance in the determination of structure-activity relationships between HS and its many interacting proteins. Unlike protein and nucleic acid structure characterization, carbohydrates and more specifically GAGs have no individual method allowing simple, reproducible structure determination of oligosaccharides of any size. In addition, obtaining a reasonable amount of pure samples in order to perform the multiple stage structural analysis is difficult due to the heterogeneous nature of HS. Nuclear magnetic resonance (NMR) is a direct method used frequently for glycan structural analysis. This method does not require multiple processing steps; however, it does require large amounts of pure sample (typically ~ mgs). In addition, an analytical technique such as mass spectrometry (MS) which is capable of determining of HS elemental composition is now emerging. Many other structural determination methods are also available; all of them benefit from breaking down the HS chain into small oligosaccharides using enzymatic or chemical methods. In addition, enzymes such as endolytic bacterial lyase enzymes and exolytic mammalian lysosomal enzymes can be used to identify the presence and positioning of the various sulfate, acetyl and carboxyl groups on the glucosamine and uronic acid subunits. The information obtained from enzymes coupled with nitrous acid digestion could allow structural determination of HS sequence (Garg *et al.*, 2005; Turnbull *et al.*, 1999). Most methods used to date are intended for structure characterization of an interesting (purified) oligosaccharide that has shown some selectivity for protein binding and particular biological importance.

1.7.1 Nuclear magnetic resonance (NMR)

NMR is based on the properties of nuclei in the magnetic field and applied electromagnetic (EM) pulse, which cause the nuclei to absorb energy from the EM pulse and radiate this energy back out. The energy radiated back out is at specific resonance frequency that depends on the strength of the magnetic field and the environment of the nuclei.

This allows the observation of specific quantum mechanical properties of an atomic nucleus. Most NMR studies involve the use of ^{1}H, ^{13}C, ^{15}N and ^{31}P isotopes. When a magnetic field applied to a solution containing HS/ heparin sample the consequence is the ^{1}H and ^{13}C atoms are lined up. When the field is switched off, the nuclei relax back to their original spin state and the energy required for change is then recorded in a NMR spectrum. The resonance of a particular atom is influenced by its environment, i.e. proximity to other atoms. The position of the peak is called chemical shift and is measured relative to that of a standard molecule, which is often tetramethylsilane (Yates *et al.*, 1996).

Simple one-dimensional NMR spectroscopy (1DNMR) is routinely used to study the entire primary structure of small oligosaccharides, indicates how many residues are there and how many of them belong to each anomeric configuration. Two-dimensional NMR techniques (2DNMR) are used to determine the structure of more complicated molecules, provided a sufficient amount of relatively pure material is available. The complete structural elucidation requires the full assignment of both the ^{1}H and ^{13}C NMR spectra of the oligosaccharide. This task typically is accomplished by a combination of two-dimensional NMR techniques. Brief description of 2DNMR techniques are listed in Table 1.4 (Varki *et al.*, 2009). NMR spectroscopy provides a full structural characterization of HS/ heparin without altering the sample. However, a large amount of pure sample is required (typically ~ 1 mg). In addition, NMR requires specialised equipment and expertise in analysis of the NMR data. NMR has been used to sequence 6-mer and 8-mer HS/ heparin saccharides (Larnkjaer *et al.*, 1995; Yamada *et al.*, 1999). In some cases, larger heparin saccharides were sequenced by NMR (Shriver *et al.*, 2000), but this is difficult, since the disaccharides units have similar structures and the carbon atoms on the rings have similar environments. HS saccharides with a distinctive chemical shift, such as 3-O-sulfated saccharides, have been found to be easier to sequence.

2D NMR technique	Description
Correlation spectroscopy (COSY)	Correlations of cross-peaks indicate protons joined by few bonds identity. Used for identifying the number and the anomeric configuration in a glycan.
Total correlation spectroscopy (TOCSY)	Identifies resonances belonging to individual spin systems, as cross-peaks define the whole spin system. In addition, identity and anomeric configuration of a monosaccharide can be revealed.
Nuclear Overhauser Effect Spectroscopy (NOESY)	Cross-peaks indicate protons close in space. It is useful in saccharide sequencing and conformational analysis
Rotating-frame NOESY (ROESY)	To determine the connectivity of the residues, its spectrum shows linkage through space, and identifies atoms, which are spatially close to each other.
Heteronuclear multiple bond spectroscopy (HMBC)	Cross-peaks indicate proton and C, N, or P atoms linked by few bonds assignment of NMR signals to atoms in structure; sequence and substitution analysis
Heteronuclear single- quantum coherence spectroscopy (HSQC)	Cross-peaks indicate proton and C, N, or P atom linked by one bond assignment of NMR signals to atoms in structure

Table 1.4 Major NMR techniques for HS/ heparin structure determination (Garg *et al.*, 2005; Varki *et al.*, 2009).

1.7.2 Mass spectrometry (MS)

MS is an analytical technique for the determination of the elemental composition of molecules. Its principle consists of ionizing chemical compounds to generate charged molecules or molecular fragments and then measure their mass-to-charge ratios (*m/z*). Structural analysis of HS by MS presents a challenge, due to its sequence heterogeneity and some characteristic features such as isomerism. In addition, the high fragmentation energy could result in the loss of important component of the HS such as sulfates.

Electro-spray ionization (ESI) MS permits ionization of HS saccharides and direct ratio determination (Gunay *et al.*, 2003; Kuberan *et al.*, 2002). Although ES-MS is used in structural determination, the HS spectra are often very complex, due to the sample often being a mixture and the sulfate groups being adducted with cations (such as sodium ions) to varying degrees.

Some problems in HS sequencing could be solved by the use of tandem MS/ MS, such as structural isomerism, by detecting differing fragmentation pathways (Naggar *et al.*, 2004; Saad and Leary, 2004). In addition, direct coupling of MS with liquid chromatography (LC-MS) will give a 2D structural analysis (Linhardt *et al.*, 1989; Henriksen *et al.*, 2006; Zaia, 2009).

Recently, the introduction of the hydrophobic phenylsemicarbazide (PSC) tag in conjunction with IP-RP-HPLC/ ES-MS is a different method in the ES-MS analysis of HS (Skidmore *et al.*, 2009). This approach does not require chromatographic elution with high levels of salt; hence, it does not suffer from a need for subsequent desalting or potential interference of the sodium ions with MS analysis as in the SAX-HPLC separation. In addition, this method could form one part of a sequential 3D chromatographic separation of HS. When it is coupled with digestion of PSC derivatives, using lyase, hydrolase and sulfatase enzymes and subsequent MS analysis of the digestion products, it provides a sensitive and rapid way to elucidate detailed structural information on the HS oligosaccharides and offers the basis for development of powerful sequencing strategies for HS glycans (Dr. A Atrih unpublished work).

Matrix-assisted laser desorption/ ionization (MALDI) MS is an ionization technique, allowing the analysis of biomolecules and large organic molecules, however, it is a harsh technique compared to the ESI. MALDI time-of-flight MS (MALDI-TOF MS) has been used for structural analysis of HS saccharides (Venkataraman *et al.*, 1999). The approach of Venkataraman et al, 1999 involved pairing the oligosaccharide with a basic peptide and determining the mass of the peptide-oligosaccharide complex (Juhasz and Biemann, 1994; Juhasz and Biemann, 1995). Hence, the mass/ charge ratio detected is for the combined mass (HS and the bound peptide). By measuring the mass before and after partial enzymatic or chemical digestion, it is possible to determine the oligosaccharide residue sequence (Venkataraman *et al.*, 1999). This approach is limited by the need to purify the HS oligosaccharide prior to the MALDI-TOF sequencing procedures and there is ~10 % loss of sulfates compared to ESI (Tissot *et al.*, 2008).

Using multidimensional MS, however, it is possible to isolate an ion corresponding to an individual oligosaccharide component in a complex mixture in the first MS dimension, eliminating the need to produce pure oligosaccharides. This ion can then be fragmented by collision induced (or activated) dissociation (CID or CAD) and the masses of the resultant fragment can be determined in the second dimension MS. Sequencing of oligosaccharides has been demonstrated using MS/ MS (Konig and Leary, 1998; Saad and Leary, 2005; Tseng *et al.*, 1999).

Recently, Tissot et al (2007) have developed a MALDI MS strategy for the analysis of HS oligosaccharides purified from cells and tissues compatible with high-throughput glycomic analysis (Dell and Morris, 2001). By utilizing crystalline matrices, such as norharmane and 2', 4', 6'- trihydroxyacetophenone (THAP), as well as ionic liquids for the detection of fully sulfated molecular species by MALDI-TOF MS, Tissot et al (2007) were able to successfully analyse heparin derived oligosaccharides as large as 10-mer carrying up to 13 sulfate groups by MALDI-MS. Moreover, it shows that MALDI-TOF MS can be employed to provide structural information using either crystalline or liquid matrices. In addition, a bioinformatics tool to help annotate HS MS data has also been developed (Tissot *et al.*, 2007).
Considerable progress that been made over the past five years in HS structure analysis by MS (Saad *et al.*, 2005; Saad and Leary, 2005; Thanawiroon *et al.*, 2004; Zamora *et al.*, 2002), and MS can be expected to be used as a routine technique for structure determination over the next few years.

1.7.3 HS synthesis

1.7.3.1 Chemical synthesis

Producing chemically synthesized HS or heparin-like structures in large quantities suitable for biochemical and biological assays and finally for use as pharmaceuticals is an exciting idea. However, chemical synthesis of HS oligosaccharides is a lengthy and challenging process, and few HS oligosaccharides have been chemically produced.

The earliest example being the anti-thrombin III binding sequence of heparin (Petitou and van Boeckel, 1992; Petitou and van Boeckel, 2004). Furthermore, a number of custom-made synthetic saccharides that have the ability to interact with the platelet binding proteins, HSV-1 glycoproteins and FGFs family and also facilitate HSV-1 entry and have been synthesised (Koshida *et al.*, 1999; Kovensky *et al.*, 1999; Lohman and Seeberger, 2004; Suda *et al.*, 1999). In addition, new synthetic approaches are now in place, which are more reliable in generating a series of diverse HS/ heparin oligosaccharides structure, such as the use of one-pot method for complex oligosaccharide synthesis (ten Dam *et al.*, 2004; Wang *et al.*, 2007; Polat and Wong, 2007).

A modular strategy to synthesize heparin oligosaccharides was develop by Orgueira et al (2003) the advantage of this method is that it can control the stereochemistry of the anomeric centre by placing a conformational constraint on the uronic acid acceptors (Orgueira *et al.*, 2003). Recently pure 48 disaccharide building blocks have been chemically generated to provide for molecular assembly of HS/ heparin oligosaccharide libraries, initially a set of tetrasaccharides (Arungundram *et al.*, 2009). Despite the recent advances in HS/ heparin chemical synthesis it is still not possible to obtain a wide range of HS structure in a short time. As the methods require many chemical preparation, modification and purification steps, and the complex use of protecting groups in order to overcome problems such as solvent incompatibilities (Avci *et al.*, 2003; Karst *et al.*, 2003; Karst and Linhardt, 2003; Noti and Seeberger, 2005; Boltje *et al.*, 2009).

1.7.3.2 **Enzymatic synthesis**

Despite the efforts of many groups in chemical synthesis it is still a challenge to produce HS/ heparin oligosaccharides that are larger than 6-mer. Hence, enzymatic synthesis has been attempted, as it has high regioselectivity and does not require any protection steps. Thus, it is easier to produce longer oligosaccharides using HS modifying enzymes.

Enzymatic synthesis of only micrograms amounts of HS polysaccharides mixture has been accomplished by using a series of recombinant sulfotransferases and C5 epimerase (Kuberan *et al.*, 2003). However, milligram amounts were achieved by generating bulk quantities of HS biosynthetic enzymes and through the use of a PAPS regeneration system or through finding a less costly sulfate donor, such as p-nitrophenol sulfate (PNPS) (Burkart *et al.*, 2000; Chen *et al.*, 2005). In addition, grams of *Escherichia coli* K5 heparosan were isolated and have been used as a substrate for HS biosynthetic enzymes (Kuberan *et al.*, 2003). Recently a chemo-enzymatic method was developed by Zhang et al (2008), which has facilitated the production of heparin-like polysaccharides resembling heparin derived from animal tissues as confirmed by heteronuclear multiple bond spectroscopy (HMBC-NMR) and is classed as a novel reagent for studying the interaction of heparin with proteins (Zhang *et al.*, 2008).

Chen et al (2007) used combinations of biosynthetic enzymes in generating HS library with various sulfations in order to identify new anticoagulant structures. Interestingly, they found that a polysaccharide (Recomparin) lacking IdoA has strong binding affinity to anti-thrombin III, anti-Xa and anti-IIa (Chen *et al.*, 2007). Chemical or enzymatic synthesis of large and well-defined oligosaccharides still represents a challenge. It could be a while before it becomes a routine procedure. Furthermore, an advance in structural analysis is required in order to characterise the newly produced saccharides completely.

1.8 HS selectivity/ specificity

The regulation of HS biosynthesis suggests that there is a high degree of specificity and selectivity in interactions of HS with proteins (Holmborn *et al.*, 2004). The notion of selectivity/ specificity has been debated in more detail in recent reviews (Coombe and Kett, 2005; Gallagher, 2001; Kreuger *et al.*, 2006; Lindahl and Li, 2009; Nakato and Kimata, 2002; Powell *et al.*, 2004).

The interactions between HS and proteins are thought to depend on specific sulfate groups which reflect the importance of the NS or NA/ NS domains in protein binding (Gallagher, 2001). This idea has been strengthened by the clear specificity of the interaction between HS/ heparin and ATIII which has been referred to as sequence specificity (Clamp *et al.*, 2006; Guimond and Turnbull, 1999; Salmivirta *et al.*, 1996). However, there are speculations for a different view (Kreuger *et al.*, 2006; Rudd *et al.*, 2007). Since the interactions may be modulated by many factors: such as the conformational flexibility (especially of the IdoA2S and the glycosidic linkage) and the selective effect of counter cations (such as Na^{+}, Cu^{++}). In addition, the influence of residues adjacent to the actual protein binding domains and domains organization should not be ignored (Chan *et al.*, 1992; Guerrini *et al.*, 2008a; Guglieri *et al.*, 2008; Rudd *et al.*, 2007; Guimond *et al.*, 2009; Rudd and Yates, 2010).

In spite of extensive investigations of the specificity of HS-protein interactions, in terms of saccharide composition and size, there is still no universal model to fit all proteins interacting with HS. However, thoroughly exploring distinct HS-protein interactions and looking into the structural components of HS in terms of presence of common or uncommon features could increase the knowledge of HS-protein selectivity/ specificity. Therefore, occurrence of an uncommon HS unit could be an indication of some degree of specificity, and there are some few examples validating this theory: the feature of an uncommon 3-O sulfate glucosamine unit that is a fundamental component of the interaction between 5-mer and ATIII (Petitou, 2003). Only one third of heparin chains will have this structure. However, certain HS species would have this rare composition, as vascular HS is one of these species and is suggested to have a major role in regulation of blood coagulation (Colliec-Jouault *et al.*, 1994). Furthermore, the 3-O sulfate that binds to anti-thrombin III was found in the extra-vascular sites, in particular the ovary, where it is involved in regulation of protease action at ovulation (de Agostini, 2006). The 3-O-sulfation has also been suggested to be important for the interactions of FGF-7 (Capila and Linhardt, 2002).

Moreover, some HS chains have 3-O sulfate groups that do not interact with ATIII, suggesting that they could be binding to proteins that are yet to be identified (Edge and Spiro, 1990; de Agostini *et al.*, 2008). N-unsubstituted glucosamine is also present as one of the uncommon HS modifications. These rare free amino groups are found in sequences that able to bind to L and P selectin (Norgard-Sumnicht and Varki, 1995). The herpes simplex glycoprotein gD (HSV) and cyclophilin B both require the presence of uncommon substitutions. Their binding sequences contain both N-unsubstituted and 3-O sulfated glucosamine residues, though it is not clear if there is a structural necessity for the free amine group or whether the unusual specificity of 3-OST-3 isoform for a free amine determines its presence in binding site (Shukla *et al.*, 1999; Vanpouille *et al.*, 2007).

On the subject of the hexuronic acid, IdoA is the major 2-O sulfated component, but most HS contain small proportion of GlcA2S, which have been catalyzed by the same enzyme (2-OST) (Fisher *et al.*, 2001). Tissue HS isolated from adult human brain showed considerable amounts of GlcA2S-GlcNS disaccharides units, however it is absent from neonatal brain. The protein-binding partner for GlcA2S is still to be determined (Lindahl *et al.*, 1995; Lortat-Jacob, 2009).

As discussed above, HS specificity could also be due to uncommon saccharides units. This hypothesis does not rule out the special arrangement of the common sulfate groups for supporting HS specificity. The best examples are the FGF family. Even though the strength of FGFs interaction with HS correlated with the overall degree of saccharide sulfation (Jemth *et al.*, 2002; Kreuger *et al.*, 2005), some of the sulfate groups (such as NS, 2-O-sulfate and 6-O-sulfate) have been found to contribute to HS protein interactions more than others. Examples include FGF-2, FGF-10, $VEGF_{165}$ and GDNF (Ashikari-Hada *et al.*, 2004; Jemth *et al.*, 2002; Rickard *et al.*, 2003; Robinson *et al.*, 2005). Furthermore, Bulow et al (2008) provided *in vivo* evidence for the importance of HS roles in selective projection of motor axons in *C elegans,* as their data suggested that both the axon guidance cue *slt-1*/Slit and its receptor *eva-1,* require specific HS modifications for activity (Bulow *et al.*, 2008).

FGF-1 needs 2-O-sulfate of the uronic acid, and 6-O-sulfate and N sulfation of the glucosamine, for strong interaction with HS, while FGF-2 requires only 2-O- sulfate and N sulfation for binding to HS (Kreuger *et al.*, 1999; Turnbull *et al.*, 1992). In addition, FGF-2 is reported to require saccharides of 10 to 12-mer in length, as well as the presence of 6-O-sulfation, to promote mitogenic activity (Guimond *et al.*, 1993; Pye *et al.*, 1998). Nevertheless, in some cases 4-mer saccharide was able to stimulate cell proliferation (Delehedde *et al.*, 2002a). FGF-2 binding was also observed in the absence of sulfate groups (Ornitz *et al.*, 1995). In addition, longer saccharide sequences were also proposed, as in the case of chemokines such as platelet factor 4 (PF-4) and IL-8; they exist as tetramer and dimer, respectively, and form 1:1 complexes with HS saccharides of 12-mer and 20-mer in length and rich in IdoA2S. It has been projected that HS saccharides wrap around these complexes, interacting with spatially separated binding sites exposed on their surface (Capila and Linhardt, 2002; Spillmann *et al.*, 1998).

Similar structural arrangements have been proposed for other proteins such as $VEGF_{165}$ and INF-γ gamma (Lortat-Jacob *et al.*, 1995; Robinson *et al.*, 2006). The NS domains of HS are composed of a maximum of 14-mer (Gallagher, 2001). Thus, special domain arrangements of HS are needed to illustrate these long binding sequences. Gallagher, (2006) proposed a "composite sulfated regions" (CSRs) which include NS domains flanked by alternating sequences of NS and NA disaccharide units that form T zones (transition zones) between the NS domains and the largely NA regions. The 6-O-sulfate of the glucosamine is present in both NS domains and T zones. Differences in position and number of 6-O-sulfates contribute significantly to the fine structural variability in HS. The 6-O-sulfates are subject to removal by SULF-1and SULF-2. The 'editing' function of these enzymes has a profound effect on the binding properties of HS, because 6-O-sulfates are a common functional group for protein recognition (Murphy *et al.*, 2004; Gallagher, 2006).

Kreuger and colleagues (2006) have anticipated that the assembly of these long binding sites requires short NS domains separated by spacer region containing NA residues (SAS) domains (Kreuger *et al.*, 2006). SAS domains may link HS-binding sites located in different proteins as in the case of thrombin and anti-thrombin, and sites composed of a wide separated clusters of basic amino acid residues within single polypeptide as in CXCL-12 gamma chemokine, or endostatin (Kreuger *et al.*, 2002; Laguri *et al.*, 2007; Turnbull *et al.*, 2001).

The interaction of heparin with some proteins such as L and P-selectin is cation-dependent, requiring micro-molar levels of free calcium. L-selectin interacts with highly sulfated regions of HS whereas, P-selectin binding individual less highly modified domains (Koenig *et al.*, 1998; Norgard-Sumnicht and Varki, 1995).

Guimond et al (2009) studied the effect of different cations with respect to HS chain conformation and FGF-1 interaction and they observed differences depending on the cation form (Guimond *et al.*, 2009b). Therefore, the question is, do specific sequences modulate HS-proteins interactions and activity?

1.8.1 Is there a sequence code?

HS specificity is still under investigation. The anti-thrombin III binding region (5-mer with its uncommon sulfate groups) provides the prototypic example for the specific saccharide sequence hypothesis. However, even in this case there are examples of AT-III binding sites that do not concur to this single sequence (Guerrini *et al.*, 2006; Guerrini *et al.*, 2008b).

Furthermore, different FGFs show extensive sharing of binding sites in HS and ability of HS oligosaccharides and polysaccharides to induce complex formation with FGF-1 or FGF-2 with various FGFRs, and activity was promoted by increasing overall sulfation in a non-specific manner, questioning this hypothesis (Jastrebova *et al.*, 2006; Kreuger *et al.*, 2005).

However, in the latter examples an affinity fractionation method was used for the estimation of binding affinities. In this method a mixture of oligosaccharides were applied to an affinity column and eluted with a concentration gradient of NaCl, such that the stronger the binding the higher the concentration of NaCl required for elution. Hence, this approach focuses only on the electrostatic interactions and ignores other interaction factors (Thompson *et al.*, 1994b). From the above debate, there is no one simple rationalization to explain the specificity or selectivity observed.

Here are some possible explanations: the presence of uncommon units in HS domains could be an indication of HS sequence selectivity for protein interactions. In addition, common sulfated saccharides units such as 2-O, 6-O and N sulfates may contribute more to certain protein interactions than other groups, a notion that has been well studied in the case of FGF-HS-FGFR ternary complexes. Special sequence arrangements within HS chains that interact and modulate protein binding and activity are the Holy Grail and may exist in sequences. This thesis aims to answer some of these issues.

1.9 Aims

From the above introduction, it is evident that HS plays an important role in regulating the activity of various proteins and therefore controls their actions. The aim of this thesis is to examine the theory that HS has specific saccharide sequence and sulfation patterns that regulate protein binding and activity.

This will be achievable by generating libraries of heparins, chemically modified heparins and porcine intestinal mucosa HS (PMHS) saccharides as reagents facilitating structure-function studies (see section 3.1.2).

Furthermore, to establish a) the sulfate requirements and an estimated minimum size for HS binding to Slit and Robo using competition ELISA and SEC generated oligosaccharide; b) the effects of heparin variants on HS/ Slit/ Robo ternary complex formation utilizing analytical SEC and competition ELISA with modified heparin chains; c) the effects of heparin variants in Slit and Robo signalling using an *in vitro* bioassay (growth cone collapse assay) (see section 4.1.9).

Finally, SAX generated oligosaccharide libraries will be screened for FGF-1 and FGF-2 binding by competition ELISA, followed by *in vitro* activity studies (BaF3 cell response assay). FGF is a model example for the HS-protein interaction, as many researchers have studied this system extensively. The study conducted by Guimond and Turnbull, (1999) on HS saccharide signalling regulation of FGF-2 via various FGFR isoforms demonstrated that HS saccharides are receptor and ligand specific modulators of activity. However, HS saccharide interactions were not fully addressed in order to relate binding data to activity data (Guimond and Turnbull, 1999; Pye , *et al.*, 2000) (see section 5.1.6).

Overall, this study will explore the role of HS saccharides in regulating protein functions, and establish in depth understanding of the structure-activity relationships involved, hoping ultimately to resolve the HS saccharide sequence selectivity/ specificity hypothesis.

2 Chapter two: Materials and Methods

2.1 Materials

2.1.1 GAGs

Porcine mucosal heparan sulfate (PMHS) was a gift from Organon (www.schering-plough.nl, Oss, Netherlands). Porcine intestinal mucosal heparin (PMH) was purchased from Celsus Laboratories (www.heparin.com, Cat. No. PH-3005, Ohio; USA). Bovine lung heparin was bought from Calbiochem (www.merck-chemicals.co.uk, Cat. No. 375093, La Jolla, USA). Chemically modified heparins were contributed by Dr. E Yates. Chondroitin sulfate (CS-C) was obtained from Sigma (www.sigmaaldrich.com, Cat. No. C4384).

2.1.2 Enzymes

Recombinant Heparinase I, II and III from *Flavobacterium heparinum* were purchased from IBEX (www.ibex.ca, Cat. No. 50-010, 50-011 and 50-012, respectively, and they were stored at -80 °C). Unit definition: one international unit (IU) is the amount of enzyme that will liberate 1 μmol of unsaturated oligosaccharides from HS per minute at 30°C and pH 7.5.

Chondroitinase ABC (cABCase) from *Proteus vulgaris* was purchased from Sigma (www.sigmaaldrich.com, Cat. No. C3667). Unit definition: One unit will liberate 1 μ mole of 2-acetamido-2-deoxy-3-O-(beta-D-gluc-4-ene-pyranosyluronic acid) 6-O-sulfo-D-galactose from CS per minute at pH 8.0 at 37°C.

2.1.3 Proteins

2.1.3.1 Antibodies

Anti-fibroblast growth factor antibodies were purchased from R&D systems, (www.rndsystems.com, Cat. Nos. anti-FGF1, AF-232-NA; anti-FGF2, AF-233-NA,). Anti goat conjugated with horseradish peroxidise (HRP) were bought from Sigma (www.sigmaaldrich.com, Cat. No. A5420).

Goat antibody for the constant region of human IgG1 (Fc), coupled with HRP, was bought from Pierce (www.piercenet.com, catalogue number; 31416). Mouse monoclonal (IgG1) anti c-myc (9E10) was acquired from Sigma, (www.sigmaaldrich.com, catalogue number M5546). Anti-biotin-HRP was purchased from Cell Signalling, (www.cellsignal.com, Cat. No. 7075).

2.1.3.2 **FGFs**

Human recombinant (rh) rhFGF1 and rhFGF2 were purchased from R&D systems, (www.rndsystems.com, Cat. No. FGF1, 232-FA-025 and FGF2 233-FB-025); FGF2 was a gift from Prof. D.G. Fernig (University of Liverpool).

2.1.3.3 **Robo**

Robo protein variants were a gift from Prof. Erhard Hohenester (Imperial College London), including *drosophila* Robo IG12 C-His, *drosophila* Robo IG12 untagged, *drosophila* Robo IG1 C-His, *drosophila* Robo IG1 untagged, *drosophila* Robo D1-5 FC.

2.1.3.4 **Slit**

Slit protein variants were a gift from Prof. Erhard Hohenester (Imperial College London) *drosophila* Slit D2 N-His, *drosophila* Slit D2 untagged, human Slit2 D2 untagged, *drosophila* Slit D1-4 His-myc. The human Slit2 or mock conditioned medium (hSlit2-CM) were also provided by Prof. Hohenester.

2.1.4 Reagents:

All common chemicals were of analytical grade; a list of chemicals, their suppliers and catalogue numbers is shown in Table 2.1.

Reagents	Suppliers and catalogue number
Acetic acid	BDH, UK, vwr.com, Cat. No. 100015N
Acrylamide/bis-acrylamide	Sigma, www.sigmaaldrich.com, 40 %, 19:1 ratio, Cat. No. A-2917; 40 %, 49:1 ratio, Cat. No. A-0924
Albumin Standard bovine	PIERCE, www.piercenet.com, Cat. No. 23209
Ammonium acetate	Sigma, www.sigmaaldrich.com, Cat. No. A7262
Aminoxybiotin **[N-(aminooxyacetyl)-N'-(D- biotinoyl) hydrazine, trifluoroacetic acid salt (ARP)]**	Invitrogen, www.invitrogen.com Cat. No. A-10550
Ammonium hydrogen carbonate	Fluka, www.sigmaaldrich.com/fluka, Cat. No. 09830
Ammonium persulfate (APS)	Sigma, www.sigmaaldrich.com, Cat. No. A3678
Azure A chloride	Sigma, www.sigmaaldrich.com, Cat. No. A6270
Biotin-x-x-hydrazide	CalBiochem, www.merck-chemicals.co.uk, Cat. No. 203110
Bovine serum albumin	Sigma, www.sigmaaldrich.com, Cat. No. A3058. Fraction V
Calcium acetate	Sigma, www.sigmaaldrich.com, Cat. No. C-8570
Calcium chloride	BDH, uk.vwr.com, Cat. No. 27588
Carbonic Anhydrase, from bovine erythrocytes,	Sigma, www.sigmaaldrich.com, Cat. No. C7025
Casein	Sigma, www.sigmaaldrich.com, Cat. No. C8654-500G
Coomassie Plus	PIERCE, www.piercenet.com, Cat. No. 1856210
Cytochrome c equine heart	Sigma, www.sigmaaldrich.com, Cat. No. C2506
Dialysis tubing	Medicell International Ltd, www.medicell.co.uk, Cat. No. DVT07000.04000. MWCO: 7000 Dalton
Di-n-butyl amine	BDH, uk.vwr.com, Cat. No. 153303J
EDTA	Sigma, www.sigmaaldrich.com, Cat. No. E5134
Ethanol	BDH, uk.vwr.com, Cat. No. 1047E
Ethylene glycol	Sigma, www.sigmaaldrich.com, Cat. No. 293237
F12 Nutrient mixture,	Invitrogen, www.invitrogen.com4T, 4TCat. No. 31765-027
Fertile chick eggs	Leas Lane Farm (Wirral, Merseyside, UK)

Fetal Calf Serum (FCS)	Invitrogen, www.invitrogen.com TCat. No. 16010-159
Glutaraldehyde	Sigma, www.sigmaaldrich.com, Cat. No. G5882-100 mL
L-glutamine	Sigma, www.sigmaaldrich.com, Cat. No. G8549
Glycerol	Fisher scientific, www.fisher.co.uk, Cat. No. G/0650/17
Hams F12 glutamax	Invitrogen/ Gibco, www.invitrogen.com Cat. No. 31765-27
Ham's F12 medium with L-glutamine	Invitrogen/ Gibco, www.invitrogen.com Cat. No. 21765-029
Hank's buffered salts solution (HBSS)	Invitrogen/ Gibco, www.invitrogen.com Cat. No. 24020-091
Hybond-ECL nitrocellulose membrane	GE Healthcare, www.gehealthcare.com, Cat. No. RPN68D
Hydrochloric acid	BDH, uk.vwr.com, Cat. No. 450023K,
Hyperfilm-ECL	GE Healthcare, www.gehealthcare.com, Cat. No. 28-9068-36
Interleukin 3 (rmIL-3)	R and D systems, www.rndsystems.com, Cat. No. 403-ML-010
Insulin from bovine pancreas	Sigma, www.sigmaaldrich.com, Cat. No. I5500
Insulin/ Transferrin/ selenium	Invitrogen/ Gibco, www.invitrogen.com Cat. No. 41400-045
Laminin-1	Invitrogen, www.invitrogen.com Cat. No. 23017
MES	Sigma, www.sigmaaldrich.com, Cat. No. 69892
Methanol	VWR, uk.vwr.com, Cat. No. 20864.320
Methocllelulose	Sigma, www.sigmaaldrich.com, Cat. No. M7027
MTT (3-(4,5-Dimethyl-2-thiazolyl)-2,5-diphenyl-2H-tetrazolium bromide)	Sigma, www.sigmaaldrich.com, Cat. No. M2128
Myoglobin equine heart	Sigma, www.sigmaaldrich.com, Cat. No. M1882
Na-HEPES	Fluka www.sigmaaldrich.com, Cat. No. 83264
OPD tablets	Serotec, www.abdserotec.com, Cat. No. BUF046A
PBS (ELISA)	OXOID, Dulbecco A Tablets, www.oxoid.com, Cat. No. BR0014
DPBS (Cell culture)	Invitrogen / Gibco, www.invitrogen.com Cat. No. 14190
Penicillin G	Invitrogen / Gibco, www.invitrogen.com Cat. No. 15140-163
Pen/ Strep 10.000 units	Invitrogen / Gibco, www.invitrogen.com Cat. No. 15140-122
Phenol red	Sigma, www.sigmaaldrich.com, Cat. No. P3532.

Poly-D-lysine	Sigma, www.sigmaaldrich.com, Cat. No. P7890
Potassium acetate	BDH, uk.vwr.com, Cat. No. 295814P
RPMI 1640 medium	Invitrogen/Gibco, www.invitrogen.com Cat. No. 21875
Selenium	Promega, Aldrich, Cat. No. 229857
Sodium acetate	Sigma, www.sigmaaldrich.com, Cat. No. S8625
Sodium borate	Sigma, www.sigmaaldrich.com, Cat. No. S9640
Sodium chloride	BDH, uk.vwr.com, Cat. No. 153274V
Sodium hydrogen carbonate	Sigma, www.sigmaaldrich.com, Cat. No. S6014-500G
Sodium hydroxide	BDH, uk.vwr.com, Cat. No. 10524X
Sodium nitrite	Fluka, www.sigmaaldrich.com/fluka, Cat. No. 71759
Streptavidin	Promega, www.promega.com, Cat. No. Z7041
Streptomycin sulfate	Invitrogen / Gibco, www.invitrogen.com Cat. No. 11860-038
Sucrose	Sigma, www.sigmaaldrich.com, Cat. No. S1174
Sulphuric acid	BDH, uk.vwr.com, Cat. No. 102761C
TEMED (*N,N,N',N'*-Tetramethylethylenediamine)	Sigma, www.sigmaaldrich.com, Cat. No. T9281
Transferrin	Sigma, www.sigmaaldrich.com, Cat. No. 51147
Tris (hydroxymethyl) methylamine	BDH, uk.vwr.com, Cat. No. 103156X
Tween 20	Sigma, www.sigmaaldrich.com, Cat. No. P7949-500 mL
Water	Deionised obtained from a water purifier or commercial supplier.
Water (Chromanorm HPLC grade)	VWR, uk.vwr.com, Cat. No. 23596.320

Table 2.1 chemicals used and suppliers

2.1.5 Buffers and cell culture media

A list of the cell culture media and buffers used, together with their composition is shown in Table 2.2.

Azure A staining solution:	0.08 % Azure A chloride in deionised water.
BaF3 medium	RPMI 1640, 10 % (v/v) FCS, 50 μM L-glutamine, 100 U/ ml penicillin G, 50 μg/ ml streptomycin sulfate
Chondroitinase ABC digestion buffer:	0.5 M Tris acetate pH 8 with glacial acetic acid
Cover-slip fixing medium:	0.12 M Sucrose in distilled H_2O, 0.5mM $CaCl_2$, 75mM Millonig's (phosphate buffer), 2% glutaraldehyde
Cover-slip mounting buffer:	30 μl PBS for each cover slip and tap with clear nail varnish.
Cover-slip preparation: **Coating with poly lysine (PL):** **Coating with Laminin (LN):**	 Dilute 1:100 of (1 mg/ ml) in 100 mM Na borate buffer pH 8.5. Dilute 1:100 of (1 mg/ ml) in autoclaved distilled H_2O.
Desalting SEC running buffer:	Deionised water degassed for ~30 minutes with helium.
Dialysis tubing:	Tubing should be cut to convenient length and boiled for 10 minutes in 2% sodium hydrogen carbonate and 1 mM EDTA, before rinsing and boiling, or autoclaving, for 10 minutes in water. Tubing should be stored fully immersed at 4 °C in 20 % ethanol and handled with gloves.
ELISA Streptavidin buffer: **Blocking buffer for FGFs:** **Oligosaccharides, FGFs and antibodies buffer:**	0.1M sodium carbonate and 0.1M sodium hydrogen carbonate mixed until pH is 9.6. Store at 4 °C 1% (w/v) BSA in; PBS 0.05 % (v/v) Tween-20 (PBST) 1% (w/v) BSA/PBST

Substrate, orthophenylene diamine (OPD):	Solution by adding 1 tablets into 3mls de-ionised water 1.25µl 30 % hydrogen peroxide and keep in falcon wrapped in foil to dissolve for 5 minutes
Blocking buffer for Slit and Robo	3 % casein (w/v) in PBST
Oligosaccharides, Slit and Robo and antibodies buffer:	0.5 % casein (w/v) in PBST
Enzyme stock aliquots:	cABCase and heparinase enzymes should be made to appropriate stock concentrations in respective enzyme digestion buffers that have been supplemented with 0.01 % BSA and filtered using an appropriate syringe filter. The solutions should be frozen using liquid nitrogen as single use aliquots for long-term storage at -20 °C or -80 °C.
Fractionation SEC running buffer:	0.5 M ammonium hydrogen carbonate filtered and degassed for ~30 minutes with helium for 1L.
Heparinase digestion buffer:	0.1 M sodium acetate, 0.1 mM calcium acetate pH 7.0 (using glacial acetic acid) – can be stored at -20 °C prior to use.
MTT	5 mg/ ml MTT (in PBS). 10 % SDS, 0.01N HCl per well overnight at 37 °C (not necessary to incubate at 5% CO_2)
PBS	140 mM NaCl, 5 mM NaH_2PO_4, 5 mM Na_2HPO_4, PH 7.2
Sodium borate	0.1 M borate buffer (0.1 M Na_2BO_3), adjusted to pH 8.5
PAGE loading gel:	9 % acrylamide, 110 mM Tris-acetate pH 7, 21.5 % ethylene glycol, 0.05 % APS, 0.0025 % TEMED, made immediately before pouring into the gel plates.
PAGE resolving gel:	33 % acrylamide, 110 mM Tris-acetate pH 7, 21.5 % ethylene glycol. 0.03 % APS, 0.0007 % Temed made immediately before pouring into the gel plates.
PAGE loading buffer:	80 % glycerol, 20 % running buffer, phenol red.
PAGE running buffer:	30 mM Tris, 20 mM MES pH 7.5.
RPIP-HPLC buffers	A1 consists of 10 % methanol, 50 mM ammonium acetate and 10 mM dibutylamine. (450 ml Milli Q H_2O, 50 ml pure methanol, 2 g ammonium acetate, and 0.8 ml dibutylamine) A2 consists of 20 % methanol, 50 mM ammonium acetate and 10 mM dibutylamine (100 methanol, 400 ml Milli Q H_2O 2 g ammonium acetate and 0.8 ml dibutylamine).

	B consists of 90 % methanol containing 50 mM ammonium acetate and 10 mM dibutyl amine (50 ml Milli Q water, 450 ml methanol, 2 g ammonium acetate and 0.8 ml dibutylamine). Buffer A1 is usually used for shorter low sulfated HS (2-mer, 4-mer and 6-mer); Buffer A2 is usually used for larger HS fragments 8-mer and 10-mer).
Retinal ganglion culture medium **Stock medium:** **Working medium:**	➢ Hams F12 glutamax 100 ml ➢ 0.5g Methocllelulose (dissolve over night) ➢ Pen/ Strep 10.000 units 1 ml, ➢ 20 ml Hams F12 glutamax ➢ 1:100 Insulin/ Transferrin/ selenium (5 µg/ ml) (200 µl/20 ml) ➢ 1: 100 Transferrin (100 µg/ ml) 10 mg/ ml (200 µl/ 20 ml) ➢ 1:1000 300 mM Seleinum (20 µl/ 20 ml) ➢ 1: 1000 0.1 mg/ ml BSA 20 µl/20 ml
SAX chromatography solvents:	Solvent A: Milli Q H_2O adjusted to ~ pH 3.5 using 1M HPLC grade hydrochloric acid. Solvent B: 2 M HPLC grade NaCl adjusted to pH 3.5 using 1 M HPLC grade hydrochloric acid. Both solvents were filtered through a 0.2 µm filter and degassed for ~ 30 minutes /litre with helium.
SEC for heparins fractionation	0.5 M NH_4HCO_3 in Milli Q H_2O. Filtered through a 0.2 µm filter and degassed for ~ 30 minutes/litre with helium
SEC for the ternary complex studies:	20 mM Na-HEPES, 150 mM NaCl pH 7.5

Table 2.2 compositions of buffers and cell culture medium.

2.1.6 Equipment

Equipment used in this study is listed in Table 2.3.

Centrifuge	Centrifuge 5804, Eppendorf, www.eppendorf.com, Cat. No. 1T5804 000.013
Centrifugal evaporator	Speed Vac SPD121P, ThermoSavant, uk.vwr.com, Cat. No. 195-227
Cover glass	VWR, uk.vwr.com, cat no: 631-0149
Desalting column	HiPrep ™ 26/10 Desalting column (26 mm I.D x 10 cm length), GE Healthcare, www.gehealthcare.com/uken)
Dissecting microscope	Motic, K401, GDC Microscopes (Surrey, UK) www.gdcmicroscopes.com
DVC camera	Model. 1310c-FW-OO; digital images recorded using DVC view version 2.2.8 software (www.dvcco.com).

Filter syringe	Sterile Minisart® 0.2µm CE, Sartorius stedim biotech, www.sartorius-stedim.com, Cat. No. 16534.
Filter Bottle top	Polysulfone Nalgene®, uk.vwr.com, Cat. No. 516-0578 with 0.2 µm, 47 mm I.D. cellulose acetate membrane filters, Nalge Nunc, Fisher Scientific, extranet.fisher.co.uk, Cat. No. 13TFDM-309-100Q.
Fraction collector	Frac-100, GE Healthcare, www.gehealthcare.com/uken
Freeze dryer	Heto PowerDry PL3000, www.thermo.com with pump
Gel electrophoresis system	Mini-PROTEAN tetra cell system, Bio-Rad, www.bio-rad.com) and power pack, EPS 601, GE Healthcare, www.gehealthcare.com/uken
Helium cylinder	BOC, www.boc-gases.com
Heat block	Grant www.grant.co.uk Cat. No. QBT2
HPLC-RPIP	Dionex consisted of a 580A pump, UVD 170S variable-wavelength detector, and an online DG-2410 degasser.
HPLC-SAX	Shimadzu HPLC with SCL-10A controller, LC-10AT pump, SPD-10 UV detector, FCV-10AL mixer, CS16150 vacuum degasser, CTO-10 AS column oven and Class-VP chromatography data system
Incubator	CO2 Incubator Model: MCO175, Sanyo, Japan
Injection syringe	1 ml Hamilton, VWR, uk.vwr.com, Cat. No. 613-1166
Inverted microscope	Zeiss Axiovert-25 Microscope, www.zeiss.co.uk
Laminar flow hood II	HERA Safe, Heraeus, Germany
Low pressure chromatography (FPLC)	An AKTA purifier 10 (GE Healthcare) with (e.g. P-900, UV-900, INV-907 and PV-908, M-925 modules), along with an automated fraction collector (e.g. FRAC 950), and UNICORN system control, data acquisition and analysis software
Microcentrifuge	Eppendorf minispin, www.eppendorf.co.uk
NuPAGE® Novex Bis-Tris Gels	Invitrogen, www.invitrogen.com NP0342BOX
PH meter	Jenway, Cat. No. 3505
Plates:	
96 wells Maxisorp:	Nunc, uk.vwr.com, Cat. No. 735-0083
96 conical-bottom wells:	Nunc, uk.vwr.com, Cat. No. 732-0191
4 wells plate:	Nunc, uk.vwr.com, Cat. No. 734-2176
Corning® 96 wells TC:	Corning, www.corning.com, Cat. No. 3595

Plate reader	Thermo MultiSKAN EX
Quartz cuvette	Hellma, www.hellma.co.uk
Rocker	Grant, BOEKEL, BFR25,
Roller Mixer	SRT1, Stuart Scientific, www.stuart-equipment.com
Rotator,	SB2, Stuart Scientific www.stuart-equipment.com
Rotary evaporator	Laborota 4000 eco Basic1, uk.vwr.com, Cat. No. 531-3717
Rotatest Shaker	Model R100, Lukham, England
RPIP-HPLC columns	C18 column (4.6 x 50 mm, 5 µm particle size, Supelco) C4 column (25 mm x 4.6 mm, 5 µm particle size, Supelco)
SAX HPLC columns	Propac PA1 column, Dionex, www.dionex.com, Analytical 4 mm I.D x 250 mm length: P/N 039658, or Semi-preparative column 9 mm I.D. x 250 mm length: P/N 040137.
Scissors (dissecting)	Agar Scientific, T5321, www.agarscientific.com
SEC column	➢ Superdex™ peptide PE 7.5/300 column (7.5 mm I.D. x 300 mm length), Cat. No. 17-5003-01 ➢ Superdex ™ 30 prep grade media, catalogue number: 17-0905-03 ➢ XK 16/100 columns (16 mm I.D. x 100 mm length), catalogue number: 18-8776-01 ➢ Superdex ™ 75 (10 / 300GL), Cat. No. 17-5174-014 GE healthcare, www.gehealthcare.com
Spectrophotometer	Shimadzu UV-1601, www.shimadzu.co.uk
Stirrer	IKA® RH basic KT/c
Tubes:	➢ 1.5 ml tubes from SARSTEDT, (autoclaved) (www.sarstedt.com, Germany) ➢ 5ml and 20 ml aseptic universal tubes from Sterilin Ltd (www.sterilin.co.uk, UK)
Tweezers, Dumont 5	Agar Scientific, T5390, www.agarscientific.com
Vortex	VWR, uk.vwr.com, Galaxy mini
Water bath	Grant JB Series, www.grant.co.uk
Water purifier	Elga Maxima water purifier, www.elgaprocesswater.co.uk
Xcell Surelock **Mini-cell**	Invitrogen, www.invitrogen.com Cat. No. EI0001

Table 2.3 Equipment used and suppliers.

2.2 Methods

2.2.1 Preparation of chemically modified heparins

Porcine mucosal heparin (PMH) was the starting material for all eight chemically modified heparins used in this study. Chemically modified heparins were prepared by Dr. Yates according to the procedure described in (Yates *et al.*, 1996) and were characterized by NMR techniques. Figure 1.8 outlines the predominant disaccharide components for each of the eight chemically modified heparins.

2.2.2 Extra purification of porcine mucosal heparan sulfate (PMHS) starting materials

One gram of porcine mucosal heparan sulfate (PMHS) powder was dissolved in 100 mM Tris acetate buffer pH 8 [chondroitin ABCase (cABCase) buffer] at 20 mg/ ml. cABCase was added at one mIU per mg of PMHS and incubated in a water bath overnight at 37 °C. The digestion was monitored by change in UV absorbance at λ_{abs} = 232 nm. The reaction was terminated by heating for two minutes at 100 °C, to denature the enzyme.

The reaction mixture was then transferred into dialysis tubing (molecular weight cut off 7000 Dalton) of sufficient length for at least a doubling in volume. Dialysis was carried out against a 20-fold excess of water for four days; water was changed each day. The solution was then concentrated using a rotor evaporator. The dried sample was reconstituted in 20 ml Milli Q H_2O and divided into four separate universal tubes (5 ml in each), followed by addition of 15 ml of ethanol to each tube. In addition, potassium acetate was added to each tube at 1.3 % (w/v) in order to aid ethanol precipitation. The tubes were stored at -20 °C for three to four hours before centrifugation at 2500-x g for 10 min at room temperature. The supernatants were carefully aspirated. The last step was repeated four to five times and finally the purified PMHS was re-suspended in Milli Q H_2O, lyophilized, and stored at -20 °C. The recovery was ~ 85-90 % of the start material.

2.2.3 Partial digestion of PMHS, heparin and chemically modified heparins

2.2.3.1 Enzyme partial digestion

Prior to large-scale enzymatic partial digestion, a small-scale trial digestion was conducted to determine a suitable type of heparinase, amount of enzyme and time needed for successful partial digestion. This trial partial digestion was analysed by monitoring the extent of digestion at periodic time points during the partial digestion or using small scale SEC or PAGE with Azure A staining (Turnbull and Gallagher, 1988; Vives *et al.*, 2001). Bulk enzyme partial digestions were carried out in 100 mM Na acetate, 0.1 mM Ca acetate (pH 7.0) buffer at 37 °C and all reactions were stopped by boiling for 2 min. Digests with multiple time points were pooled at the end of the partial digestion process. About 100 mg PMH was digested with heparinase I at 1 mU/ mg (57 mU/ ml) for 3, 4 and 5 hours; 100 mg BLH digested with heparinase I at 1 mU/ mg (33 mU/ ml) for 4, 6 and 8 hours.

In addition, 10 mg of the 2-O-desulfated heparin was partially digested with heparinase II at 5 mU/ mg (5 mU/ ml) for 6 and 8 hours. 10 mg 6-O-desulfated heparin digested with heparinase II at 5mU/ mg (5 mU/ ml) for 1 and 2 hours. 10 mg 2, 6-O-desulfated heparin digested with heparinase II at 5 mU/ mg (5 mU/ ml for 16 hours; 10 mg N-acetyl heparin digested with heparinase II 5 mU/ mg (5 mU/ ml) for 6 hours. Furthermore, 413 mg PMHS was digested with of heparinase III 0.1 mU/ mg (5 mU/ ml) for two hours, 10 mU heparinase III was added and incubated for 24 hours then a further 10 mU was added for two hours. All enzymatic partial digested saccharides were lyophilized and kept at -20 °C for further uses.

2.2.3.2 Nitrous acid partial digestion

Prior to large-scale nitrous acid partial digestion, a small-scale trial digestion was conducted to determine suitable time points for successful partial digestion. The trial partial digest was analysed by PAGE with Azure A staining (Turnbull and Gallagher, 1988; Vives *et al.*, 2001).

The bulk nitrous acid partial digestion was conducted as follow: freshly made 0.5 M sodium nitrite in Milli Q H_2O was added to an equal volume of 0.5 M HCl. The reaction mixture was kept on ice; this reaction gave 0.25 M nitrous acid (pH ~ 2.0). After partial digestion, samples were neutralized by the addition of 1:10 volume of 1 M $NaHCO_3$ solution to bring the pH up to 6-7. The pH of the solution was tested to ensure that the reaction had stopped. For heparin, solution at 100 mg/ ml was diluted with the newly generated nitrous acid at room temperature. Aliquots were taken at different time points, (10, 20, 30 and 40 minutes) from the reaction mixture. Chemically modified heparins (2-de-O-sulfate, 6-de-O-sulfate and 2,6-de-O-sulfate) were nitrous acid digested as follow: newly made 0.04 M sodium nitrite in Milli Q H_2O was added to an equal volume of 0.04 M HCl. The reaction mixture was kept on ice; this reaction gives 0.02 M nitrous acid. Heparin solution at 12.5 mg/ ml was diluted with the newly generated nitrous acid at room temperature. Aliquots were taken at different time points, (20, 45 and 90 minutes) from the reaction mixture all the nitrous acid partially digested fractions were stored at -20 °C.

2.2.4 Oligosaccharides separation by polyacrylamide gel electrophoresis (PAGE)

A mixture of the enzyme or nitrous acid partial digest saccharides and size separated oligosaccharide fractions were analysed using polyacrylamide gel electrophoresis (PAGE) (Turnbull and Gallagher, 1988). Samples were diluted in sample buffer (70 % glycerol/ 30 % running buffer) with 10 % phenol red added. Samples were loaded into the wells using gel loading tips and then electrophoresis initially through a 1.5 cm loading gel (7.5 % acrylamide) at a constant voltage of 200 V for one hour. Followed by, electrophoresis through a resolving gel at constant voltage of 110 V for 16 hours, until the phenol red marker migrated ~ 2/3 of the way down the gel.

The running buffer used was 30 mM Tris, 20 mM MES (pH 8.0). After electrophoresis, oligosaccharide bands were visualised by staining with 0.08 % aqueous Azure A for 10 min under constant agitation (Turnbull and Gallagher, 1988; Turnbull *et al.*, 1999). Excess dye was removed by washing the gel several times in

deionised water. The gel image was recorded using DVC camera and software (www.dvcco.com).

2.2.5 Size separation

2.2.5.1 Size-exclusion chromatography (SEC)

The lyophilized partially digested samples were re-suspended in Milli Q H_2O at 100 mg/ ml for PMH and BLH, 50 mg/ ml for PMHS and 10 mg/ ml for chemically modified heparins. The 5ml injection loop of the AKTA purifier 10 (GE Healthcare) was loaded with 1 ml of sample using a Hamilton syringe, after ensuring that the sample was free of air bubbles. This volume was less than 1 % of column volume for ideal separation and less than 50 % of the loop volume for minimum sample loss. The flow rate was set at 0.5 ml/ min with 0.5 M ammonium hydrogen carbonate (isocratic buffer) for the Superdex ™ 30 and the elevated flow was started after injecting the sample; the elution was monitored at λ_{abs} = 232 nm for the enzyme digested saccharides and at λ_{abs} = 215nm for the nitrous acid generated saccharides. Fractions of 1 ml were collected (sample elution typically occurs between 300 and 700 minutes of elution time equivalent to 150-350 ml of elution buffer). Fractions were pooled individually according to the selected partially resolved SEC peaks. The pooled fractions were then concentrated by lyophilisation and stored at -20 °C ready for desalting (Feyzi *et al.*, 1997b).

2.2.5.2 Desalting SEC fractions

The lyophilised pooled fractions were re-suspended in 1–2.5 ml of Milli Q H_2O, loaded into the 5 ml injection loop of the AKTA purifier 10, using a suitable Hamilton syringe, ensuring that the sample was free of air bubbles. The fraction pool was less than 1 % of column volume and less than 50 % of loop. The flow rate was set at 5 ml/ min buffer through the HiPrep ™ 26/ 10 desalting column (packed with Sephadex G-25 fine). The programme was started by injecting the sample into the injection loop and monitoring the elution at λ_{abs} = 232 nm and at λ_{abs} = 215nm.

The fraction collector was set up to collect 2 ml fractions immediately after eluting the loop with 5 ml of Milli Q H_2O. The fractions corresponding to the oligosaccharide peak (which eluted first) were pooled together, after ensuring that the salt peak (which eluted later) did not overlap with the saccharide peak. Volatile ammonium hydrogen carbonate (SEC buffer) was also removed by serial cycles of lyophilisation. Pooled SEC fractions were frozen at -80 °C, or by dipping into liquid nitrogen. Frozen samples were freeze-dried until the samples were dry powder. The samples were then re-suspended in Milli Q H_2O, frozen and lyophilized; this lyophilisation cycle was repeated twice, giving a total of three cycles of lyophilisation; however, in some cases an additional fourth cycle of lyophilisation was employed dependent on individual sample needs (Goodger *et al.*, 2008).

2.2.6 Quantification of oligosaccharide fractions

Fraction pools were re-suspended in a known volume of water. The fraction absorbance was recorded at λ_{abs} = 232 nm using a quartz cuvette and spectrophotometer (Shimadzu). The volume of the solution was adjusted until λ_{abs} = 232 nm was in the linear range of the spectrophotometer (e.g. 0-1 absorbance units). The molar concentration of the oligosaccharides present in the solution was then determined using the Beer-Lambert law with an extinction coefficient of 5500 mol^{-1} cm^{-1} for the unsaturated bond chromophore generated by heparinase enzymes (Linhardt *et al.*, 1988). In addition, weighing was also performed where larger amounts of oligosaccharides were available (≥ 1 mg). Briefly, an empty 1.5 ml Eppendorf tube was weighed three times on a sensitive balance (accurate to 0.1 mg).

Oligosaccharide sample were re-suspended in 1 ml and added to the empty tube. The oligosaccharide sample was lyophilised and the total tube weight recorded three times post-lyophilisation. The average weight reading of the empty tube was subtracted from the average weight of the tube post lyophilisation. This method was particularly useful for nitrous acid partial digested oligosaccharides due to their low sensitivity of detection, also their lack of a strong chromophore.

2.2.7 Oligosaccharide size validation

A new method was developed for oligosaccharides size validation. This technique is based on the change in absorbance at λ_{abs}= 232 nm on complete digestion of a known amount of sample with a mixture heparinases I, II and III. The Δ 4, 5-uronate double bond extinction coefficient was used to calculate the ratio of moles of double bond before and after digestion to specify the number of disaccharides present in the oligosaccharide fraction. The method in brief, is based on the unsaturated disaccharide extinction coefficient (5500 $M^{-1}cm^{-1}$), and Beer's law (A=Ecl), where 1.8 nmoles of double bond gives 0.1 units of absorbance in a 100 µl volume. Thus, 10 µl of the unknown fraction was taken into 100 µl Milli Q H_2O, the absorbance was read at λ_{abs}= 232 nm and the concentration at mol/l was calculated and number of nmol in 100 µl was obtained. A volume equivalent to 1.8 nmol was taken from this sample into a new tube, 20 µl of lyase enzyme buffer (500 mM Na acetate, 0.5 mM Ca acetate, pH 7.0) was added and the volume made up to 100 µl with Milli Q H_2O (this mixture should read 0.1 absorbance λ_{abs}= 232 nm).

For the blank, 20 µl of lyase enzyme buffer (500 mM Na acetate, 0.5 mM Ca acetate, pH 7.0) was added to 80 µl Milli Q H_2O. Each of the heparinase I, II and III (0.25 mU each) were added to the sample and blank and incubated overnight at 37 °C. The final absorbance was then read the following day; a reading of 0.1 indicates a disaccharide sample, whereas an increase of 0.1, defines a 4-mer, and so on. This method can be used for both enzyme and nitrous acid digested fractions (though in the latter case the starting concentration must be estimated by weight).

Oligosaccharide size assignments were also confirmed (without absorbance) by electrospary mass spectrometry (ES-MS) with assistance of Dr. Atrih and Miss Miller; see appendices.

2.2.8 Charges separation

2.2.8.1 Strong anion exchange high performance liquid chromatography (SAX-HPLC)

The desalted SEC fraction pools were further fractionated on the basis of their charge using strong anion exchange (SAX) chromatography, performed on Shimadzu SCL-10AVP system equipped with a Propac-PA1 column, (9 x 250 mm, Dionex); (Turnbull *et al.*, 1999). The samples were re-suspended in Milli Q H_2O at a concentration of 10 mg/ ml. An analytical trail run (~50-100 µg) was performed in order to establish where fraction collector racks should be changed, followed by preparative fractionation. Briefly, tubes were placed in adequate fraction collector racks sufficient for the whole duration of the elution gradient i.e. 180 minutes. About 5 µl of 0.1 M ammonium hydrogen carbonate was added to each tube, this amount being sufficient to neutralise 0.25 ml of elution solvent (pH 3.5). Sample (maximum 5 mg) was made up to a final volume of 0.5 ml in Milli Q H_2O and injected into the pre-washed 1 ml injection loop using Hamilton syringe. The column was pre-washed for 10 min with 2 M sodium chloride in water, pH 3.5 (solvent B) at 1 ml/ min flow rate and then equilibrated with Milli Q H_2O, pH 3.5 (solvent A) for 10 min at the same flow rate. The flow was isocratic in Milli Q H_2O (pH 3.5) for 1 min at flow rate 1 ml/ min for sample loading onto the column.

Samples were eluted with a linear gradient of 0-50 % solvent B (0-1 M NaCl) over 180 min, except for heparin where the gradient used was 0-1.8 M over 180 min. The flow rate was 1 ml/ min. The column temperature was set at 40 °C using column oven. Detection was performed online using a UV detector set at λ_{abs} = 232 nm. Fractions were collected at 15 second intervals (0.25 ml volume) using a fraction collector calibrated at 1 ml/ ml flow rate and fraction collector racks changed at suitable time points where peak elution was absent.

The column was washed after the run by increasing the sodium chloride gradient concentration from 1 M to 2 M for 30 min and re-equilibrated with Milli Q H_2O (pH 3.5) for 10 minutes. Fractions corresponding to the partially resolved SAX peaks were pooled into a suitable tube, after considering the calculated delay time between the UV detector and fraction collector. The pooled fractions were concentrated by lyophilisation and stored at -20 °C for further use (Guimond and Turnbull, 1999).

2.2.8.2 **Desalting of SAX-HPLC fractions**

The lyophilised pooled fractions were re-suspended in a suitable volume of Milli Q H_2O, and loaded into the injection loop of the AKTA purifier 10, using a suitable syringe and ensuring that the sample was free of air bubbles. The fraction pool volume was less than 1 % of column volume and less than 50 % of loop volume. The flow rate was 5 ml/ min. Two desalting columns (HiPrep™ 26/10, packed with Sephadex G-25 fine) were connected in series. The columns were equilibrated by flushing through with Milli Q H_2O for 20 minutes at flow rate 5 ml/ min. The programme was started by injecting the sample into the injection loop. The separation of oligosaccharides from sodium chloride was achieved using isocratic Milli Q H_2O at a flow rate of 5 ml/ min using online UV detection at 215nm and 232 nm over period of ~ 40 min. Fractions of 2 ml were collected throughout the run using a fraction collector. The salt peak eluted after ~ 15 min. The fractions corresponding to the saccharide peak (which elutes first) were pooled together, after ensuring that the salt peak did not overlap with the saccharide peak.

2.2.9 Compositional analysis of HS, heparin and chemically modified heparins

The structural composition of each of the chemically modified heparins and the parent heparin were confirmed by complete heparinase (Zuck *et al.*, 1992) digestion. The resultant data were confirmed by SAX-HPLC against known disaccharides standards. In brief, about 20 µg of sample was added to 20 µl of 5x lyase enzyme buffer (500 mM Na acetate, 0.5 mM Ca acetate, pH 7.0).

The volume was made up to 97 µl with Milli Q H_2O, followed by addition of 1 µl (0.25 mU) of each of the heparinase enzymes (I, II and III) and incubation overnight at 37 °C. Samples were heated to 100 °C for 2 min to terminate enzyme action. Milli Q H_2O (100 µl) was added to the sample. Digested samples were then analyzed using SAX HPLC as described in section 2.2.8.1 but using a linear gradient 0-1 M NaCl over 0-45 minutes. SAX elution was monitored by absorbance at λ_{abs}= 232 nm. Disaccharide components were identified by comparison to known disaccharide standards eluted under the same conditions.

2.2.10 Biotinylation

Heparin 10-mer oligosaccharide generated by nitrous acid partial digestion was biotinylated at the reducing end. The lyophilised 10-mer heparin was dissolved in Milli Q H_2O (pH 5.0) at 10 mg/ ml. A five-fold excess of 2.5 mM aminoxybiotin [(N-(aminooxyacetyl)-N'-(D- biotinoyl) hydrazine, trifluoroacetic acid salt (ARP)] was added, and the reaction mixture was incubated for a minimum of 16 hours at 50 °C. Sequential runs over a 0.5 ml DEAE-Sephacel column were used to purify the biotinylated 10-mer heparin oligosaccharide. The DEAE column was equilibrated with 50 mM NaCl/ 10 mM phosphate buffer (pH 7.0). Following a comprehensive wash with the PBS to remove un-reacted biotin (~ 50 column volums), the bound oligosaccharides were eluted with 1 ml of 2 M NaCl. The absorbance of eluted fractions was monitored at λ = 232 nm using a spectrophotometer. Selected fractions were pooled and desalted using a HiPrep™ desalting column 26/10 (as described in section 2.2.5.2). The desalted biotin-10-mer heparin was lyophilised, quantified and stored at -80 °C for furthermore. PAGE and dot blot were used to assess the success of the biotinylation.

2.2.10.1 Detection of 10-mer heparin-biotin by dot blot

A dot blot technique was used to confirm the biotinylation of the nitrous acid digested 10-mer heparin oligosaccharides. Samples with different biotinylation conditions and control (immunoassayed biotinylated heparin 10-mer) were detected by dot blot.

Briefly, 1 µl of 10-mer heparin-biotin at concentration 10 mg/ ml were spotted onto nitrocellulose membrane (Hybond-ECL nitrocellulose membrane, GE Healthcare). Circles were drawn around each spot; the nitrocellulose membrane was set aside to dry for 30 minutes at room temperature and then blocked with 5 % (w/v) BSA/ PBST for one hour. Anti-biotin-HRP (Cell Signalling) was added to the membrane and incubated at room temperature for one hour. Membrane was washed four times (10 min each) with PBST; after the fourth wash, the membrane was incubated with ECL reagents (GE Healthcare) for 5 minutes. The membrane was covered with cling film, after ensuring that excess ECL buffer was removed. In the dark room, the membrane was exposed to ECL film (Hyperfilm-ECL, GE Healthcare) for 5 minutes, then transferred to a developer tray for 2 minutes, fixer for 2 minutes and finally washed with water and air-dried.

2.2.11 Enzyme-linked immunosorbant assay (ELISA)

2.2.11.1 Competition ELISA

Competition ELISA was used to study protein interactions with heparin chains and oligosaccharides. In brief, 3 mg/ ml streptavidin in 0.1M Na_2CO_3/ $NaHCO_3$ was incubated for 16 hours at 4 °C in Maxisorp 96-well microtiter plates (Nunc Maxisorp) (Powell *et al.*, 2002). Plates were blocked with 1 % (w/v) BSA in PBS for 2 hours at room temperature; washed with PBS 0.05 % (v/v) Tween 20 (Sigma) (PBST), and then incubated with biotinylated 10-mer heparin in 1 % (w/v) BSA/ PBST for 2 hours at room temperature. Plates were then washed five times with PBST, and a constant concentration of protein was incubated with variable concentrations of soluble competitors in 1 % (w/v) BSA / PBST at 4 °C for 16 hours for binding to reach equilibrium (for saccharide dose response experiments). Concerning the protein oligosaccharide size required, a constant concentration of the oligosaccharide was incubated with a constant concentration of protein. Following the overnight incubation at 4 °C, the plate was washed in PBST, and then primary antibody diluted in 1 % (w/v) BSA / PBST was added to the plates and incubated for 1 hour at room temperature.

The plates were then washed in PBST and incubated with secondary antibody-horseradish peroxidise conjugates diluted in 1 % (w/v) BSA/ PBST for 1 hour at room temperature. After washing in PBST the plate was developed with the substrate (100 µl of O-phenylenediamine (OPD) solution to each well, prepared according to the manufacturer's instructions), the reaction was then stopped by adding 100 µl to each well of 0.5 M sulphuric acid. The absorbance values (at λ_{abs} = 492 nm) were measured using a microtiter plate reader (Powell *et al.*, 2002).

2.2.11.2 **Direct ELISA**

Direct ELISA was used as a screening method for ternary complex formation as described previously (Hussain *et al.*, 2006). Briefly, Slit D1-4 was diluted in 0.1 M Na_2CO_3/ $NaHCO_3$ (pH 9.6) and was added at 5 µg/ ml into 96-well microtiter plates (Nunc Maxisorp), incubated for 16 hours at 4 °C. The plate was washed with PBS and blocked with 3% (w/v) casein in PBST for 2 hours at room temperature. The plate was washed five times with PBST. Serial dilutions of Robo IG1-5 Fc protein in 0.5 % (w/v) casein in PBST were prepared. The start concentration was 100 µg/ ml and then 1:10 dilutions down to 100 pg/ ml were prepared. Heparin, chemically modified heparins and 2-20-mer heparin oligosaccharides were added to Robo IG1-5 Fc at 10 µg/ ml. Goat anti-human IgG-HRP conjugate (Pierce) diluted at 1:5000 in 0.5 % (w/v) casein in PBST was added to each well and incubated for 1 hour at room temperature. Freshly made orthophenylenediamine solution was added into the wells at 100 µl to each well. The reaction was then stopped by adding 100 µl of 0.5 M sulphuric acid. The absorbance values (at λ_{abs} =492 nm) were measured using a microtiter plate reader.

2.2.12 Analytical SEC

Analytical SEC chromatography (Superdex™ 75) was used to measure peak shifts due to the formation of a ternary complex of isolated 10 µM Drosophila Slit D2, 10 µM Robo IG1–2 and 10 µM heparin, chemically modified heparins or 10 µM oligosaccharides.

The column was calibrated with protein standards (Insulin, Cytochrome c, Myoglobin, Carbonic Anhydrase, and Albumin with molecular weight of 5.7, 12.4, 17.6, 29.0 and 66.0 KDa respectively). Samples were mixed in a 1:1:1 ratio and incubated for 30 min at room temperature and then were made up to 100 µl in 20 mM Na-HEPES 150 mM NaCl, pH 7.5. The 1 ml injection loop of the AKTA purifier 10 (GE Healthcare) was loaded with 100 µl of samples volume using a Hamilton syringe, after ensuring that the sample was free of air bubbles. This volume was less than 1 % of column volume and less than 50 % of the loop volume. The flow rate was set at 0.5 ml/ min with 20 mM Na-HEPES 150 mM NaCl pH 7.5 buffer for the Superdex ™ 75 column (10 x 300 mm) and the programme was started after injecting the sample; elution was monitored at λ_{abs}= 280 nm , and fractions of 0.5 ml were collected (sample elution typically occurs between 18 and 26 minutes).

2.2.13 Sodium dodecyl sulfate polyacrylamide gel electrophoresis (SDS-PAGE)

SDS-PAGE was used to evaluate analytical SEC fractions of Slit/ Robo/ HS complexes. The system used was XCell Surelock Mini-cell system (Invitrogen). In brief, 10 µl of the sample was prepared by heating at 70 °C for 10 min in the presence of 5 µl GE LDS sample buffer (4x), 2 µl GE Reducing agent (10x) and 3 µl Milli Q H_2O. The running buffer was made by adding 25 ml of 20X NuPAGE® MES to 475 ml of Milli Q H_2O, and loaded into the Mini-cell tank. The upper buffer chamber was filled with 200 ml 1X NuPAGE® SDS running buffer; 500 µl of antioxidant (NuPAGE®) was added. The lower chamber was filled with 300 ml of 1X NuPAGE. Samples (15 µl) were loaded into the wells of a NuPAGE® Novex 12% Bis-Tris gel. The gel was run for 40 min at a constant voltage of 200 V.

2.2.14 Growth cone collapse assays

Growth cone collapse assays were used to explore the collapse promoting activity of Slit proteins on retina growth cones (Kapfhammer *et al.*, 2007; Piper *et al.*, 2006). Changes in the morphology of the growth cones were observed and counted in blind conditions as described previously (Hussain *et al.*, 2006; Kapfhammer *et al.*, 2007; Piper *et al.*, 2006). The percentage of collapsed growth cones against spread growth cones was determined. The procedure was divided into stages: preparing the cover-slips, dissecting and culturing the retina cells, adding the Slit protein ± (heparinase and heparins), followed by fixing, mounting onto glass slides and finally counting.

2.2.14.1 **Preparations of cover-slips**

Cover-slips were sterilized by oven heat and then coated with poly-L-lysine (PL). PL (1 mg/ ml) was diluted 1:100 in 100 mM Na borate buffer pH 8.3; 70 µl was enough to coat two cover-slips, and was added to the first cover-slip, and then a second cover-slip was overlaid on top of the first cover-slip, and incubated for 1 hr. After incubation, the cover-slips were washed by dipping twice into HBSS medium. Following the PL coating, the cover-slips were coated with laminin (LN). LN (1 mg/ ml) was diluted 1:100 in autoclaved distilled H_2O. A glass plate covered with parafilm, washed with 70 % ethanol, and then with distilled H_2O was prepared.

The PL coated side of the cover-slips were placed on the 30 µl of the LN pipette onto the Parafilm surface. The cover-slips were incubated for 1hr in a Laminar flow hood II at room temperature and then washed by dipping into HBSS. They were then placed into a 4-wells cell culture plate (Nunc) with their coated side facing up. Each well was covered with 0.5 ml of retina culture medium (see Table 2.2). The plates were incubated at 37 °C ready for retina cell culture.

2.2.14.2 **Dissection of E7 chick eye**

The dissecting step was started by removing the whole eye from E7 chick embryos and then placing in Hans's medium. All the subsequent steps were performed in Hans's medium and under sterile conditions. Incubating the eye for 5 minutes at 37 °C also helps in the dissection step. The dissection of the chick retina was started by removal of the connective tissues (the whitish layer surrounding the eye), and followed by removing the retinal pigmented epithelium (RPE) (the dark brown or black layer) from the eye. The lens was removed by cutting around the lens, taking away the lens with vitreous humor (gelatinous ball). The retina was peeled off the RPE and any other attached tissues. It was observed that the retina began to curl after several minutes in Hans's medium. The retina pieces were transferred into fresh medium. Dissecting scissors were used to cut the retina into pieces of the required size (~ 1 mm x 1 mm).

2.2.14.3 **Retina cell culture**

Retinal pieces were transferred to the cover-slips in a four well plate (3-4 pieces on each cover slip) and incubated at 37 °C for 24 hours. Cover-slips were then checked for the growth of well-defined growth cones by microscopy using an inverted microscope. To test the effect of the hSlit2 protein on the chick retina growth cones, 200 µl of the retina culture medium was replaced with 200 µl of hSlit-2 conditioned medium (hSlit-2-CM); the medium was well mixed by pipetting gently up and down on the well side 2-3 times and then incubated for 20 minute at 37 °C. The growth cone collapse rescue experiments were performed by adding heparin or chemically modified heparins with hSlit-2-CM at 200 µg/ ml, following pre-treatment of the culture with heparinase (I, II and III at 2.5 mU) for three hours. Bright field microscopy was used to read the slides and to count collapsed growth cones versus normal growth cones.

2.2.14.4 **Fixing axons onto cover-slips**

Cover-slips were fixed by gently adding 250 µl of fixing medium (**see** Table 2.2) on one side of the well (so as not to disturb the growth cone) and incubation for 30 min at room temperature.

2.2.14.5 **Mounting onto glass slide**

Cover-slips were lifted up off the wells and washed twice with distilled water, air dried at room temperature and mounted on a glass slide (two cover-slips per slide). PBS was found to be the best mounting solution; as many other commercially available mounting solutions were tested but failed, due to the problem of air bubbles under the cover-slips, making it difficult to properly access the morphology of the growth cones. The cover slip was sealed around the edges using clear nail varnish.

2.2.15 BaF3 bioassay of FGF signalling

Lymphoblastoid cell line (BaF3 cells) was used as a bioassay for studying fibroblast growth factor signalling. BaF3 cells lack both endogenous HS and fibroblast growth factor receptor, and normally require addition of IL-3 for survival and growth (Guimond and Turnbull, 1999; Venkataraman *et al.*, 1996). BaF3 cells transfected with FGFR1c were maintained in RPMI 1640 growth medium supplemented with 10 % (v/v) foetal calf serum, 1 mM L-glutamine, 1 mM penicillin G, 1 mM streptomycin, and 1 ng/ ml rmIL 3 (R & D systems). Cells were routinely maintained at a density of 5 x 10^4 - 1 x 10^6 cells/ ml at 37 °C in 5 % CO_2.

For testing of growth factor responses 1 nM of rhFGF1 or rhFGF2 (R&D Systems) were used, in the presence of 10 µg–1 ng/ ml of PMH (Celsus Laboratories) or selected 8-mer PMHS (3 µg/ ml) saccharides, prepared in RPMI growth medium. The cells were added to a final density of 10^4 -10^5 cells/ ml in medium without IL-3 and incubated at 37 °C in 5 % CO_2 for 72 hours. Cells growth was assessed by measuring viable cells using 3-[4, 5-dimethylthiazol- 2-yl]-2, 5-diphenyltetrazolium bromide (MTT).

About 5-10 µl of the MTT (5 mg/ ml in PBS) was added to each well and incubated for four hours at 37 °C in 5 % CO_2 before solubilisation by the addition of 10 % (w/v) SDS /0.01 M HCl for 16 hours. The absorbance at λ_{abs} = 570 nm values were measured using a microtiter plate reader (Thermo). As a positive control, the cells were incubated as above in growth medium containing 1 ng/ ml rmIL-3; in negative controls medium alone was used. Controls for growth factor alone or heparin alone were also performed, and assays were carried out in triplicate (Guimond and Turnbull, 1999; Venkataraman *et al.*, 1996).

2.2.15.1 **RPIP and RP HPLC conditions for saccharide separation**

(In collaboration with Dr. Atrih)

Reverse phase ion-pairing (RPIP) HPLC was performed as follows, for separation of phenylsemicarbazide (PSC) tagged saccharides. Samples were diluted in 400 µl loading buffer (5 % methanol containing 10 mM dibutylamine and 50 mM ammonium acetate, adjusted to pH 7.0 with acetic acid) and injected onto a C18 column (4.6 x 50 mm, 5 µm particle size, Supelco) without a guard column. Elution buffers were A: 5 % methanol or 20 % methanol, B: 90 % methanol, both containing 10 mM dibutylamine and 50 mM ammonium acetate (pH 7.0 with acetic acid). The column was equilibrated in buffer A (5 % methanol, when separating 2-mers and 4-mers or 20 % methanol when separating 6-mers or larger oligosaccharides) at a flow rate of 0.7 ml/ min for 30 min prior to sample injection.

The elution was carried out using a linear gradient (0-100 % buffer B over 300 min) at a constant flow rate of 0.7 ml/ min. Phenylsemicarbazide derivatized oligosaccharides, which are detected at both 232 nm and 242 nm were manually collected and dried. The presence of the tag was checked by ESI-MS and the derivatized saccharides were further purified by Reverse phase (RP)-HPLC on a C4 column (25 mm x 4.6 mm, 5 µm particle sizes, Supelco). In this second purification, buffer A consisted of 5 mM ammonium acetate (pH, 7.0) and buffer B contained 5 mM ammonium acetate containing 90 % methanol (pH, 7.0). Elution was achieved using a linear gradient of 0-100 % B over 200 min.

3 Chapter three: Production of HS oligosaccharide libraries for use in structure-function studies

3.1 Introduction

In this investigation, oligosaccharide libraries were produced from tissue-derived heparin, chemically modified heparins and HS polysaccharide chains. This was achieved by an enzymatic and a chemical partial digestion, and then separation based on their hydrodynamic volume, (dictated by the number and identities of the constituent disaccharide units) and by charge (which is dependent on the quantity of O and N sulfates groups). The techniques used for separation were size-exclusion chromatography (SEC) followed by strong anion exchange (SAX-HPLC) (Powell *et al.*, 2010).

Tissue derived heparin, chemically modified heparins and HS oligosaccharide libraries cover a broad level of structural diversity not readily available in synthetic oligosaccharides. Oligosaccharides generated by partial enzymatic digestion can be exploited in finding out the minimum length of saccharides that interact with a particular protein. Furthermore, they can also be used to investigate the type of sulfates required for particular interactions (Ostrovsky *et al.*, 2002; Robinson *et al.*, 2005; Hussain *et al.*, 2006; Goodger *et al.*, 2008). In addition, purified oligosaccharides can be used in co-crystallography studies of HS-protein interaction (Pellegrini *et al.*, 2000; Schlessinger *et al.*, 2000). Chemically partially digested oligosaccharides also have a reactive reducing end, which is useful for immobilization of oligosaccharides on surfaces (such as ELISA assays) in order to study saccharide protein interactions. Oligosaccharides generated in this study have been used to explore the selectivity and specificity of HS-protein interactions.

3.1.1 Methods for HS/ heparin oligosaccharides production

3.1.1.1 Partial digestion

Digestion of heparin, chemically modified heparin and HS chains can be accomplished via enzymatic and chemical methods that cut at specific glycosidic linkages within the chain to produce mixtures of structurally diverse oligosaccharides of different (even-numbered) lengths (Bohmer *et al.*, 1990; Linhardt *et al.*, 1990; Shively and Conrad, 1976). The partial digestion of the HS polysaccharides influences the content of the oligosaccharide mixture generated, and therefore will control the final product.

Enzymatic cleavage: The heparinases are enzymes (purified from *Flavobacterium heparinum*) that digest heparin and HS. There are three heparinases I, II and III (also known as heparin lyases I, II or III or heparitinases III, II and I respectively) that as a mixture can convert heparin, chemically modified heparin and HS to disaccharides (Linhardt *et al.*, 1986). The cleavage reactions are elimination reactions, which result in the formation of an unsaturated uronic acid at the non-reducing end (losing the identity of GlcA/ IdoA as both become ΔUA), but conserve the glucosamine residue on the reducing end of the cleavage product (Figure 3.1). The reported specificity of the enzymes is shown in Table 3.1 (Linhardt *et al.*, 1986; Linhardt *et al.*, 1990).

Heparin lyases	Size	EC number	Glycosidic link cleavage site	Heparan sulfate	Heparin
Heparinase I	43 kDa	EC 4.2.2.7	GlcNR*(± 6S) α (1–4) IdoA 2S	<5%	+ve
Heparinase II	86 kDa	Not given	GlcNR*(± 6S) α (1–4) GlcA/ IdoA	+ve	+ve
Heparinase III	74 kDa	EC 4.2.2.8	GlcNR*(± 6S) α (1–4) GlcA	+ve	<5%

*Where (R= N-acetyl or N-sulfate)

Table 3.1 Heparinase (I, II and III) enzyme specificity for the depolymerisation of heparan sulfate/heparin. +ve represent the main substrate for heparinase enzymes.

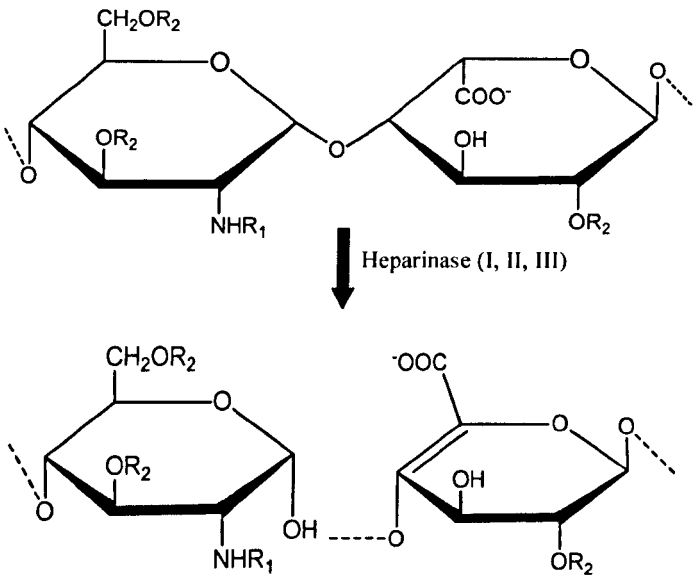

Figure 3.1 Schematic showing partial digestion of heparin/HS by heparinase enzymes, resulting in oligosaccharides having an unsaturated bond at their non-reducing end (D-glucuronic acid and L-iduronic acid both degrade to Δ 4, 5-unsaturated uronic acid). R_1 =H, Ac or SO_3; R_2= H or SO_3.

Nitrous acid cleavage: Low pH nitrous acid cleavage is an additional method for the degradation of heparin and modified heparins, but also HS. It results in selective cleavage of the glycosidic bonds in the NS domains of these polysaccharides. A high pH nitrous acid version of the procedure can be applied, which is more specific to the unmodified (N-acetylated) areas of the HS polysaccharides chains. Briefly, N-acetyl groups on the glucosamine residues in the unmodified areas are first de-N-acetylated with hydrazine in a procedure known as hydrazinolysis, to convert the GlcNAc to GlcN (Shaklee and Conrad, 1984; Shaklee *et al.*, 1985; Shaklee and Conrad, 1986; Guo and Conrad, 1989). Then, the glycosidic bonds of the resulting N un-substituted amino sugars become sensitive to cleavage at room temperature with nitrous acid at pH 3.9. Both types of cleavage with nitrous acid leave the uronic acid at the non-reducing end of unchanged, while the reducing end is modified to an anhyromannose residue (Powell *et al.*, 2004) (Figure 3.2).

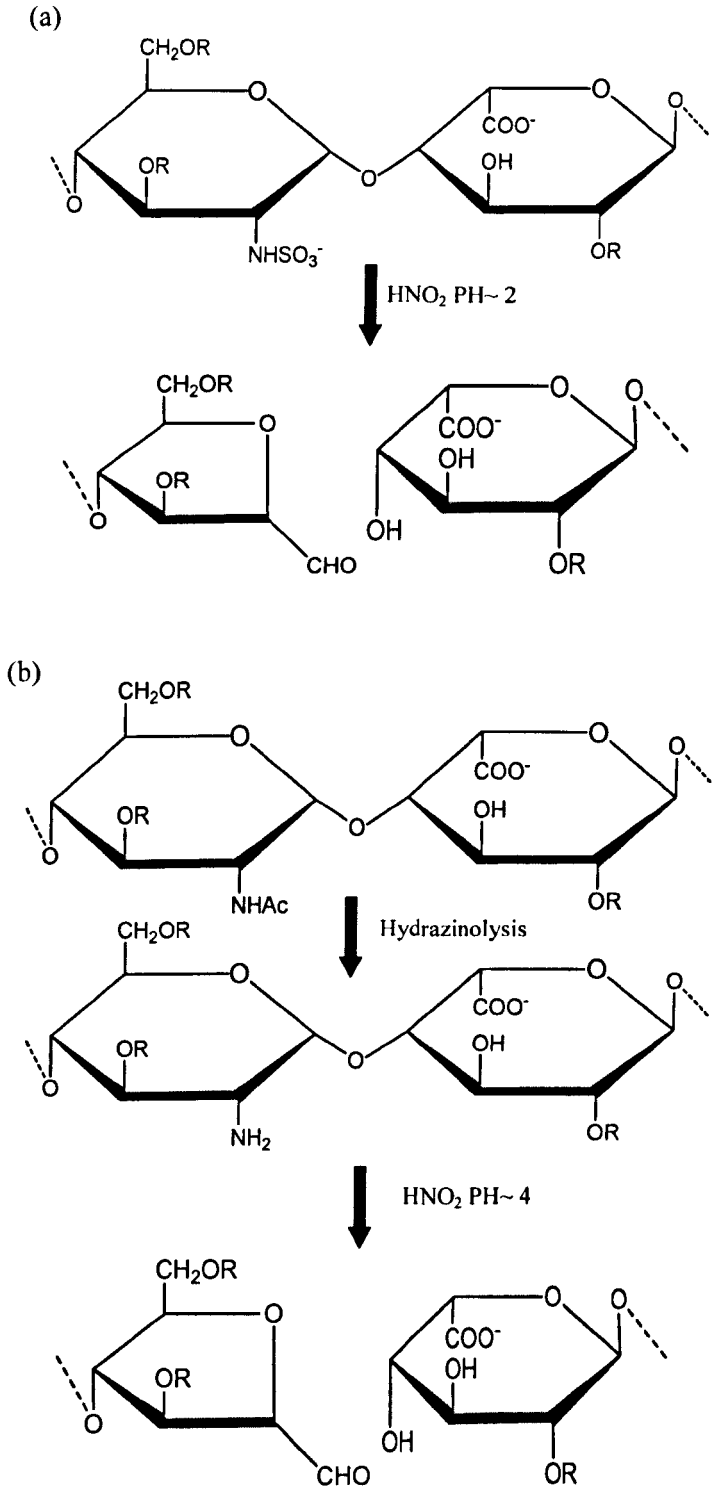

Figure 3.2 Schematic showing the result of partial digestion of heparins/ HS with nitrous acid. The linkage of N-sulfated glucosamine and uronic acid is cleaved at pH 1.5 (A) while the linkage of N-acetylated glucosamine and uronic acid is cleaved by hydrazinolysis followed by cleavage by nitrous acid at pH 3.9 (B). R =SO_3 - or H.

3.1.1.2 SEC

Size-exclusion chromatography (SEC) (also called gel filtration or gel permeation chromatography) fractionates according to hydrodynamic volume (which is broadly proportional to size). This separation is performed by the interaction of the mobile phase with a stationary phase. The matrix beads that comprise the stationary phase have a specific variety of pore sizes, which gives rise to a fractionation range within which molecules can be separated. SEC is carried out twice during oligosaccharide production, first in the fractionation of the partially digested materials and secondly during desalting (i.e. removing ammonium hydrogen carbonate and sodium chloride). Removal of inorganic salts, such as sodium chloride (NaCl), needs a column with a relatively small pore size. An example is Sephadex™ G25 medium (GE Healthcare; e.g. PD-10 pre-packed columns), which will rapidly and conveniently separate oligosaccharides greater in size than a 4-mer from inorganic salts. Similar columns with improved fractionation properties for disaccharides can be poured using Sephadex™ G-25 Superfine as the matrix of choice, and by increasing the column length. For semi-preparative separations, Hi-Prep 26/10 columns (Sephadex™ G-25 fine) provide a preparative load desalting option which can be easily connected to a fast protein liquid chromatography (FPLC) system (e.g. AKTA purifier).

For the separation of oligosaccharide fragments generated from partial digestion of heparin, chemically modified heparins and HS chains, it has been determined that separations of 2-20-mer can be effectively carried out using columns of diameter 1-2 cm by 1-2 m length, using either Bio-Gel P10 (BioRad) or G-50 Sephadex™ (GE Healthcare). The flow rates for these columns are low so the runs take between 24-48 hours. Bio-Gel P10 (Walker *et al.*, 1994) gives the highest resolution but, the matrix is unstable due to its soft gel nature and therefore it is less consistent. Instead, a different matrix such as Superdex™ 30 can be employed and gives excellent and consistent resolution. Superdex™ 30 is also a robust matrix so the column can be connected to an FPLC system and run at faster flow rates (Feyzi *et al.*, 1997b).

The buffer of choice is 0.1-0.5 M ammonium hydrogen bicarbonate used to ion pair with the negative charges carboxyl and sulfate groups, and hence reduce the likelihood of ionic interactions with the matrix beads. Ammonium hydrogen carbonate is also volatile, so it can be removed by serial freeze-drying.

3.1.1.3 SAX-HPLC

Strong anion exchange high performance liquid chromatography (SAX-HPLC) separates anionic molecules based on their net charges. In anion exchange chromatography, the matrix possesses positive charges and interacts with the negative charges on heparin and HS. The positive charges on the matrix are due to a strong base (e.g. quaternary ammonium) derivatized onto a support medium, which remains positively charged across the pH range of 1-14. Oligosaccharide fraction mixtures introduced into the mobile phase will bind ionically to the positive charged matrix. The content of sulfate and carboxyl groups, and the buffer pH, largely determines the strength of the interactions. The pH of the buffers must be above the pKa of the sulfate and carboxyl groups to de-protonate the acidic groups. If the pH is less than the pKa of the acidic groups, they will not participate efficiently in interactions with the column matrix. Oligosaccharides are eluted from the column by introducing a gradient of counter ion (e.g. sodium chloride).

The Propac PA1 column (Dionex) is a high-resolution SAX column utilized for separation of heparin and heparan sulfate oligosaccharides. The Propac PA1 column provides reliable elution times, which are necessary for oligosaccharide separation and disaccharide analysis. Two types of Propac PA1 column are available; analytical columns (4 x 250 mm) for sample loads of between 0.5 to 1 mg, and semi-prep scale columns (9 x 250 mm) for samples up to 5 mg.

An alternative high resolution method is the derivatization of the silica based C18 columns with cetyltrimethylammonium (CTA) hydroxide in order to provide the basic group used for anion exchange (Mourier and Viskov, 2004); however this column has poor longevity compared to the Propac PA1 column, requiring re-derivatization every 3-4 months. However, this column does provide better resolution than the Propac PA1 for disaccharide analysis as seen by the excellent resolution of α and β anomers with some of the disaccharide standards.

3.1.1.4 PAGE

Polyacrylamide gel electrophoresis (PAGE) is also used for analysis of heparin and heparan sulfate oligosaccharides (Turnbull *et al.*, 1999). PAGE is a high-resolution technique, which separates molecules based on their charge, size and conformations. Separation results from "sieving" of charged molecules through pore in the gel matrix, with migration towards an electrode of opposite charge. Commonly, polyacrylamide gels of high viscosity are used (in the order of 30 %). Polyacrylamide gels are created by the polymerization of acrylamide monomers with the N, N'-methlylenebisacrylamide cross linker. The pore sizes formed within the gel are dependent on the proportion of cross-linking agent and the total acrylamide concentration. Ammonium persulfate is usually used as the free radical initiator while N, N, N', N'-tetramethylenediamine (TEMED) stabilizes the polymerization chain reaction. A common method for visualization of unlabeled oligosaccharides is the blue dye Azure A. Staining occurs due to ionic interactions with the highly negative charge sulfate and carboxylic acid groups present in this class of carbohydrate. Background staining can easily be removed by washing with double-distilled water. The limit of detection is in the order of micrograms (Turnbull and Gallagher, 1988).

3.1.2 Aims and strategy

The principal aim of this chapter is to describe production of three sets of novel oligosaccharide libraries from heparin, modified heparins and HS polysaccharides.

These were achieved by employing enzymatic and chemical partial digestion, followed by chromatographic fractionation by SEC and SAX-HPLC. The oligosaccharides libraries were then exploited in structure-function selectivity and specificity studies of HS-protein interactions in two model systems: Slit and Robo (Chapter 4) and FGF proteins (Chapter 5). The strategy has been summarized in Figure 3.3. Further examples of the use of these oligosaccharides are also mentioned.

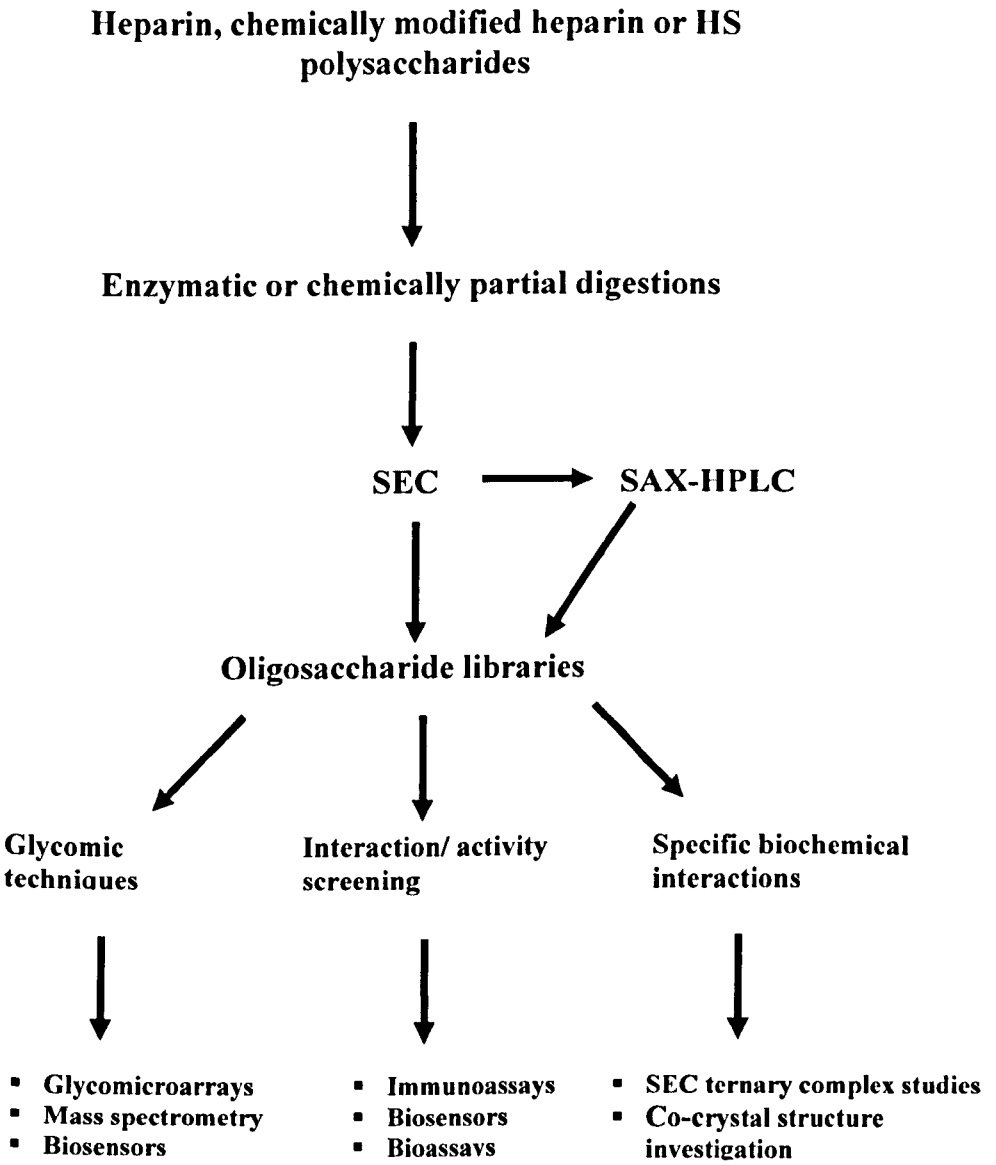

Figure 3.3 Strategy for making and exploiting oligosaccharide libraries

3.2 Results

3.2.1 Heparin oligosaccharides produced by heparinase I and their applications

Two sources of heparin starting material were chosen as a supply for the heparin oligosaccharide libraries, namely porcine mucosal heparin (PMH) and bovine lung heparin (BLH). They were both partially digested by heparinase I over time courses optimised in order to obtain oligosaccharides within the desired size ranges followed by SEC and SAX-HPLC separation.

3.2.1.1 Heparinase I partial digestion

In order to obtain a successful heparin partial digestion, a test digestion was performed. The test digestion is valuable in determining the quantity of the enzyme and the length of digestion required to obtain an oligosaccharide mixture with an appropriate range of sizes. Figure 3.4a shows test partial digestion of BLH with the products at various time points tested by PAGE analysis. Here it is clear that there is an increase for products corresponding to the smaller oligosaccharides and a reduction of the large polysaccharide chains. The test digestion has confirmed that the heparinase I partial digestion was successful for particular time points (2, 4 and 6 hours) which produce a spread of different oligosaccharide sizes.

The information obtained from the test digests was used to determine large-scale partial digestions using the three time points (2, 4 and 6 hours) (Figure 3.4b). These time points showed an appropriate spread of large, medium and small oligosaccharides. The products of large-scale partial digestion were pooled, freeze-dried, and stored at -20 °C ready for the SEC.

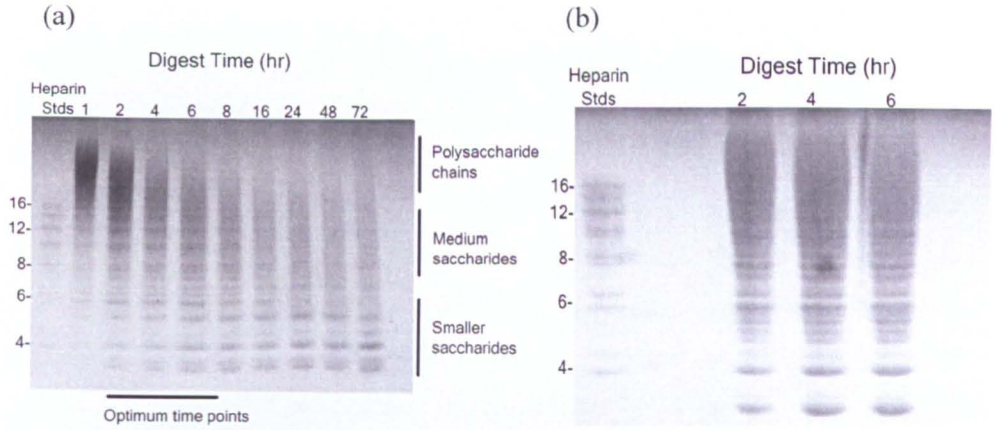

Figure 3.4 Kinetic analysis of heparinase digestion using PAGE. a) Trial digests. b) Bulk digests show three time points picked from the trial digest. Bovine lung heparin was incubated with 1 mU/ mg (33 mU/ ml) heparinase I, and aliquots removed at sequential time points, heated to 100 $^{\circ}$C to terminate the digestion, and analysed by PAGE alongside a pool of size-estimated SEC fractions from bovine lung heparin (heparin standards). PAGE gels were stained with Azure A and digital images recorded using a DVC camera operated with DVC view version 2.2.8 software.

3.2.1.2 Separation of heparinase I digested oligosaccharides by SEC

The pooled sample was then size fractionated over Superdex 30^{TM}; with elution monitored at 232 nm to detect the non-reducing end double bond generated by the enzymatic cleavage. A typical profile of Superdex 30^{TM} separation and the pooling regime (illustrated with horizontal bars) is shown in Figure 3.5a and b. Here, two different heparin sources (BLH and PMH) were used for SEC separation; they produce roughly similar profiles, although better resolution is evident for the lower amount (100 mg PMH) Figure 3.5b.

The largest peak eluting earlier than the total column volume contains disaccharides and this was confirmed by further analysis of the peak (by PAGE, HPLC and ES-MS). Then the peaks were assigned by increasing degrees of polymerisation by counting in disaccharide repeat units from the disaccharide peak (shown by even integers). However, these pooled peaks may exhibit degree heterogeneity due to the lack of baseline resolution, and the size and sulfation diversity of heparin.

The sizes of the oligosaccharides in the pooled fractions were determined by PAGE (Figure 3.5c and d). PAGE analysis has proved to be a useful tool for oligosaccharide size determination, with commercially available and laboratory produced standards run side by side with the oligosaccharides in question. In this study, the assignments of heparin oligosaccharide sizes were also confirmed by changes in absorbance at λ_{abs}= 232 nm following complete digestion of the fraction with heparinases I, II and III (Powell *et al.*, 2010), and moreover, by electro-spray mass spectrometry (with the help of Dr. Atrih and Miss Miller; see Appendix 1). PAGE was also performed to check the outcome of the SEC of five different runs of 10-mers and three different runs of 18-mer heparin oligosaccharides (Figure 3.6). The result confirmed the consistency of the method.

Superdex 30™ medium used in the SEC separation proved to be a tough reliable matrix column (the column used in this project continues to be useful after for more than six years). However, the resolution was not as high as with BioGel P10, which was previously used in separating HS oligosaccharides (Guimond and Turnbull, 1999). The problem with the P10 columns are that they are only effective for a few runs and then become unreliable due to the more fragile matrix; also, they ran at much lower flow rates compared to Superdex 30™. Thus, an improvement in the resolution of Superdex 30™ column would be useful. The possibility of running the sample through a combination of Superdex matrixes (mentioned in section 3.3) could improve the resolution of SEC and the purity of larger oligosaccharides. An additional way to improve SEC resolution might be by adding an extra ultra filtration step prior to the SEC step.

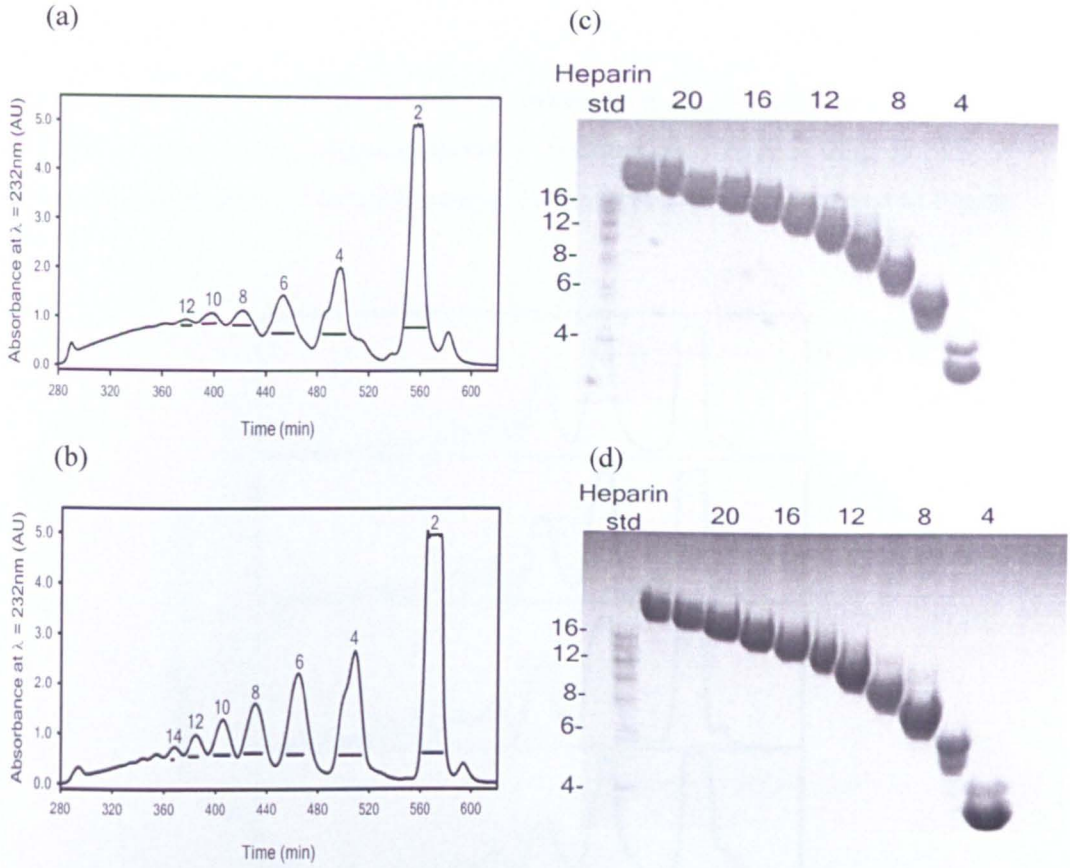

Figure 3.5 Profiles of heparinase I partial digest of BLH and PMH. Size-exclusion chromatography fractionation of heparinase partial digests of 200 mg BLH (a) and 100 mg PMH (b). Fraction pooling and PAGE analysis for size-exclusion chromatography fractionation of heparinase partial digests of BLH (c) and PMH (d). Briefly, Superdex ™ 30 SEC chromatography (16 mm I.D. x 200 cm length), was run using an AKTA purifier 10 at a flow rate of 0.5 ml/ min in 0.5 M ammonium hydrogen carbonate and monitoring the elution profile by absorbance at λ_{abs} =232 nm, was used to fractionate a pooled mixture of 3, 4 and 5 hr time points of 100 mg PMH digested with 1 mU/ mg (33 mU/ ml) heparinase I. Data were recorded using the Unicorn 5.0 software and exported into SigmaPlot 11. Fractions across selected peaks were roughly estimated to contain heparin saccharides displaying increasing degrees of polymerization (shown by even integers in b) and pooled as shown by horizontal bars (in a). Multiple separations of 100 mg per run were performed, and profiles were consistent (n > 50 runs).

Figure 3.6 PAGE analyses of selected heparinase digestion oligosaccharides SEC (10-mer and 18-mer). Five 10-mer and three 18-mer fractions were analysed by PAGE alongside a pool of size-estimated SEC fractions from bovine lung heparin (heparin standards). PAGE gels were stained with Azure A and digital images recorded using DVC camera operated with DVC view version 2.2.8 software.

Subsequent to trial experiments and confirmation of oligosaccharide sizes, large amounts of sized heparin oligosaccharides (~1-30 mg per size pool from 100 mg of heparin) were produced. The consistency of the procedure is demonstrated in Figure 3.7.

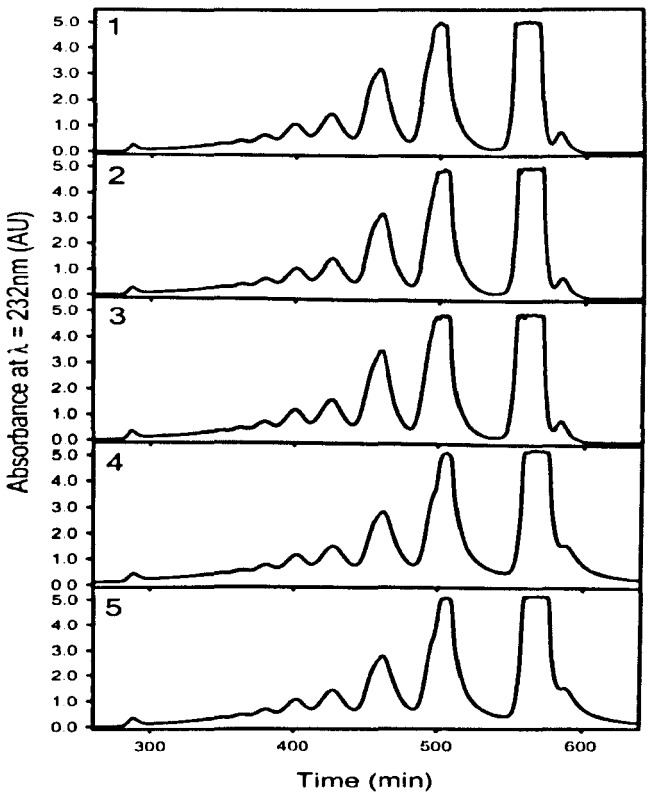

Figure 3.7 Size-exclusion chromatography profiles of five heparinase I partial digests. Size-exclusion chromatography fractionation of independent heparinase partial digests of 100 mg PMH. Chromatography was carried out as described in Figure 3.5.

Size-defined heparin oligosaccharide fractions produced in this way were useful in binding studies for HS/ Slit/ Robo interactions (Chapter 4) and to study FGF-1 and FGF-2 interactions with HS (Chapter 5). In addition, these oligosaccharides were used in the development of glyco-microarrays in two different platforms (aminosilane and gold) (Powell *et al.*, 2009; Zhi *et al.*, 2008; Zhi *et al.*, 2006). A further list of oligosaccharide applications is described in Appendix 2.

3.2.1.3 Purification of SEC separated oligosaccharides by SAX-HPLC and their applications

BLH was used as the source material for the production of 4-mer, 6-mer, 8-mer and 10-mer SAX-HPLC purified heparin oligosaccharides. This is due to its high trisulfated disaccharide content (IdoA2SGlcNS6S) and because it has simpler SAX-HPLC, profile compared to PMH (Figure 3.8) and hence it is easier to purify the major oligosaccharides. However, different BLH batches have shown more complexity than others have (data not shown). This observation also demonstrates that there is heterogeneity in heparin within species.

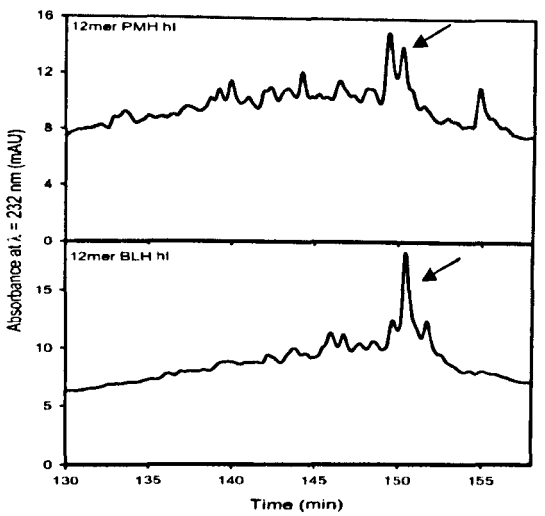

Figure 3.8 SAX-HPLC profiles for the trisulfated peak of 12-mer PMH and BLH. 100 µg of 12-mer fraction from PMH or BLH were subjected to SAX-HPLC analysis performed on Propac PA1 columns (9 x 250 mm) equilibrated in Milli Q H_2O, at flow rate of 1 ml/ min. Samples were eluted with a linear gradient of sodium chloride (0 – 1.8 M over 180 min), sub-fractioned oligosaccharides were detected by absorbance at 232 nm. The figure shows a typical preparative run. Multiple separations of 1-5 mg per run were performed and identical peak fractions corresponding to selected trisulfated peaks (illustrated by arrows) were pooled, desalted on Hiprep desalting columns, freeze dried and quantified. Data were recorded using Shimadzu Class-VP 4.2 Chromatography data system software and exported into SigmaPlot 11.

Figure 3.9 shows a series of SAX-HPLC purified enzyme digested BLH oligosaccharides (4-mer, 6-mer, 8-mer and 10-mer fractions); it is clear that there are increasing numbers of peaks and peak complexity within the larger size fractions. In addition, the trisulfated peaks (denoted by the arrows) shifted (as expected) to higher salt elution positions with increasing the oligosaccharide size.

It is noticeable that the individual peak areas shrank with increasing oligosaccharide size, meaning that large quantities are needed to obtain workable amount of the purified trisulfated peaks. Hence, multiple runs of SAX-HPLC of particular sizes were prepared to milligram quantities (using the method described above) in order to obtain sufficient purified saccharides for further studies.

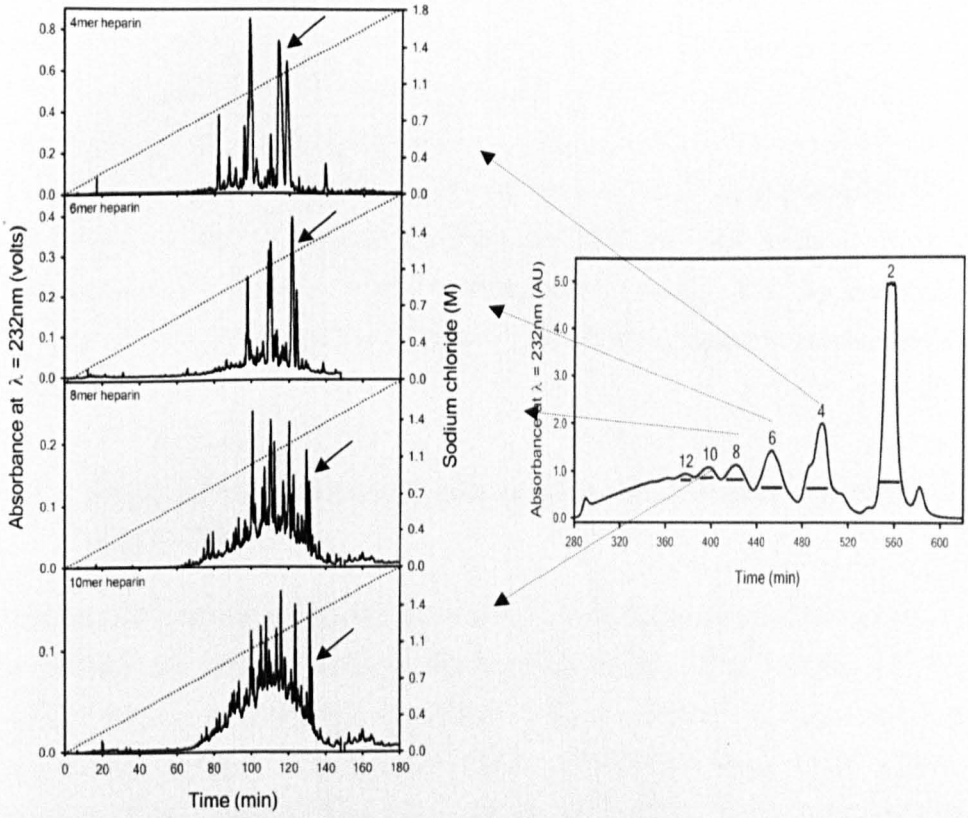

Figure 3.9 SAX-HPLC profiles for 4, 6, 8 and 10-mer SEC pools from BLH subjected to heparinase de-polymerization. Saccharide fractions were further resolved by high resolution SAX-HPLC, performed on Propac PA1 columns (9 x 250 mm) equilibrated in Milli Q H_2O, at flow rate of 1 ml/ min. Samples were eluted with a linear gradient of sodium chloride (0 – 1.8 M over 180 min), sub-fractioned oligosaccharides were detected by absorbance at 232 nm. The figure shows a typical preparative run. Multiple separations of 1-5 mg per run were performed and identical peak fractions corresponding to selected trisulfated peaks (illustrated by the arrows) were pooled, desalted on Hiprep desalting columns, freeze dried and quantified. Data were recorded using Shimadzu Class-VP 4.2 Chromatography data system software and exported into SigmaPlot 11.

Heparin SAX-HPLC showed that most of the peaks are clustered in the end of the salt gradient, this reflecting the high sulfate contents of heparin. Hence, a higher concentration of salt is needed, this was also been confirmed by the disaccharide compositional analysis, which showed the trisulfated peak is the predominant species within heparin.

In collaboration with the Hohenester lab (Imperial College, London), purified heparin 10-mer was used in studies that established that HS plays an essential part in formation of the Slit-Robo signalling complex (Hussain *et al.*, 2006); (Appendix 2, Figure A1). In other collaborative studies SAX-HPLC purified heparin oligosaccharides (4-mer and 6-mer) were sent to Dr. Tissot (Imperial College, London) for validation of novel MALDI-TOF/TOF MS/ MS methods using ionic lipid matrices (Tissot *et al.*, 2007) (Appendix 2, Figure A2). Appendix 2 also contains other examples of applications of these purified heparin saccharides (SEC and SAX).

3.2.2 Heparin oligosaccharides produced by nitrous acid and their applications

Competition binding assays (ELISA) used in this thesis required biotinylation of saccharides for immobilisation of the oligosaccharides on the streptavidin coated surface. Internal biotinylation, using NHS ester derivatives, has been used in long polysaccharide chains, but is thought to react with the free amino group that occurs on some GlcN residues of HS, and could also label GlcNS residues engaged in the binding of proteins with HS. This could result in loss of binding ability through steric hindrance, especially in the case of oligosaccharides (Powell *et al.*, 2004). However, nitrous acid generated oligosaccharides have a reactive reducing end anhydromannose residue, which can be exploited for efficient biotinylation.

3.2.2.1 **Nitrous acid partial digestion**

PMH was partially digested using low pH nitrous acid; using the same digestion strategy as in enzyme digestion i.e. small-scale trial digestion followed by large scale. Figure 3.10a and b shows PAGE analysis of trial and bulk nitrous acid digested PMH fractions. These data were similar to the ones obtained by enzyme digestion, however, the nitrous acid digestion was rapid compared to heparinase I digestion, with time points in minutes rather than hours.

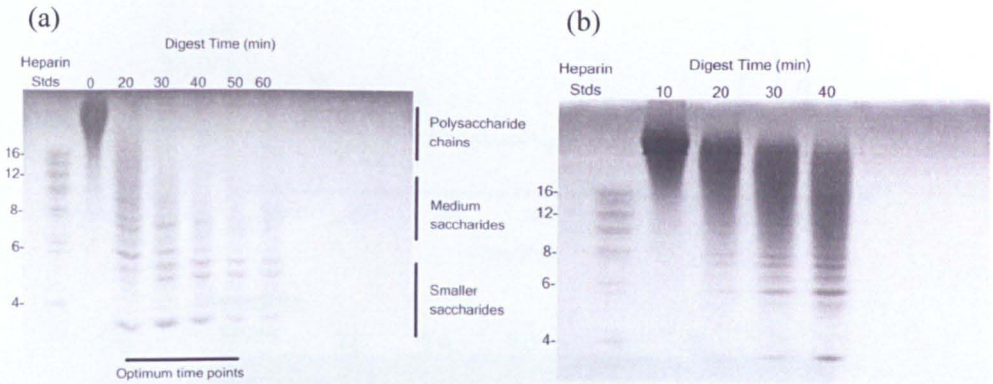

Figure 3.10 Analysis of kinetics of low pH nitrous acid digestion of PMH using PAGE. Porcine mucosal heparin was incubated with an equivalent volume of 250 mM HNO_2 at room temperature; aliquots were removed at sequential time points, and neutralized with $NaHCO_3$ to terminate the digestion. The resulting oligosaccharides were analysed by PAGE alongside a pool of size-defined SEC fractions from bovine lung heparin (heparin standards). PAGE gels were stained with Azure A and digital images recorded using DVC camera operated with DVC view version 2.2.8 software. a) Trial digest demonstrating increased amounts of smaller saccharides with time and b) bulk digest showing four selected time points picked (10, 20, 30 and 40 minutes) with an appropriate spread of large, medium and small saccharides.

3.2.2.2 **SEC separation of nitrous acid digested heparin**

Samples digested for appropriate times were then pooled and separated by SEC (Figure 3.11a). Selected peak fractions were then pooled and analysed by PAGE (Figure 3.11b). The amounts of size fractions were less compared to the same amounts digested by heparinase I. Therefore, optimisation of the nitrous acid digestion was needed to achieve larger amounts of the required size fractions. This was tested by controlling the time course of the digestion.

Figure 3.12 shows examples of two different chromatograms for different time point pools. Once the desired product profile was achieved (20, 30 and 40 min), scale-up production of nitrous acid generated oligosaccharides was carried out and tens of milligrams were prepared (Figure 3.13).

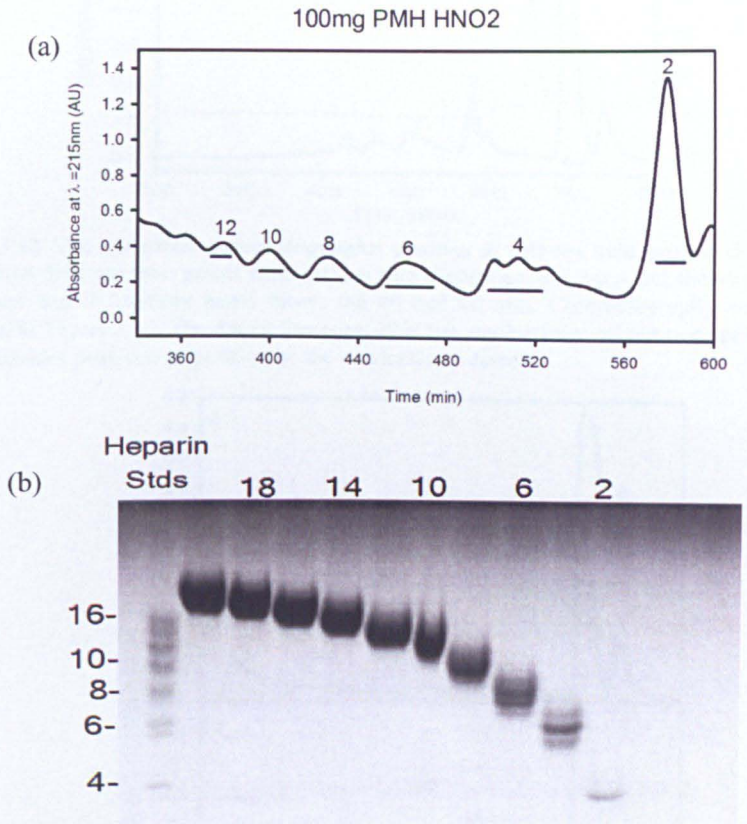

Figure 3.11 Size-exclusion chromatography profile of nitrous acid partial digests 100 mg PMH. a) Size-exclusion chromatography fractionation of nitrous acid partial digests of 100 mg PMH. Superdex ™ 30 SEC chromatography (16 mm I.D. x 200 cm length), run using an AKTA purifier 10 at a flow rate of 0.5 ml/min in 0.5 M ammonium hydrogen carbonate and monitoring the elution profile by absorbance at λ_{abs} =215 nm. Fractions across selected peaks were roughly estimated to contain HS/heparin saccharides displaying increasing degrees of polymerization (shown by even integers). b) Fraction pooling and PAGE analysis for size-exclusion chromatography fractionation of nitrous acid partial digests of heparin.

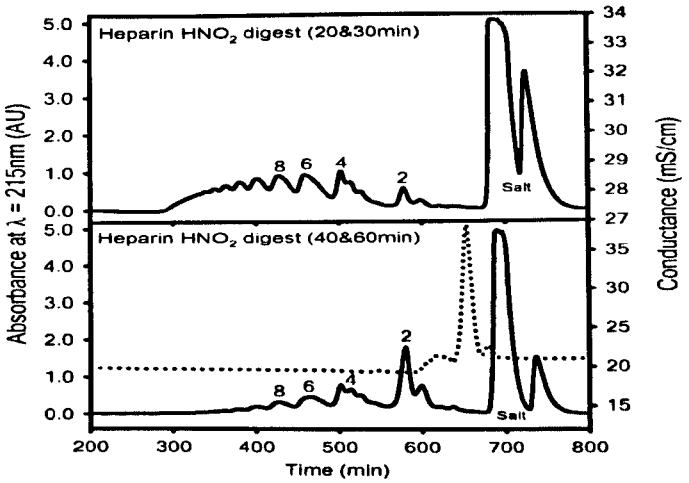

Figure 3.12 Size-exclusion chromatography profiles of nitrous acid partial digests of 100 mg PMH. Two different time points from nitrous acid digestions; the top panel shows pooled 20 and 30 min digest and the bottom panel shows the 40 and 60 min. Chromatography was carried out as described in Figure 3.11. The dotted line represents the conductivity, which was appeared earlier than the saccharides peak due to position of the conductivity detector.

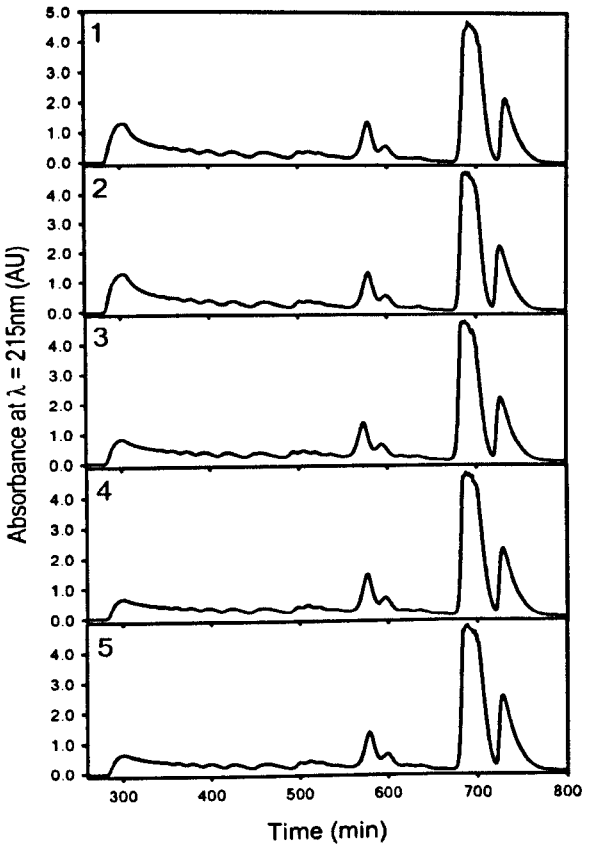

Figure 3.13 Size-exclusion chromatography profiles of five independent nitrous acid partial digests of 100 mg PMH. Size-exclusion chromatography of 5 representative individual digest (1-5) were performed as described in Figure 3.11 the data demonstrate that the profiles are highly consistent (n >30).

Nitrous acid generated oligosaccharides were biotinylated in order to be immobilised on microtiter plates in competition ELISA experiments. The biotinylation was performed with a 5-fold excess of aminoxybiotin (pH 5.0) and incubated overnight at 50 °C. Biotinylation efficiency was assessed by executing a dot blot on nitrocellulose membrane Figure 3.14.

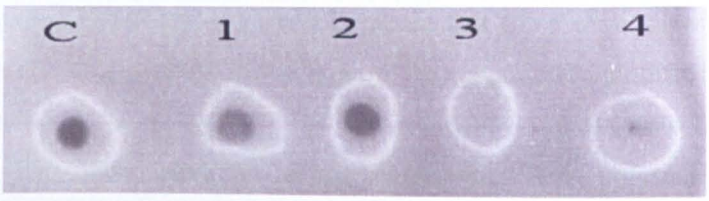

Figure 3.14 Dot blot of biotinylated 10-mer heparin oligosaccharides. Briefly 1 µl of oligosaccharides heparin-biotin 10 mg/ ml were spotted onto nitrocellulose membrane (Hybond-ECL nitrocellulose membrane, GE Healthcare). Followed by incubation for 30 min at room temperature and then blocked with 5 % (w/v) BSA / PBST then anti-biotin-HRP (Cell Signalling) was added before washing with PBST followed by adding ECL detection reagents (GE Healthcare) and then exposed to ECL film (Hyperfilm-ECL, GE Healthcare). The ECL film was then developed and fixed finally washed with water and air-dried. The biotinylation method of choice was the aminoxybiotin; the numbers represent different biotinylation conditions 1=5x, 2=4x, 3=2x, and 4=1x, x represent fold excess; C represents control, is a tested biotinylated 10-mer heparin (for details see section 2.2.11.1).

Apart from biotinylation, nitrous acid derived oligosaccharides were also used in the development of the glyco-microarray fabrication on a gold platform (Powell *et al.*, 2009; Zhi *et al.*, 2006); and on aminosaline platform (paper in preparation by Powell and co-workers). Moreover, in collaboration with Dr Jonathan Popplewell (Farfield Group, Ltd), 10-mer heparin oligosaccharides (nitrous acid generated) were used in developing a dual polarisation interferometry (DPI) surface capable of looking at the interactions, and also the complex geometry, of proteins binding to carbohydrate (Popplewell *et al.*, 2009). This technique will add a new angle to the progressing Slit and Robo studies (see Chapter 4).

3.2.3 Chemically modified heparin oligosaccharides

The structural compositions of each of the chemically modified heparins used in the oligosaccharide production were confirmed by complete heparinase (I, II and III) digestion followed by SAX-HPLC, with reference to known disaccharide standards.

Figure 3.15 shows the SAX-HPLC profile of the eight common disaccharide standards. Figure 3.16 summarizes the relative levels of the disaccharide components present within the different chemically modified heparins expressed as a percentage of total disaccharides.

This analysis confirmed the expected alterations in the structure of the chemically modified heparins. However, it should be noted that there were minor amounts of residual unmodified disaccharides in most of the chemically modified heparins as observed previously (Yates *et al.*, 1996). These should be taken into consideration in interpreting any data obtained using these modified polysaccharides and oligosaccharides.

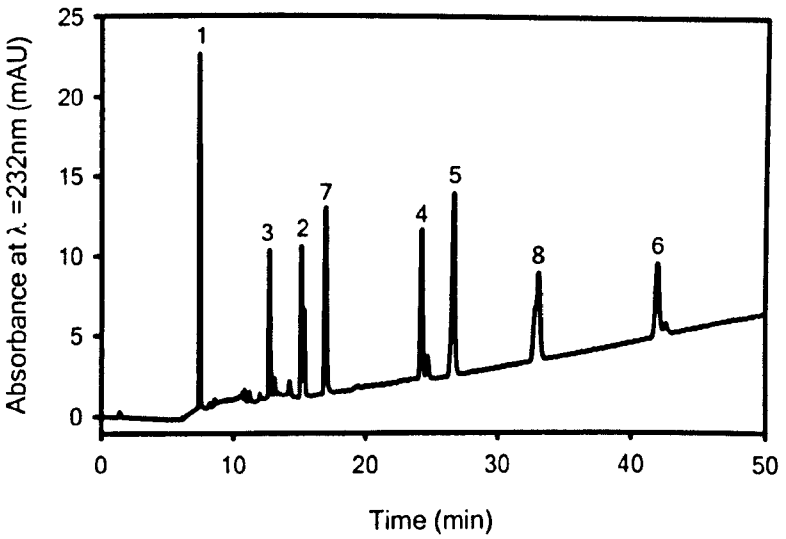

Figure 3.15 Disaccharide compositional analyses of the eight common naturally occurring disaccharides standards. Separation was achieved using SAX-HPLC on a Propac-PA1 analytical column (Dionex) with linear gradient of 0-1 M over 0-45 min and flow rate 1ml/ min. 1.ΔUA-GlcNAc 2. ΔUA-GlcNAc (6S) 3. ΔUA-GlcNS 4. ΔUA-GlcNS (6S) 5. ΔUA (2S)-GlcNS 6.Δ UA (2S)-GlcNS (6S) 7. ΔUA (2S)-GlcNAc 8. ΔUA (2S)-GlcNAc (6S). Disaccharide standards were from Dextra Laboratories Ltd, UK.

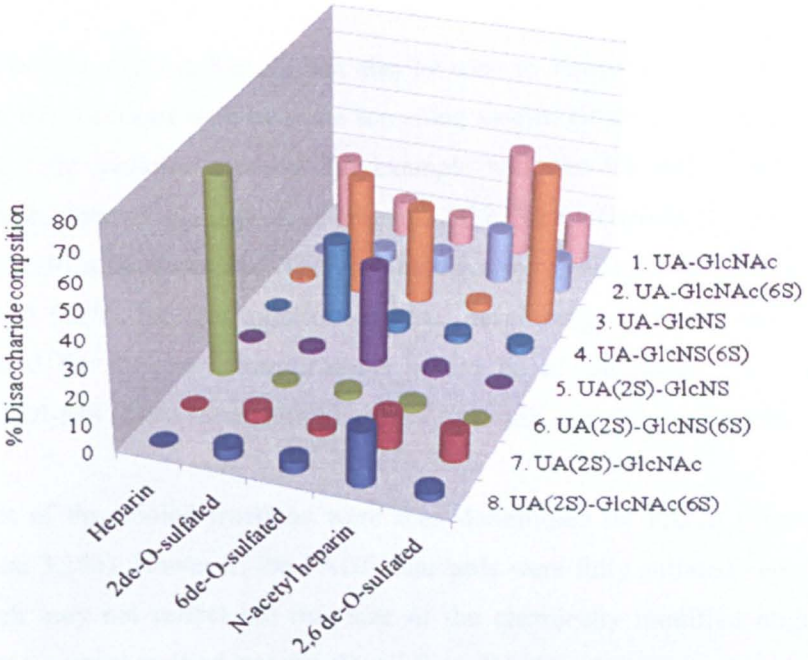

Figure 3.16 Disaccharide compositions of heparin and chemically modified heparins. Disaccharide composition was determined by SAX-HPLC with reference to authentic standards, as described in Figure 3.15.

Chemically modified heparins (2 de-O-sulfated, 6 de-O-sulfated, N Acetyl heparin and 2, 6 de-O-sulfated heparin) were partially cleaved with heparinase II enzyme or nitrous acid. The procedures for partial digestion followed the same optimization principles used in generation of heparin saccharides i.e. trial digestion and then scaled up digestion (data not shown). Following the digestion, pooled samples were applied to the SEC column; the resulting chromatogram profiles were more complex compared to heparin (Figure 3.17a and Figure 3.18a). Some of the peaks were split with several shoulders, and the occurrence of peaks in between the well-defined peaks was observed. Most of these observations could be explained by a combination of the heterogeneous nature of the source material (PMH) and the diverse structural features of the partially digested materials.

Most of the SEC chromatogram profiles showed that the separation was not at baseline resolution. This problem may be due to the heterogeneity of the saccharides. This difficulty was dealt with by employing a strict pooling regime, ignoring the borders between peaks to get high purity oligosaccharides size fractions.

The border oligosaccharides can also be used in assays that do not require entirely pure size fractions such as some screening assays. However, sometimes SEC peaks were only partially resolved, for example with the HS and chemically modified heparin chromatogram profiles (Figures 3.17, 3.18). Therefore, another method for size verification is needed. The enzyme digestion method mentioned in section 3.2.2 proved useful for this application; also, developing a routine mass spectrometry method for all size determinations would be of significant, for example using MALDI-MS (Tissot *et al.*, 2007) or ES-MS (Atrih et al, in preparation).

Sizes of the pooled fractions were then determined by PAGE (Figure 3.17b and Figure 3.18b). However, the PAGE standards were fully sulfated heparin standards, which may not reflect the true size of the chemically modified oligosaccharides. Hence, a novel method was developed for validating oligosaccharide size assignment (Powell *et al.*, 2010).

Briefly, the method is based on the change in the absorbance at λ_{abs} = 232 nm on complete digestion with heparinases I, II and III of a known amount of a fraction. Use of the double bond extinction coefficient to calculate the ratio of moles of double bond before and after digestion allows the number of disaccharides present in the oligosaccharide fraction to be calculated. From the extinction coefficient (5500 $M^{-1}cm^{-1}$) and Beer-Lambert law, 1.8 nmoles of double bond gives 0.1 units of absorbance in a 100 µl volume. Therefore, if there are 1.8 nmoles of 4-mer in 100 µl which has been completely digested with the three heparinase enzymes it should yield one double bond and show an absorbance increase of 0.1 confirming the size as 4-mer. However, if there is more than one double bond has been digested to completion, the absorbance will increase by absorbance more than 0.1.

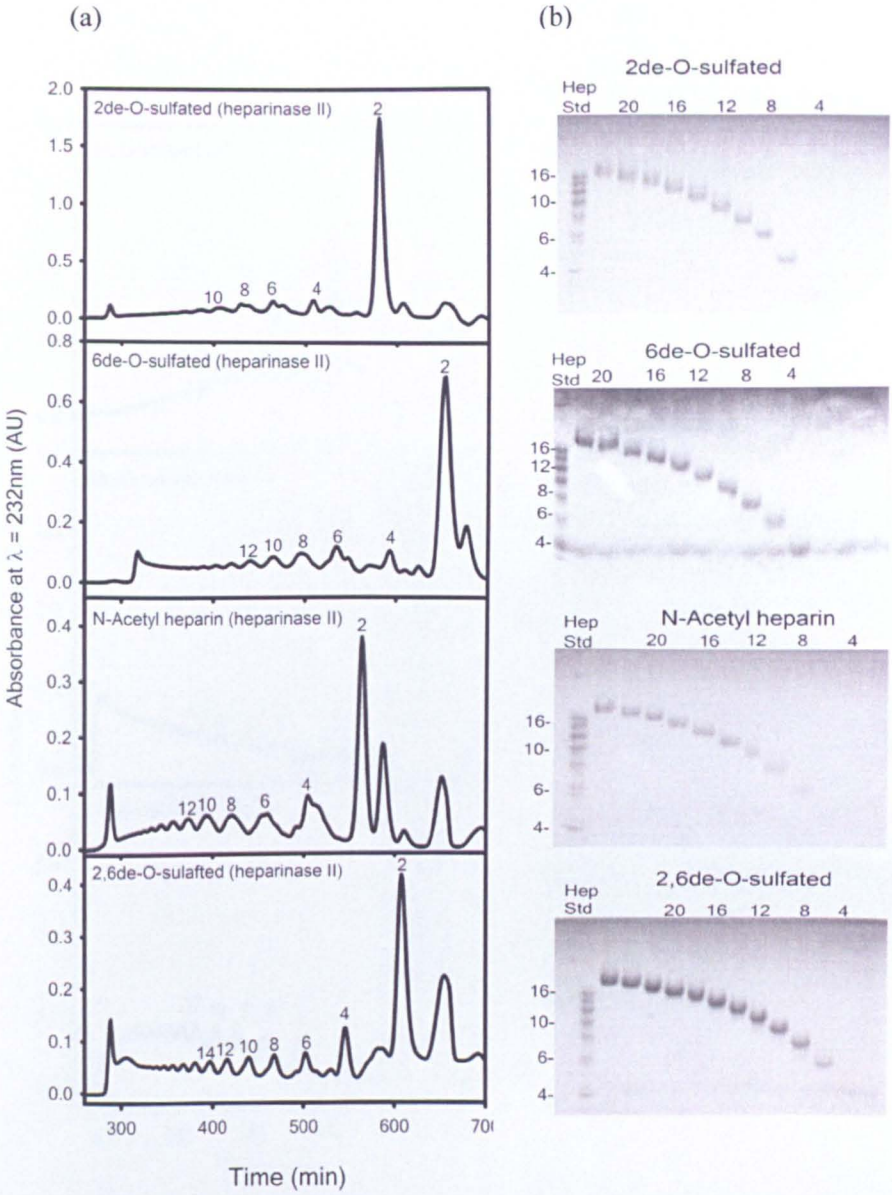

Figure 3.17 Size-exclusion chromatography profiles of heparinase II partial digests of chemically modified heparins. a) Size-exclusion chromatography fractionation of heparinase II partial digests of chemically modified heparin variants. Briefly, 10 mg of 2 de-O-sulfated, 6 de-O-sulfated, NAc and 2,6 de-O-sulfated heparin was digested with 5 mU/ mg (5 mU/ ml) heparinase II for 6, 1, 6 and 8 hours respectively before heating to 100 °C to terminate digestion. Chromatography was carried out as described in Figure 3.13. b) Fraction pooling and PAGE analysis for size-exclusion chromatography fractionation of heparinase II partial digests of modified heparins variants. Fractions across selected peaks were roughly estimated to contain HS/heparin saccharides displaying increasing degrees of polymerization (shown by even integers). Two runs of 10 mg per run were performed for each variant and the profiles were consistent. Chemically modified heparin polysaccharides were a gift from Dr. Ed Yates and were prepared and characterized by NMR as described previously (Yates *et al.*, 1996).

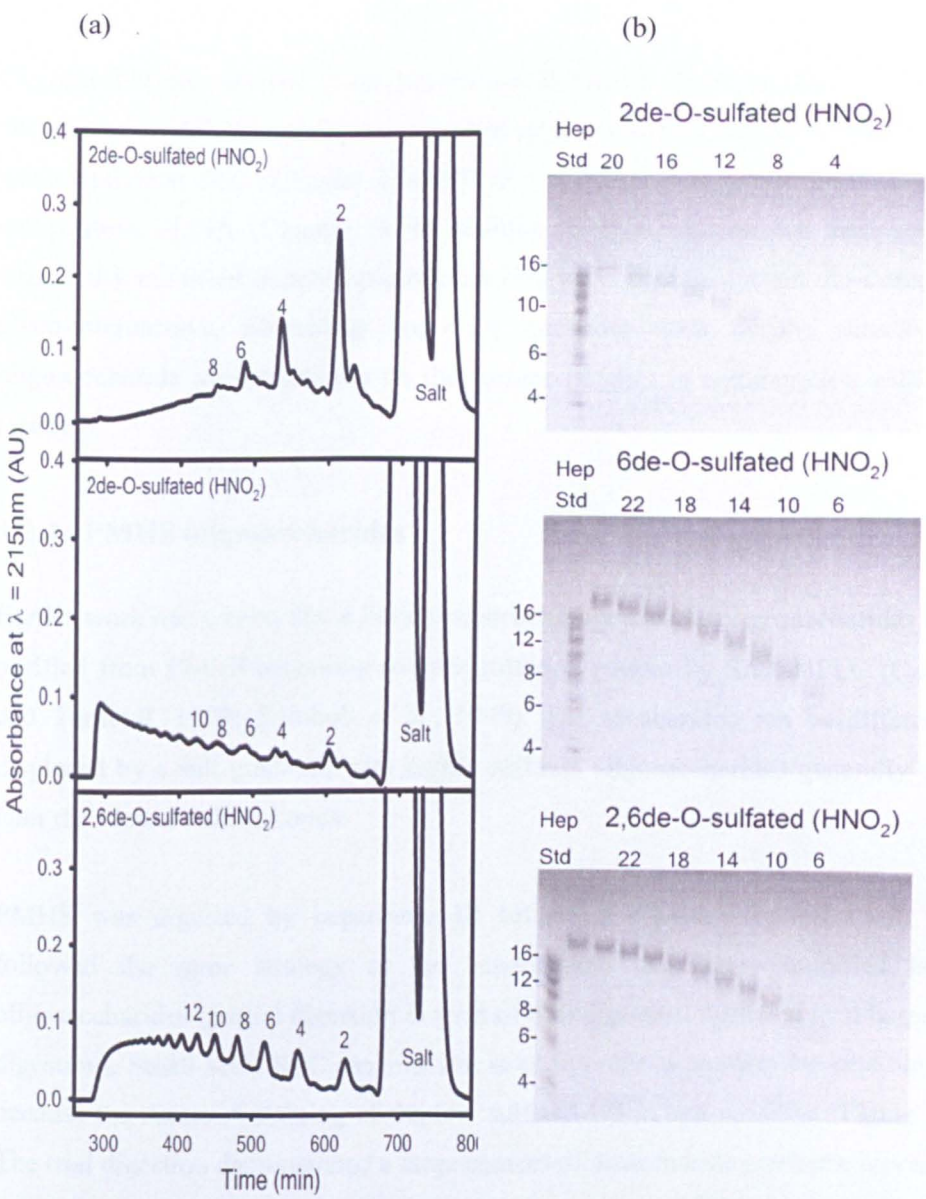

Figure 3.18. Size-exclusion chromatography profiles of nitrous acid partial digests of chemically modified heparins. a) Size-exclusion chromatography fractionation of nitrous acid partial digests of chemically modified heparin variants. Briefly, 10 mg of 2 de-O-sulfated, 6 de-O-sulfated and 2, 6 de-O-sulfated heparins were digested with 10 mM HNO_2 for 20, 45 and 90 min before neutralizing with 1M $NaHCO_3$ to terminate digestion. Chromatography was carried out as described in Figure 3.13 apart from monitoring the elution profile by absorbance at λ_{abs} =215nm. b) Fraction pooling and PAGE analysis for size-exclusion chromatography fractionation of nitrous acid partial digests of modified heparins variants. Fractions across selected peaks were roughly estimated to contain modified heparin saccharides displaying increasing degrees of polymerization (shown by even integers). Two runs of 10 mg each were performed for each variant and the profiles were consistent.

Oligosaccharides derived from heparinase II partial digestion from a panel of chemically modified heparins were used in ternary complex studies of Slit and Robo using analytical SEC (Chapter 4) and FGF-1 and FGF-2 sequence selectivity using competition ELISA (Chapter 5). In addition, enzyme and nitrous acid generated chemically modified heparin oligosaccharides were used in current development of glyco-microarrays, addressing important questions such as the sensitivity of oligosaccharide immobilization on the surface [studies in collaboration with Dr. A Powell].

3.2.4 PMHS oligosaccharides

Earlier work has shown that a library of structurally diverse oligosaccharides can be purified from PMHS according to their sulfation pattern by SAX-HPLC (Guimond and Turnbull, 1999; Turnbull *et al.*, 1999). The saccharides can be differentially displaced by a salt gradient, with highly sulfated oligosaccharides generally eluting later than lower sulfated ones.

PMHS was digested by heparinase III following digestion optimization, which followed the same strategy as the heparin and chemically modified heparin oligosaccharides (partial digestion in term of trial digestion followed by a large-scale digestion). Small-scale SEC analysis was used in order to confirm the trial digestion because the Azure A staining of the low sulfated HS is less sensitive (Figure 3.19). The trial digestion demonstrated a large content of disaccharide products, represented by the predominant peak, and to a lesser extent a range of different oligosaccharides sizes, as observed previously for this type of digest (Turnbull and Gallagher, 1990).

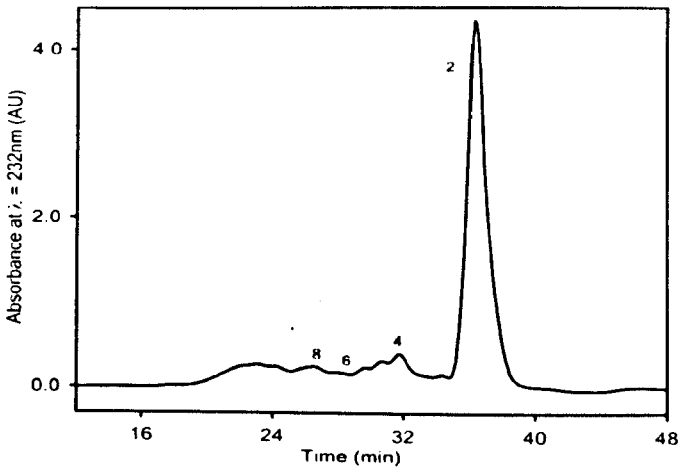

Figure 3.19 Test PMHS partial digestion followed by small-scale size-exclusion chromatography. Porcine mucosal heparan sulfate (100μg) was partially digested using heparinase III at 0.1mU/ mg, and the products were fractionated using a Superdex ™ peptide 7.5/300 small scale SEC column run (using an AKTA 10 purifier at a flow rate of 0.2 ml / min in 0.5 M ammonium hydrogen carbonate), monitoring the elution profile by absorbance at λ_{abs} = 232nm. Data was recorded using Unicorn 5.0 software and exported into SigmaPlot 11.

Subsequent to the test digestion and the analytical SEC, large-scale separation was conducted to obtain different size pools (Figure 3.20a). The SEC profile for the PMHS was shown to have more complex peaks than heparin and chemically modified heparins with some size fractions having multiple peaks. In addition, the profile did not display base line resolution, emphasising the heterogeneous nature of the HS.

Size assignment was carried out by PAGE (Figure 3.20b); however, Azure A staining for the small oligosaccharide sizes was poor due to their low sulfation (data not shown). Thus, PAGE alone was not sufficient to determine the exact oligosaccharide size. Therefore, Electro-spray mass spectrometry (ES-MS) analysis was conducted on these samples for further size confirmation (with assistance of Dr. Abdel Atrih).

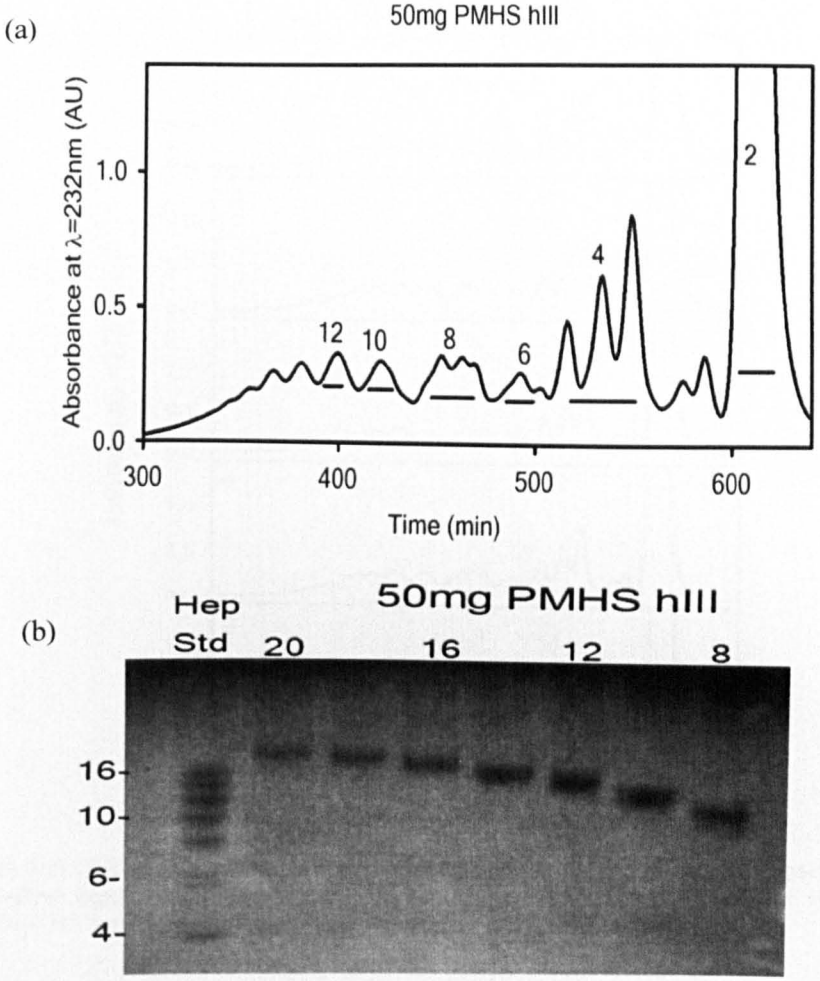

Figure 3.20 Size-exclusion chromatography profiles of heparinase III partial digests of PMHS a) Size-exclusion chromatography fractionation of heparinase partial digests of HS variants. b) Fraction pooling and PAGE analysis for size-exclusion chromatography fractionation of heparinase partial digests of HS variants. Briefly, 50 mg aliquot of 413 mg porcine mucosal heparan sulfate was digested with 0.1 mU/ mg (5 mU/ ml) of heparinase III for 2hr, adding a further 10 mU heparinase III and then again at 24 hours, before heating to 100°C to terminate digestion. Chromatography was carried out as described in Figure 3.13. Fractions across selected peaks were roughly estimated to contain HS/heparin saccharides displaying increasing degrees of polymerization (shown by even integers). More than 25 runs of 50 mg each were performed and the profiles were consistent.

Following SEC separation and size determination, scale-up production of SEC fractions was carried out; the separations were shown to be highly consistent (Figure 3.21). Relevant size-defined SEC fractions were then pooled and stored after desalting for further analysis. From the SEC profiles, it is clear that the peaks are more heterogeneous than for heparin.

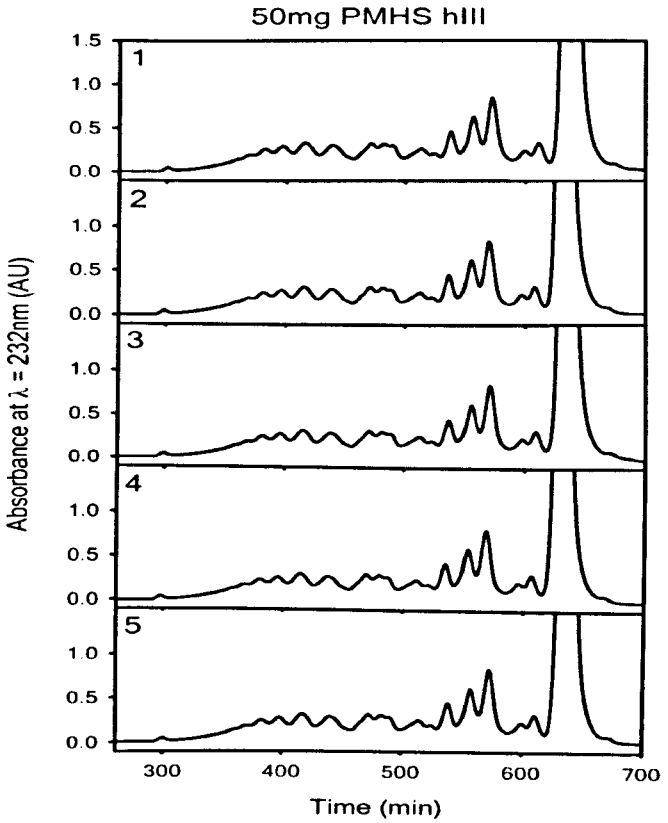

Figure 3.21 Size-exclusion chromatography profiles of five separate runs of heparinase III partial digest of PMHS. Partial digestion and chromatography was carried out as described in Figure 3.20.

Two SEC size pools (6-mer and 8-mer) were initially selected for further purification using SAX-HPLC. These particular sizes were selected due to previous investigations by many researchers confirming their interactions with FGF-1 and FGF-2 (Wong and Burgess, 1998; Sasaki *et al.*, 1999; Loo *et al.*, 2001; Ostrovsky *et al.*, 2002; Robinson *et al.*, 2005; Kreuger *et al.*, 2005).

One of the goals of this project is to generate oligosaccharides for structure-function studies for FGF-1 and FGF-2. Figure 3.22a shows the SAX profile of the 6-mer pool and Figure 3.23a the 8-mer pool. HS saccharides showed a spread of peaks across the gradient. Some of the peaks were single symmetrical peaks, others had shoulders, and some groups of 2-4 peaks bunched together, suggesting that they might represent isomers with slight structural variations.

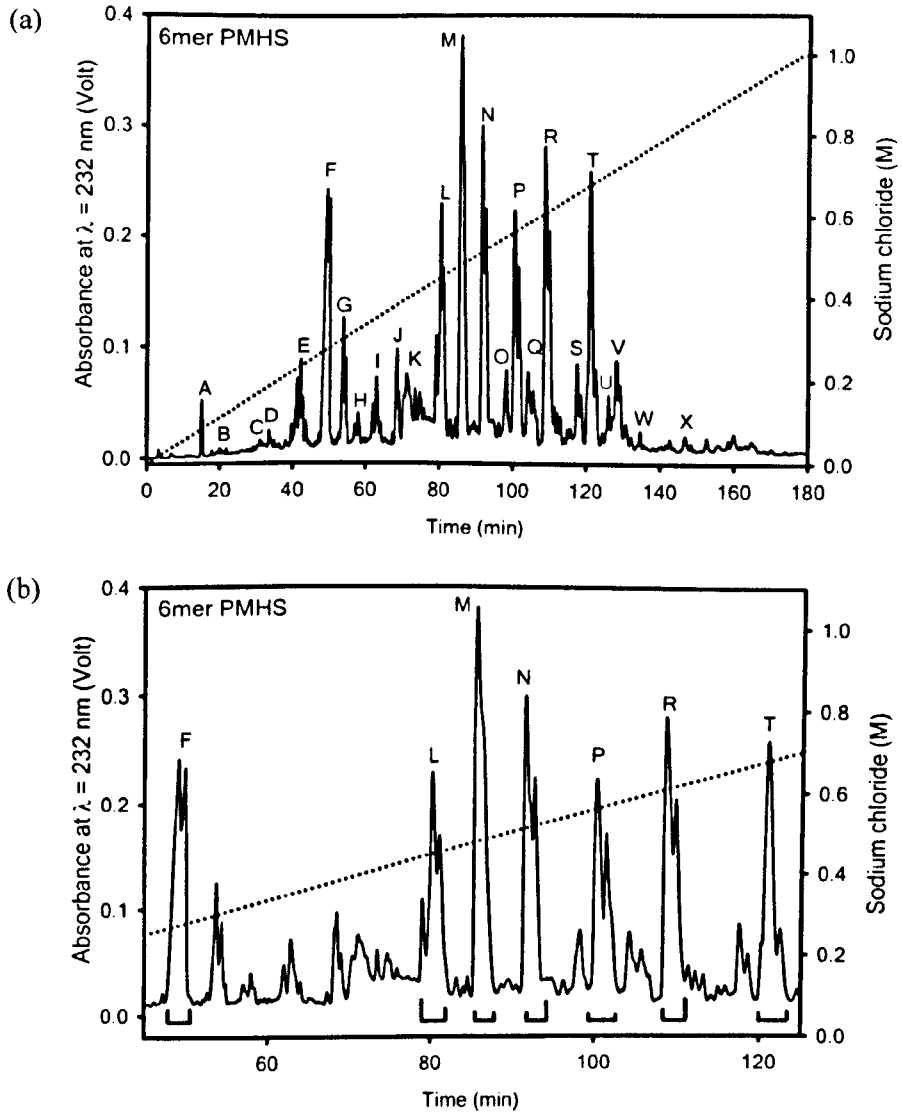

Figure 3.22 SAX-HPLC profiles for 6-mer PMHS gel filtration pool saccharides. 6-mer pools obtained by heparinase III digestion followed by SEC were further resolved by high resolution SAX-HPLC. Performed on Propac PA1 columns (9 x 250 mm) equilibrated in Milli Q H_2O, pH 3.5 at flow rate of 1 ml/min. Samples were eluted with a linear gradient of sodium chloride pH 3.5 (0 - 1 M over 180 min), detecting by absorbance at λ = 232 nm. A) Shows a typical preparative run. Multiple separations for 3 mg per run were performed and identical peaks labelled fractions corresponding to selected peaks were pooled. B) Shows a region of the porcine mucosal HS 6-mer SAX-HPLC chromatogram, where fractions were pooled for individual peaks, or across groups of partially resolved peaks. Fractions corresponding to selected peaks were pooled, desalted on Hiprep desalting columns, freeze-dried and quantified. Data were recorded using Shimadzu Class-VP 4.2.

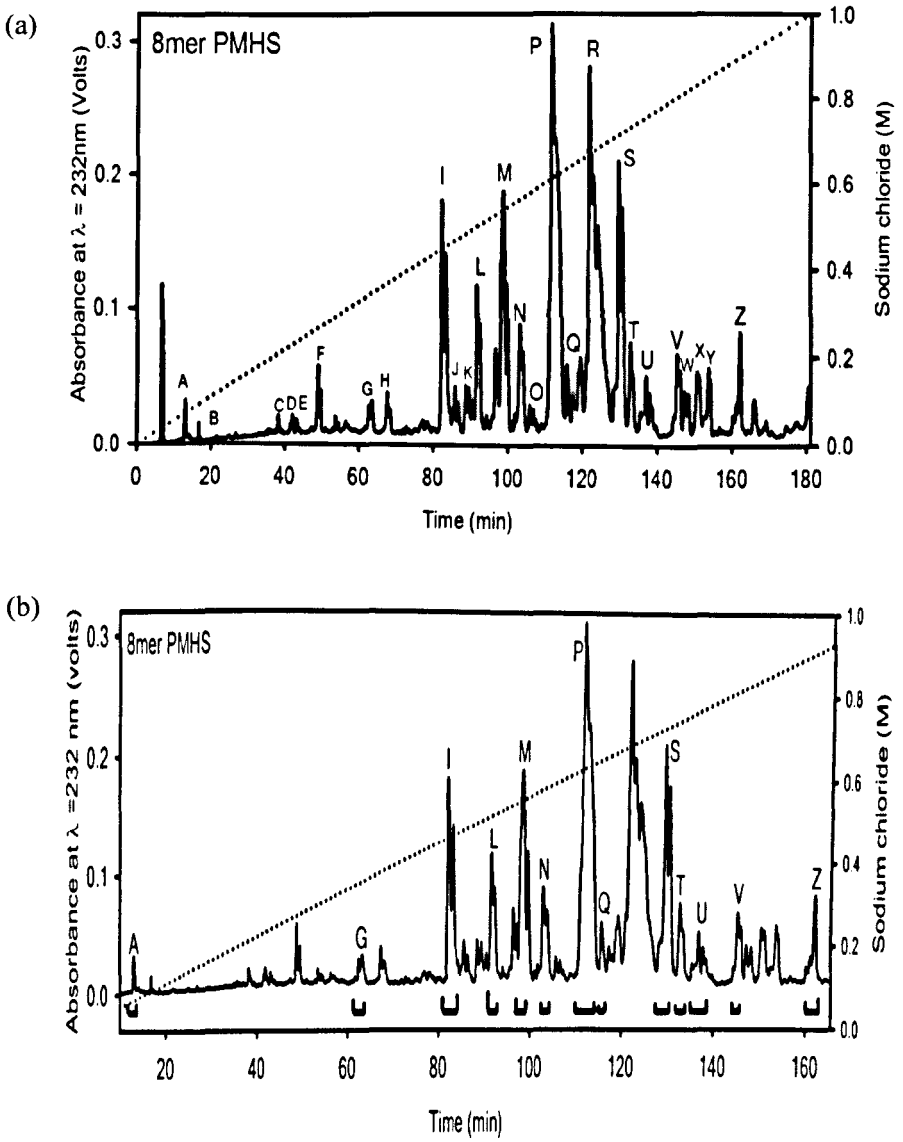

Figure 3.23 SAX-HPLC profiles for 8-mer PMHS gel filtration pool saccharide. 8-mer pools obtained by heparinase III digestion followed by SEC were further resolved by high resolution SAX-HPLC, as described in figure 3.24. A) Shows a typical preparative run. Multiple separations for 5 mg per run were performed and identical peaks labelled fractions corresponding to selected peaks were pooled. B) Shows a region of the porcine mucosal HS 8-mer SAX-HPLC chromatogram, where fractions were pooled for individual peaks, or across groups of partially resolved peaks. Fractions corresponding to selected peaks were pooled, desalted on Hiprep desalting columns, freeze-dried and quantified. Data were recorded using Shimadzu Class-VP 4.2.

Diversity in their structures was confirmed for several of them by disaccharide compositional analysis (Figure 3.24). Furthermore, there was still heterogeneity in HS oligosaccharide SAX-HPLC separation (Figure 3.22, 3.23), this issue can be resolved by collecting these contaminated peaks and applying an additional SAX-HPLC step using a series of SAX columns, and possibly using a shallower gradient.

Following SAX separations fractions were desalted and then quantified using the absorbance at λ_{abs}= 232 nm and the extinction coefficient for the non-reducing end double bond (5500 $mol^{-1}cm^{-1}$) (Linhardt *et al.*, 1988). Table 3.2 shows the estimated amount of SAX sub-fractions derived from 10 mg of 8-mer PMHS starting material. As seen in the table, the oligosaccharides were obtained in microgram quantities (varying from 11 to 970 μg, but most typically 50-100 μg); it should be noted that these amounts would limit the use of these oligosaccharides to appropriate interaction and biological assays, which do not require large amounts of material.

Disaccharide composition analysis was conducted for selected SAX fractions obtained from the 6-mer and 8-mer pools. These fractions were selected from the start, the middle and the end of the salt gradient. Figure 3.24 shows the disaccharide analyses profiles, and demonstrate the complex composition for each of the 6-mer and 8-mer fractions, consistent with expected structure variations. In addition, it shows that these saccharides have a minor trisulfated disaccharide content compared to heparin. This structural variability is explored further in Chapter 5.

Selected fractions of SAX-HPLC generated 6-mer and 8-mer PMHS were used in FGF-1 and FGF-2 interaction and activity studies (Chapter 5; Turnbull, 2010 #5650}. In addition, 6-mer and 8-mer PMHS were subject to sequencing using a method developed by Dr. Atrih involving tag separation, HS degradation enzymes and mass spectrometry (Atrih et al, manuscript in preparation). Selected 6-mer and 8-mer PMHS fractions were also used in glyco-microarray development.

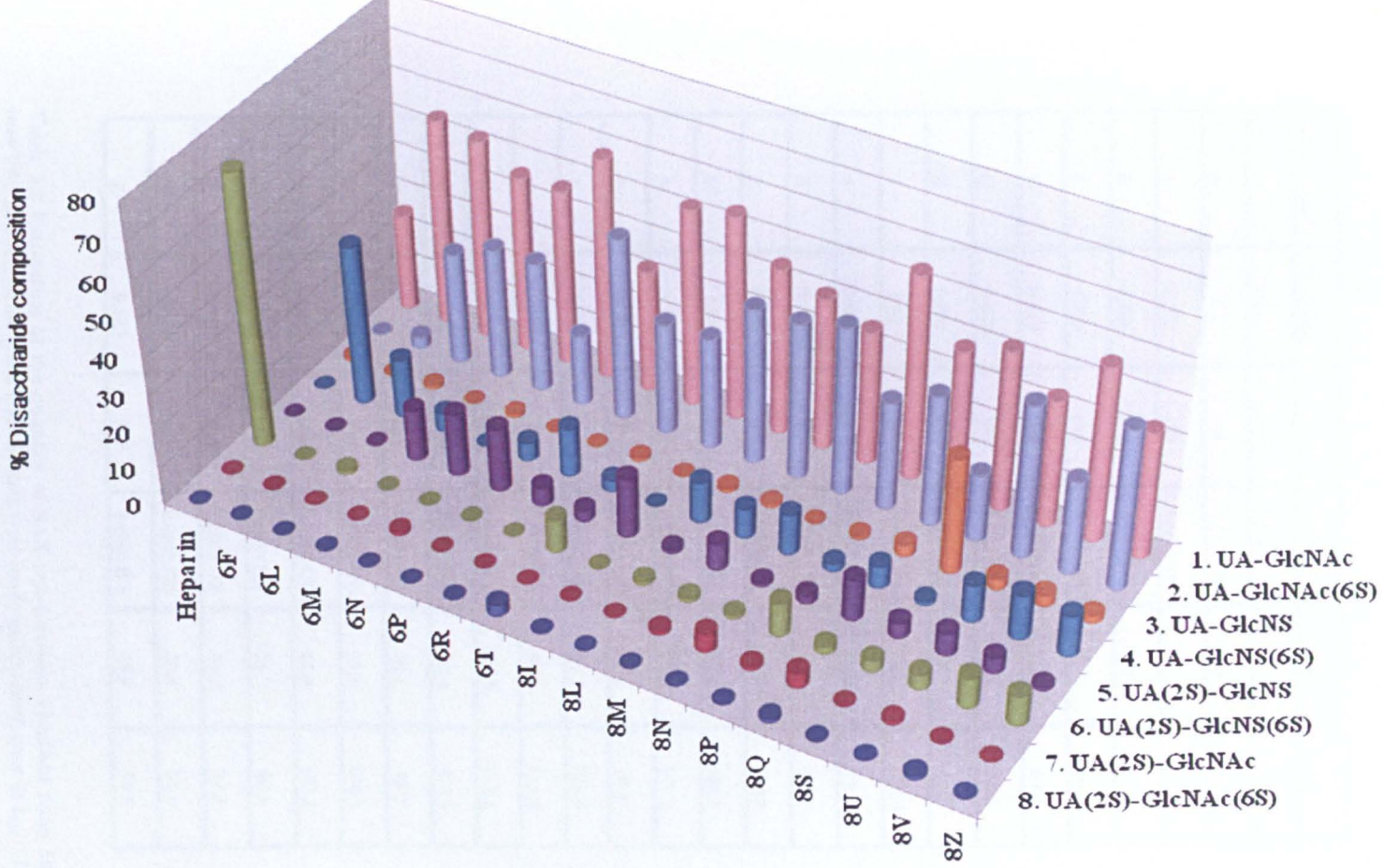

Figure 3.24 Disaccharide composition profiles of selected SAX-HPLC purified 6-mer and 8-mer PMHS saccharide fractions. Disaccharide composition was determined by SAX-HPLC with reference to authentic standards, as described in Figure 3.15.

8mer PMHS	A. 232nm	µls	moles/l	nmol	µg
A	0.518	100	9.42E-05	9.4	20.7
B	0.4	100	7.27E-05	7.3	16.0
C	0.532	100	9.67E-05	9.7	21.3
D	0.286	100	0.000052	5.2	11.4
E	0.399	100	7.25E-05	7.3	16.0
F	0.618	200	0.0001124	22.5	49.4
G	0.683	200	0.0001242	24.8	54.6
H	0.802	200	0.0001458	29.2	64.2
I	0.92	500	0.0001673	83.6	184.0
J	0.896	200	0.0001629	32.6	71.7
K	0.646	200	0.0001175	23.5	51.7
L	0.562	600	0.0001022	61.3	134.9
M	1.06	900	0.0001927	173.5	381.6
N	1.08	300	0.0001964	58.9	129.6
O	0.76	200	0.0001382	27.6	60.8
P	1.05	2300	0.0001909	439.1	966.0
Q	0.925	300	0.0001682	50.5	111.0
R	1.03	1500	0.0001873	280.9	618.0
S	1.01	1000	0.0001836	183.6	404.0
T	0.727	200	0.0001322	26.4	58.2
U	0.868	400	0.0001578	63.1	138.9
V	0.86	300	0.0001564	46.9	103.2
W	0.706	200	0.0001284	25.7	56.5
X	0.953	200	0.0001733	34.7	76.2
Y	0.645	200	0.0001173	23.5	51.6
Z	0.823	300	0.0001496	44.9	98.8

Table 3.2 Estimation of the quantity of SAX sub-fractions obtained from 10 mg of 8-mer PMHS saccharide pool. Calculations were made using absorbance at λ_{abs}= 232 nm and the extinction coefficient for the double bond (5500 $mol^{-1}cm^{-1}$).

3.3 Discussion

HS has been shown to interact with hundreds of proteins (Bishop *et al.*, 2007; Capila and Linhardt, 2002; Ori *et al.*, 2008). Nevertheless, the variable structures/ sequences of HS polysaccharide chains made it difficult to interpret the selectivity of these interactions, due to the structural diversity along the chain and between individual chains, as well as the potential presence of multiple protein binding sites within one chain. Therefore, oligosaccharides produced from chains by enzyme or nitrous acid cleavage would simplify this task and enable the minimum size of HS sequences required for binding and activity to be explored (Powell *et al.*, 2010). Oligosaccharides can also be used to investigate the selectivity of HS-protein interactions by determining the sequences of oligosaccharides that bind, and activate or inhibit particular proteins.

Here it has been demonstrated that, oligosaccharides can be produced from heparin, chemically modified heparin and HS chains, exploiting partial enzymatic or chemical cleavage it should be noted that both methods produced unnatural terminal residues, and partial digestion of heparin, chemically modified heparin and HS polysaccharides influenced the composition of the resulting oligosaccharide mixtures generated.

Enzyme partial digestion produces a Δ 4, 5-unsaturated uronic acid derivative at the non-reducing end which has the advantage of being a chromophore (λ absorbance = 232 nm), but results in loss of identity of both uronic acid monosaccharides (GlcA and IdoA), each giving the same product structure. Oligosaccharides produced by enzymatic cleavage were found to be easy to monitor and to quantify due to the action of the heparinases enzymes (Linhardt *et al.*, 1988; Linhardt *et al.*, 1986; Linhardt *et al.*, 1990). The cost of heparinases I, II and III used in the enzymatic partial digestion is high compared to nitrous acid. Therefore, a great deal of time was spent on optimizing the reaction conditions. Trial digests proved to be very useful to determine the minimum amount of enzyme needed and the optimum conditions required for digestion.

Recombinant protein expression has been used to produce heparinase enzymes. Therefore, a quality control procedure was needed to compare enzymes from batch to batch before use. Partial enzymatic digestion proved helpful in generating large quantities (milligrams) of heparin oligosaccharides as shown in Figure 3.5a and b. The peaks were relatively well resolved especially for sizes range between 2-12-mers, and to a lesser extent to 14-20-mers. This was an advantage because most known proteins that bind to HS require between 4-12-mer oligosaccharides. Mass production of heparin oligosaccharides by enzyme generation required grams of starting material. PAGE analysis was used for size assignment, and proved to be a valuable size screening method, however, disaccharides has a low molecular weight, around 576 Dalton, and hence runs too fast on the gel (before other sizes are resolved), so it is not recommended to separate large and small oligosaccharides on the same gel. Disaccharides from different species run the same as the commercially available disaccharide standards (Dextra Labs) (results not shown). PAGE analysis was useful in quality control and pooling samples of the same oligosaccharide sizes and the same species as shown in Figure 3.5c and d. However, PAGE is not able to determine the absolute size, and another method such as mass spectrometry is needed for confirmation. Thus, in this thesis, heparin oligosaccharides produced by SEC were also analysed by ES-MS with the help of Dr. A Atrih and Miss R Miller (see Appendix 1). Furthermore, a MALDI-TOF mass spectrometry technique was developed for analysing highly sulfated heparins using oligosaccharides generated by partial enzyme digestion, in collaboration with Dr. B Tissot (Imperial College, London) (Tissot *et al.*, 2007).

Nitrous acid partial digestion of heparin yields an oligosaccharide with a 2, 5 anhydromannose residue at the reducing end, which has the advantage of been highly reactive, while leaving the non-reducing end uronic acid moiety unaffected. This particular set of oligosaccharides was very useful in labelling and immobilization on surfaces; via their reducing ends in the latter case the remaining oligosaccharide is available to interact with proteins. However, a disadvantage is the difficulty of oligosaccharide detection due to lack of a strong chromophore.

Thus, it is wise to label these oligosaccharides at the reducing end with fluorophores to improve the sensitivity of detection, or to work with limited detection sensitivity and exploit the reactivity of the reducing end in other ways. Zhi et al (2006) have used heparin 10-mer saccharides generated by nitrous acid digested on a gold microarray platform and found that they had better detection sensitivity compared to the enzyme digested oligosaccharides (Powell *et al.*, 2009; Zhi *et al.*, 2006). In addition, these type of oligosaccharides (due to their reactive reducing end) were easy to label and this was useful in competition assays (e.g. competition ELISA where oligosaccharides were labelled with biotin and immobilized on the streptavidin coated ELISA plate); the same principle was used in competition biosensor assays (Ostrovsky *et al.*, 2002; Powell *et al.*, 2002).

SEC was used in the primary fractionation of partial digested oligosaccharides with ammonium hydrogen carbonate as the running buffer to prevent the interaction of oligosaccharides with the column matrix and improve resolution. It is noticeable that the SEC chromatograms did not achieve baseline resolution for most heparin variants and HS. In addition, the ammonium hydrogen carbonate has high pH, and it is well known that HS structure is sensitive to high pH (Liu and Perlin, 1992; Skidmore *et al.*, 2009). Hence, development of a new SEC buffer would be an advantage. The SEC matrix used in this project was Superdex 30™ which, has proven to be a tough reliable matrix (the column used in this project continues to be useful after for more than six years). However, the resolution was not as high as with BioGel P10, which was previously used in separating HS oligosaccharides (Guimond and Turnbull, 1999). The problem with the P10 columns is that they are only effective for a few runs and then become unreliable due to the more fragile matrix; also, they ran at much lower flow rates compared to Superdex 30™. Thus, an improvement in the resolution of Superdex 30™ column would be useful. Despite that, large oligosaccharides from heparin and HS have molecular weights less than 10 kDa (e.g. 20-mer heparin ~ 5.760 kDa) which positions them within the Superdex 30™ separation range.

The oligosaccharides always have larger hydrodynamic radius than anticipated (i.e. the 10-mers have molecular weights of about ~ 2.880 kDa but a hydrodynamic radius similar to ~19.5 kDa globular proteins (Robinson *et al.*, 2005). Thus using Superdex™ matrix (for it is durability) with different pore sizes can be beneficial. There are ranges of Superdex™ matrixes available on the market include Superdex™ 75 (separation range 3-70 kDa) and Superdex™ 200 (range between 10-600 kDa). Thus, in order to improve resolution, two Superdex™ columns with different pore sizes could be connected, so if Superdex™ 75 (larger pores sizes) were connected in series with Superdex™ 30 (smaller pores sizes) this could improve the separation and purity of larger oligosaccharides. In some of the SEC profiles there are noticeable broad peaks just before 300 minutes of elution time, which is expected to be undigested polysaccharide chains; the application of methods such as ultra filtration could possibly improve the SEC separation by removing undigested material prior to chromatography.

In contrast to enzyme-generated oligosaccharides, the peaks obtained by nitrous acid depolymerisation are more complex, as shown in Figure 3.11a. The peaks were less resolved, which implies requirements for more starting material if large amounts of oligosaccharides are desired. In addition, some peaks have multiple small peaks within a size class, which may reflect the complex mixture of structures within each size fraction. One other issue is the presence of the huge salt peak (Figure 3.13); it is not known whether salt interferes with the oligosaccharide separation. Hence, a desalting step before conducting the SEC may be required.

Subsequent to SEC fractionation, some selected sizes were further purified according to their charge using SAX-HPLC, eluting with a linear gradient of sodium chloride. Here, the separation was performed at pH 3.5, so that the carboxylate groups of the uronic acids would be protonated, making the SAX separation depend solely on the sulfation content and patterns. The acid needs to be neutralized as soon as possible after separation because low pH could affect the chemical structure by de-N-sulfation (Drummond *et al.*, 2001; Liu and Perlin, 1992).

It is also worth taking into consideration the amount of neutralizing materials used because if there is excess base, this could also alter the structure of the saccharides by forming an epoxide between C-2 and C-3 of the IdoA2S (Jaseja *et al.*, 1989).

The Propac PA1 columns were used in all SAX-HPLC separations as they have proved to give the most reliable and high-resolution oligosaccharide separations, with consistent profiles and elution times. The cost of this column compared to other SAX columns is high. However, it represents good value for money when reliability and longevity are considered (lasting for over 10 years with consistent usage and several hundreds of runs performed). A hindrance in using this column is the limited temperature range, which, according to the manufacturer is a maximum of 40 °C; thus, using a higher temperature (50 °C) which could improve the SAX separation, is not possible. The maximum flow rate restriction for both Propac PA1 columns (analytical and preparative) necessitates a lengthy gradient. The maximum amount that can be loaded on the preparative column is about 5 milligrams; this may be insufficient if large quantities of SAX purified saccharides are needed.

SAX chromatogram profiles of BLH 4-mer, 6-mer, 8-mer and 10-mer (Figure 3.9) showed an increase in the complexity of the SAX profile with the size of the oligosaccharides. In addition, the tri-sulfated peaks (the two adjacent peaks between 115 and 135 minutes elution) have been analysed by mass spectrometry and found to have the same number of sulfates, hence, the split peaks could be classed as anomers or structural isomers, with both peaks being tri-sulfated species. Figure 3.8 shows SAX profiles of two 12-mer heparin from different sources PMH and BLH, enzyme digested fractions, separated by SEC in the same way. However, there was a difference in their SAX profiles. This observation demonstrates the complexity of heparin between species.

Chemically modified heparins were partially digested using either an enzyme (heparinase II) or nitrous acid. Figure 3.17a shows the chromatograms of four of the chemically modified heparins digested by heparinase II; it is clear that each one of the chemically modified heparins has its unique profile. It is also noticeable that in the four profiles the peaks are not single peaks. In addition, the elution times of the disaccharides varied with each compound.

Figure 3.17b shows the PAGE analysis of the pooled fractions from Figure 3.17a; the gel shows there is a step increase in size from small in the bottom to the large sizes at the top. However, there could be missing bands at the bottom of the gels that may not stain with Azure A due to low sulfation, or low molecular weight, or both. In addition, the oligosaccharide size standards used for all gels were BLH enzyme partially digested, which will not have the same structure, as for the chemically modified heparins. Hence, this method will not give an accurate size determination of the SEC fractions. Nitrous acid partial digestion of chemically modified heparins creates another challenge as the peaks are not well resolved and more complex, with many sub-peaks (Figure 3.18a). The PAGE analysis (Figure 3.18b) for the pooled peak fractions was also less clear. For all these reasons, a new method for size determination was needed. One of the methods could be mass spectrometry; however, it is not always available and requires experience and sophisticated equipment. The simple method mentioned in section 3.2.2 provides a solution to the challenge of size determination.

The structure and the purity of the chemically modified heparins were confirmed by NMR spectrometry (information from Dr. Yates). However, disaccharide composition analysis was performed to evaluate the heterogeneity of modified heparins. There was typically about 5 % heterogeneity according to the disaccharide compositional analysis (Figure 3.16). It is not known if this 5 % will hinder interpretation of data from using these modified saccharides or not, but since HS-protein interactions are thought be quite subtle in detecting small differences, these residual amounts of non-modified saccharides should be considered, and the data should not be over-interpreted.

SEC chromatogram of PMHS is shown in Figure 3.20a, and is more complex than for heparin saccharides, with the peaks less well-resolved, split peaks and with minor peaks in between large peaks. The PAGE analysis revealed that what was thought to be an 8-mer was a 6-mer and the smaller sizes failed to stain by Azure A.

Applying PMHS SEC fractions to any assay will be challenging due to the complex mixtures they contain. Thus, SAX-HPLC was introduced. PMHS SAX chromatogram profiles showed structures that are more complex and the peaks spread across the whole gradient, compared to the heparin SAX profile (Figure 3.9), indicating the heterogeneity and diversity within the PMHS SAX saccharide structures. In addition, PMHS requires less salt to elute compared to that of heparin with the full SAX separation of the PMHS occurred at around 0.9 M NaCl while in heparin, around 1.5 M NaCl is required (Figure 3.22 and Figure 3.9). This observation indicated as expected that there are fewer sulfates in PMHS saccharides than heparin ones. The SAX pooling procedure is shown in Figure 3.22b and 3.23b, although some SAX-purified peaks represent single oligosaccharides of high purity, other contain shoulders or multiple peaks, which could be due to the presence of anomers (α and β) or structural isomers. Here, it is recommended that an additional SAX run with the same gradient be performed if extra-pure oligosaccharides are required. However, it is wise to consider the quantity of the starting materials and the potential losses.

Compositional disaccharide analysis of the 8-mer PMHS SAX-HPLC fractions (Figure 3.24) demonstrated that each peak has unique sulfate content, and all of these structures have lower levels of sulfation compared to heparin. Hence, these saccharides would be model candidates for HS-protein selectivity studies. Table 3.2 shows the amount of purified 8-mer PMHS SAX fractions, it is clear that the quantities were typically in micrograms, the completely recovered amount is about 40 % of the starting material. Hence, more than a half of the starting material was lost in the multi-step separation procedure.

These quantities from SAX fractions limit the variety of assays that can be used. However, microarrays would be an ideal technique for utilizing these quantities of oligosaccharides, and in recent years, our lab has been involved in developing microarray techniques using two platforms (aminosilane and gold) (Zhi *et al.*, 2008; Zhi *et al.*, 2006).

A major concern of using SAX-HPLC as a method for further fractionation for oligosaccharides is elution with sodium chloride, which could be an obstacle even after desalting, in terms of determining the structure of the oligosaccharides by mass spectrometry. The sodium adduct present in the SAX oligosaccharides can interfere with the mass determination (Dr. Atrih, personal communications). Using an alternative method employing volatile buffers such as ion pairing reverse phase high performance liquid chromatography IPRP-HPLC would be an option, as the volatile buffer will not interfere with mass spectrometry analysis.

SEC oligosaccharides were desalted using commercially available columns (Hiprep™ Desalting 26/ 10, GE Healthcare) to speed up oligosaccharide production. This step can be replaced by serial lyophilisation, as the ammonium hydrogen carbonate is volatile and can be removed by three cycles of freeze-drying. However, serial lyophilisation is not an option in the case of SAX fractions because the elution buffer is sodium chloride, which it is not volatile. There are always losses of between 1-5% of oligosaccharides in the desalting step. This is acceptable if heparin and chemically modified heparins were used as the starting materials; however if precious tissue HS is used any loss will be undesirable. Ultimately, pure oligosaccharides are needed, so it is advisable to use a combination of techniques to obtain single purified species.

From what has been mentioned in the results and discussion, a wide range of applications would benefit from generating these saccharide libraries. Oligosaccharide libraries have also contributed to other projects; examples of these projects are listed in Appendix 2. It is clear that they have a major potential as model structures and are useful in a variety of interaction investigations, with a wide range of heparin binding proteins, whose number continue to increase.

Finally, producing HS oligosaccharide libraries is a laborious technique with microgram amounts being prepared from grams of starting materials. However, finding sequences with unique protein regulation characteristics would justify the hard work.

4 Chapter four: Involvement of Heparan Sulfate in Slit-Robo Interactions and Activity

4.1 Introduction

4.1.1 Background

Slits are a family of large proteins secreted by midline glial cells that are ligands for a transmembrane protein called roundabout (Robo) (Wang *et al.*, 1999). Slit and Robo play a major role in the nervous system, for example, regulating the growth of axons and their guidance to the correct region of the brain; they also function as a repellent, preventing axons from crossing to non-targeted areas (Keleman *et al.*, 2002; Wang *et al.*, 1999). In addition, axon branching and migration of neurons have been found to be influenced by Slit and Robo interactions (Young *et al.*, 2004). Furthermore, Slit and Robo have been shown to have many other regulatory functions such as inhibition of the chemokine-induced chemotaxis in leukocytes (Wu *et al.*, 2001) and endothelial cell migration (Fernandis and Ganju, 2001; Wu *et al.*, 2001). Organs such as heart, lung and kidney require Slit and Robo for their development (Xian *et al.*, 2001; Grieshammer *et al.*, 2004). Slit and Robo also play an important role in inflammation, angiogenesis, and tumour metastasis (Yang *et al.*, 2003).

4.1.2 Slit

Slit was first discovered in *Drosophila* (Wang *et al.*, 1999). Slit homologues are found in *C. elegans* and various vertebrate species such as fishes, birds and mammals (Hao *et al.*, 2001; Vargesson *et al.*, 2001; Yee *et al.*, 1999; Zugmaier *et al.*, 1999). There are three genes encoding Slit. Slit-1, Slit-2 and Slit-3 were isolated from mammals and a single Slit from invertebrates (Itoh *et al.*, 1998; Wang *et al.*, 1999). Slits from different species have about 60 % sequence homology and they all encode a large extracellular matrix (ECM) glycoprotein of about 200 kDa (Wang *et al.*, 1999; Zugmaier *et al.*, 1999; Niclou *et al.*, 2000).

Slit are multi-domain proteins incorporating, from their N-terminus to C-terminus, four leucine rich repeats (LRR) joined by disulfide bonds and seven (invertebrate) to nine (vertebrate) epidermal growth factor (EGF) repeats. Also, an ALPS domain (Agrin-Laminin-Perlecan-Slit) or laminin G-like module one (invertebrate), or three (vertebrate) between EGF-6 and EGF-7, and a cysteine knot (Howitt *et al.*, 2004; Kobe and Kajava, 2001; Nguyen-Ba-Charvet *et al.*, 2002) (Figure 4.1).

Proteolytic cleavage of Slit-2 was observed between EGF-5 and EGF-6 producing two fragments, a large N terminal fragment (140 kDa) and a small C terminal fragment (55-60 kDa) (Nguyen Ba-Charvet *et al.*, 2001).

Crystallography studies have uncovered the crystal structures of D2, D3 and D4 of the Slit LRR domains (Howitt *et al.*, 2004; Morlot *et al.*, 2007). Every LRR domain is made of an N-terminal cysteine-rich cap, a range of five to seven LRRs, and a C-terminal cysteine rich cap. Each LRR includes a central LXXLXLXXN motif that donates one β-strand to the coiled sheet that makes up the concave face of the LRR domain (Howitt *et al.*, 2004; Kobe and Kajava, 2001). The four LRR domains of Slit are joined by small linkers containing a cysteine residue that forms a disulfide link with the cysteine residue at the convex back of the previous domain (Howitt *et al.*, 2004).

Drosophila Slit, human Slit-2, Slit-3 and Slit-1 (Itoh *et al.*, 1998; Little *et al.*, 2002; Tanno *et al.*, 2004) all have other spliced transcripts. In zebrafish, two Slit-1 isoforms were recognized because of gene duplication (Hutson *et al.*, 2003). There are two mammalian Slit-2 isoforms originating in the brain, a large 200 kDa and small 150 kDa (Slit-2-N), the small one being due to the proteolytic cleavage of full-length Slit-2 (Niclou *et al.*, 2000; Wang *et al.*, 1999; Zugmaier *et al.*, 1999). Slit cleavage fragments appear to have different cell organization characteristics, the shorter C-terminal fragment is more diffusible and both the larger N-terminal fragment and the full-length form are more firmly associated with the cell (Whitford *et al.*, 2002).

Distinct Slit fragments have different binding properties and thus different functional activities. This finding is supported by *in vitro* data showing that the full length Slit-2 functions as a competitor of Slit-2 N-terminus fragments in the dorsal root ganglion (DRG) branching assay, and that Slit-2 N-terminus, not full-length Slit-2, causes collapse of olfactory bulb (OB) growth cones (Whitford *et al.*, 2002). Structure function investigations in vertebrates and *Drosophila* demonstrated that the LRRs of Slits are necessary and sufficient to mediate their repulsive activities in neurons (Couchman *et al.*, 2001; Nguyen Ba-Charvet *et al.*, 2001). Recently, in-depth structure function analysis of the LRR domains of *Drosophila* Slit, revealed that the active site of Slit is located on the second of the four LRR (D2) (Howitt *et al.*, 2004), which is highly conserved between Slits. Slit can also dimerize through the D4 domain and the cysteine knot (Tanno *et al.*, 2004).

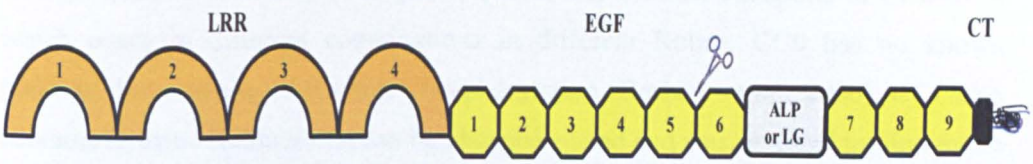

Figure 4.1 Schematic showing the domain structure of Slit. LRR, leucine-rich repeat; EGF, epidermal growth factor-like domains; ALPS domain (Agrin-Laminin-Perlecan-Slit)LG, laminin G-like domain; CT, C-terminal cystine-knot. A pair of scissors indicates the proteolytic cleavage site of Slit.

4.1.3 Robo

The earliest Robo gene was recognized in *Drosophila* during an inclusive screen for genes controlling midline crossing in the central nervous system (CNS) (Seeger *et al.*, 1993). There is a single Robo in C. *elegans* (SAX-3) (Hao *et al.*, 2001), whereas, there are three Robo genes found in *Drosophila*, Zebrafish and chick (Piper *et al.*, 2000; Simpson *et al.*, 2000; Vargesson *et al.*, 2001; Yuan *et al.*, 1999). Mammals have four Robos (Robo1-4) (Huminiecki *et al.*, 2002). Robo proteins belong to the immunoglobulin (Ig) superfamily.

They have five Ig like domains followed by three fibronectin type III (FNIII) repeats, a transmembrane part and an extended intracellular tail containing up to four conserved cytoplasmic motifs, CC0-CC3, with no recognizable catalytic domains (Figure 4.2) (Bedell *et al.*, 2005; Huminiecki *et al.*, 2002). The first two Ig domains are the most highly conserved parts and are found in the Robo-4 (or magic roundabout) which is expressed exclusively by endothelial cells and plays a part in angiogenesis (Thomas *et al.*, 2003). Robo-4 lacks the last three Ig domains, some of the FNIII domains and the CC1 and CC3 motifs found in other Robo proteins. The interaction of Robo-4 with Slit is not documented (Thomas *et al.*, 2003; Suchting *et al.*, 2005). The crystal structures are available for IG-1 and IG-2 of human Robo-1 and of *Drosophila* Robo. They show two canonical I-set Ig domains with evidence of considerable flexing at the domain junction (Fukuhara *et al.*, 2008).

The cytosolic Robo domains are poorly preserved, with the exception of CC0-CC3, which occur in different combinations in different Robos. CC0 has no known function, but is a site of tyrosine phosphorylation (Bashaw *et al.*, 2000). CC1 also contains tyrosine residues that can be phosphorylated and was revealed to bind to the P3 domain of the netrin-1 receptor, which is known as deleted in colorectal cancer (DCC) (Yunmbam and Wellstein, 2001). CC2 is a proline-rich sequence that matches the consensus-binding site for *Drosophila* Enabled (Ena); CC3 is also a polyproline stretch (Piper *et al.*, 2000). *Drosophila* Robo-2 and Robo-3 lack the CC2 and CC3 domains (Rajagopalan *et al.*, 2000; Simpson *et al.*, 2000) and the second half of CC2 is also not preserved in mouse and Zebrafish Robo-3. In addition, mouse Robo-3/ Rig-1 (Rig-1 for retinoblastoma inhibiting gene 1) lacks the CC1 motif (Yuan *et al.*, 1999), however, Zebrafish Robo-3 has the CC1 motif (Sleeman *et al.*, 2001). Furthermore, there are some spliced variants of mouse Robo-3/ Rig-1 (Couchman *et al.*, 2001) (Figure 4.2).

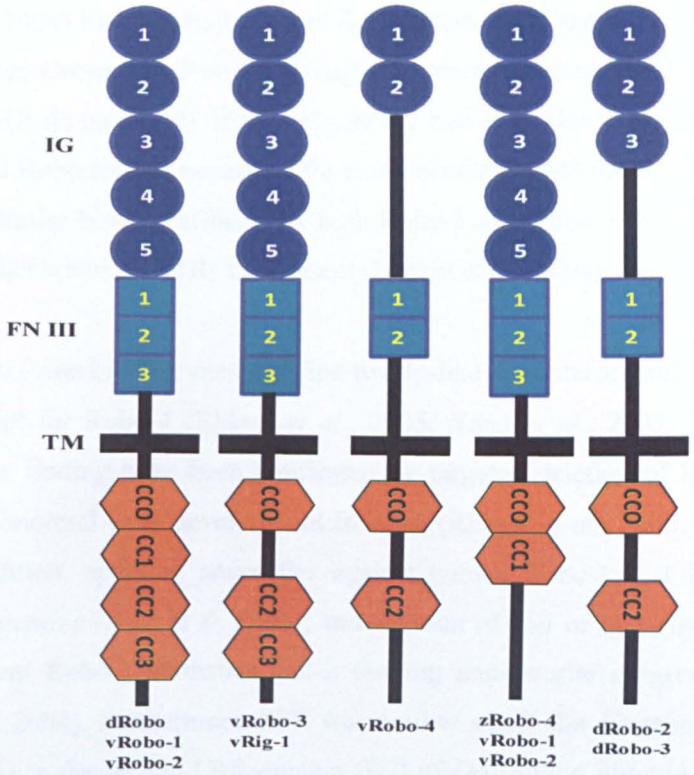

Figure 4.2 Schematic showing the domain structure of Robo. Robo IG1-5, immunoglobulin-like domains; FN3, fibronectin type 3-like domain; TM, transmembrane; CC0–3, conserved cytosolic motifs (d: *Drosophila*; v: Vertebrate; z: Zebrafish).

4.1.4 Slit and Robo binding

Many biologically important processes such as the crossing of axons at the midline are dependent on Slit interactions with Robo (Dickson and Gilestro, 2006; Tessier-Lavigne and Goodman, 1996). Genetic and biochemical data established that Slit is a ligand for the *Drosophila* Robo-1 and Robo-3 receptors (Hussain *et al.*, 2006). Slit and Robo bind to each other with dissociation constants of about 10 nM (Hohenester, 2008). The Slit and Robo interaction is evolutionarily conserved because *Drosophila* Slit can bind mammalian Robos, and the other way round (Hussain *et al.*, 2006). In addition, proteolytically cleaved Slit C-fragments do not bind to the Robo (Xian *et al.*, 2001). Several studies have shown that the LRR domains of Slit are necessary for Robo binding and biological activity *in vitro* (Couchman *et al.*, 2001; Zhang *et al.*, 2001b).

Howitt et al (2004) have studied Slit and Robo interactions and mapped the binding site for all three *Drosophila* Robos to a highly protected area on the concave face of the second LRR domain (D2) of Slit (Figure 4.1 and 4.2). However, FNIII domains and dimerized Robo are not necessary for Robo binding to Slit (Howitt *et al.*, 2004). Slit D2 has similar binding affinity for both Robo-1 and Robo-3. Nevertheless, Slit affinity is higher when all LRRs are present (Howitt *et al.*, 2004).

With regard to Robo binding sites, the first two Ig-like domains are important for Slit binding, except for Robo-4 (Rhiner *et al.*, 2005; Yang *et al.*, 2003; Zhang *et al.*, 2001b). These finding have been confirmed by targeted deletion of Ig-1 and Ig-2 resulting in abnormal lung development in mice (Rhiner *et al.*, 2005; Yang *et al.*, 2003). In addition, applying antibodies against human Robo-1 Ig-1 blocks Slit-2 tumour angiogenesis (Xian et al, 2003); and deletion of Ig-1 or Ig-2 (Ig-like domain 2) from human Robo-1 abolishes Slit-2 binding and neurite outgrowth *in vitro* (Tiwari *et al.*, 2004). Furthermore, SPR was used to verify the direct interactions in real time between the second LRR domain (D2) of *Drosophila* Slit and the Ig-1 and Ig-2 of the *Drosophila* Robo (Tiwari *et al.*, 2004). The other domains did not interact with Slit. The dissociation constant for the Slit-Robo complex was in the micromolar range, suggesting that the interaction between the full-length proteins is significantly enhanced by oligomerization of Slit and Robo (Hohenester, 2008). None of these studies provides a clear understanding of how the binding of Slit to the ectodomain of Robo translates into an intracellular signal. However, there are some suggested mechanisms of action; that Slit binding could result in Robo clustering, disorder of the preformed Robo oligomer, or induction of conformational changes in Robo without affecting the oligomeric status (Hohenester, 2008).

4.1.5 Slit/ Robo/ HS

Several studies suggest that Slit-Robo signalling strictly requires HS (Song *et al.*, 2004). Slit-Robo signalling *in vitro* can be eliminated by enzymatic degradation of cell-surface HS (Piper *et al.*, 2006; Zhang *et al.*, 2001b).

In addition, Slit-Robo signalling *in vivo* can be abolished by genetic removal of enzymes involved in HS biosynthesis, or of HSPG core proteins (Bulow and Hobert, 2004; Inatani *et al.*, 2003; Li *et al.*, 2004; Steigemann *et al.*, 2004). Genetic research in *Drosophila* has suggested that HSPG syndecan controls both the distribution and efficiency of Slit (Li *et al.*, 2004). However, syndecans have not been implicated in regulation of mammalian Slits. Instead, glypican-1 HSPG has been identified as the controller of receptor for human Slit-2; it has been shown that both cleavage fragments of Slit-2 are recognized by glypican-1 (Ronca *et al.*, 2001).

HS/ heparin binding sites were mapped for two different regions of the *Drosophila* Slit, the N-terminal LRR domains D1 and D2, and the C-terminal cystine knot domain (Steigemann *et al.*, 2004). The C-terminal domain has stronger preference for HS, however, it is unlikely to account for its strict Slit-Robo signalling function, supported by the fact that the N-terminal and not the C-terminal Slit fragment is biologically active *in vitro* (Ronca *et al.*, 2001). HS binding to Slit D2 could be the key to understanding HS involvement in Slit and Robo signalling as this domain also contains the Robo binding site (Zhang *et al.*, 2001b). Hussain et al (2006) found that *Drosophila* Slit D2 and Robo IG-1 and IG-2 linked with a 10-mer heparin oligosaccharide in solution formed a ternary complex of 1:1:1 stoichiometry (Hussain *et al.*, 2006). This complex appears to summarize the signalling complex at the axon cell membrane. These residues are in a conserved basic patch in the C-terminal cap of the human Slit-2 D2 (Lys 461, Arg 462, Lys 466, Arg 467, Lys 472 and Lys 475) are required not only for heparin binding, but also for the HS-dependent Slit-2 D2-induced collapse of *Xenopus* retinal axon growth cones *in vitro* (Hussain *et al.*, 2006). The crystal structure of the ternary Slit-Robo-HS signalling complex is still under investigation. However, the crystal structure of the binary complex of human Slit-2 D2 and Robo1 IG1 have shown that the HS-binding site of Slit-2 D2 remains fully uncovered and formation of a ternary complex is thus structurally possible (Morlot *et al.*, 2007).

Robo residues involved in HS binding have not been recognized but are likely to exist, given that *Drosophila* IG1–IG2 binds heparin quite avidly. Recent structural studies by Fukuhara et al (2008) revealed that the binding of heparin oligosaccharides to the Robo involved only the IG-1.

This domain contains a highly conserved basic patch of Lys 69, Arg 117, Lys 122, and Lys 123 in both invertebrates and vertebrates. The Arg 117 is located on the border of the domain and is involved in the Slit binding. Fukuhara et al (2008) suggested that at least five HS disaccharide residues are needed to make a connection between both the Slit D-2 and the Robo IG-1. This proposal was also confirmed previously by Hussain et al (2006) corresponding to the minimal HS size capable of disturbing the *Xenopus* retinal axon targeting.

The question of specificity of Slit-HS interactions has also been investigated, because HS is a highly heterogeneous molecule with variable sulfated domains. Shipp and Hsieh-Wilson (2007) used microarrays of limited heparin polysaccharide derivatives and human Slit-2, and found that binding of hSlit-2 to heparin was strongly dependent on 6-O and N sulfates, whereas 2-O sulfate was less significant. They also validated their results using bioactivity assays (brain explants), in which the different heparin derivatives were examined for their ability to inhibit axon guidance and neuronal cell migration (Shipp and Hsieh-Wilson, 2007), although this was an *in vitro* study which may involve multiple target effects. These findings contradict what has been suggested by Irie et al (2002) that both 2-O and 6-O sulfates have powerful bypass inducing activity (Irie *et al.*, 2002). The recent structural data obtained by Fukuhara et al (2008), shows that a flexible 10-mer oligosaccharide was required to assist Slit and Robo complex formation. The flexibility of HS is dependent on the 2-O sulfate of the iduronic acid and the glycosidic linkages, whereas the 6-O sulfates of the glucosamine is less flexible, which supports the importance of the 2-O sulfates (Powell *et al.*, 2004; Rudd and Yates, 2010; Yates *et al.*, 1996).

4.1.6 Solid phase immunoassays for determination of binary and ternary complexes

Competition Enzyme-Linked ImmunoSorbent Assay (ELISA) has been used to confirm and characterise the interaction of proteins with heparin and chemically modified heparins (Powell *et al.*, 2002).

Competition ELISAs exploit the ability of heparin oligosaccharides to be labelled with biotin and then immobilised on microtitre plates by streptavidin. This method of immobilisation is thought to present the oligosaccharides, away from the surface, and increase the ease of contact of binding sites within the immobilised oligosaccharide to proteins (Figure 4.3). Bound protein can then be measured using immunodetection with appropriate primary and secondary antibodies.

Heparin oligosaccharides can be biotinylated at the reducing end (Ostrovsky *et al.*, 2002). Nitrous acid generated oligosaccharides have been used in the present studies (see Chapter 3). These size-defined oligosaccharides have a highly reactive reducing end aldehyde group. The method for labelling nitrous acid oligosaccharides with biotin is described in Methods (section 2.2.11). This method has advantages over internal biotinylation of the heparin chains using NHS-ester derivatives, since it was thought that reaction would occur with the free amino groups that occur on some glucosamine residues of heparin/ HS, but also with GlcNS residues. As N-sulfates are regularly involved in the interaction of proteins with heparin/ HS, such a labelling procedure may lead to a loss of binding sites, as well as possibly altering the conformation of binding sequences. Reducing end labelling through the reaction of biocytin hydrazide with the reducing end aldehyde is expected to be the most effective approach as the selective labelling at one end of the oligosaccharide chains leaves the remainder of saccharide binding sites exposed for interaction with proteins.

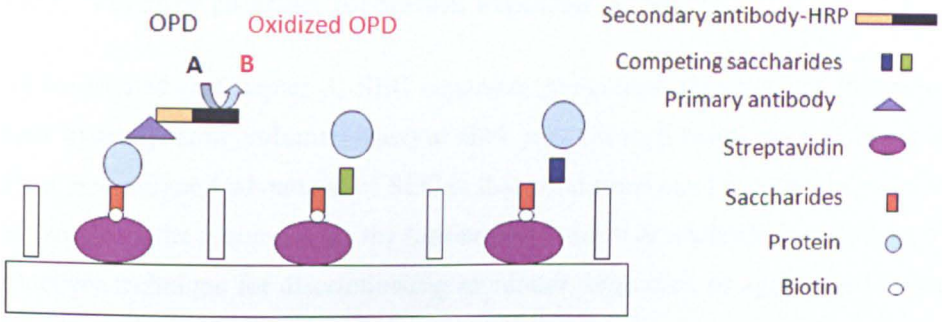

Figure 4.3 Schematic of competition ELISA. Biotinylated saccharides are immobilised on streptavidin coated microtiter plate. Protein and competitor saccharides are added, then primary antibody, and quantified using a secondary antibody [Horse radish peroxidase (HRP) conjugate. The latter is detected by oxidation of Ortho-Phenylenediamine (OPD) substrate to a coloured product (read at $\lambda = 492$nm).

Direct ELISA can also be used as a screening method for studying ternary complex formation. In this case, one of the protein partners can be coated on the microtiter plate surface, with binding of the other protein partner (Fc labelled) detected via use of HRP labelled antibody (Figure 4.4). The ability of HS or heparin to modulate this complex formation can thus be measured (Hussain *et al.*, 2006) (Figure 4.4).

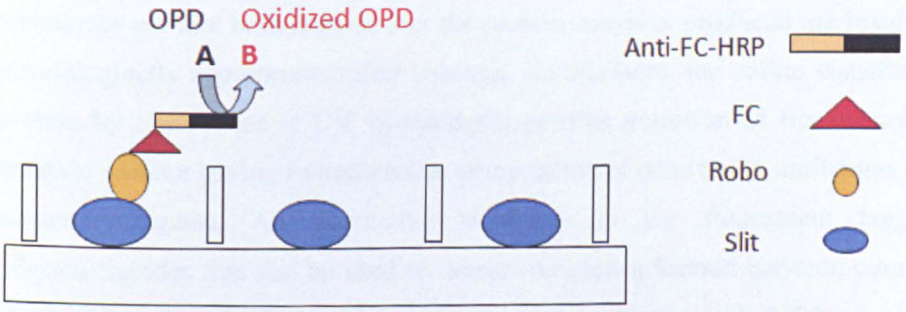

Figure 4.4 Schematic of direct ELISA. Slit D1-4 was diluted with Na_2CO_3/ $NaHCO_3$ pH 9.6, and coated onto microtiter plates and incubated overnight at 4 ° C. Then, blocked and washed. Robo IG1–5 Fc protein was incubated for 2 hours, followed by wash; bound protein was detected by HRP-conjugated goat anti-human Fc antibody which then oxidises the substrate Ortho-Phenylenediamine (OPD) to a coloured product (read at $\lambda = 492$nm).

4.1.7 Ternary complex formation explored by SEC

As mentioned in Chapter 3, SEC separates molecules according to differences in their hydrodynamic volume (sizes) as they pass through beads packed in a column. Thus, a significant advantage of SEC is that conditions can be varied to suit the type of sample or the requirements for further purification or analysis. In addition, it is an excellent technique for discriminating monomer, oligomer, or aggregated forms of a target protein. Superdex™, which has been discussed earlier, is a composite matrix of dextran and agarose, which provides excellent SEC properties of cross-linked dextran (Sephadex™) with the physical and chemical stability of highly cross-linked agarose to produce separation media with excellent selectivity and high resolution. The mean bead size in Superdex 75 media is 13 μm, with a recommended separation range of 3-70 kDa for globular proteins. They can be used for monitoring changes in molecular size and analysis of protein-protein interactions.

SEC is also an established technique for studying heparin-protein complexes (Robinson *et al.*, 2005). The advantages of this technique compared to other techniques are that both heparin and the protein complex produced are resolved in a physiologically appropriate buffer solution. Furthermore, the online visualization of protein by absorbance at UV wavelengths permits detection of free complexes in solution without having to immobilize components or detect with antibodies or other secondary agents. An alternative technique is the fluorescent tagging of oligosaccharides that can be used to detect complexes formed between components incubated at physiologically relevant concentrations (Lyon *et al.*, 2004).

4.1.8 Biological activity studies for Slit-Robo using growth cone collapse assay

The growth cone collapse assay can be used to characterize the signalling activity present in the chick retina that induces the collapse of retinal ganglion cells (RGC) growth cones.

This technique is a standard approach for proteins with repellent activities such as Slits. The growth cone collapse assay has been used for the recognition of molecules that are repulsive to growth cones or inhibit axonal outgrowth (Kapfhammer *et al.*, 2007; Piper *et al.*, 2006). The morphology of the growth cone changes after exposure to a test protein as the readout. This assay does not require very specialized equipment and can be established by any laboratory with experience in neuronal cell culture. Growth cones extend over long distances to make contact with their proper targets and respond to guidance cues in their environments, which direct them along accurate and reproducible routes. A large number of signalling molecules that serve as axonal guidance cues, however, some act as attractants whereas others act as repellents (Kapfhammer *et al.*, 2007). The localization of the repellent signalling molecules could induce the growth cones to turn away. When a growth cone is not able to escape a repellent signal it loses its spread morphology and becomes temporarily collapsed. This action is referred to as growth cone collapse.

Collapse was originally reported following contact between growth cones and axons growing from sympathetic ganglia and retinal explants (Chilton, 2006; Tessier-Lavigne and Goodman, 1996). Growth cone collapse serves as a very sensitive and consistent marker of repellent activity. It can be used as a bioactivity assay to identify repulsive guidance cues and to determine whether particular axons are responsive to known repellent signals or not. In this assay, the readout is the morphology of the growth cone. This assay exploits the finding that many embryonic axons grown over laminin have well spread growth cones. Contact with a cellular surface that expresses a repellent cue, for instance a plasma membrane preparation containing a repellent cue, or even with reconstituted extracts of purified or recombinant repellent proteins, induces growth cones to lose their spread morphology and instead assume a shrunken shape of lamellipodia or filopodia (Figure 4.5). The change in morphology can occur in a few minutes and last for several hours if the repellent is not removed. The morphologies of growth cones can be preserved by fixation and the percentage of collapsed versus intact growth cones can then be determined. Alternatively, immunostaining can be used (Piper *et al.*, 2006).

Using growth cone collapse to detect repellent activity allows quantification of repellent activity contained within a preparation. It has been successfully used to generate concentration response curves of collapsing activity (Raper and Kapfhammer, 1990). Growth cone behaviour can be observed during the collapse response using video recording, as the response of a growth cone to repellent is highly characteristic. The growth cone stops forward motion, lamellipodial activity is halted, lamellipodia shrink while filopodia thicken and retract. These morphological changes can be monitored and counted by the naked eye or by using photographic images and analysed using an image analysis programme, and the proportion of the collapsed against spread can be determined (Figure 4.6a and b).

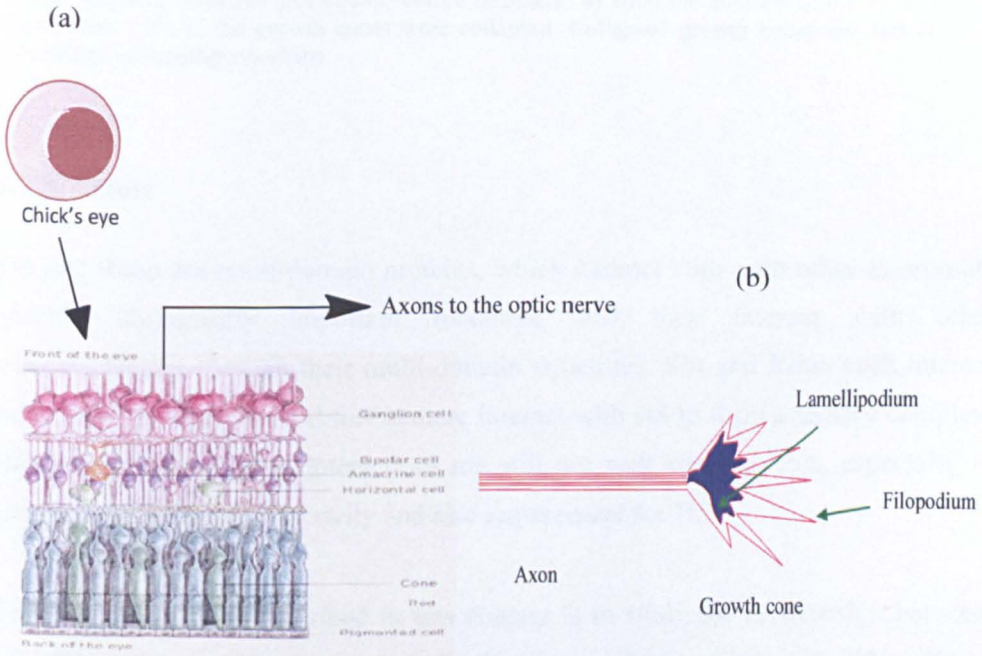

Figure 4.5 Retinal cell layers and a schematic of the growth cone. a) Shows different layers of retina cells adopted from (Cepko, 2000). b) Schematic of the growth cone showing the axon and lamellipodium and filopodium.

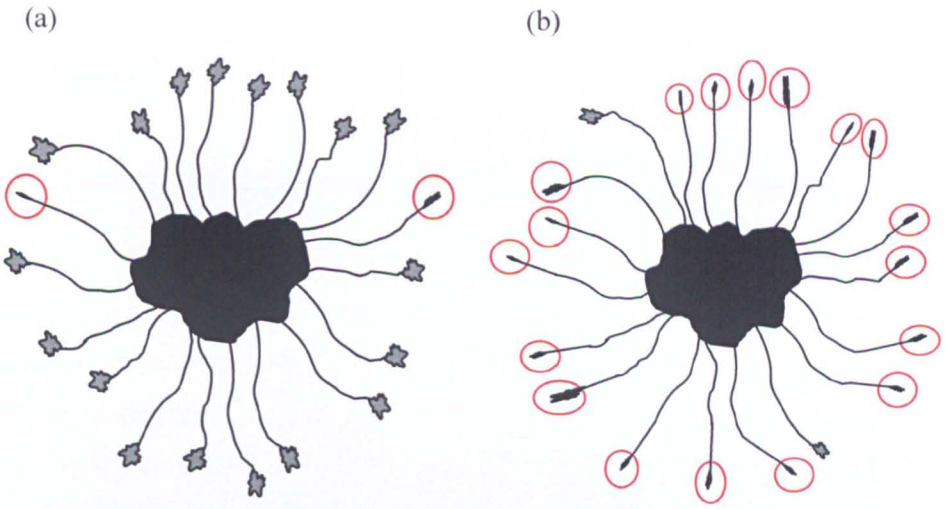

Figure 4.6 Schematic drawing shows the characteristics of a growth cone collapse assay of E7 chick retina. The collapsed growth cones are circled red. a) Before the addition of hSlit2-CM, most of the axons have a well-characterized lamellipodia, generally about 10% of growth cones appeared collapsed (red circles) before treatment. b) After the addition of the hSlit2-CM, more than 75% of the growth cones were collapsed. Collapsed growth cones are defined by shrinkage of lamellipodia shape.

4.1.9 Aims

Slit and Robo are multi-domain proteins, which interact with each other to promote specific biologically important functions, and they interact with other macromolecules through their multi-domain structures. Slit and Robo each interact independently with HS, and furthermore interact with HS to form a ternary complex. However, these complex interactions are still not well characterized, especially in terms of the sequence selectivity and size requirement for HS.

The aim of the work described in this chapter is to study the relationship between HS, Slit and Robo. First, to explore the binary complexes of HS with either Slit or Robo and determine the saccharide sequence requirements and minimum oligosaccharide sizes required to interact with both proteins. Second, to establish the minimum size and the sulfation pattern requirements necessary for the Slit-Robo-HS ternary complex formation. Finally, to investigate the Slit-Robo-HS structure-activity relationship using an *in vitro* bioassay (growth cone collapse assay). The outcomes of this study will add new insights into HS, Slit and Robo interactions, and the related structure-activity relationships.

4.2 Results

4.2.1 Analysis of chemically modified heparin polysaccharides

Estimated molecular weights for the GAG polysaccharides chains used in this study are listed in Table 4.1. The molecular weights for the chemically modified heparins generated from PMH were calculated according to the predominant structure of PMH disaccharide for each type. The chemically modified heparins used in this study were 2-de-O-sulfated (2-de), 6-de-O-sulfated (6-de), N Acetyl heparin (NAc), 2-de-O-sulfated NAc, (2-de NAc), 6-de-O-sulfate NAc, (6-de NAc), 2, 6-de-O-sulfated (2, 6-de), 2, 6-de-O-sulfated NAc (2, 6-deNAc) and persulfated (over sulfated) heparin (perS). Also, disaccharide mass ratios were calculated for all modified heparins, using heparin disaccharide as a reference (Table 4.1).

Chemically modified heparins were characterised by NMR (Yates et al, 1996) (see Appendix 3). In addition, disaccharide compositional analysis was performed for eight of the chemically modified heparin chains and porcine intestinal mucosal heparin. In brief, the heparin derivatives were comprehensively digested to completion by heparinase I, II and III enzymes (Yates *et al.*, 2004). The resultant disaccharides were separated according to the sulfate charges using SAX-HPLC and then identified by comparison to the eight commercially available disaccharides standards (Dextra Lab). The percentage of each disaccharide was then calculated to construct a distinctive profile for each chemically modified heparin chain (Figure 4.7.). The molecular weight for the porcine intestinal mucosal heparin (PMH) is 12 kDa according to the manufacturer's information (Celsus Ltd).

GAGs	Disaccharide mass (Da)	Disaccharide mass ratio	MW (kDa)
Heparin	576	1.0	12.0
2-O-desulfated heparin	496	0.9	10.3
6-O-desulfated heparin	496	0.9	10.3
N-Acetylated heparin	539	0.9	11.2
2-O-desulfated N-Acetylated	459	0.8	9.6
6-O-desulfated N-Acetylated	459	0.8	9.6
2, 6-O-desulfated N sulfated	416	0.7	8.7
2,6-O-desulfated N-Acetylated	337	0.6	7.0
Over-sulfated heparin	737	1.3	15.4
Chondroitin sulfate C	568	1.0	11.8

Table 4.1 Estimated molecular weight of various GAGs used in this study and their calculated disaccharides mass ratio. The disaccharide mass ratio was calculated by dividing the molecular mass of predominant modified disaccharides by the molecular mass of predominant heparin disaccharide (see figure 4.7). Porcine intestinal mucosal heparin PMH (Celsus) starting material is ~12 kDa (manufacturer's estimate). The chemically modified polysaccharides molecular weight were estimated based on their predominant disaccharides units and the mw of their original start material.

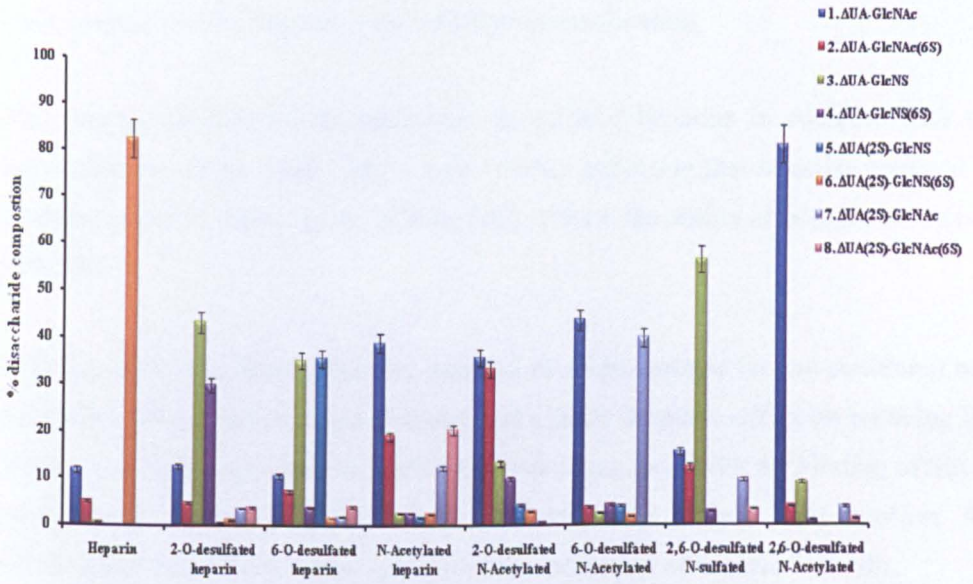

Figure 4.7 Disaccharide compositional analysis for heparin and chemically modified polysaccharides.

4.2.2 Competition ELISA: investigating Slit heparin binary complexes

The type of sulfate groups involved in the HS interaction with Slit protein were examined by competition ELISA utilizing the c-myc tagged Slit which was then detected by a primary anti-c-myc antibody and a secondary HRP-conjugated antibody. This method proved practical in determining the relative effectiveness of a series of selectively chemically modified heparins. The molecular weights for these polysaccharides were estimated based on altered sulfation, in order to allow approximately equivalent concentration of inhibitors to be used. The systematically modified set of chemically modified heparins lacking specific types of sulfate groups were used as competitors of the interaction of the Slit protein with 10-mer heparin is shown in Figure 4.8. Removal of one sulfate at the 2-O position of the iduronic acid (2-de), or the 6 position of glucosamine (6-de), or N-acetylation of the glucosamine (NAc) all reduced the ability of soluble modified heparins to compete with binding of Slit to immobilised 10-mer heparin by ~10-fold (Figure 4.8a). It can then be proposed that each of these three sulfate groups are involved directly in the interaction of heparin with Slit, or that they impart a required change of conformation on the heparin chain which promotes binding.

The relative abilities of the selectively de-sulfated heparins to compete with the interaction are of the order 2-de > 6-de = NAc, indicating that selective removal of different types of sulfate group differentially affects the ability of heparin to interact with Slit.

In Figure 4.8b, the effect of further removal of sulfate groups (at two positions) was examined. The removal of two sulfates had a more dramatic effect on reducing the ability of soluble chemically modified heparins to compete with the binding of Slit to immobilised 10-mer heparin (more than 100-fold). These data confirm the involvement of all three sulfate groups in the interaction of heparin with Slit.

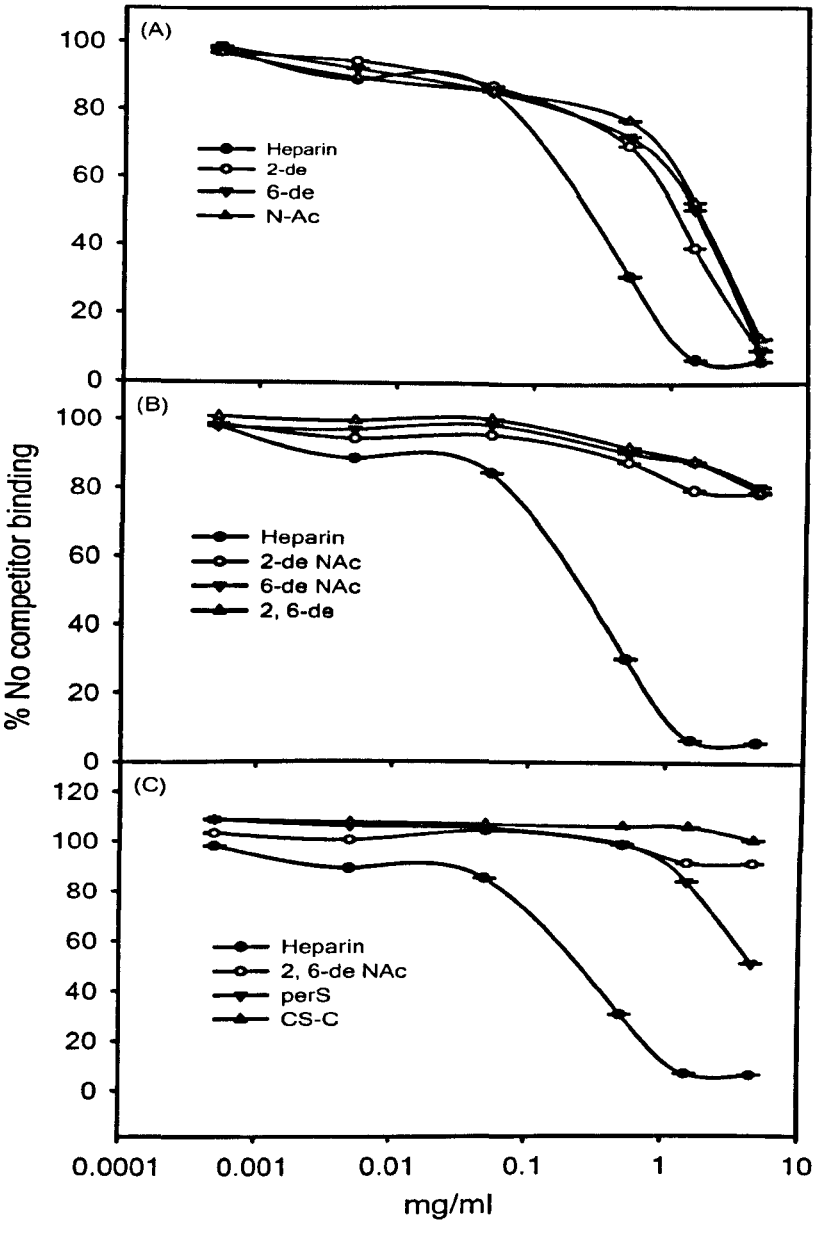

Figure 4.8 Binding of Slit to immobilized heparin oligosaccharide in the presence of soluble native or selectively de-sulfated heparins competition ELISA assays. a) Heparin, 2-de, 6-de and N Ac. b) Heparin, 2-de NAc, 6-de NAc and 2, 6-de. c) Heparin, 2, 6-de, perS and CS. Porcine mucosal heparin (PMH) 10-mer (produced by nitrous acid depolymerisation) was biotinylated at the reducing end and immobilised on streptavidin-coated 96-well microtitre plates. Equilibrium binding of 115 µg/ ml Slit to immobilized 10-mer PMH in the presence of varying concentrations of soluble competitors (selected chemically modified heparins) was quantified as a percentage of no competitor binding, using horseradish peroxidase protein and O-phenylenediamine substrate read at absorbance 492 nm and reported as a percentage of no competitor binding. Values are the mean of triplicate samples and error bars represent the STDEV of binding, and data are representative of four separate experiments.

All three double-modified heparins displayed similar abilities to compete with 10-mer heparin, though the 2-de NAc polymer was possible a slightly better inhibitor. In contrast, chondroitin-6-sulfate (C-6-S) was a very poor competitor of the interaction; CS has on average one sulfate per disaccharide, compared to ~3 for heparin; however, C-6-S has a similar charge to the doubly modified heparins, yet is a much poorer competitor (> 100-fold). This is likely to be due to both its lower charge, but also lack of structural features required to interfere specifically with interactions between heparin and Slit. In addition, over-sulfated chemically modified heparin (perS) was tested as a competitor. If a non-specific electrostatic interaction is responsible for the binding then this compound might be expected to be a better competitor than heparin. Figure 4.8c shows clearly that for heparin with respect to perS, native heparin is a better competitor than perS by > 10-fold. Totally de-sulfated chemically modified heparin had a similar activity to that of CS (more than 100-fold reduction). This finding indicates that there is no clear correlation between the number of negative charges per disaccharide and the capability of different chemically modified heparins and CS polysaccharides to compete with 10-mer heparin oligosaccharides for binding to Slit. These data suggest that the interactions are mediated selectively by sulfate groups within heparin/ HS chains indicating a likely conformational role for the display of sulfate groups on these particular backbone structures. However, compositional analyses of the chemically modified heparins (Figure 4.7) showed that the modifications are not achieved to absolute completion, and thus a degree of caution must be exercised in the interpretation of data using these compounds.

The interaction affinity of Slit to heparin derivatives was also assessed by determining the IC_{50} values for these interactions. The IC_{50} is the concentration of the inhibitor (heparin derivatives) that generates 50 % inhibition of protein binding to immobilised 10-mer heparin.

The IC_{50} for some of the screened heparins derivatives is shown in Figure 4.9. Heparin has the lowest IC_{50}, 230 µg/ml, followed by 2-de, 6-de, NAc and, finally, per-sulfated heparin. However, chemically modified chains with two or more sulfates removed, and CS, were unable to inhibit sufficiently to allow the IC_{50} to be calculated (Figure 4.9).

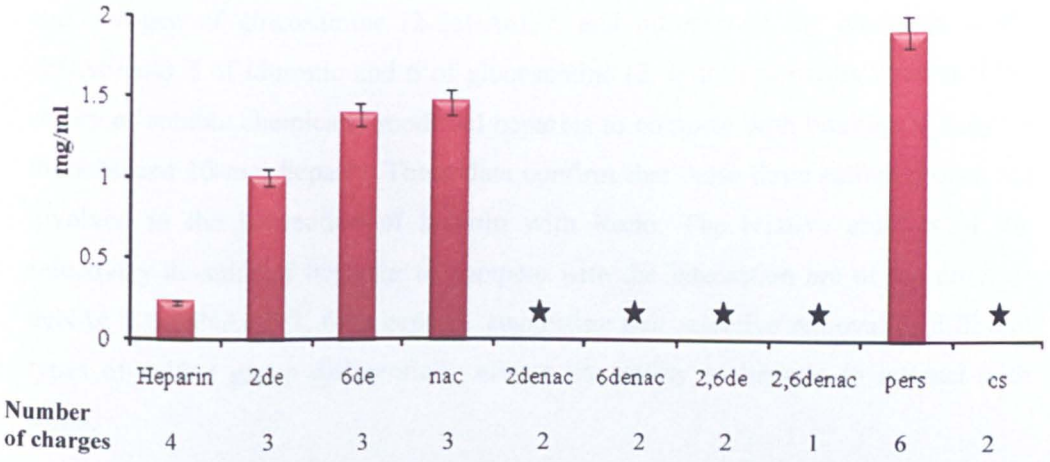

Figure 4.9 IC_{50} values for inhibition of slit binding to binding to immobilised 10-mer heparin by modified heparin variants. IC_{50} values were calculated as the concentration of inhibitor saccharide needed for 50 % inhibition of the Slit binding to immobilised 10-mer heparin obtained from Figure 4.8. Values are the average of triplicate samples, error bars represent the STDEV. The data are representative of two separates experiments. The stars represent saccharides unable to compete adequately to calculate the IC_{50}.

4.2.3 Competition ELISA: investigating Robo-heparin binary complexes

The types of sulfate groups associated with the Robo-HS interaction were also examined by competition ELISA; in this case, the Fc labelled Robo was detected by a primary anti-Fc antibody and a secondary HRP-conjugated antibody. The same chemically modified heparins used in the Slit study were used here (Figure 4.7). The removal of one sulfate at the 2 position of the iduronic acid (2-de) or the 6 position (6-de) or nitrogen of the glucosamine (NAc) reduced the ability of soluble chemically modified heparins to compete with Robo binding to immobilised 10-mer heparin by ~50-fold in the case of NAc and 2-de, and more strongly (~100-fold) for the 6-de (Figure 4.10a). It can then be proposed that all these three sulfate group types are involved in the interaction of heparin with Robo.

The relative abilities of the selectively de-sulfated heparins to compete with the interaction are of the order NAc = 2-de > 6-de, suggesting as for Slit protein that selective removal of different types of sulfate groups differentially affects the ability of heparin to interact with Robo.

In Figure 4.10b further selective removal of sulfates at positions 2 of iduronic acid and nitrogen of glucosamine (2-deNAc), 6 and nitrogen of the glucosamine (6-deNAc) and 2 of iduronic and 6 of glucosamine (2, 6-de) essentially abolished the ability of soluble chemically modified heparins to compete with binding of Robo to immobilised 10-mer heparin. These data confirm that these three sulfate groups are involved in the interaction of heparin with Robo. The relative abilities of the selectively de-sulfated heparins to compete with the interaction are of the order 2-deNAc > 6-deNAc = 2, 6-de heparin, suggesting that selective removal of different types of sulfate group differentially affects the ability of heparin to interact with Robo.

As observed for Slit, CS is a 100-fold poor competitor of the interactions than heparin and perS is a weaker competitor than native heparin by greater than 10-fold (Figure 4.10). Totally de-sulfated chemically modified heparin had a similar activity to CS, with more than 100-fold less inhibitory effect than heparin. These findings indicate that there is no clear connection between the number of negative charges per disaccharide and the capability of different chemically modified heparins and CS polysaccharides to compete with 10-mer heparin oligosaccharides for binding to Robo. This suggests that sulfate groups within the heparin polysaccharide chain mediate the interactions selectively.

The interaction affinity of Robo to heparin derivatives as also assessed by determining the IC_{50} values for these interactions. Heparin had the lowest IC_{50} of 25 µg/ ml, followed by per-sulfated heparin, NAc, 2-de and finally the 6-de heparin (Figure 4.11). IC_{50} values could not be calculated for the other four chemically modified heparins and CS. It is notable that the IC_{50} of Robo for heparin is ~10-fold lower than for Slit (Figure 4.9)

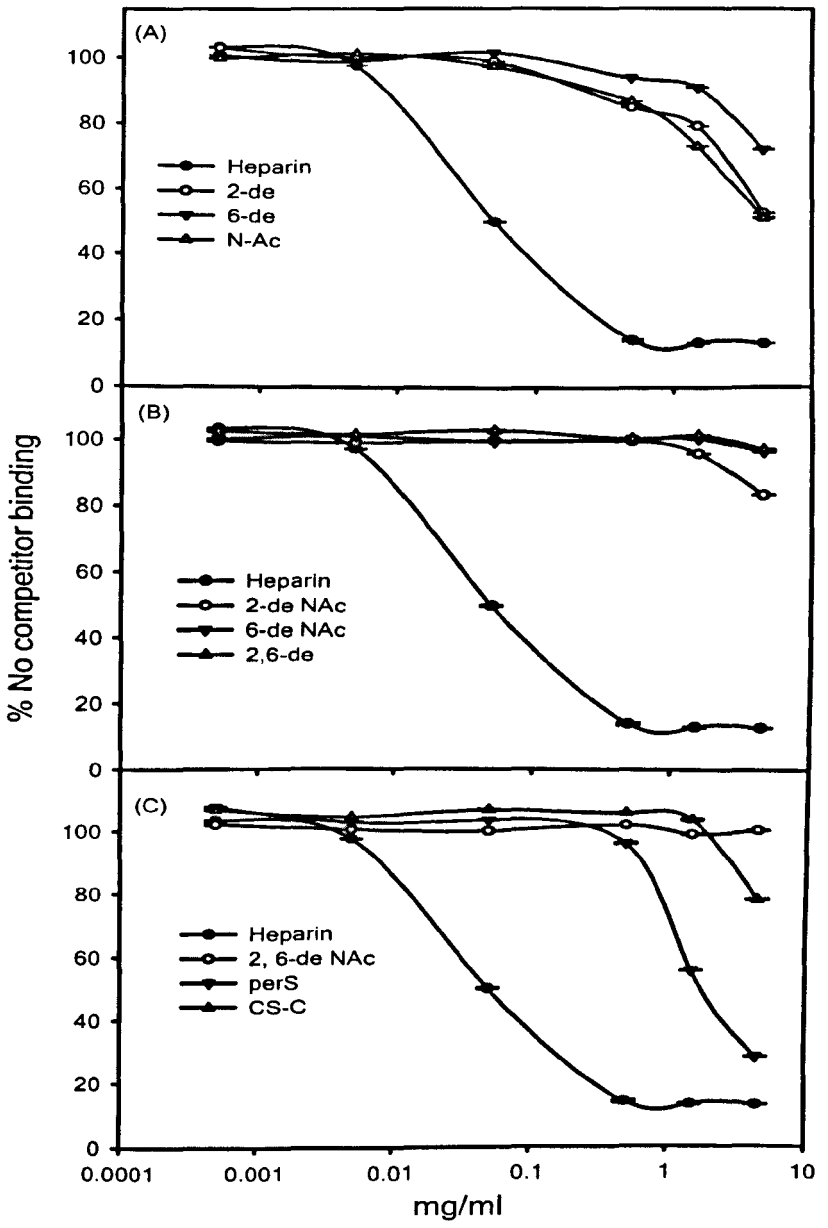

Figure 4.10 Binding of Robo to immobilized heparin oligosaccharide in the presence of soluble native and selectively desulfated heparins. a) Heparin, 2-de 6-de and NAc. b) Heparin, 2-deNAc, 6-deNAc and 2, 6-de. c) Heparin, 2,6-deNAc, perS and CS. Competition ELISA experiment was conducted as described in Figure 4.8. The concentration of Robo was 65 µg/ ml. Data are representative of four separate experiments.

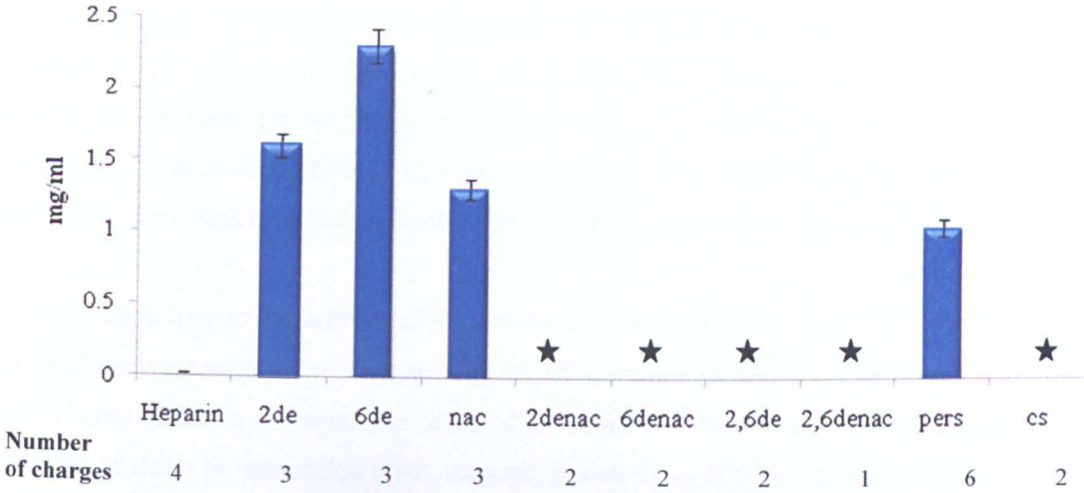

Figure 4.11 IC_{50} values for inhibition of Robo binding to immobilised 10-mer by heparin derivatives. IC_{50} values were calculated as in Figure 4.8, from data in Figure 4.10. The IC_{50} for heparin was 25 μg/ml.

4.2.4 Direct ELISA: investigating Slit-Robo-heparin ternary complexes

A solid phase protein assay was performed to test the effect of heparin and chemically modified heparins on the formation of a ternary Slit-Robo-heparin complex. In order to investigate whether heparin or chemically modified heparins have an effect on the Slit-Robo interaction the experiment was first carried out in the absence of polysaccharides. In this method, Slit D1-4 (5 μg/ ml) was coated onto 96-well microtiter plates (NUNC Maxisorp). Wells were blocked with PBS/casein and then washed with PBS. Robo IG1–5 Fc protein (100 μg/ ml) was added and bound protein was detected by HRP conjugated goat anti-human Fc antibody (Sigma).

Heparin and chemically modified heparins were added to Robo IG1–5 Fc at 10 μg/ ml; this addition resulted in a marked shift in the observed binding of Robo to immobilised Slit (> 70-80-fold) (Figure 4.12a). In contrast, addition of 10 μg/ ml of the 2-de or 6-de heparins only resulted in a 10-15-fold increase in the interaction of Slit and Robo (~10-15-fold) suggesting that both 2-de and 6-de are equally important in enhancing Slit-Robo interactions. In contrast, NAc heparin produced a ~25-30-fold increase in the Slit and Robo interaction (Figure 4.12b).

In contrast, removal of two sulfates in the case of 2-de NAc and 6-de NAc heparins resulted in no ability to promote the Slit-Robo interaction (Figure 4.12b). Addition of the perS heparin resulted in a very slight increase (~ 5-fold) in the Slit-Robo interaction, whereas addition of 2, 6-de (both O sulfates removed) or totally de-sulfated heparin had no effect promoting the Slit-Robo interaction (Figure 4.12c).

The selective interaction affinity of the ternary complexes of Slit, Robo and heparin derivatives were assessed by determining the EC_{50} values for these interactions. The EC_{50} is the effective concentration required to induce a 50 % of maximal increase in binding of Robo to immobilized Slit. Heparin has an EC_{50} of 5 ng/ ml whereas NAc heparin had a slightly higher EC_{50} of 14 ng/ ml. Eliminating, either one of the 2-O or 6-O sulfate groups resulted in higher EC_{50} values of 25 ng/ ml. Over-sulfation of heparin resulted in an EC_{50} of 66 ng/ ml. In contrast, removal of two or three sulfates from heparin resulted in very high EC_{50} values, which were similar to the control condition (no added heparin) (Figure 4.13).

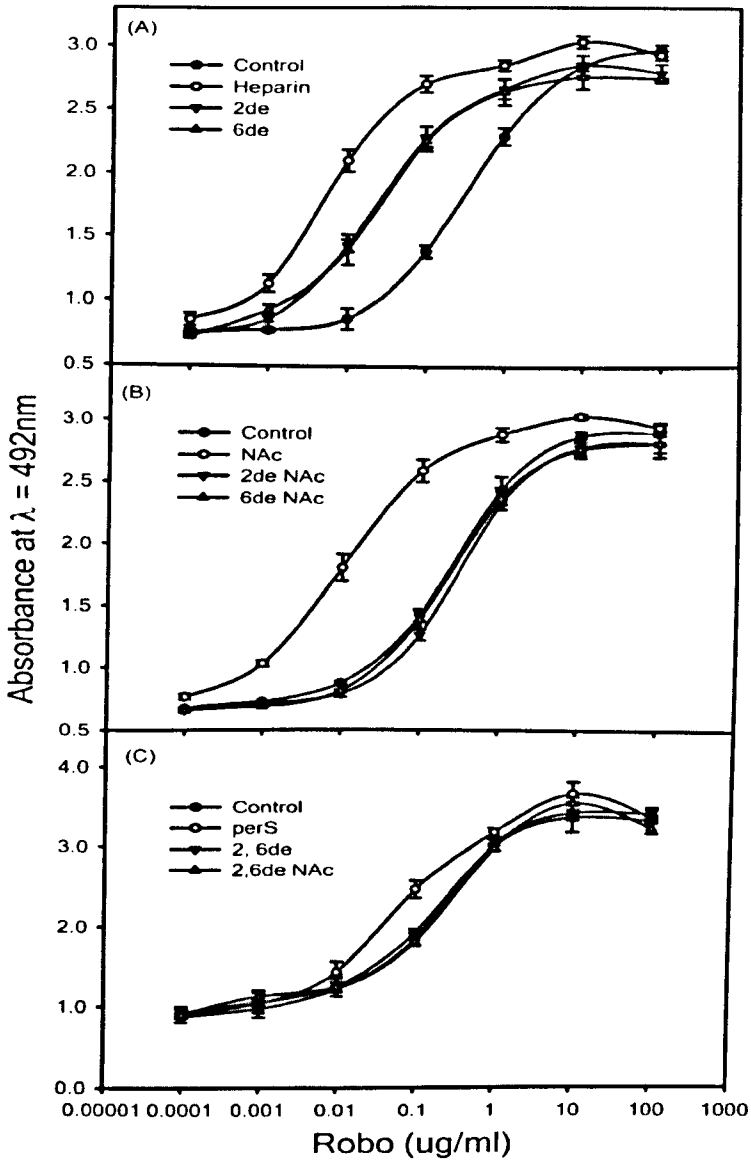

Figure 4.12 Heparin and some chemically modified heparins enhance the Slit-Robo interaction. Binding of varying concentrations of soluble Robo IG1–5 Fc to Slit D1–4 immobilized on 96-well microtitre plates in the absence or presence of 10 μg/ ml of heparin or chemically modified heparins. a) Heparin, 2-de and 6-de. b) NAc, 2-denac, and 6-denac. c) perS, 2,6-de and 2,6-denac. Bound Robo IG1–5 Fc was detected using an anti-FC horseradish peroxidase protein and O-phenylenediamine substrate read at absorbance 492 nm as described in Methods. The values are the means of triplicate samples, error bars represent the STDEV, and data are representative of three separate experiments.

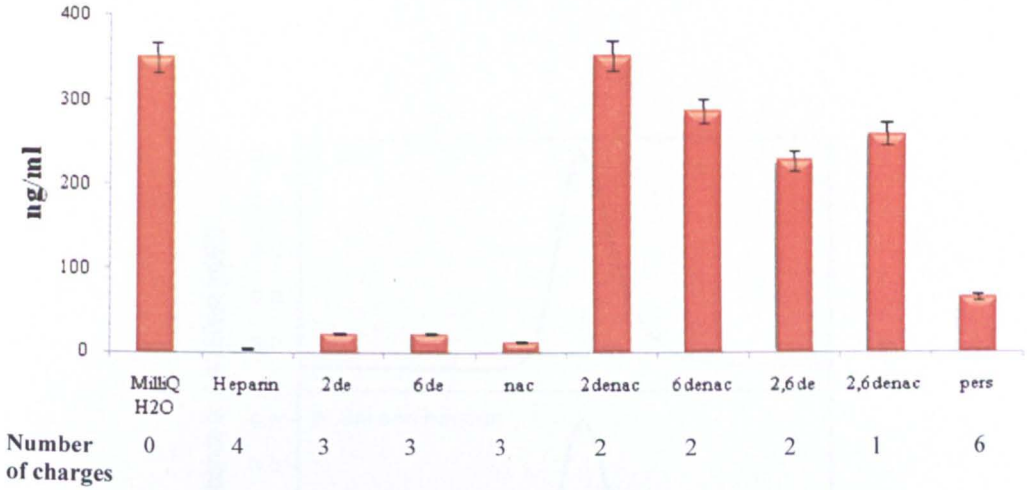

Figure 4.13 EC_{50} of increase binding of Robo to immobilized Slit in the presence of 10 µg/ ml heparin derivatives. EC_{50} values were calculated as the concentration of Robo needed for a 50% maximal increase of the interaction of the Robo with immobilised Slit (obtained from Figure 4.12). Values are the average of triplicate samples and error bars represent the STDEV. The data are representative of two separates experiments.

4.2.5 Heparin-mediated interaction of Slit-Robo explored by SEC

To obtain direct evidence for ternary complex formation, analytical SEC was used. The column used was Superdex™ 75 that has the capability of separating globular proteins in the size range 3-70 kDa. The column was calibrated with suitable standards. In Figure 4.14a *Drosophila* Slit D2 was applied separately to the calibrated column; its elution time indicated a size of 27.4 kDa, consistent with a monomer (Figure 4.14a). However, addition of heparin had no significant effect on the elution time as reported previously by Hussain et al (2006), indicating that it continues to run as a monomer (Figure 4.14b).

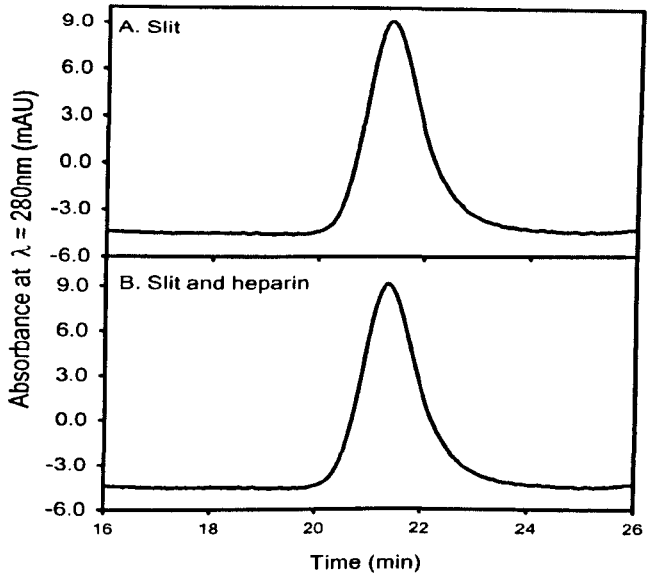

Figure 4.14 Size-exclusion chromatography (SEC) analysis of Slit and Slit / heparin. SEC chromatograms of isolated (a) 10 μM Drosophila Slit D2; (b) 10 μM Drosophila Slit D2 and 10 μM heparin mixed in 1:1 ratio. Briefly, Superdex ™ 75 SEC chromatography, was run using an AKTA purifier 10 at a flow rate of 0.5 ml / min in 20 mM Na-HEPES 150 mM NaCl pH 7.5 and monitoring the elution profile by absorbance at λ_{abs} = 280 nm. The void volume of the column is 8.0 ml. Data was recorded using the Unicorn 5.0 software and exported into SigmaPlot 11. Three runs were performed and the profiles were consistent.

The elution time of *Drosophila* Robo IG1–2 (24.1 kDa) is also most compatible with that of a monomer. Adding heparin also had no effect on the elution time of the Robo peak (Figure 4.15b).

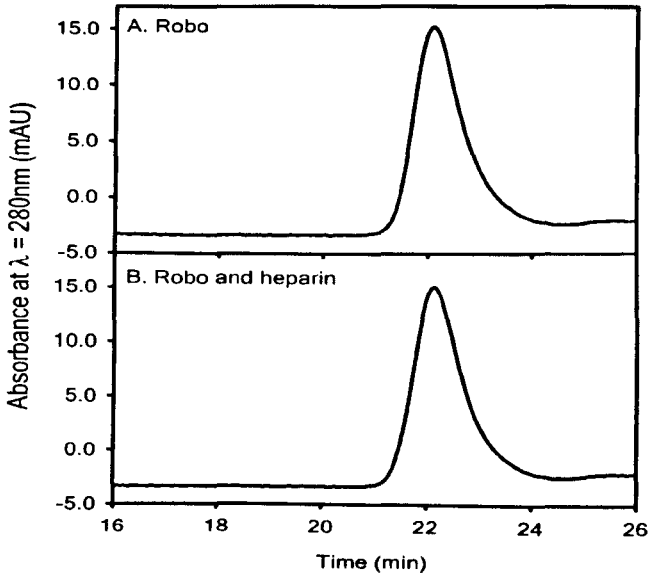

Figure 4.15 Size-exclusion chromatography (SEC) analysis of Robo and Robo/ heparin. SEC chromatograms of isolated (a) 10 μM Drosophila dRoboIG1-2; (b) 10 μM Drosophila dRobo IG 1-2 and 10μM heparin mixed in 1:1 ratio. Chromatography was carried out as described in Figure 4.14. Three runs were performed and the profiles were consistent.

When 10 μM Slit D2 and 10 μM Robo IG1–2 were mixed in a 1:1 ratio, two peaks were observed (Figure 4.16). However, these peaks coincided exactly with the individual dSlit D2 and dRobo IG1-2 elution profiles providing no evidence of a shift to the left, which would indicate that a stable binary complex had formed.

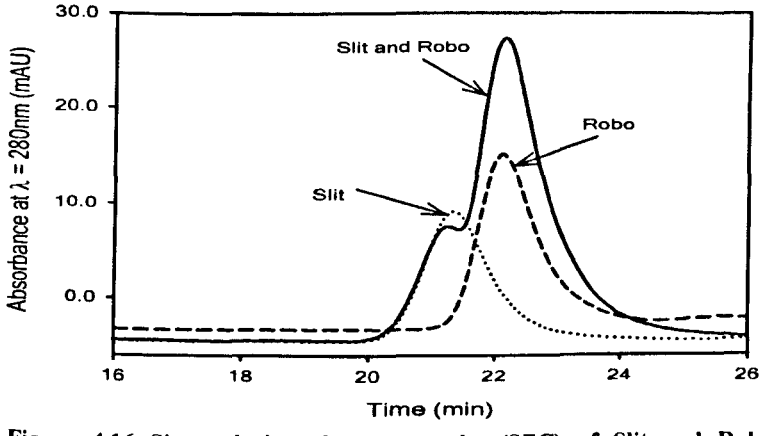

Figure 4.16 Size-exclusion chromatography (SEC) of Slit and Robo mixture. SEC chromatograms of 10 μM Drosophila Slit D2 and 10 μM Robo IG1–2, mixed in 1:1 ratio; the individual Slit (dotted line) and Robo (dashed line) peaks are shown in comparison with the combined profile. Chromatography was carried out as described in Figure 4.14. Three runs were performed and the profiles were consistent.

A selection of heparin, chemically modified heparins and CS-C were next examined to answer the question as to whether there are selective sulfate requirements for ternary complex formation. The SlitD2 and RoboIG1–2 were mixed in 1:1 ratio, the complex was eluted at 22.16 min (Table 4.2). When Slit and Robo were mixed in a 1:1:1 molar ratio with heparin a great peak shift to the left was observed (eluted at 20.33 min) suggesting that heparin has significant effect on Slit-Robo complex formation (Table 4.2). However, due to the large mass and the polydisperse nature of heparin it is difficult to estimate the complex hydrodynamic radius. Note that linear polysaccharides in solution have larger than anticipated hydrodynamic volume (Robinson *et al.*, 2005).

Chemically modified heparin (2-de or 6-de, and NAc) peaks were shifted partially to the left, with NAc producing a more pronounced shift than the others. In contrast, the chemically modified heparins 2-deNAc, 6-deNAc, 2, 6-de and 2, 6-deNAc, and CS-C, did not produce significant changes in the elution profiles (Figure 4.17). Over-sulfated heparin polysaccharide (perS) was eluted in the void volume (data not shown). This could be because its molecular weight is larger than anticipated, but is more likely the result of non-specific binding between the perS heparin and the gel filtration matrix environment, or its promotion of protein aggregation.

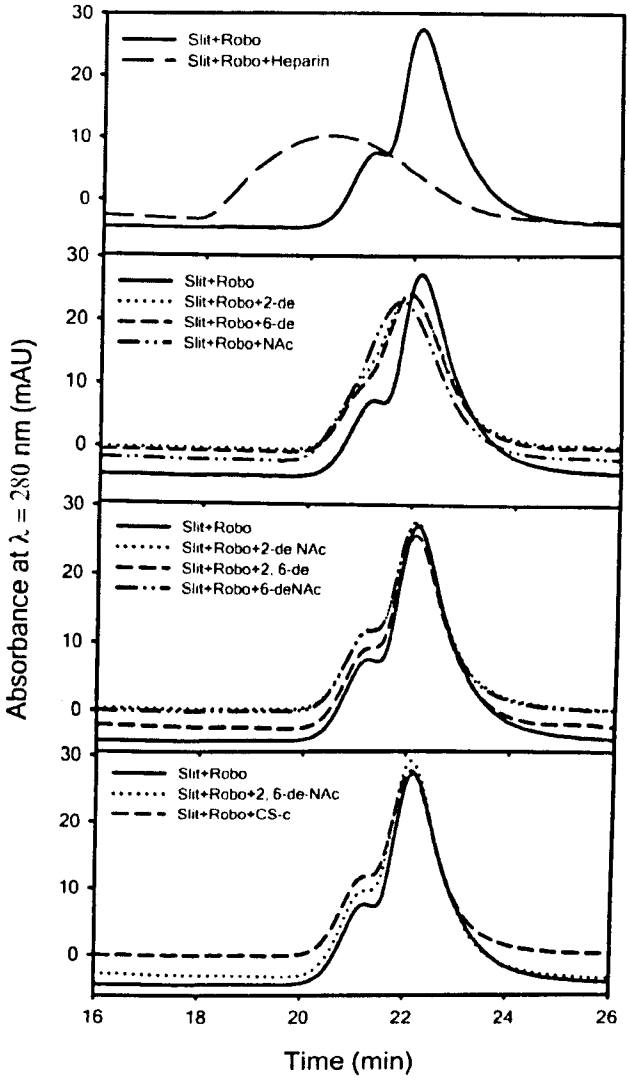

Figure 4.17 Size-exclusion chromatography (SEC) analysis of ternary Slit/Robo/heparin derivative complexes. SEC chromatograms of isolated 10 μM Drosophila Slit D2 and 10 μM Robo IG1–2, a 1:1 mixture of the two proteins, and a 1:1:1 mixture of the two proteins with 10μM heparin or chemically modified heparins. Chromatography was carried out as described in Figure 4.14. Three runs were performed and the profiles were consistent.

Complex	Peak maxima (min)	Average charges per disaccharide unit
Slit/ Robo	22.16	-
Slit/ Robo+Heparin	20.33	4
Slit/ Robo+2-de	21.92	3
Slit/ Robo+6-de	21.95	3
Slit/ Robo+NAc	21.79	3
Slit/ Robo+2-deNAc	22.11	2
Slit/ Robo+6-de NAc	22.11	2
Slit/ Robo+2, 6-de	22.13	2
Slit/ Robo+2, 6-de NAc	22.13	1
Slit/ Robo+CS-C	22.13	2

Table 4.2 showing the peak maxima of Slit and Robo plus modified heparin polysaccharides; and the number of average charges per disaccharide unit for each of the polysaccharides used in the gel filtration experiment.

SDS-PAGE was performed on SEC fractions for dSlitD2 and RoboIG1-2 complexes, with and without heparin, to confirm the presence of the two proteins in equivalent amounts (Figure 4.18a and b). The results showed that the earlier eluted peak fractions contained both Slit and Robo protein in the presence of heparin, whereas comparable fractions from the dSlitD2 and dRoboIG1-2 complex confirmed that Slit and Robo eluted in later fractions.

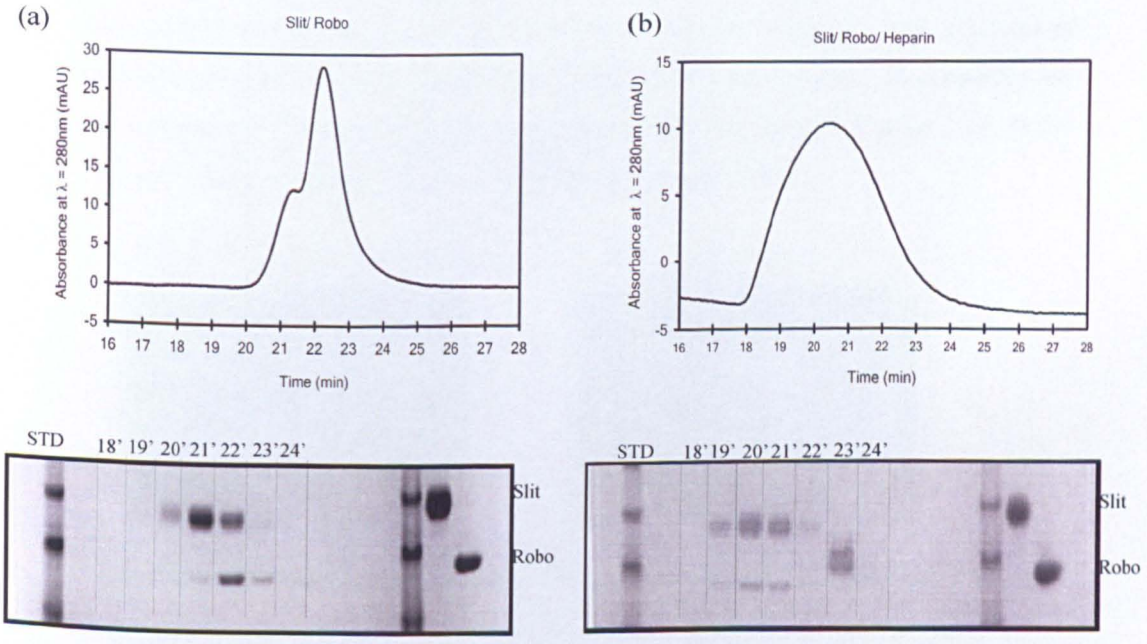

Figure 4.18 Size-exclusion chromatography (SEC) analysis of ternary Slit/ Robo/heparin derivative complexes and PAGE analysis of the eluted fractions. SEC chromatograms of isolated 10 μM Drosophila Slit D2 and 10 μM Robo IG1–2, a 1:1 mixture of the two proteins, and a 1:1:1 mixture of the two proteins with 10 μM heparin or chemically modified heparins. Chromatography was carried out as described in Figure 4.14. B) Coomassie Blue-stained SDS-PAGE gel of the peak fractions indicated in A. The fraction numbers are shown at the top of the gel. Three runs were performed and the profiles were consistent.

4.2.6 Activity studies: hSlit-2 growth cone collapse assay

From previous biochemical data, it has been shown that HS plays an important role in the Slit-Robo interaction. It has been hypothesized that if heparin (or HS) form a ternary complex with Slit and Robo and are crucial for their interactions, enzymatic removal of endogenous HS by heparinases will affect Slit-Robo interactions and disrupts the biological activity (e.g. collapse of growth cones). However, addition of exogenous HS or heparin to heparinases treated cells should restore Slit and Robo biological activity. Bioassay data provides an insight into the structure-activity relationship of HS with Slit and Robo, to confirm the biochemical findings and show whether binding and activity are correlated.

To explore whether HS has a role in Slit and Robo biological activity, an *in vitro* collapse assay was carried out, utilizing the growth cones of chick retinal explants. As developing chicken embryos, express two Slits receptors (Robo-1 and Robo-2) (Vargesson *et al.*, 2001). However, only Robo-2 has been identified as the major receptor required for axon guidance (Thompson *et al.*, 2009a). Retinal explants from chick embryonic age day 7 (E7) were cultured for 24 hours prior to the addition of conditioned medium (CM) of cells expressing hSlit2, appropriate CM concentration was determined in a dose response experiment (data not shown). Figure 4.19 shows the morphology of non-collapsed and collapsed growth cones.

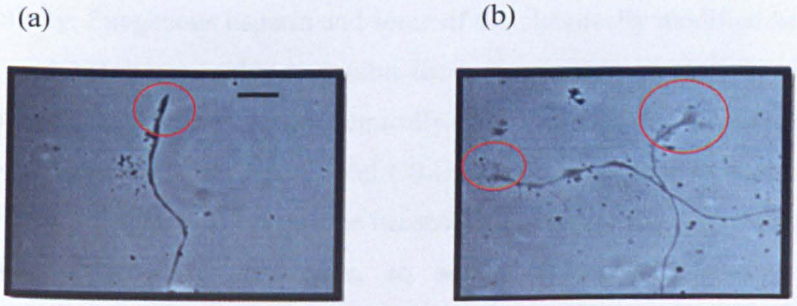

Figure 4.19 Effect of hSlit2-CM on chick retinal growth cones. (a) Non-collapsed growth cones in cultures treated with PBS buffer; (b) Collapsed growth cones in cultures treated with conditioned medium of hSlit2-expressing cells (hSlit2-CM); scale bars: 10 μm.

Assay development was performed to confirm the requirement for endogenous HS (response abolished by heparinase treatment) and the ability of exogenous heparins to rescue heparinase treated cells (Figure 4.20).

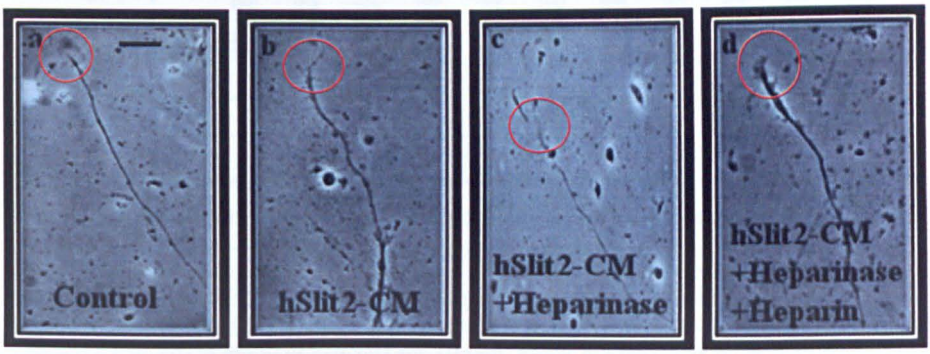

Figure 4.20 Assay development showing changes in the morphology of the growth cone in rescue experiments. Growth cones were treated with PBS buffer control (a), conditioned medium of hSlit2-expressing cells (hSlit2-CM) (b), growth cones were pre-treated with heparinase 1, II, III (5mU/ ml) for 3 hours (c) growth cones were pre-treated with heparinase 1, II, III (5mU/ ml) for 3 hours, then rescued with heparin at 200 µg/ ml (d), scale bars: 10 µm.

HSlit-2-CM caused significant collapse activity of the growth cones compared to the control (PBS) (Figure 4.21). The maximum level of collapse was about ~ 90 %, compared to ~15% in PBS control. Mock medium (collected under the same conditions as the hSlit2-CM from cells transfected with an empty vector) was added to test the non-specific effect of the culture medium on the growth cone. Collapse activity for the mock medium was about ~30 % demonstrating only a small change in activity. Exogenous heparin and some of the chemically modified heparins (2-de, 6-de and NAc), were able to inhibit the collapse inducing activity of hSlit2-CM (Figure 4.21). However, other chemically modified heparins (2-de NAc, 6-de NAc, 2, 6-de, 2, 6-de NAc and perS) and CS-C had no significant effect on the collapse activity of hSlit2-CM. This may be because endogenous HS chains were involved in modulating Slit/Robo interaction, so adding exogenous heparin or particular chemically modified heparins could competitively inhibit this event by saturating relevant sites of interaction.

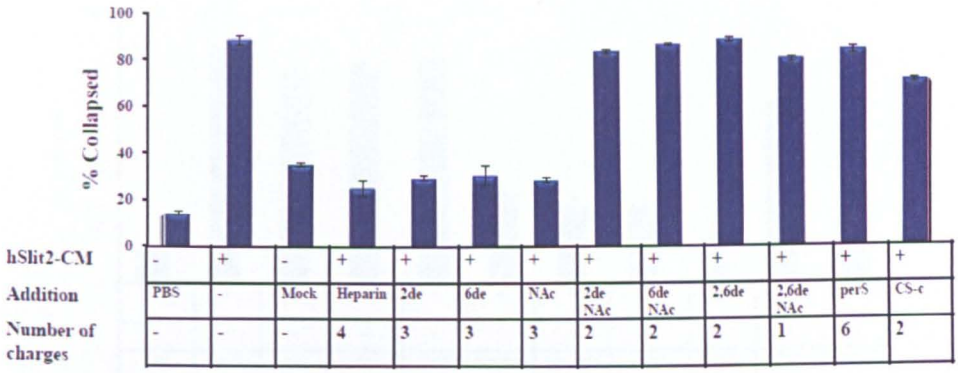

Figure 4.21 Inhibitory effects of heparin and chemically modified heparins on growth cone collapse promoted by hSlit2-CM. The retinal growth cone collapse assay was performed as described in Methods. Briefly, chick eyes were dissected from stage E7 embryos and cultured at 37 °C on cover-slips coated with 10 µg/ ml poly-L-lysine (Sigma) and 10 µg/ml laminin (Sigma) for 24 h. Heparin or chemically modified heparins, or CS-C (200 µg/ ml), were added immediately prior to the addition of hSlit2-CM, or PBS (negative control) to cultured explants for 10 min. Mock medium was collected under the same conditions as the hSlit2-CM from cells transfected with empty vector. Cultures were then fixed for 1 h in 2 % paraformaldehyde 7.5 % (w/v) sucrose and then mounted. The number of collapsed growth cones was counted in blind conditions. Each experiment was conducted independently a minimum of three times.

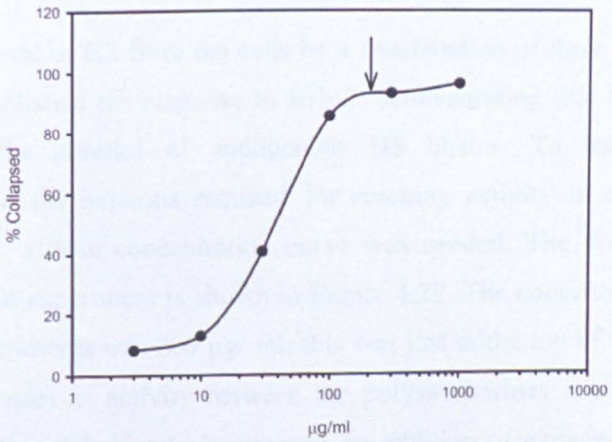

Figure 4.22 Dose concentration curve for heparin rescue activity on chick retinal growth cones. The data shows the ability of heparin to rescue growth cone collapse promoted by h Slit2-CM on ganglion cells subjected to enzymatic removal of endogenous HS. Concentrations ranged from 3-1000 µg/ ml. The percentage of collapsed growth cones was plotted against the heparin concentration. The arrow represents the 200 µg/ ml the concentration used in the rescue experiments.

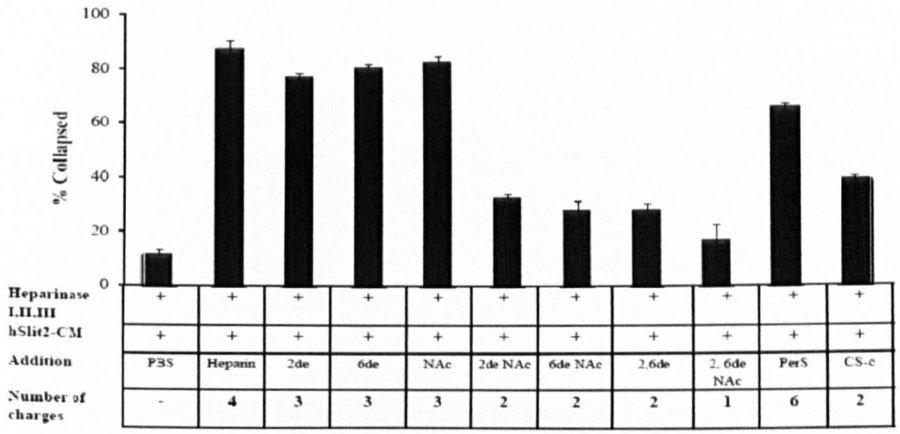

Figure 4.23 Chick retinal growth cone collapse promoted by hSlit2-CM is dependent on heparin and chemically modified heparins. The growth cone assay was carried out as described in **Figure 4.21**. Heparinase 1, II, III (5 mU / ml, IBEX), enzymes were added 3 hours before the addition of hSlit2-CM, or PBS (negative control), to cultured explants for 10 min. Then heparin, or chemically modified heparins, or CS-C, (200 µg/ ml) were added immediately prior to the addition of hSlit2-CM. Each experiment was conducted independently a minimum of three times.

Enzymatic removal of HS from the cells by a combination of three heparinase (I, II, III) enzymes abolished the response to hSlit2, demonstrating that Slit activity does not occur in the absence of endogenous HS chains. To test the structural characteristics of the heparins required for rescuing activity in cells depleted of endogenous HS, a dose concentration curve was needed. The dose concentration curve for heparin experiment is shown in Figure 4.22. The concentration chosen for subsequent experiments was 200 µg/ ml; this was just at the top of the slope, so that potential differences in activity between the polysaccharides could be monitored. Remarkably, this activity could be rescued by addition of exogenous heparin, and some of the chemically modified heparins (2-de, 6-de and NAc), to heparinase-treated cultures restored their sensitivity to hSlit2-CM (Figure 4.23), indicating that selectively de-sulfated heparins can substitute for endogenous HS to support productive signalling. Heparin had the highest rescue activity for the collapsed growth cones (~ 90 %) while removing one sulfate from heparin in the case of 2-de, 6-de and NAc modified heparins only moderately reduced their rescue activity to about ~ 75-80 % (Figure 4.23).

In contrast, removing two sulfates (2-deNAc, 6-deNAc or 2, 6-de) resulted in a low level of rescue activity (~25-30 %). Complete desulfation (2, 6-deNAc) resulted in a complete loss of rescue activity. Over-sulfated heparin (perS), which has in total six negative charges per disaccharide, has a modest rescue activity of about ~ 65 %, whereas CS-C have produced only partial rescue activity (~30 %), a level comparable with the double desulfated heparins. These data provided further support that HS has a functional role in regulating Slit-Robo biological activity.

4.2.7 Competition ELISA: studying oligosaccharide size requirements

4.2.7.1 Effect of heparin oligosaccharides on Slit and on Robo complexes

Competition ELISAs were also carried out to determine the minimum size required for Slit and Robo binding to heparin. As has been mentioned in Chapter 3, using oligosaccharides has advantages over working with polysaccharide chains, because native heparin is large and polydisperse thus, knowing the minimum oligosaccharide size of heparin will be instructive, and will simplify interpretation of binding data. Furthermore, it will assist in the on-going attempt to determine the crystal structure of ternary complexes of Slit, Robo and HS.

Figure 4.24 shows that 10-mer heparin is a significantly better competitor than 8-mer and 6-mer heparin for binding to Slit; in agreement with the proposal of Hussain et al (2006) that 10-mer is the minimum size of heparin oligosaccharide necessary for formation of the ternary complex. However, 6-mers and even 4-mers are able to compete, suggesting that these could be the minimum size required for binding to Slit. However, it is unknown if oligosaccharides this size are long enough for biological activity, as all investigators have used full-length polysaccharide chains in their interaction activity studies. Furthermore, Figure 4.24 shows that considerably higher concentrations of oligosaccharides were needed (1 mg/ ml). This concentration was used after several optimization steps. This high concentration of competitors is achievable for heparin oligosaccharide, but not HS oligosaccharides.

The oligosaccharide study will therefore be limited to heparin derivatives. 10-mers gave maximal binding competition with Robo (Figure 4.25), which agrees with the minimum size of heparin oligosaccharides that are necessary for the ternary complex proposed by Hussain et al (2006). However, 8-mers, 6-mers and even 4-mers also inhibit the interaction as observed for the Slit.

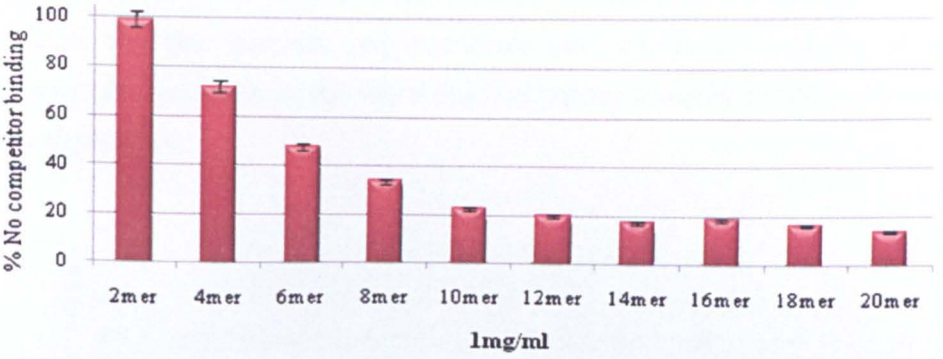

Figure 4.24 Binding of Slit to immobilized heparin oligosaccharide in the presence of soluble 2-20-mer heparin saccharides. Competition ELISA experiments were conducted as described in Figure 4.8. Data are representative of three separate experiments.

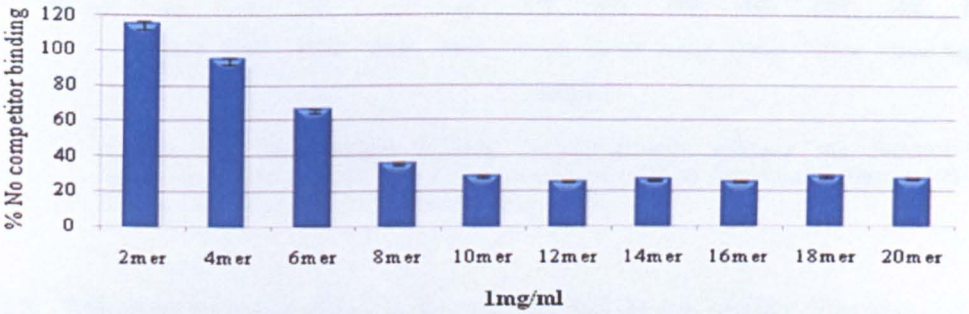

Figure 4.25 Binding of Robo to immobilized heparin oligosaccharide in the presence of soluble 2-20-mer heparin saccharides. Competition ELISA experiments were conducted as described in Figure 4.8. Data are representative of three separate experiments.

4.2.7.2 Effect of heparin oligosaccharides on Slit-Robo binary complex using direct ELISA

It is important to study in more detail the characteristics of heparin/ HS saccharides that are essential for enhancing Slit-Robo interactions. Thus, there is a need to determine the minimum size of oligosaccharides that support formation of the Slit-Robo-HS ternary complex.

In Figure 4.26, size-defined heparin oligosaccharides (2-20-mer) were applied at 10 µg/ ml to study Slit-Robo complex formation in a solid phase assay. It is clear those oligosaccharides of size 10-mer or longer provided enhancement of Slit-Robo interactions, with a steady increase with increasing size, and the strongest enhancement observed by adding 20-mers. Heparin polysaccharide had an even greater effect (~30 %) than the 20-mers on the Slit and Robo interaction. This result suggests that the minimum oligosaccharide size able to assist in the co-crystal structure determination of the Slit/ Robo/ HS ternary complex would be 10-mer-12-mer saccharides.

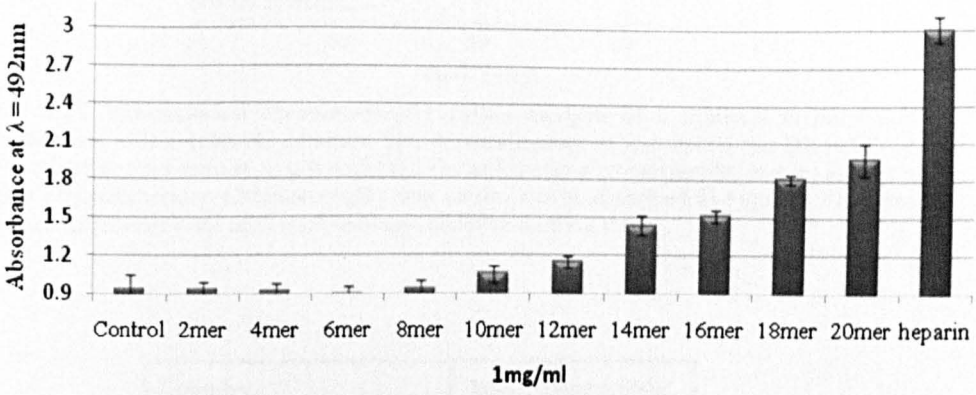

Figure 4.26 Size defined heparin oligosaccharides enhance the Slit-Robo interaction. Direct ELISA experiments were conducted as described in **Figure 4.11**. Data are representative of three separate experiments.

4.2.8 Effect of heparin oligosaccharides on Slit-Robo binary complex using SEC

The ability of size defined heparin oligosaccharides to interact with Slit and Robo was investigated using a range of sized heparin oligosaccharides and SEC. Selected oligosaccharides were incubated with dSlitD2 and dRoboIG1-2 in 1:1:1 ratio. Sizes from 2, 4 and 6-mer had no effect on the elution position of Slit and Robo complex, indicating that no stable complex formed (Figure 4.27). Larger oligosaccharide sizes (8-14-mer) shifted the elution peak to the left, with 12-mer and 14-mer showing the most clear shifts, indicating that complexes with larger hydrodynamic volumes were formed (Figure 4.27a and b).

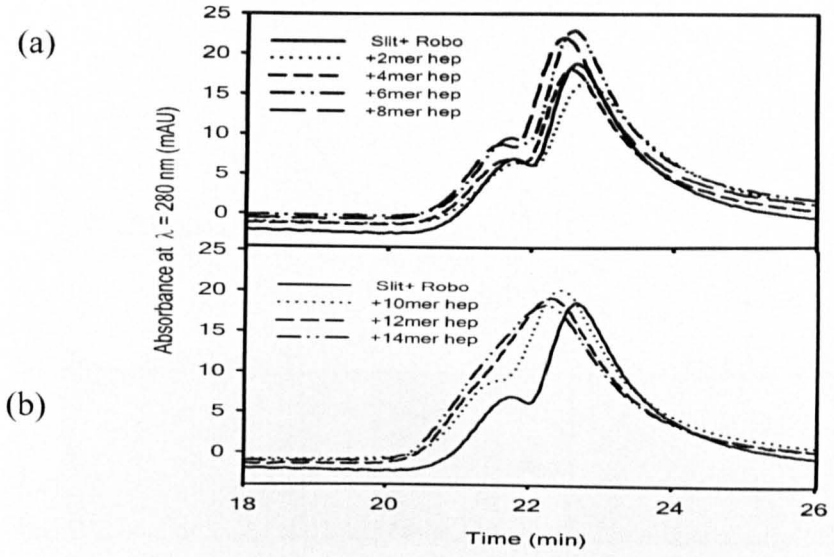

Figure 4.27 Size-exclusion chromatography (SEC) analysis of a minimal ternary Slit/ Robo/heparin oligosaccharide complex. SEC chromatograms of Drosophila Slit D2 and Robo IG1–2 mixed in 1:1:1 ratio at 10 μM with (a) 2-6-mer heparin oligosaccharides and (b) 8-14-mer heparin oligosaccharides. Chromatography was carried out as described in Figure 4.14. Three separate experiments were performed and representative data are shown.

Complex	Peak maxima (min)
Slit/ Robo+2-mer heparin	22.76
Slit/ Robo+4-mer heparin	22.55
Slit/ Robo+6-mer heparin	22.59
Slit/ Robo+8-mer heparin	22.44
Slit/ Robo+10-mer heparin	22.37
Slit/ Robo+12-mer heparin	22.27
Slit/ Robo+14-mer heparin	22.23

Table 4.3 Elution times of the peak maxima of heparin oligosaccharides with Slit-Robo.

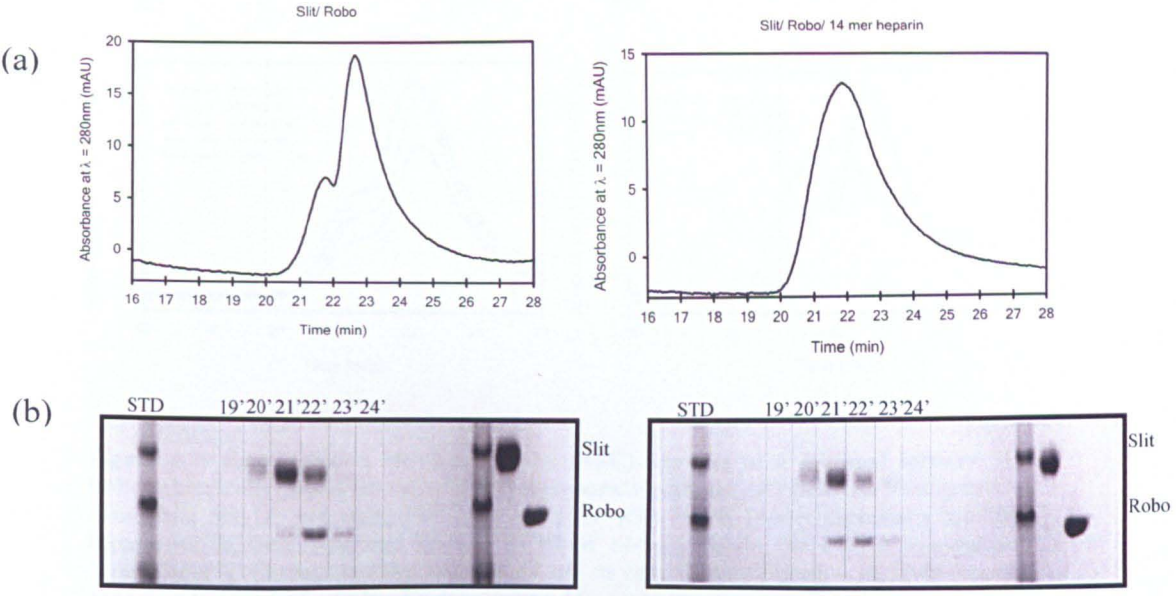

Figure 4.28 Size-exclusion chromatography (SEC) analysis of a minimal ternary Slit/ Robo/heparin oligosaccharide complex and PAGE analysis of eluted fractions. A) SEC chromatograms of isolated 10 μM Drosophila Slit D2/ 10 μM Robo IG1–2 mixed with 10 μM 14-mer heparin oligosaccharide. Chromatography was carried out as described in Figure 4.14. B) Coomassie Blue-stained SDS-PAGE gel of the peak fractions indicated in A. The fraction numbers are shown at the top of the gel. Three separate experiments were performed and representative data are shown.

Several different 14-mer oligosaccharides fractions prepared from chemically modified heparin were each mixed in 1:1:1 molar ratio with Slit and Robo to examine their abilities to promote ternary complex formation. 14-mers from 2-de, 6-de and NAc heparins produced slight shifts in the peaks to left, indicating their abilities to promote the interaction (Figure 4.29a). Furthermore, removal of two sulfates (e.g. 2, 6-de) resulted in no effect on the complex formation. 14-mer heparin produced a clear shift of the elution peak to the left, whereas adding 14-mer perS heparin saccharides produced no significant effect on complex formation (Figure 4.29b).

SDS-PAGE was performed for dSlitD2-d-Robo IG1-2 and 14-mer heparin SEC fractions as examples to confirm the presence of the two proteins in the putative complexes (Figure 4.28). Peak fractions contained both Slit and Robo in the earlier eluted fraction for 14-mer heparin compared to the control dSlitD2 and dRoboIG1-2 complex in the absence of oligosaccharides.

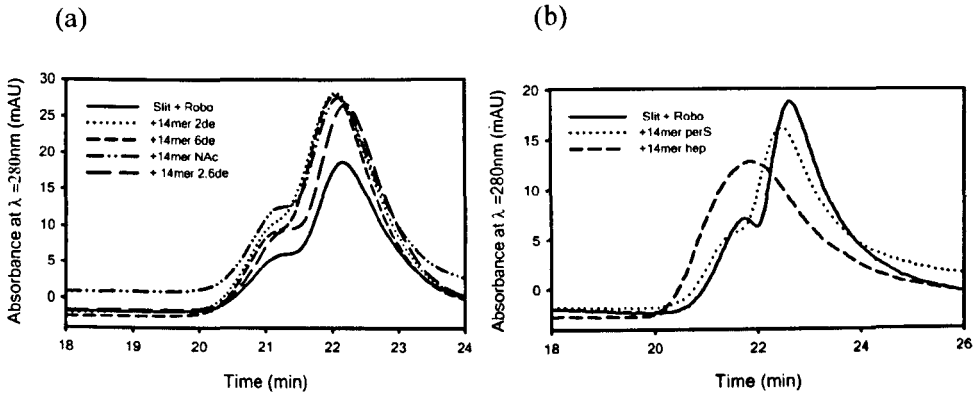

Figure 4.29 Size-exclusion chromatography (SEC) analysis of a minimal ternary Slit/ Robo/ chemically modified heparin oligosaccharide complex. A) SEC chromatograms of Drosophila Slit D2 and Robo IG1–2, mixed 1:1:1 with 10μM 14-mer chemically modified heparins (2-de, 6-de, NAc and 2.6-de). B) 10μM 14-mer heparin and 14-mer over-sulfated heparin (perS). Chromatography was carried out as described in Figure 4.14. Two separate experiments were performed and representative data are shown

4.3 Discussion

HS is needed for *in vitro* and *in vivo* Slit signalling through its receptor Robo (Hohenester, 2008). Nevertheless, the molecular mechanism by which HS controls these interactions is not yet clear. Robo has been shown to bind to a highly conserved region on the concave area of the Slit second LRR (D2). HS was also found to bind to a basic patch next to the Robo binding sites on Slit D2 and it has proved to be critical for its bioactivity (Howitt *et al.*, 2004). Hussain et al (2006) have established that HS forms a ternary complex with Slit and Robo, using heparin oligosaccharides purified in the early stages of the current project. Further studies have focused on Slit and Robo and their binary interactions with HS and also, on attempting to establish the essential sulfate groups and size requirements needed for a viable interaction with HS; and finally, to explore the ternary complex between Slit-Robo-HS and its biological significance.

Heparin derivatives	Competition ELISA Binary complexes		Direct ELISA Ternary complex	Elution time of GFC peaks maxima in min	Growth cone collapse rescue	Number of charges
	Slit	Robo	Slit and Robo	Slit and Robo= 22.16		
Heparin	++++	++++	++++	20.33	++	4
2-O-desulfated heparin	+++	++	++	21.92	++	3
6-O-desulfated heparin	++	+	++	21.95	++	3
N-Acetylated heparin	++	++	+++	21.79	++	3
2-O-desulfated N-acetylated heparin	-	-	-	22.11	-	2
6-O-desulfated N-acetylated heparin	-	-	-	22.11	-	2
2,6-O-desulfated heparin	-	-	-	22.13	-	2
2,6-O-desulfated N-acetylated heparin	-	-	-	22.13	-	1
Over sulfated heparin (perS)	+	+++	+	-	+	6

Table 4.4 Competition and direct ELISA data of chemically modified heparin interaction with the Slit, Robo, Slit and Robo complex; – no significant interaction; +, weak, ++ moderate; +++, strong and ++++ very strong interaction. Also showing the peaks maxima of the GFC in min and the ability of modified heparins for rescuing the collapse of the growth cone.

Competition ELISA data have shown that Slit binding involves 2-O, 6-O, and N sulfate groups in their interactions with HS (Table 4.3). However, there is a slight preference for the 6-O-sulfate and N sulfate more than the 2-O sulfate. This finding agreed to some extent with data from Shipp and Hsieh-Wilson (2007), that the 6-O sulfate and N sulfate of the glucosamine are essential for Slit binding to HS. However, the present study suggests the importance of 2-O sulfate as well, which had been played down by Shipp and Hsieh-Wilson (2007); the binding method used in their study involved microarrays of surface-bound chemically modified heparin polysaccharides. In their experiments, they tested three concentrations (50, 25 and 15 μM) of heparin and used a limited range of chemically modified heparins. As has been mentioned, the molarities of the polysaccharide chains are difficult to establish owing to their polydisperse nature. Importantly, the surface binding of the polysaccharides may alter their apparent specificity. Furthermore, it is documented that full length Slit-2 protein (that they were using) has two binding sites for heparin, one with high affinity which is in the C-terminus and one with lower affinity in the N-terminus (specifically on D2 of the LLR). The N-terminal Slit D2 is thought to be responsible for its biological function (Hussain *et al.*, 2006). Their data also differ with what had been suggested by Irie et al (2002), that the 2-O and the 6-O sulfate groups are important in axon guidance assays *in vivo* in which the promoter protein was suspected to be Slit. However, these data are more complex to interpret and could involve other target proteins.

Recently, Fukuhara and co-workers (2008) revealed the structural details of binding between dRoboIG1-2 and heparin oligosaccharide and confirmed that at least 10-mers are needed. Different structural data on the Slit binding sites to heparin were found to be adjacent to the Robo binding site in basic patches of the Slit D2 (Fukuhara *et al.*, 2008). This position requires a great deal of conformational change to allow access of the saccharides to their binding sites. The structural flexibility of the HS chain is enhanced by the presence of iduronic acid with 2-O sulfates, as well as the glycosidic bonds (Rudd and Yates, 2010; Yates *et al.*, 2004). This information suggests that to have conformational flexibility in HS, iduronic acid with a 2-O sulfate would be advantageous.

In the current investigation, competition ELISA data were obtained from a wider range of heparin concentrations, equivalent approximately to 300 μM to 80 nM, which could reveal more insight into the interactions. Eight of the chemically modified heparins and CS-C were also tested for interactions. In addition, the competition ELISA experiments were conducted on fragments of Slit2 D1-4, which contains the D2 domain this site involves in HS interaction and also, in binding. Most previous binary interaction work focused on the ligand (Slit). This is the first study to examine the receptor (Robo) binary interaction with HS. Robo has shown a 10-fold preference for heparin binding affinity compared to Slit based on their IC_{50} data (Figures 4.9 and 4.11). Chemically modified heparin competition data showed that Robo binding involves the 6-O sulfate, and to a lesser extent the 2-O and N sulfates. Thus, Robo selects a sulfation pattern distinct from its ligand (Slit) (Table 4.3). It has been mentioned in the introduction that there are different types of Robos with distinct structures. This finding could be significant as in the case of FGF system, where different HS/ FGFR interactions are vital in determining the output of FGF signalling and cell fate (Guimond and Turnbull, 1999).

Both Slit and Robo showed stronger affinities to heparin compared to chemically modified heparins. These results do not rule out a non-specific involvement of electrostatic interactions. However, the data obtained on the interactions of over-sulfated (perS) heparin with both Slit and Robo showed it to be a poorer competitor compared to heparin, indicating that a simple charge density is not the main criterion for supporting these interactions (Table 4.3). This idea is supported also by the data from CS-C, which is also a very poor competitor.

The results from direct ELISA have shown that heparin yielded about a 70-fold shift in the dose response curve for Slit-Robo complex formation whereas NAc heparin enhanced the interaction by 25-fold, and the 2-de or 6-de by about 14-fold (Figure 4.13). Removing two or more sulfates resulted in negligible effects on promoting the Slit-Robo interaction. The presence of extra negative charges, as in the case of over-sulfated heparin (perS) produced only about a 5-fold enhancement in complex formation.

These results provide "foot printing" data to explore sulfation selectivity; they suggest that O-sulfation (both 2-O and 6-O) are most critical for promoting complex formation, and are distinct from the binding preferences observed for both Slit (6-O = N > 2-O) and Robo (6-O > N = 2-O) as individual proteins. In particular, they suggest a more prominent role for the 2-O-sulfates (Table 4.3).

To obtain direct evidence for ternary complex formation, analytical SEC was employed. *Drosophila* Slit D2 (27.4 kDa + 2 *N*-linked glycans) eluted as a monomer (Figure 4.14a). The elution volume of *Drosophila* Robo IG1–2 (24.1 kDa) is also well matched with a monomer (Figure 4.15a). When Slit D2 and Robo IG12 were mixed in a 1:1 ratio, only individual peaks were observed, which demonstrated a lack of formation of a binary complex (Figure 4.16). Addition of heparin in a 1:1:1 ratio to Slit-Robo complex results in the formation of a ternary complex with a much broader and higher molecular weight peak (Figure 4.17). This peak could be explained by the polyvalent effect of heparin; because it has many binding sites, multiple complexes could assemble on the chain. Interestingly, when heparin was added to the individual Slit D2 and Robo IG-12 proteins, no interaction was detected. These data suggest that a high affinity-binding site (sufficient to be observed in SEC chromatography) is only formed in the presence of the Slit-Robo complex. This view is supported by the much lower concentration of heparins needed to support complex formation compared to individual protein interactions. The different modified heparins were mixed with the same ratio 1:1:1 to the Slit and Robo. Only three of the modified heparins supported the ternary complex formation (NAc, 6-de and 2-de). The chemically modified heparins with more than one sulfate missing, and CS-C did not significantly promote ternary complex formation. Thus, there seems to be a key requirement for at least two sulfate groups on heparin for a productive interaction. However, 6-de has weaker interaction with Robo according to Table 4.3. SEC under the above conditions proved to be a fast and simple method to run with a high degree of consistency. Calibration using protein standards gave mass estimates for heparin protein complexes that, when combined with information on the molarities of the incubated components, allowed stoichiometries to be estimated. This technique could be modified to study a wide range of protein-polysaccharide interactions.

The importance of HS structures that can form a ternary complex with Slit and Robo was examined by using analytical SEC (Robinson *et al.*, 2005). Different modified heparins were mixed in the same ratio 1:1:1 to the Slit and Robo. Only three modified heparins supported the formation, of a ternary complex formation these were NAc, 6-de and 2-de. The chemically modified heparins with more than one sulfate missing and CS-C did not promote the ternary complex formation.

This data have confirmed to some extent the earlier direct ELISA data where the fact that losing 6-O or 2-O sulfate groups were 50 % lesser than NAc. This difference could be due to larger Slit proteins (dSlitD1-4) and larger Robo proteins (dRoboIG1-5) were used in the direct ELISA and also, dSlitD1-4 was C-myc and His tagged and the dRoboIG1-5 was Fc tagged and so a dimer. It is not clear if these factors could affect the direct ELISA data. They may explain the differences in the two assays. Analytical SEC was a more concise assay, as one fragment dSlitD2 that contained the Robo binding sites, was mixed with dRoboIG1-2 in 1:1:1 ratio with heparin derivatives. dSlitD2 contains the binding site for dRoboIG1-2 and it has been recently confirmed that HS binding is next to the Robo binding site on Slit D2. However, other parts of the proteins might contribute to the formation of the complexes, so the direct ELISA data cannot be disregarded.

The effects of HS sulfation have also been examined on axon guidance promoted by Slit. Chick retina isolated from embryonic day seven (E7) embryos, were co-cultured with hSlit-2-CM. Adding heparin and some of the chemically modified heparins (2-de, 6-de and NAc) inhibited the collapse-inducing activity of hSlit-2-CM. From the structural information on full length Slit, it has been proposed that there are two sites for heparin binding; one at the C-terminal (which has no involvement with Slit and Robo interactions) and one on the N-terminal (involved in Robo and heparin binding). By adding heparin to full length Slit, competition with the endogenous HS is expected to result in inhibition of the activity of the full-length hSlit-2. Earlier investigations have established that Slit requires HS to mediate axon guidance, as treatment of the cell cultures with heparinase abolished the repulsive activity of Slit (Hussain *et al.*, 2006).

Here, chemically modified heparins were investigated for their role in rescuing Slit activity of cells that had been heparinase treated (to create a deficiency in endogenous HS). Enzymatic removal of endogenous HS by heparinase treatment eliminated the response to hSlit2, indicating that HS chains at the cell surface are crucial for Slit-Robo signalling. Surprisingly, it was found that heparin, 2-de, 6-de and NAc all rescued the collapse activity of Slit (Figure 4.2). In contrast, removing two or more sulfates completely abolished the rescue activity. Over-sulfated heparin and CS-C had only weak rescue effects. These data are broadly consistent with data obtained biochemically using SEC chromatography, except that the presence of N-sulfate groups seems to be more critical in the biological assays.

However, it should be noted that the same mass of heparin and chemically modified heparins were used for all retina experiments at a single screening dose concentration. It will be useful in the future to perform dose responses for the modified heparins to assess whether there are any quantitative differences in their activity. In addition, the molecular weight of the chemically modified heparins should also be taken into consideration in the interpretation of the data. Overall, the activity data provide additional support for the view that 2-O, 6-O and N sulfates are all important for HS promotion of Slit-Robo activity, though none appear to be essential in their own right, demonstrating possible redundancy in the structural requirements. Nevertheless, these data suggest that changes in HS structure (particularly 2-O or 6-O sulfation) could result in altered ability to promote Slit activity. Further studies with natural HS saccharide structures are now needed to help elucidate this possibility. It is worth noting that altered 2-O and 6-O sulfation in HS2ST and HS6ST1 knockout mice have been found to result in altered axon guidance phenotype (Pratt *et al.*, 2006).

Most of the binding and bioassay data were obtained using polysaccharide chains, which it has been argued in this thesis are useful for screening purpose, but to discover more details of interactions and structure-activity relationships, structurally defined oligosaccharides would be useful. The effect of oligosaccharide sizes on the Slit and Robo complex formation were also examined as this information is required to understand complex formation and for many follow-up studies such as establishing the crystal structure of the co-complexes.

Heparin oligosaccharides are an essential tool for studying heparin/HS proteins interactions (see Chapter 3). The minimum sizes of oligosaccharides that interact with Slit and Robo have been confirmed by competition ELISA. Slit and Robo require at least 8-mer oligosaccharides for inhibition, but 10-mer and larger oligosaccharides achieve complete inhibition essentially equivalent to intact chains. These findings will assist in the ongoing attempt to obtain the crystal structure of the ternary complex of Slit/Robo/HS. In addition, a range of size-defined (2-mer-14-mer) heparin oligosaccharides was tested for their ability to maintain the ternary complex. They were mixed in a 1:1:1 molar ratio to Slit-Robo.

Well-defined shifts were observed with 12-mer and 14-mer, whereas, 8-mer and 10-mer both created only a modest shift, indicating some complex formation. Heparin and 14-mer heparin SEC complex data were confirmed by SDS-PAGE and Coomassie blue staining to demonstrate the presence of both Slit and Robo in the putative complex peak. Chemically modified heparin oligosaccharides (14-mers) were selected to be screened for Slit and Robo ternary complex formation. The results gained from the analytical SEC provide additional proof for the necessity of two sulfates per disaccharide unit in heparin for their promotion of Slit-Robo complexes. In future work, HS oligosaccharides should be tested for activity in the growth cone assay in order to study in more detail the potential different activities of HS oligosaccharides in Slit-Robo ternary complex formation. Overall, the Slit-Robo-HS biochemical and bioactivity data described in this chapter provide insights into the nature of these interactions and assist further in understanding the structure-activity relationships (SARs).

5 Chapter five: A new insight into the structure selectivity of HS: how 8-mer sub-fractions regulate FGF-1 and FGF-2 signalling

5.1 Introduction

5.1.1 FGFs

Fibroblast growth factors (FGFs) are proteins, found in organisms ranging from invertebrates (e.g. nematodes) to vertebrates (e.g. human). The human and mouse FGFs are encoded by 22 genes, *Xenopus* and chicken by seven, four in zebrafish, two in the nematode *C elegans* and only one in *Drosophila.* There is 13-71% amino acid similarity between FGFs and their molecular weights range in size from 18-34 kDa (Itoh and Konishi, 2007). The human FGFs are divided into seven subfamilies, each subfamily containing between two to four members (Figure 5.1). The FGF-11 sub-family, also called fibroblast homologous factors (FHFs), is different from the other FGF sub-families, as they do not signal through activation of FGF receptors (FGFRs). Instead, their main targets are the intracellular domains of voltage-gated sodium channels (Beenken and Mohammadi, 2009; Goetz *et al.*, 2009). All others FGF subfamilies have relatively strong affinities to heparin, (confirmed by their salt elution from affinity columns) apart from FGF-19 subfamily, which has modest or no affinity (Asada *et al.*, 2009; Goetz *et al.*, 2007).

FGFs are involved in many developmental processes, such as cell proliferation, differentiation and morphogenesis. Development most organs, such as the nervous system, lenses, kidneys and skeleton are dependent on FGFs (Abdel-Rahman *et al.*, 2008; Bates, 2007; Chikazu *et al.*, 2000; Mason, 2007; Robinson, 2006). FGFs are important in many physiological processes, such as regulation of tissue homeostasis, wound healing, tissue repair and angiogenesis (Kroger and Schroder, 2002; Ornitz and Itoh, 2001; Werner and Grose, 2003; Yamashita *et al.*, 2002).

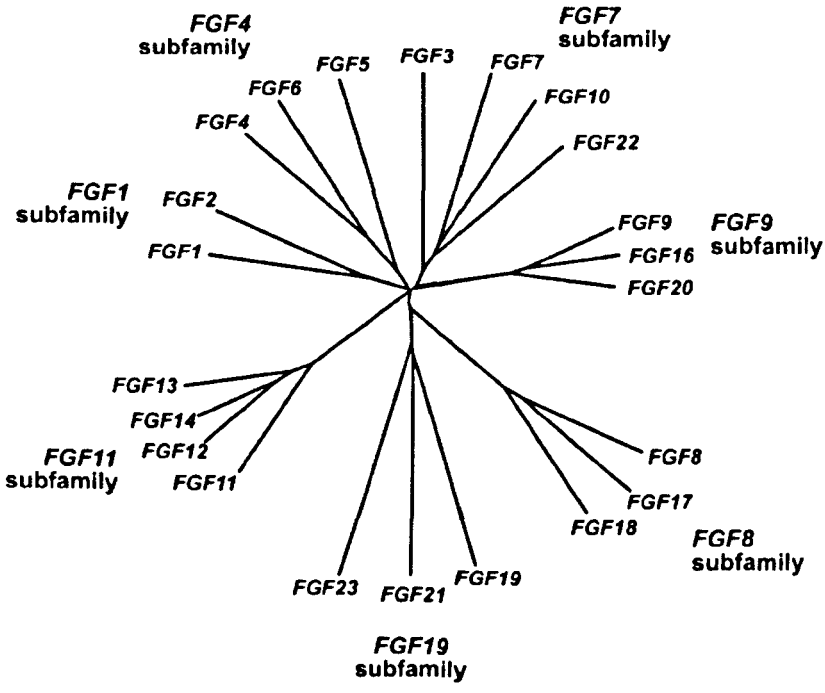

Figure 5.1 Human *fgf* gene families and their evolutionary relationships. Twenty-two FGFs have been identified. Phylogenetic analysis suggests that the FGFs can be arranged into seven subfamilies containing two to four members each. Branch lengths are proportional to the evolutionary distance between each gene. Adopted from (Itoh and Ornitz, 2004).

Genetic studies of knockout mice have shown that a lack of some FGFs, such as FGF-8, is lethal (Meyers *et al.*, 1998). Miller et al., (2000) and Ortega et al., (1998), however, found that lack of the FGF-1 or FGF-2 had either no effect or only a mild effect on phenotype, respectively. Mutations in FGFs have also been linked to many human hereditary diseases. This is due to the loss of the FGF functions in most cases. Here are some examples of these diseases and their malfunctioning FGFs. Michel aplasia, a disease characterised by congenital deafness, is caused by a mutation in FGF-3 (Tekin *et al.*, 2007; Yuguchi *et al.*, 2005). Spinocerebellar ataxia is linked to mutations in FGF-14 (van Swieten *et al.*, 2003). FGF-23 is involved in the regulation of phosphate and vitamin D homeostasis and mutation of this growth factor results in phosphate wasting disorders (Yuguchi *et al.*, 2005). The FGF knockout mice have provided much of the physiological information available. Table 5.1 summarize some of this information (Beenken and Mohammadi, 2009).

Fibroblast growth factor (FGF)	Phenotype of knockout mouse	Physiological role
FGF1	Normal	Not established
FGF2	Loss of vascular tone; slight loss of cortex neurons	Not established
FGF3	Inner ear agenesis in humans	Inner ear development
FGF4	Embryonic lethal	Cardiac valve leaflet formation; limb development
FGF5	Abnormally long hair	Hair growth cycle regulation
FGF6	Defective muscle regeneration	Myogenesis
FGF7	Matted hair; reduced nephron; branching in kidney	Branching morphogenesis
FGF8	Embryonic lethal	Brain, eye, ear and limb development
FGF9	Postnatal death; gender reversal; lung hypoplasia	Gonadal development; organogenesis
FGF10	Failed limb and lung development	Branching morphogenesis
FGF16	Embryonic lethal	Heart development
FGF17	Abnormal brain development	Cerebral and cerebellar development
FGF18	Delayed long-bone ossification	Bone development
FGF19	Increased bile acid pool	Bile acid homeostasis; lipolysis gall bladder filling
FGF20	No knockout model	Neurotrophic factor
FGF21	No knockout model	Fasting response; glucose homeostasis Lipolysis and lipogenesis
FGF22	No knockout model	Presynaptic neural organizer
FGF23	Hyperphosphataemia; hypoglycaemia; immature sexual organs	Phosphate homeostasis; vitamin D homeostasis

Table 5.1 The physiology of FGFs adopted from (Beenken and Mohammadi, 2009).

5.1.2 FGFRs

FGFRs are tyrosine kinase class IV receptors. There are four classic FGFRs (FGFR1-4), encoded by a family of four genes (*fgfr1-4)* (Groth and Lardelli, 2002; Houssaint *et al.*, 1990; Neilson and Friesel, 1996; Powers *et al.*, 2000; Sleeman *et al.*, 2001). FGFs interact with the FGFRs and provoke FGFR dimerization followed by phosphorylation of specific cytoplasmic tyrosine residues through triggering the intracellular signalling pathways that regulate cell fate (Itoh and Ornitz, 2004; Johnson and Williams, 1993).

FGFRs consist of an extracellular region consisting of a signal peptide followed by three immunoglobulin (Ig)-like domains (I-III) with an acid box between IgI and IgII (Figure 5.2). A heparin-binding region and a cell adhesion molecule (CAM) homology domain (CHD) are located downstream from the acid box. At the end of the extracellular region is a transmembrane (TM) domain followed by an intracellular region. The latter consists of a juxtamembrane domain, a tyrosine kinase domain (which is split into two TK1 and TK2 by a kinase insert) and a short c-terminal tail (CT) (Doherty and Walsh, 1996; Groth *et al.*, 2002; Walker *et al.*, 1994) (Figure 5.2).

A fifth *fgfr* gene encodes a receptor lacking a kinase domain required for signal transduction by transphosphorylation, termed fibroblast growth factor receptor- Like FGFRL1 (Trueb *et al.*, 2003).

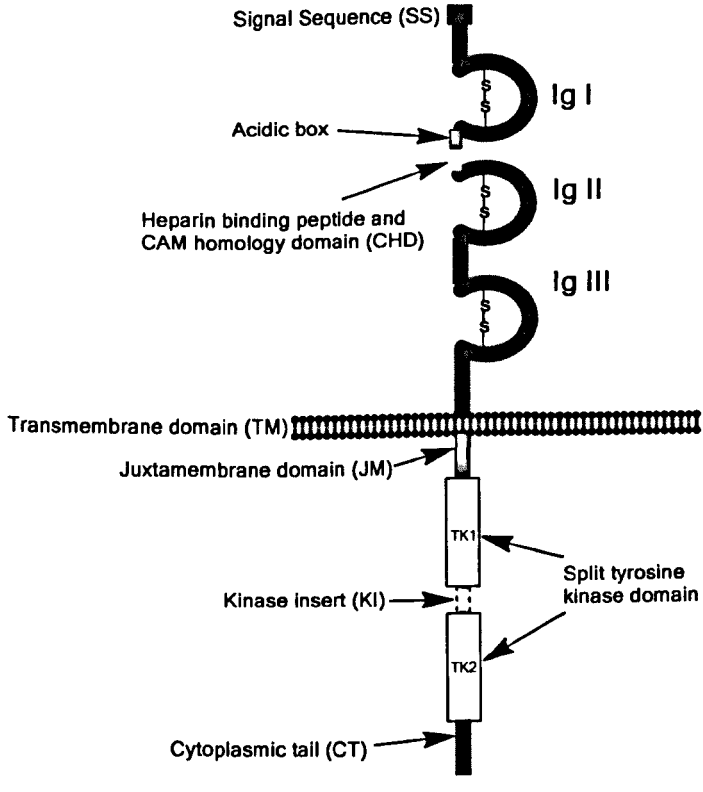

Figure 5.2 Schematic depicting the main structural features of FGFRs.

FGFRs are subjected to alternative splicing of their gene transcripts resulting in diverse FGFR1, 2, 3 and 4 isoforms that are differentially expressed in cells and tissues (Fernig and Gallagher, 1994; Ornitz *et al.*, 1996). The FGFR isoform splice variants are III a, b and c, but FGFR isoform may contain two or three Ig domains and the specific sequence of the three variants of the Ig-like III domain (IIIb and IIIc) also known as (a, b and c) (Ornitz *et al.*, 1996). These variants are essential to the functions of the FGF signalling system and they exhibit diverse specificity for FGFs (Ornitz *et al.*, 1996; Venkataraman *et al.*, 1996). FGFR-1 is reported to have at least 48 isoforms ranging between soluble receptors and transmembrane variants (Groth and Lardelli, 2002). FGF-1 is the only FGF that has the capability of activating all receptor isoform splice variants (Eswarakumar *et al.*, 2005) (Table 5.2). In contrast, FGF-22 is an excellent activator of only FGFR-2b (Umemori *et al.*, 2004).

FGFR isoform	Ligand specificity
FGFR1b	FGF1, -2, -3 and -10
FGFR1c	FGF1, -2, -4, -5 and -6
FGFR2b	FGF1, -3, -7, -10 and -22
FGFR2c	FGF1, -2, -4, -6, -9, -17 and -18
FGFR3b	FGF1 and -9
FGFR3c	FGF1, -2, -4, -8, -9, -17, -18 and -23
FGFR4	FGF1, -2, -4, -6, -8, -9, -16, -17, -18 and -19

Table 5.2 Ligand specificities of FGFR isoforms and splice variants in the presence of heparin (Eswarakumar *et al.*, 2005).

The role of the different receptors has been investigated by targeted gene modification in mice. Mice lacking FGFR-1b or FGFR-1c die due to defects in their cell migration (Deng *et al.*, 1994; Deng *et al.*, 1993; Partanen *et al.*, 1998), whereas, mice lacking the Ig domain III of FGFR2 die due to malfunctions in the placenta (Xu *et al.*, 1998). There are several human hereditary disorders connected to mutations in FGFR-1, FGFR-2 and FGFR-3 (Wilkie, 2005). Mutations in FGFRs, which lead to gain of function, were recognized in a variety of human cancers such as lymphomas, prostate and breast cancers (Deng *et al.*, 1994).

FGFR-1 and FGFR-2 mutations result in craniosynostosis syndromes (premature closure of one or more cranial sutures), such as Crouzon, Pfeiffer and Apert syndromes. Other disorders, relating to dwarfism, such as chondrodysplasia syndromes, hypochondroplasia, achondroplasia and thanatophoric dysplasia, are associated with mutation in FGFR-3 (i.e. increasing activity) (Eswarakumar *et al.*, 2005; Wilkie, 2005).

The FGFs transmit their signals via high-affinity binding to the FGFRs, however, there is evidence that non-FGFR or FGFR-interacting proteins such as an integrin αvβ3, neural cell adhesion molecule (NCAM), N-cadherin and anosmin, are important players in FGF signalling (Cai and Chen, 2008; Hu *et al.*, 2009; Kim *et al.*, 2008; Kiselyov *et al.*, 2005; Kochoyan *et al.*, 2008; Murakami *et al.*, 2008; Suyama *et al.*, 2002).

5.1.3 Involvement of HS in the regulation of FGF signalling

The signalling of FGF involves high affinity binding of FGF to FGFRs followed by receptor dimerization and activation (Neufeld and Gospodarowicz, 1985; Powers *et al.*, 2000). The receptor activation triggers trans-phosphorylation of specific tyrosine residues in the cytoplasmic kinase domain creating binding sites for Src homology 2 (SH2) and phosphotyrosine binding (PTB) domain-containing proteins leading to the initiation of downstream signalling cascades (Boilly et al., 2000). For example, adaptor proteins interacting with activated FGFR trigger downstream signalling involving Ras-mitogen activated protein kinase (MAPK) (Dailey *et al.*, 2005; Katz *et al.*, 2007).

HS is known to function as a co-receptor for the FGFs by participating in the formation of a ternary complex, mediated by specific interactions of the HS with both the FGF and its receptor. It was first suggested that the HS is necessary for high affinity binding of FGF-2 to FGFR-1 and for cell growth and differentiation; however, low affinity binding was also possible (Rapraeger *et al.*, 1991; Yayon *et al.*, 1991).

The mechanism of the interaction between HS and the FGFs is thought to rely on an electrostatic interaction between the negatively charged sulfate and carboxyl groups in the HS chain, and the basic amino acids (Lysine and Arginine) in FGFs, with Arg favoured due to its high pKa (more than 12) (Fromm *et al.*, 1995). However, the interaction of FGF-2 was shown to be only 30 % ionic, hence, other forces, such as hydrogen bonding, hydrophobic and van der Waal's interactions, would certainly contribute to the interaction (Pantoliano *et al.*, 1994; Thompson *et al.*, 1994a; Zhu *et al.*, 1998).

The exact method by which HS interacts with FGF and FGFR to form a ternary complex is still debatable (Harmer *et al.*, 2004; Yu *et al.*, 2005). There are a number of anticipated models; Yayon et al (1991) have proposed conformational changes similar to the interaction of HS with ATIII (Yayon *et al.*, 1991). However, structural and biochemical studies of FGF-1 and FGF-2 with heparin saccharides do not support this idea (Springer *et al.*, 1994; Faham *et al.*, 1996; DiGabriele *et al.*, 1998) (Figure 5.3a and b). The ternary complex of HS saccharides, FGF and FGFR was subsequently analysed by co-crystallography. The two main proposed models are the symmetric and the asymmetric. In the symmetric model there are two HS saccharides, two FGFs and two FGFRs, and the HS functions as regulator for both FGF-FGFR and FGFR-FGFR interactions (Figure 5.4a) (Schlessinger *et al.*, 2000).

In contrast, in the asymmetric model, there are one HS, two FGFs and two FGFRs, and here HS functions as a bridge between the FGF and the FGFR (Figure 5.4b) (Pellegrini *et al.*, 2000). Recently, Goodger et al, (2008) have suggested that both interaction models are possible, dependent on the length and structure of the heparin oligosaccharide used (Goodger *et al.*, 2008). Despite the importance of these studies, they have not explained how a short heparin oligosaccharide (4-mer) can activate FGF-2 signalling (Delehedde *et al.*, 2002a). In addition, it must be remembered that all of these studies used highly sulfated heparin and not lower sulfated heterogeneous HS.

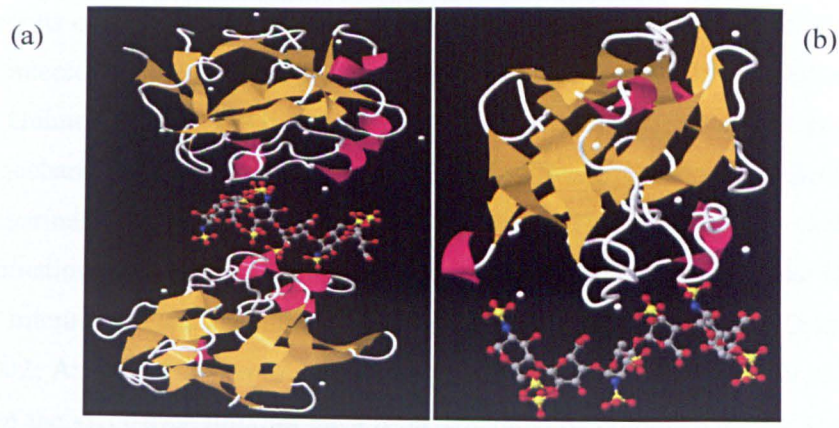

Figure 5.3 Top view of the co-crystallography structures of the FGF-1 (2AXM, a) (DiGabriele *et al.*, 1998) with 10-mer heparin and FGF-2 (1BFC, b) with 6-mer heparin complexes. (Faham *et al.*, 1996). Oligosaccharides are shown in ball and stick form, and the protein in cartoon form and the water molecules in white.

Figure 5.4 Two co-crystallography structures of the HS-FGF-FGFR ternary complex. Oligosaccharides are shown in ball and stick form, the protein in cartoon form and the water molecules in white. a) The symmetric model (2FGF-2, 2FGFR1, 2 10-mer) 1FQ9 (Schlessinger *et al.*, 2000). b) The asymmetric model (2FGF-1, 2FGFR1, 1 10-mer) 1E0O (Pellegrini *et al.*, 2000).

5.1.4 HS and heparin derivative saccharides are important tools for studying structure-activity relationship of HS-FGF-FGFR system

Decoding the sulfation specificities of the FGF/ FGFR system will be critical for understanding the structure-activity relationships of HS and the molecular mechanisms of important biological processes. Several approaches have been used to study HS-FGF interactions (Powell *et al.*, 2004). One approach is using heparin and chemically modified heparin variants for screening the selectivity of HS in regulation of the FGF/ FGFR system.

The results obtained could emphasize the importance of a particular sulfation types in the interaction of FGFs and FGFRs with HS (Belford *et al.*, 1992; Belford *et al.*, 1993; Guimond *et al.*, 1993; Powell *et al.*, 2002). Another approach is to produce oligosaccharide libraries from naturally occurring heparin, HS or modified heparin by heparinase or nitrous acid partial digestion. This approach is helpful in determination of the size, as well as specific sulfate motifs required for the HS-FGF-FGFR interactions and signalling (Loo *et al.*, 2001; Jemth *et al.*, 2002; Ostrovsky *et al.*, 2002; Ashikari-Hada *et al.*, 2004; Robinson *et al.*, 2005; Goodger *et al.*, 2008). Most of the saccharide libraries have been generated by chromatography. Hence, the oligosaccharides may encounter some degree of heterogeneity in terms of size purification. This should be taken into consideration when analysing the interaction or activity data. In addition, an appropriate method for structural characterization is essential in order to relate sequence information to activity.

5.1.5 HS sequence selectivity in HS-FGF-FGFR system

The structural determinants of the HS chain binding to FGFs have been extensively studied. In FGF-2, the interactions between the amino acid side chains and the sulfate groups of the IdoA2S and the GlcNS were shown to be crucial for binding (Turnbull *et al.*, 1992; Guimond *et al.*, 1993; Walker *et al.*, 1994; Ishihara, 1994). In addition, the minimum size of the HS oligosaccharide needed is thought to be in the range between 4-12-mer in length (Turnbull *et al.*, 1992; Ishihara *et al.*, 1993; Maccarana *et al.*, 1993; Delehedde *et al.*, 2002a).

Kreuger et al (1999) have shown that there are differences in HS binding of FGF-1 and FGF-2. The 6-O-sulfation of IdoA2S-GlcNS units in HS is more important for FGF-1 binding than FGF-2 (Sasaki *et al.*, 1999; Kreuger *et al.*, 2001; Kreuger *et al.*, 2003; Guglieri *et al.*, 2008). In a broader study, Kreuger and colleagues investigated the interactions between HS and various FGFs and concluded that the nature of many FGF-HS interactions depends largely on the organization of the HS domains rather than their subtle structure (Kreuger *et al.*, 2005; Kreuger *et al.*, 2006). This finding challenges the notion of selectivity/ specificity in the HS-FGF interactions.

The biochemical techniques used by most researchers in pursuing the HS-FGF selectivity of interactions are affinity column chromatography or filter trapping (Sasaki *et al.*, 1999; Kreuger *et al.*, 2001; Ashikari-Hada *et al.*, 2004; Jastrebova *et al.*, 2006; Guglieri *et al.*, 2008). In these techniques, a mixture of oligosaccharides is fractionated throughout an affinity column or a filter traps saccharide-protein complexes. Bound saccharides are then eluted with a concentration gradient of salt (NaCl); the stronger the binding, the higher the concentration of NaCl required for elution. However, these techniques may not be ideal for investigating the selectivity/ specificity as the presence of a high concentration of a particular oligosaccharide may dictate its binding affinity to the protein (i.e. the mass action effect). In addition, as mentioned previously for FGF-2, in some cases only about 30 % of the interaction is thought to be ionic, hence the fractionation of mixtures on an affinity column and elution with salt may be biased towards these types of interactions. Furthermore, the nature of the proteins may be altered (i.e. they may unfold) due to the immobilization of proteins onto columns or filters (Powell *et al.*, 2004).

HS/ heparin interact independently with FGFRs via a specific heparin binding sequence (K18K) found between the Ig I and Ig II (Figure 5.2) (Kan *et al.*, 1993, McKeehan, 1993; Kan *et al.*, 1999). Mitogenic bioassays revealed that signalling of FGFR was mediated by specific HS saccharides (Pye *et al.*, 1998; Guimond and Turnbull, 1999; Pye *et al.*, 2000). The HS binding sequence for FGFR-4 has been suggested to be an 8-mer with IdoA2S and GlcNS6S residues (Zhang *et al.*, 2001a). Powell et al (2002) studied the FGFR-1 and FGFR-2 binding to heparin chains and found that the kinetics and affinities of the interactions for each receptor differed significantly. Despite both the FGFR-2 and the FGFR-1 requiring 6-O, 2-O, and N sulfate, FGFR-1 bound to heparin chains with a lower affinity (63 nM) than FGFR-2 (13 nM) (Powell *et al.*, 2002).

Several studies have investigated the length and structural characteristic of HS that promote FGF activity (Guimond *et al.*, 1993; Ishihara, 1994; Pye *et al.*, 1998; Guimond and Turnbull, 1999; Pye *et al.*, 2000). Delehedde et al (2002) found that 4-mer heparin sequences are sufficient for partial FGF-2 binding to, and activation of, FGFR.

This observation was thought to be because the heparin saccharides are rich in 2-O sulfate, 6-O sulfate and the N-sulfate content, which is considered important for FGFR interaction with HS (Ostrovsky *et al.*, 2002; Powell *et al.*, 2002). However, longer HS saccharides (about 12-mer) are thought to be required in order to promote efficient receptor signalling in response to FGF-2, with regions in the saccharide that bind to both FGF-2 and another to the receptor. A requirement for both 2-O and 6-O sulfate groups was also demonstrated (Guimond *et al.*, 1993). Pye et al (1998) found that 10-mer and 12-mer HS are involved in promoting FGF-2 activity, and that 6-O sulfation of GlcNS, in addition to 2-O sulfation of IdoA, is vital in promoting FGF-2 activity (Pye *et al.*, 1998; Pye *et al.*, 2000). In addition, Guimond and Turnbull (1999) have studied the mitogenic activity of the SAX purified 10-mer HS saccharides with FGF-2 and various FGFRs and showed that signalling activity is dependent on modification types of different HS saccharides. They proposed a model in which specific sequences with selective sulfate positions of the 10-mer saccharides can differentially enhance or inhibit different FGF-FGFR signalling complexes (Guimond and Turnbull, 1999). However, some other investigators have proposed that, lack of one type of sulfate will not cause a serious effect and can be balanced by the overall sulfate and sequence structure (Kariya *et al.*, 2000; Merry *et al.*, 2001; Kamimura *et al.*, 2006). Furthermore, there are additional parameters that could contribute to the HS-FGFs signalling system such as saccharide conformation (Rudd *et al.*, 2007). Most recently, it has been reported that changing the cation associated with modified heparins from sodium to potassium or copper causes a dramatic change in the ability to promote FGF-2 and FGF-1 signalling and activation (Rudd *et al.*, 2007; Guimond *et al.*, 2009b).

5.1.6 Aims

The above introduction has highlighted the importance of HS in FGF-FGFR complex formation. Although the interaction and activity of FGF-1 and FGF-2 and their receptors with HS has been extensively investigated, there is still no clear picture of the structural selectivity of the system. In addition, most investigators have used heparin or modified heparins instead of physiologically relevant HS saccharides. Work presented in this chapter aims at acquiring more insight into the influence of the HS structure in FGF interaction and activity events.

The FGFs studied will be FGF-1 and FGF-2, using binding and activity assays to examine whether they exhibit selectivity or specificity for particular HS characteristics. Hence, heparin and chemically modified heparins were used in order to investigate basic sulfate requirements for FGF-1 and FGF-2 binding. Size separated oligosaccharides derived from heparin and chemically modified heparins were used to determine the oligosaccharide size and the type of sulfate groups sufficient for FGF-1 and FGF-2 interactions. Finally, size/ charge separated tissue-derived HS oligosaccharides were used in order to elucidate the effect of different HS oligosaccharide structures on the interaction and activation of FGF-1 and FGF-2 with FGFR1c.

5.2 Results

5.2.1 Interactions

5.2.1.1 Competition ELISA analysis of FGF-1 and FGF-2 binding to heparin

As been pointed out in previous sections, various techniques such as affinity chromatography and filter trapping employing elution with a salt gradient do not provide conclusive information on whether interactions are mediated by specific sequences, or are simply non-specific electrostatic interactions. Therefore, the results obtained by these methods make it difficult to understand the true selectivity/ specificity of the interactions. On the other hand, competition ELISAs was used to explore the specificity of the HS-FGF system. This method can also determine the specific and non-specific interactions on the surface.

Specific binding is considered to be the saturated binding over serial concentrations and can be obtained by subtracting the non-specific binding from total binding (van Zoelen, 1989). Furthermore, competition ELISA takes advantage of the ability of nitrous acid generated heparin oligosaccharides to be labelled at their reducing end with biotin and then immobilised onto immunosorbant microtitre plates through streptavidin-biotin interaction. This method could partially resemble physiological HS, which exists in nature attached to a core protein in the form of HSPGs. Heparin 10-mer oligosaccharides were selected for surface immobilisation. This size proved to be of sufficient length for FGF-1 and FGF-2 binding (Mach *et al.*, 1993; Ishihara, 1994; Fromm *et al.*, 1997; Pellegrini *et al.*, 2000; Schlessinger *et al.*, 2000).

Furthermore, the use of the competition ELISA benefits from analysis of different binding reactions at the same time, due to the multi-well design of the microtitre plates. Hence, the concentration of the immobilised saccharides on the surface and the protein applied for interaction are constants, and the ability of different competitors to influence the interaction can be evaluated. The success of this method is dependent on various controls and optimization procedures.

5.2.1.2 Determination of optimum FGF-1 and FGF-2 concentrations for competition ELISA

Optimization of the competition ELISA assays involves knowing the amount of protein and saccharide needed to obtain the best conditions for the interaction (i.e. maximum signal to noise ratio). The optimum setting involved the use of 1nM FGF-2, measuring binding of FGF-2 to immobilized 10-mer heparin (and non-specific binding in presence of 100-fold excess of soluble 10-mer) (Figure 5.5b). The molar concentration needed for the FGF-1 protein is about 10-fold higher (10 nM) than FGF-2 (Figure 5.5a); these points were selected because they were before the complete saturation of the dose response curves, which will enable subtle differences in the binding to be detected. The concentrations selected were used in all subsequent competition ELISA experiments for FGF-1 and FGF-2.

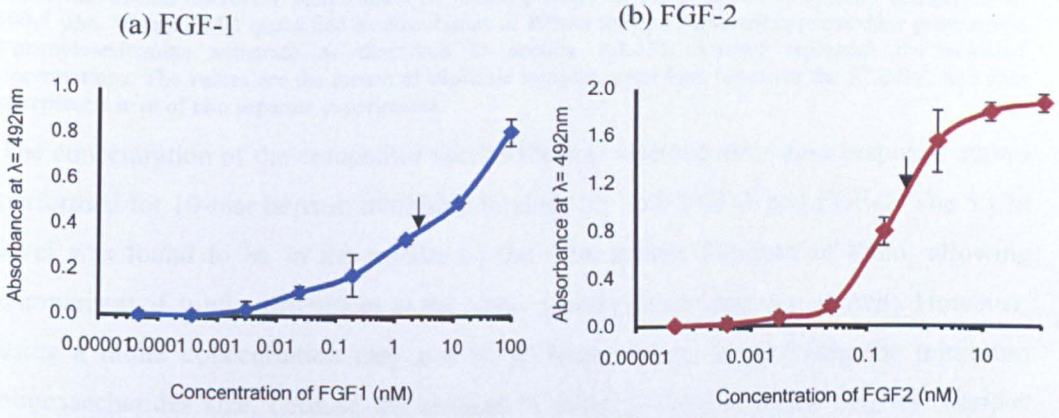

Figure 5.5 Binding of FGF-1 and FGF-2 to immobilised 10-mer heparin. Porcine mucosal heparin 10-mer was generated by nitrous acid partial digestion and SEC fractionation. 10-mer PMH was biotinylated at the reducing end, immobilised on a streptavidin-coated 96 well microtitre plate and the binding of different concentrations of (a) FGF-1 and (b) FGF-2 to the 10-mer heparin quantified as absorbance 492nm (using mouse anti-FGF primary antibodies and secondary anti mouse-HRP conjugated protein and OPD substrate, as described in the methods section 2.2.12). Arrows represent the selected concentrations.The absorbance values shown represent values calculated after subtraction of FGF background binding. Values are the mean of triplicate samples and error bars represent the STDEV. The data are representative of two separate experiments.

5.2.1.3 Determination of optimum oligosaccharides concentrations for competition ELISA

The concentration of the oligosaccharide competitor was also optimized. Heparin 8-mer was found to be long enough to support FGF-FGFR-complex formation with both FGF1 and FGF2. Therefore, with respect to length, 10-mer is thought to be sufficient to promote FGF binding and activities. Figures 5.6a and b shows the concentrations of the oligosaccharides needed to compete with 10-mer heparin. The molar concentration of 10-mer heparin was established for both FGF-1 and FGF-2. Competition doses of a heparin 10-mer shown by the arrows represent the 5 μM as it will be sufficient for FGF1 binding, but will be in the borderline for FGF2.

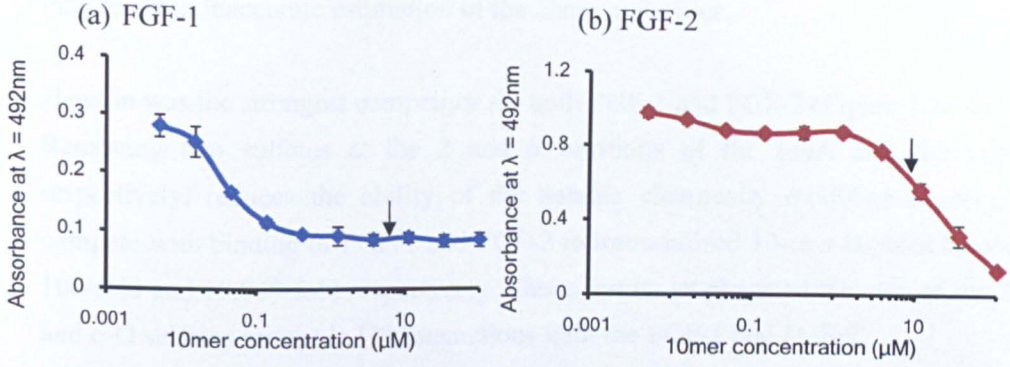

Figure 5.6 Binding of 10 nM FGF-1 and 1 nM FGF-2 to immobilized heparin oligosaccharide in the presence of 10-mer heparin. Biotinylated 10-mer from chemically digested PMH was immobilized on streptavidin-coated microtiter plates and FGF binding tested in the presence of soluble competitor of (100-5 μM, 10-mer PMH quantified as absorbance at 490nm using a horseradish peroxidase protein and O-phenylenediamine substrate as described in section 2.2.12). Arrows represent the selected concentrations. The values are the means of triplicate samples, error bars represent the STDEV, and data are representative of two separate experiments

The concentration of the competitor saccharide was selected after dose response curves performed for 10-mer heparin inhibition binding for both FGF-1 and FGF-2. The 5 μM level was found to be in the middle of the dose curves for both of them, allowing comparison of subtle differences at the same concentration (data not shown). However, using a molar concentration may not be an ideal choice for defining the minimum oligosaccharides size, because the amount of binding sites in larger oligosaccharides such as 12-mer is not the same as for the 2, 4, 6 and 8-mer. On the contrary, using molarity is an excellent way for discovering differences within the same oligosaccharide size. The amount of proteins needed for FGF-1 and FGF-2 are about 10 nM and 1 nM respectively, which is a reasonably low, physiologically relevant concentration, compared to other interaction assays such as ITC.

5.2.2 FGF-1 and FGF-2 interaction with HS/ heparin requires diverse charge and sulfation

5.2.2.1 Screening with GAG chains

In order to determine how many charges are involved in the interaction of HS with FGF-1 and FGF-2, a number of GAGs with different numbers of charges were screened. These were heparin, chemically modified heparins and CS. Competition ELISA was the method used for screening the heparin derivative and CS-C chain binding with FGF-1 and FGF-2. Equal masses of competitors (polysaccharides chains) were used since the polydisperse character of the polysaccharides chain makes it difficult to calculate the molecular weight of the full-length chain, which may result in inaccurate estimation of the chain molarities.

Heparin was the strongest competitor for both FGF-1 and FGF-2 (Figure 5.7a and b). Removing two sulfates at the 2 and 6 positions of the IdoA and the GlcNS respectively, reduces the ability of the soluble chemically modified heparins to compete with binding of FGF-1 and FGF-2 to immobilised 10-mer heparin by about 100-fold and 10,000-fold respectively. These results emphasized the role of the 2-O and 6-O sulfates groups in HS interactions with the FGF-1 and FGF-2.

Moreover, CS is shown to be a much poorer competitor compared to heparin by approximately 100000-fold (Figure 5.7a and b). CS-C has an average of two less charges per disaccharide compared to heparin, but comparable charge to the 2, 6-de heparin (Figure 1.8), so the poor competition may be due to its lower charge reducing its ability to interfere non-specifically with the 10-mer heparin interaction with FGF-1 and FGF-2. CS-C and 2, 6-O-desulfated have similar charge contents but 2, 6-O-desulfated is a much better competitor with FGF-1. Interestingly, for FGF-2 the 2, 6-O-desulfated heparin is only a slightly better competitor than CS-C, perhaps reflecting a non-specific mechanism of inhibition for the 2, 6-de heparin. Completely de-sulfated heparin (with one charge) did not compete with the 10-mer heparin for FGF-1 and FGF-2 binding.

These data indicate that there is a clear difference in the capability of different modified heparins and other polysaccharides with diverse amount of charges to interact with FGF-1 and FGF-2, which could be an indication of sequence selectivity in their binding.

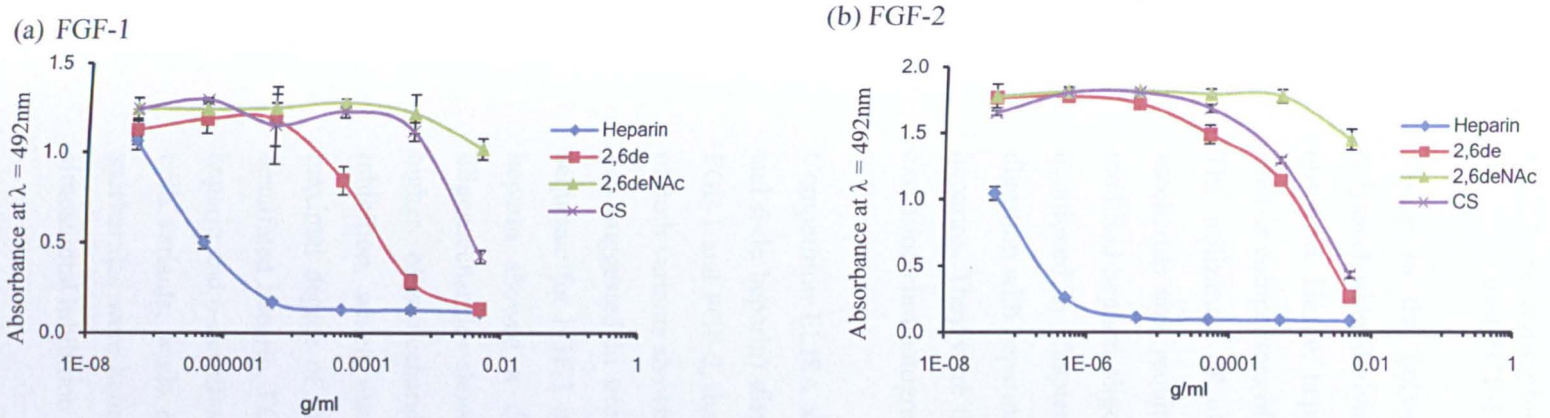

Figure 5.7 Binding of FGF-1 and FGF-2 to immobilised heparin in the presence of soluble heparin, de-sulfated heparins and CS. Porcine mucosal heparin 10-mer was biotinylated at the reducing end, immobilised on a streptavidin-coated 96 well microtitre plate and the equilibrium binding of different concentrations of binding of (a) 10 nM FGF-1 and (b) 1 nM FGF-2 to immobilised 10-mer heparin, in the presence of varying concentrations of soluble competitors (heparin; 2, 6-de; 2, 6-de NAc and CS-C). Competition ELISA uses horseradish peroxidase protein and O-phenylenediamine substrate read at absorbance at λ=492 nm as described in methods. The values are the mean of triplicate samples and error bars represent the STDEV. The data are representative of two separate experiments.

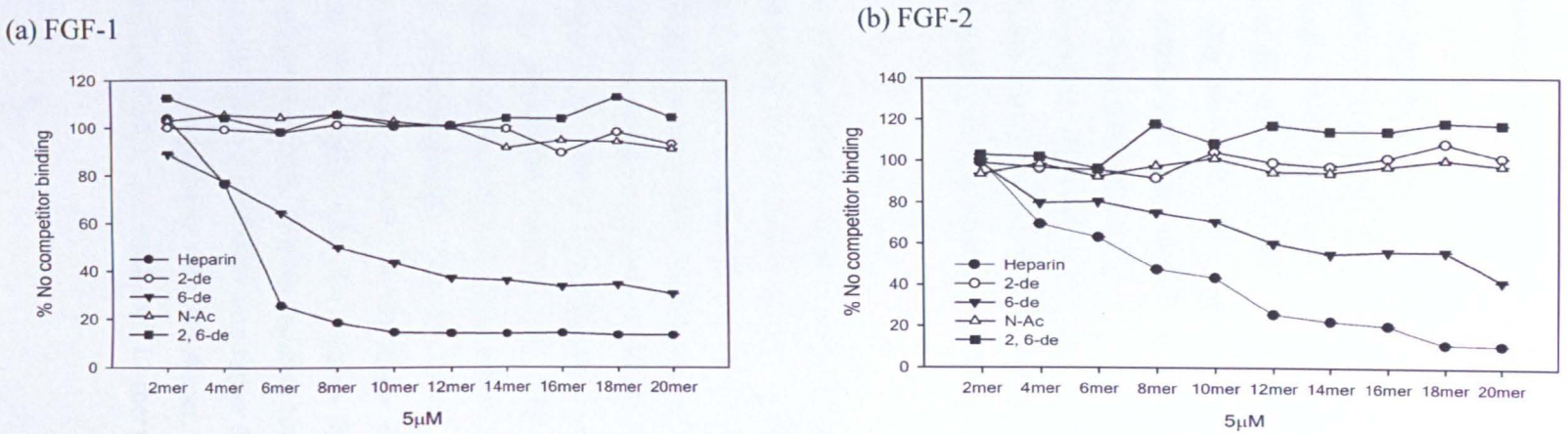

Figure 5.8 Binding of FGF-1 (a) and FGF-2 (b) to immobilized heparin oligosaccharide in the presence of soluble 2-20-mer heparin derivatives. Porcine mucosal heparin (PMH) 10-mer was chemically degraded with low pH nitrous acid, biotinylated at the reducing end and immobilised on a streptavidin-coated 96-well microtitre plate. Binding of 1nM FGF-2 to immobilized 10-mer PMH in the presence of 5 μM of soluble competitors of 2-20-mer PMH, 2-de, 6-de, NAc and 2, 6-de were quantified as a percentage of maximal binding of FGF-1 or FGF-2 in the absence of competing oligosaccharides. Competition ELISA uses horseradish peroxidase protein and O-phenylenediamine substrate read at absorbance at λ=492 nm and reported as a percentage of no competitor binding. Values are the mean of triplicate samples and error bars represent the STDEV of binding. Data are representative of three separate experiments.

5.2.2.2 Screening binding of oligosaccharides of heparin derivatives with FGF-1 and FGF-2

Owing to the poly-disperse nature and multi-valency effect of the heparin polysaccharide derivatives, fine details of any sequence requirements could be obscured. Hence, heparin and chemically modified heparin oligosaccharides were used as competitors of the interaction of the FGF-1 and FGF-2 with 10-mer heparin. The utilization of oligosaccharides also provides more information about the saccharide size requirements for the interaction. The heparin and the chemically modified heparin oligosaccharides have been generated according to the procedures mentioned in Chapter 3. Briefly, competitor oligosaccharides were produced by digestion with heparinase I for heparin and heparinase II for the chemically modified heparins. They were then separated according to hydrodynamic volume using size-exclusion chromatography.

Competition ELISA showed that two of the heparin variants (unmodified heparin and 6-de heparin) displayed more inhibition of the 10-mer heparin binding to the FGF-1 and FGF-2, than other variants do (Figure 5.8a and b). For FGF-1, the 6-mer of both variants showed increased inhibitory activity. This finding concurs with what was suggested in previous studies, that the smallest heparin binding saccharides sequence for FGF-1 is 5-7-mer (Kreuger *et al.*, 1999). However, the 6-de sulfated heparin showed a different trend for interaction with FGF-1; while heparin oligosaccharides showed near-maximal inhibition (~80 %) from 6-mer onward to higher oligosaccharides. The 6-de oligosaccharides showed more moderate inhibition, which was obvious from the 6-mer onward to the larger sizes. The maximal degree of inhibition is about 20 % higher with the heparin than the 6-desulfated heparin. FGF-2 showed weaker inhibition for both variants (unmodified heparin and 6-desulfated heparin), since the level of inhibition was rather diverse for both variants, while heparin showed some competition with the 4-mer, 8-10-mer saccharides were better inhibitors, and larger oligosaccharides ($\geq$ 12-mer) achieved almost total inhibition (~ 80 -90 %).

In contrast, the oligosaccharides from the 6-desulfated heparin showed modest inhibition, it was observable from ~ 6-mer onwards, but with a much shallower trend. The maximal extent of inhibition was about 30 % higher with heparin oligosaccharides than the 6-desulfated heparin.

Other chemically modified heparin variants (2-de, NAc and 2, 6-de) failed to compete with heparin 10-mer. These data suggested that the 2-O sulfate of the IdoA and the N sulfate of the GlcNS are most essential for IIS binding to FGF-1 and FGF-2. Interestingly, this finding is different to what was reported in the case of the FGF-binding to modified heparins (Table 5.3).

Binding with	Present information		Previous information		References
modified heparin oligosaccharides	FGF-1	FGF-2	FGF-1	FGF-2	
2-desulfated heparin	No	No	No	No	(Turnbull *et al.*, 1992; Guimond *et al.*, 1993; Kreuger *et al.*, 1999; Kreuger *et al.*, 2001; Jemth *et al.*, 2002; Ostrovsky *et al.*, 2002; Ashikari-Hada *et al.*, 2004; Goodger *et al.*, 2008)
6-desulfated heparin	Yes	Yes	No	Yes	
N-acetylated heparin	No	No	No	No	
2,6-desulfated heparin	No	No	No	No	

Table 5.3 Binding of modified heparins with FGF-1 and FGF-2, in present and previous studies, (NO, there is no interaction and Yes, there is interaction).

It should be noted that binding of FGF-1 to the 6-mer heparin oligosaccharides and binding of the FGF-2 to the 4-mer heparin oligosaccharides does not mean these are the length of saccharides required for activity. As it has been documented from previous crystal structure studies that the 8-mer or 10-mer heparin are the minimum lengths required to span between FGF-2 and FGFR to form a ternary complex (Pellegrini *et al.*, 2000; Schlessinger *et al.*, 2000).

From these data, it is clear that the binding of heparin and 6-desulfated heparin with FGF-1 and FGF-2 improved with increasing oligosaccharide length. This result was expected for heparin, as the positive charges in the binding sites on the surface of the proteins will improve the attraction towards the extended length of heparin oligosaccharides. Also, as the heparin oligosaccharides length increase, the electrostatic forces driving the FGF-heparin interaction also increase and act as a guide to bring FGFs and the oligosaccharides towards each other in a favourable orientation for their molecular interaction.

Previous data on FGF interactions with chemically modified heparins have emphasized the role of the 6-O-sulfate in binding to FGF-1. Here, it was shown that the 6-de-O-sulfated heparin was able to bind to FGF-1 in a manner more potent than with FGF-2. This may be because the interaction with FGF-2 is more complex than with FGF-1, which is needed to be stabilized to be reactive (Rudd *et al.*, 2010).

5.2.3 SAX-HPLC purified 6-mer and 8-mer PMHS saccharides-selectivity of binding with FGF-1 and FGF-2

Studies investigating the structural characteristics of HS-FGF interactions have often used heparin as a proxy for HS (Mach *et al.*, 1993; Thompson *et al.*, 1994a; Faham *et al.*, 1996; DiGabriele *et al.*, 1998; Pellegrini *et al.*, 2000; Schlessinger *et al.*, 2000). However, heparin is synthesised by the oligodendrocyte-type 2 astrocyte progenitors (O-2As) and mast cells (Mabie *et al.*, 1997; Stringer *et al.*, 1999), and the interaction between heparin and FGFs is of restricted physiological significance. On the contrary, HS is on the surface and extracellular matrix of almost all cells, where many proteins are expressed and interact with their related receptors (Merry *et al.*, 2001). Thus, the interaction between oligosaccharides from heparin (and certainly chemically modified heparins) with FGFs is unlikely to play a major role *in vivo*. Heparin is also highly sulfated, so the features of its interactions with proteins may be different to those of lower sulfated HS (Kett *et al.*, 2003). Despite this, the availability of heparin, and its sharing of the same backbone subunits and the same biosynthetic route as HS, has meant that it has played a major role in initial studies investigating the structure-function relationship of HS-protein complexes.

In previous interaction studies, Kreuger et al (1999) looked at the binding of FGFs with HS oligosaccharides using a filter-trap assay. In the assay the protein-bound oligosaccharides were eluted with 2 M salt, so this method has the same reservations as those regarding salt elution in affinity chromatography (i.e. as the interactions observed under these conditions could be due entirely to the electrostatic interactions between the negatively charged HS and the positively charged amino acids on the FGFs). In addition, these studies neglected the complex structure of HS oligosaccharides, as some of them have low amounts of sulfation.

In the current investigation, competition ELISA was used to study the interaction of FGF-1 and FGF-2 with tissue-derived HS, isolated from porcine intestinal mucosa, a source of HS that has highly complex mixtures of N and O sulfated saccharides (Guimond and Turnbull, 1999). PMHS oligosaccharides were generated by heparinase III partial digestion and separation according to hydrodynamic volume on a SEC column, followed by further separation according to charge on a SAX column. The SAX peaks were a mixture of individual peaks and clusters of peaks, which would probably represent isomers (Figure 5.9a and 5.10a). Charge separation was performed on the SEC generated 6-mer and 8-mer PMHS saccharides. These two oligosaccharide sizes were selected based on information generated from the interactions of heparin oligosaccharides with FGF-1 and FGF-2 (Figure 5.8a and b). In addition, previous studies have suggested that the 6-mer and 8-mer saccharides are sufficient to bind and promote signalling for the FGF-1 and FGF-2 (Kreuger *et al.*, 1999; Kreuger *et al.*, 2001; Jastrebova *et al.*, 2006; Goodger *et al.*, 2008).

5.2.3.1 **Interaction of 6-mer PMHS with FGF-1 and FGF-2**

The 6-mer PMHS SAX HPLC sub-fractions were selected from the start, middle and end of the salt gradient to give a wide variability in sulfation levels. At the start of the gradient saccharides would be less sulfated than at the end of the gradient (Figure 5.9a). The selected fractions were screened for their ability to compete with binding of FGF-1 and FGF-2 with an immobilised 10mer heparin. Heparin 6-mer competition was used as a control (Table 5.4). Fractions 6 F, 6 M, 6 N and 6 T showed similar competition for FGF-1, while 6 L, 6 P and 6 R did not compete. Instead, the latter saccharides augmented binding of FGF-1 binding to the immobilised 10-mer heparin (Figure 5.9b). This may reveal the occurrence of additional structural motifs in these fractions that strengthen the interaction (possibly through dimerizarion) of FGF-1 with the immobilised 10-mer heparin (DiGabriele *et al.*, 1998).

For binding with the FGF-2, fractions 6 F, 6 M and 6 N were less inhibitory while 6 L and 6 P displayed intermediate inhibitory activity; 6 R and 6 T were the best competitors and they were even better competitors than heparin 6-mer that has the highest sulfation and charge (Figure 5.9c). Thus, the HS 6-mer fractions displayed different, but also partially overlapping, interactions with FGF-1 and FGF-2.

(a) 6-mer PMHS SAX profile

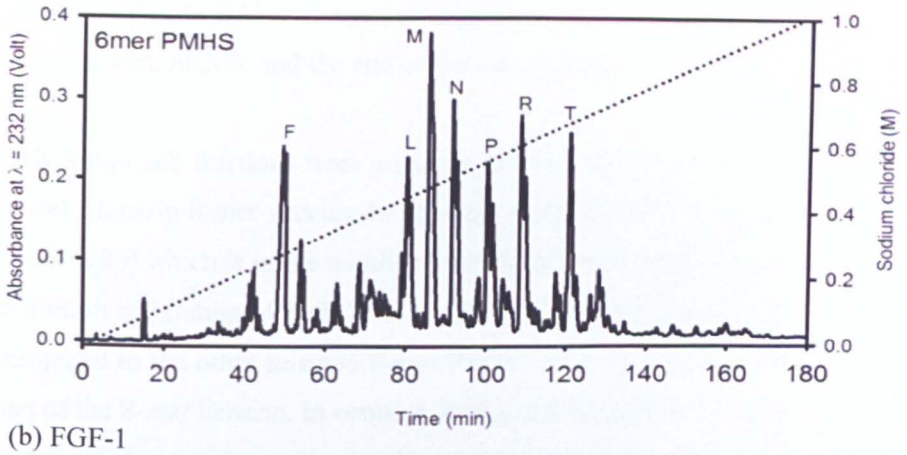

(b) FGF-1

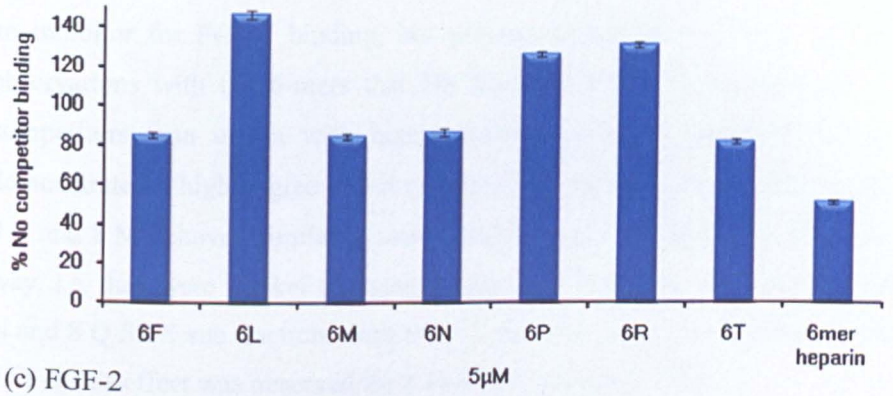

(c) FGF-2

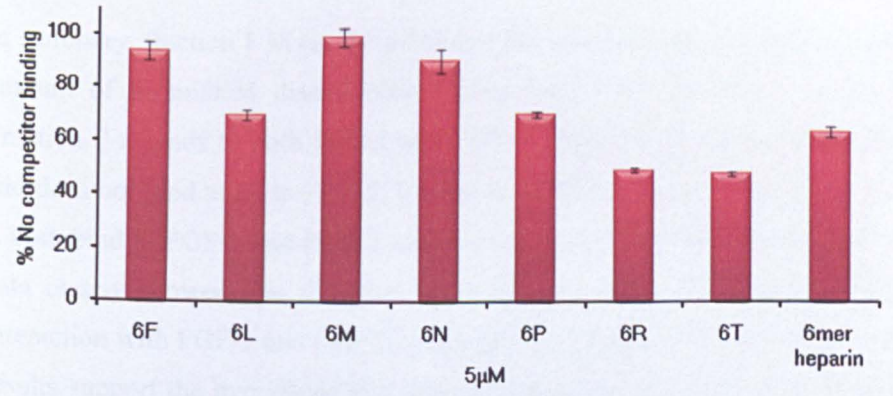

Figure 5.9 Binding of 10 nM FGF-1 and 1 nM FGF-2 to immobilized heparin oligosaccharide in the presence of soluble 6-mer PMHS. a) PMHS SAX-HPLC profile of 6-mer; b) Binding 10 nM FGF-1 to immobilized 10-mer PMH in the presence of 5 μM selected 6-mer PMHS SAX-HPLC fractions (competitors); c) Binding 1 nM FGF-2 to immobilized 10-mer PMH in the presence of 5 μM of selected 6-mer PMHS SAX-HPLC fractions (competitors). Competition ELISAs were performed as described in figure 5.7.

5.2.3.2 **Interaction of 8-mer PMHS with FGF-1 and FGF-2**

The 8-mer PMHS SAX sub-fractions were picked the same way as for the 6-mer, i.e. from the start, middle and the end of the salt gradient.

SAX 8-mer sub fractions were screened for binding with FGF-1 and FGF-2 (Figure 5.10a). Heparin 8-mer was used as a control for both FGF-1 and FGF-2 (Table 5.4). Fraction 8 P which is in the middle of the salt gradient demonstrated a high degree of inhibition of binding of both FGF-1 and FGF-2 to the immobilised 10-mer heparin, compared to the other selected 8-mer PMHS SAX sub-fractions, and was similar to that of the 8-mer heparin. In contrast, 8 M and 8 N were poor inhibitors. 8 U and 8 Z were partial competitors compared to 8 P, but better than the 8 M and 8 N. 8 Q was an inhibitor for FGF-1 binding, but promoted binding of FGF-2. These confirm observations with the 6-mers that HS fractions with low sulfation can be better competitors than others with higher sulfation (Figure 5.10b). For FGF-2, 8 P demonstrated a high degree of competition but, slightly less than for heparin 8-mer. 8 L and 8 M behaved similar to modest inhibitors. 8 U and 8 Z performed the same way, i.e. they were weaker competitors than P8. There was no inhibition with 8 I, 8 N and 8 Q SAX sub fractions with FGF-2, and they all in fact enhanced binding. For FGF-1 this effect was observed for 8 I and 8 L (Figure 5.10c).

In summary, fraction 8 M (in the middle of the gradient) which contains a negligible amount of tri-sulfated disaccharide (Table 5.4), binds to FGF-2 and to FGF-1. Fraction P 8 binds to both FGF-1 and FGF-2 while 8 N is a low binder for FGF-1 and does not bind at all to FGF-2. 8 L binds to FGF-2 rather than FGF-1. 8 U and 8 Z both bind to FGF-1 and FGF-2 and 8 Q binds to FGF-1 rather than FGF-2. These data clearly showed that different fractions have different extents of competitive interaction with FGF-1 and FGF-2, excluding the charge contents (Table 5.4). These results support the hypothesis that selective sequence rather than the simple degree of sulfation is important FGF-1 and FGF-2 binding to HS.

(a) 8-mer PMHS SAX profile

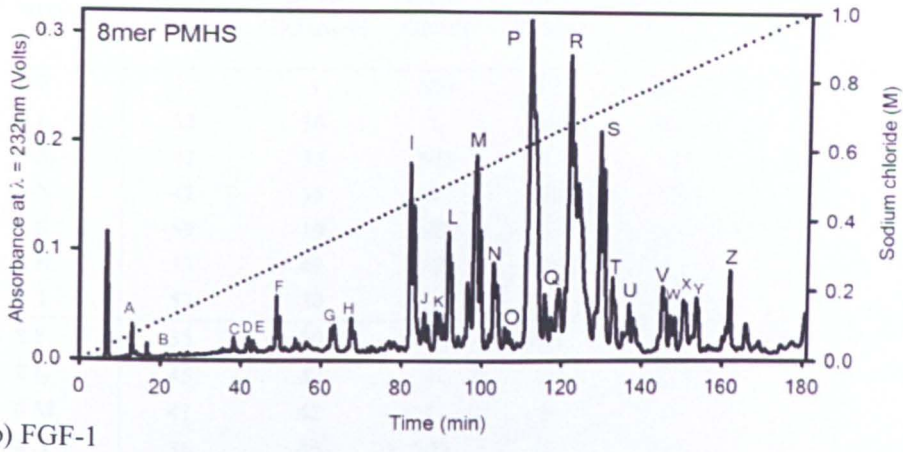

(b) FGF-1

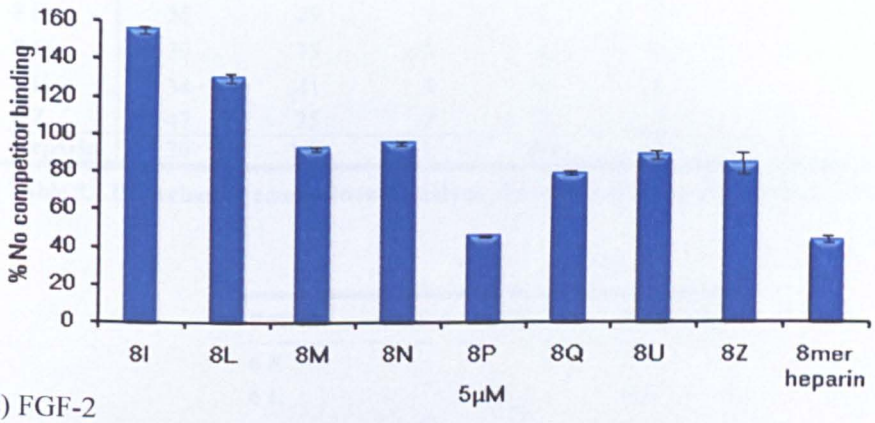

(c) FGF-2

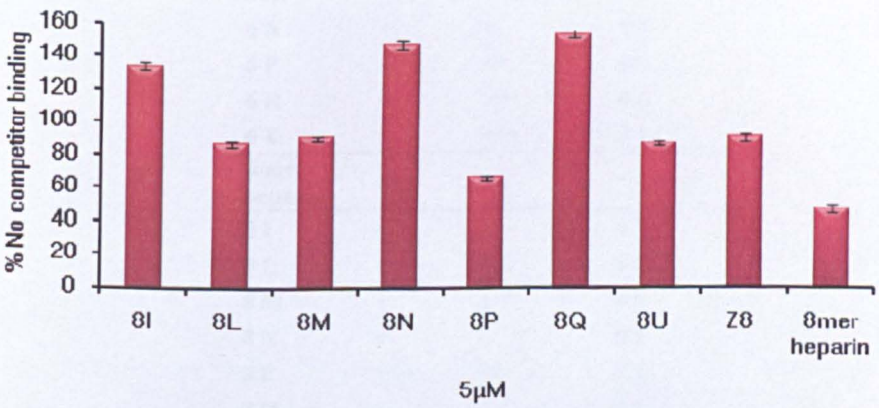

Figure 5.10 Binding of 10 nM FGF-1 and 1 nM FGF-2 to immobilized heparin oligosaccharide in the presence of soluble 8-mer PMHS. a) PMHS SAX-HPLC profile of 8-mer; b) Binding 10 nM FGF-1 to immobilized 10-mer PMH in the presence of 5 μM selected 8-mer PMHS SAX-HPLC fractions (competitors); c) Binding 1 nM FGF-2 to immobilized 10-mer PMH in the presence of 5 μM of selected 8-mer PMHS SAX-HPLC fractions (competitors). Competition ELISAs were performed as described in figure 5.7.

PMHS	ΔUA-GlcNAc	ΔUA-GlcNAc6S	ΔUA-GlcNS	ΔUA-GlcNS6S	ΔUA2S-GlcNS	ΔUA2S-GlcNS6S	ΔUA2S-GlcNAc	ΔUA2S-GlcNAc6S
6 F	55	3	ND	43	ND	ND	ND	ND
6 L	53	30	1	16	ND	1	ND	ND
6 M	47	35	ND	5	14	ND	ND	ND
6 N	47	35	1	ND	17	ND	1	ND
6 P	59	19	ND	5	17	ND	ND	ND
6 R	33	49	ND	13	5	ND	ND	ND
6 T	53	30	1	3	3	9	ND	3
8 I	55	30	ND	ND	16	ND	ND	ND
8 L	45	42	1	11	1	1	ND	ND
8 M	41	42	1	8	7	1	1	ND
8 N	36	45	ND	11	1	1	5	ND
8 P	55	29	1	2	2	9	1	ND
8 Q	39	35	3	6	11	2	4	1
8 U	34	41	3	10	6	4	1	ND
8 Z	47	25	3	12	4	8	ND	1
Heparin	26	ND	1	ND	ND	73	ND	ND

Table 5.4 Disaccharide compositional analysis of 6-mer and 8-mer PMHS SAX-HPLC fractions.

PMHS	FGF-1	FGF-2	NaCl (M)
6 F	+	-	0.3
6 L	-	++	0.5
6 M	+	-	0.5
6 N	+	+	0.5
6 P	-	++	0.6
6 R	-	+++	0.6
6 T	+	+++	0.7
6-mer heparin	+++	++	1-1.1
8 I	-	-	0.4
8 L	-	+	0.5
8 M	+	+	0.5
8 N	+	-	0.6
8 P	+++	++	0.6
8 Q	++	-	0.6
8 U	++	+	0.8
8 Z	++	+	0.9
8-mer heparin	+++	+++	1-1.2

Table 5.5 Different FGF-1 and FGF-2 binding abilities of the 6-mer and 8-mer PMHS SAX-HPLC fractions from (Figure 5.9 and 5.10). – no significant interaction; +, weak, ++ moderate; +++, strong interaction. Also, showing the molar concentration of NaCl for fractions elution.

5.2.4 Cellular mitogenic assays reveal important HS-FGF signalling information

5.2.4.1 Previous BaF3 assay data

In order to test the potential physiological significance of the binding data generated in the previous section, bioassays looking at the mitogenic activity of the HS oligosaccharides were undertaken to test their ability to promote signalling through cell surface receptor expressed on tissue culture cells (Pye *et al.*, 1998; Guimond and Turnbull, 1999; Pye and Gallagher, 1999; Pye *et al.*, 2000).

Previous studies have recognized that HS with its diverse domain structure binds to both FGFs and FGFRs (Rapraeger *et al.*, 1991; Yayon *et al.*, 1991; Walker *et al.*, 1994; Pye *et al.*, 1998; Powell *et al.*, 2002). Furthermore, signalling by FGFs through FGFRs requires HS (Rapraeger *et al.*, 1991; Guimond and Turnbull, 1999; Pye *et al.*, 2000). Guimond and Turnbull (1999) looked at various 10-mer HS saccharide SAX-HPLC fractions in an FGF bioactivity assay (using BaF3 cells). They found that some saccharides have specificity related to both FGF ligands and FGFRs; furthermore, some saccharides were activators of FGF signalling, while others were inhibitors. They concluded that regulation of cellular responsiveness to HS binding FGF is regulated through fine-tuning of HS structures. In addition, Pye et al (2000) utilized a similar approach examining FGF-1 and FGF-2 mitogenic activation by various HS saccharides and found that there are differences in FGF-1 and FGF-2 signalling activation. These differences were controlled by the length and sulfation of HS saccharides; high sulfated 8-mer HS SAX-HPLC fractions were capable of activating FGF-1 rather than FGF-2 (Pye *et al.*, 1998; Pye *et al.*, 2000). These studies have emphasized the importance of HS saccharide structure and size in controlling FGF signalling. However, the complexity of the SAX-HPLC saccharide fractions used in these two studies may well hide interesting and complex sequences. Furthermore, in some studies 8-mer HS SAX-HPLC saccharides were unable to activate the FGF-2 signalling, possibly due to limited structural diversity of 8-mer SAX fractions (Pye *et al.*, 2000).

In the current investigation, structurally diverse 8-mer HS saccharides generated by SAX-HPLC (according to disaccharide compositional analysis, Table 5.4) displayed differential interactions with FGF-1 and FGF-2 ligands; the next question was to determine whether these interaction studies correlated with bioassay data (i.e. structure-function relationships based on activity data). HS SAX 8-mer sub fractions including the ones selected in the FGF-1 and FGF-2 binding studies were subjected to signalling bioassays expressing FGFR1c.

The BaF3 cells are a murine pro-B cell line, which is deficient in both endogenous HS and FGFRs. The survival, growth and proliferation of these cells depend on the presence of interleukin-3 (IL-3). Alternatively, BaF3 cells undergo programmed cell death (apoptosis) upon removal of IL-3. BaF3 cells transfected with FGFRs survive and proliferate in the absence of IL-3 when stimulated with FGF and HS (Sakaguchi, 1992; Ornitz *et al.*, 1996; Venkataraman *et al.*, 1996). To test the ability of HS oligosaccharides to regulate FGF signalling, BaF3 cells transfected with FGFR1IIIc were incubated with an FGF in the presence of heparin or HS saccharides. Activation of signalling is detected through a mitogenic response using a tetrazolium salt (MTT) colorimetric assay where viable cells metabolise MTT generating a coloured product (which can be read at λ = 570 nm). The colour produced is proportional to the number of viable cells (Guimond and Turnbull, 1999).

5.2.4.2 HS 8-mer oligosaccharides regulate FGF-1 and FGF-2 signalling via FGFR1c

Activity screening of the 8-mer SAX sub-fractions selected from the start, middle and the end of the salt gradient showed that they had differential capabilities to activate signalling by FGFR1c in response to FGF-1 (Figure 5.11a). Some of the fractions showed a high degree of activation, while others exhibited lower activity levels or were incapable of supporting FGF-1 signalling. Fraction P 8 was the highest activator, with about 140 % activity compare to the 8-mer heparin of the same concentration. 8 M was less active compared to the 8-mer heparin by, whereas other fractions (e.g. 8 G, N 8, 8 Q, 8 U, 8 V and 8 Z) were weaker activators and fractions 8 A, 8 I, 8 L and 8 S had the lowest degree of FGF-1 activation with FGFR1c.

There are some differences apparent compared to the binding data obtained by competition ELISA; for example 8 M and 8 N, which have similar binding profile (Figure 5.10b), were different in their signalling activity. Fraction P 8 was similar to the 8-mer heparin in its competition ELISA binding, but displayed more enhanced activity in BaF3 cells compared to the 8-mer heparin (Figure 5.11b).

The BaF3 bioassay was also performed for FGF-2 with the FGFR1c isoform as it has been documented that the FGFR1c has the same proliferative response for FGF-1 and FGF-2 (Guimond and Turnbull, 1999). The screening of the 8-mer SAX sub-fractions demonstrated diverse capacities to activate signalling by FGFR1c in response to FGF-2 (Figure 5.11b). A number of fractions showed elevated levels of activation, while others displayed lesser levels of activation, or were unable of support FGF-2 signalling (Table 5.6). The 8 P and 8 M fractions were about 300 % and 200 % compared to 8-mer heparin control, with 8 Q about 130 % compared to 8-mer heparin.

Fractions 8 L, 8 N and 8 Z were moderate activators with similar activity to the 8-mer heparin. The fractions 8 S, 8 U and 8 V were weak activators (about 85 % of 8-mer heparin). Finally, fractions A 8 and G 8 were unable to activate FGF-2 with the FGFR1c.

As for FGF-1, the FGF-2 binding data obtained by competition ELISA showed differences compared to mitogenic activity, 8 P and 8 M were weaker inhibitors than 8-mer heparin, but were three and two times better activators than 8-mer heparin (Figure 5.11b). In addition, the fractions 8 Q and 8 N were not inhibitors of binding but they displayed moderate abilities to activate FGF-2 compared to 8-mer heparin respectively (Table 5.6).

(a) FGF-1

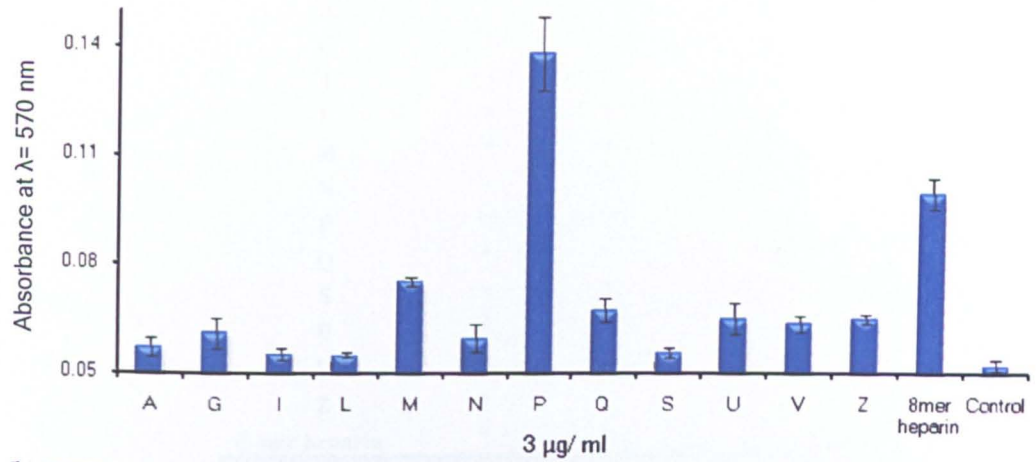

(b) FGF-2

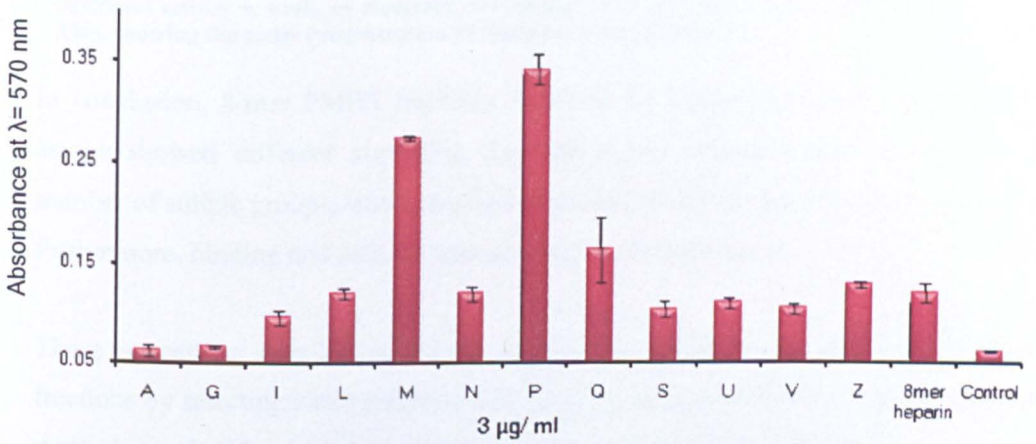

Figure 5.11 Specific HS saccharides regulate FGF-1 and FGF-2 through FGFR1c signalling. Activation of FGF signalling was measured in bioassays of mitogenesis using HS-deficient BaF3 cells transfected with FGFR1c. a) BaF3 cells were grown in the presence of 1 nM FGF-1. b) BaF3 cells were grown in the presence of 1 nM FGF-2. Briefly, BaF3 cells were grown in the presence of 1 nM FGF-1 or 1 nM FGF-2 and HS 8-mers SAX-HPLC fractions 3 µg/ ml (A,G,I,L,M,N,P,Q,S,U,V and Z) or a positive control of 8-mer heparin and full length heparin. Cell proliferation was measured at absorbance λ = 570 nm using a 3-[4, 5-dimethylthiazol-2-yl]-2, 5-diphenyltetrazolium bromide (MTT) colorimetric assay, as described under Methods. Values are the mean of triplicate samples. *Error bars* represent the *STDEV*, and the data are representative of two separate experiments.

8-mer PMHS	FGF-1	FGF-2	NaCl (M)
A	-	-	0.1
G	-	-	0.3
I	-	+	0.4
L	-	++	0.5
M	+	+++	0.5
N	-	++	0.6
P	++	++++	0.6
Q	+	++	0.6
S	-	+	0.7
U	+	+	0.8
V	+	+	0.8
Z	+	++	0.9
8-mer heparin	+	+	1-1.2

Table 5.6 Ability of different 8-mer SAX-HPLC fractions in FGF-1 and FGF-2 signalling, – no significant activity +, weak, ++ moderate; +++, strong and ++++ very strong activity, Also, Also, showing the molar concentration of NaCl for fractions elution.

In conclusion, 8-mer PMHS fractions screened for signalling activity using BaF3 assays showed different signalling capabilities not related simply to charge or number of sulfate groups, which implied structural selectivity for biological activity ; furthermore, binding and activity data are clearly not equivalent.

These interesting data led to further exploration of the 8-mer HS SAX purified fractions by selecting some fractions without clear single peaks (which likely contain multiple saccharide species) for further separation and activity screening.

5.2.5 Regulation of FGF-1 and FGF-2 mitogenic activity dependent on selective 8-mer HS structures

From the complexity of overlapping peaks, some of the PMHS 8-mer oligosaccharides separated according to size (SEC) followed by charge (SAX-HPLC) were not entirely pure species, as mentioned previously in Chapter 3. Therefore, enhanced purification was required. Hence, ion-pairing reverse phase HPLC (RPIP-HPLC) method was used as a third level of separation. Two of the 8-mer SAX fractions were selected for further purification. These were 8 M and 8 S; both of them have shown a diverse level of activity with the FGF-1 and the FGF-2 in the BaF3 assay (Table 5.6). The SAX profile for the 8 M fraction showed a major peak with two shoulder peaks, while the 8 S fraction showed a split peak.

The chromatogram of the RPIP-HPLC for M8 SAX sub fraction yielded three peaks (designated M1, M2 and M3), while the S fraction gave two peaks (S1 and S2) (Figure 5.12). These sub-fractions generated by the RPIP-HPLC were then tested in the bioassay screening with both FGFs and FGFR1c.

The BaF3 assay data for the IPR-HPLC fractions with FGF-1 showed low signalling activity compared to the 8-mer heparin, the activity responses were almost equivalent for the 8 M sub fraction (M 1, M 2 and M 3), and the 8 S sub fractions S1 was possibly more active than S2 (Figure 5.13a). On the other hand, with FGF-2 a surprisingly high level of activity was observed for the M 2 fraction compared to the 8-mer heparin, whereas the other two M 8 sub-fractions were inactive, despite the fact that M 3 was the predominant peak in the RPIP-HPLC profile. In addition, for the 8 S sub fractions with FGF-2, a relatively high level of activity of S 2 was noted compared to S 1, which was essentially inactive (Figure 5.13b).

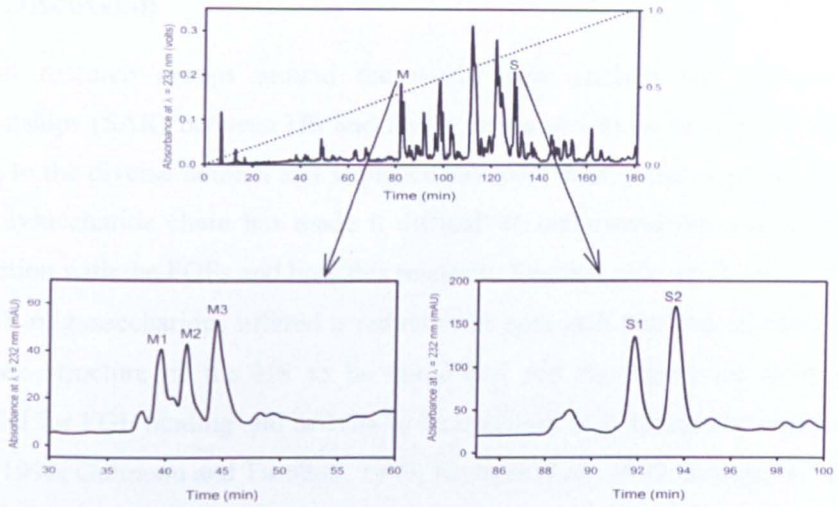

Figure 5.12 SAX-HPLC separation and RPIP-HPLC separation of the 8-mer sub-fraction M and S from PMHS.

(a) FGF-1

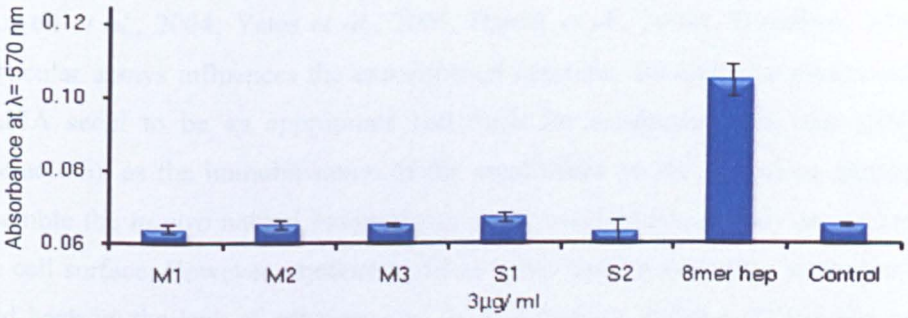

(b) FGF-2

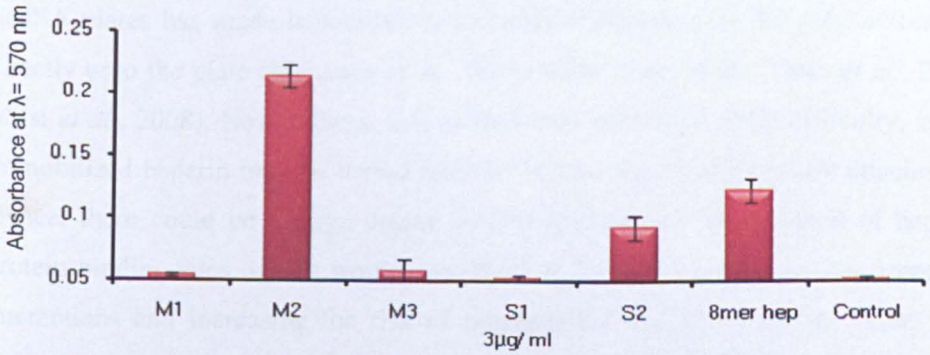

Figure 5.13 Specific HS saccharides regulate FGF-1 and FGF-2 through FGFR1c signalling. Activation of FGF signalling was measured in bioassays of mitogenesis using HS-deficient BaF3 cells transfected with FGFR1c. Briefly, BaF3 cells were grown in the presence of 1 nM FGF-1 or 1 nM FGF-2 and HS 8-mers SAX-HPLC fractions 3 µg/ ml (M1, M2, M3, S1 and S2) or a positive control of 8-mer heparin and full length heparin. As described in figure 5.12. a) BaF3 cells were grown in the presence of 1 nM FGF-1. b) BaF3 cells were grown in the presence of 1 nM FGF-2.

5.3 Discussion

Several research groups around the world have studied the structure-activity relationships (SAR) between HS and FGFs. It has proven to be a challenging task, owing to the diverse domain and sequence structure of HS, and in addition, the long HS polysaccharide chain has made it difficult to understand the true nature of its interaction with the FGFs and how this relates to function. The production of heparin and HS oligosaccharides offered a reductionist approach that has allowed the long complex structure of the HS to be simplified and the minimum sizes that are essential for FGF binding and activity to be explored and structurally analysed (Pye *et al.*, 1998; Guimond and Turnbull, 1999; Kreuger *et al.*, 1999; Kreuger *et al.*, 2001; Merry *et al.*, 2001; Allen and Rapraeger, 2003; Asada *et al.*, 2009).

A number of biochemical and biophysical assays have been used to investigate HS-FGFs interaction; many of these assays have their own merits and weaknesses (Powell *et al.*, 2004; Yates *et al.*, 2006; Hamel *et al.*, 2009). Therefore, selecting particular assays influences the experimental outcome. Biochemical assays such as ELISA seem to be an appropriate technique for conducting this task (HS-FGF interaction), as the immobilisation of the saccharides on the microtiter plate could resemble the *in vivo* natural environment of the saccharides, as they are located on the cell surface. However, conducting ELISA on standard microtiter plates has been held back by the lack of adherence of HS to the plates, making ELISA-like assays difficult to perform; for example the development of allylamine-coated EpranEx ELISA plates has made it possible to immobilise heparin and HS polysaccharides directly onto the plate (Mahoney *et al.*, 2004; Barth *et al.*, 2006; Yates *et al.*, 2006; Mitsi *et al.*, 2008). Nevertheless, this method may encounter some difficulty, as the immobilised heparin may be buried into the surface via its electrostatic attachment. Hence, there could be a large degree of difference in the presentation of heparin protein binding sites, which would contribute to lowering or altering the degree of interactions and increasing the risk of non-specific binding. A further issue, it is difficult to determine the exact amount of immobilised saccharides. Hence, in the current investigation competition ELISA has been carefully selected for studying the HS-FGFs interactions (Powell *et al.*, 2002; Rickard *et al.*, 2003).

The immobilisation of biotinylated heparin oligosaccharides via streptavidin makes it easy to bind saccharides on the surface selectively via their reducing end, with the remaining saccharide free to interact with proteins. It also takes advantage of the immunoassay approach, in which the signal is amplified by the use of primary and secondary antibodies. It offers the use of proteins in physiological buffer (as many other assays do), so that optimal protein characteristics such as conformation or folding are maintained, and it can be used to compare the interaction between ranges of saccharides. However, one obstacle of employing competition ELISA is the need for a relatively large amount of competitor, since the biotinylated 10-mer on the surface is a strong binder for the FGFs. This could be improved by using microplates with smaller radius (e.g. 384 wells), or indeed using glycoarray platforms for future experiments (Zhi *et al.*, 2006; Zhi *et al.*, 2008; Powell *et al.*, 2009). Some other biophysical techniques such as biosensors (e.g. IASys) rely on the same immobilization principal as the competition ELISA; however, the need for sophisticated expensive equipment is the major drawback. In preliminary studies of FGF-1 and FGF-2 on the IASys, FGF-1 failed to interact with the immobilised heparin 10-mer oligosaccharides on the biosensor surface (data not shown).

Many factors could explain the failure of FGF-1 in the biosensor experiment, one reason may be the fragile nature of FGF-1 protein that needs to be stabilized by addition of other proteins such as BSA, but adding mixtures of proteins to a biosensor surface will complicate the data, as changes in refractive index are monitored. In contrast, FGF-2 gave viable data in the biosensor study, possibly because FGF-2 is a more stable protein than FGF-1 (Rudd *et al.*, 2010). However, problems were also encountered in biosensor experiments with FGF-2 such as the limitation of the competitor concentration; if the concentration of the competitor increases to generate full concentration dose curves, the biosensor surface (cuvette) can become clogged with the high concentration of the saccharides, and may interfere with subsequent results. A new generation of biosensors are now available in the market. Some of these may resolve the issues encountered with the IASys system, for example, an Octet biosensor was on trial in the department and preliminary data showed marked improvements in the data generated compared to the IASys.

Heparin 10-mer oligosaccharide were selected as sufficient to interact with the FGF-1 and FGF-2, as many different studies have indicated that both FGF-1 and FGF-2 need saccharides shorter than the 10-mer in length for interaction and signalling (Kreuger *et al.*, 1999; Kreuger *et al.*, 2001; Delehedde *et al.*, 2002a; Wu *et al.*, 2003). The use of chemically modified heparins for FGF studies was previously reported (Ashikari-Hada *et al.*, 2004; Kariya *et al.*, 2000; Ostrovsky *et al.*, 2002). They were particularly useful in identifying which sulfate groups are important in the HS-FGF interaction and signalling. In the current study, it was confirmed that the interaction between FGF-1 or FGF-2 and HS is not due to a general electrostatic interaction. This is because CS-C with the two negative charges in its disaccharide repeat, failed to bind to both FGF-1 and FGF-2 better than the 2-O and 6-O de-sulfated heparins, which have only the N sulfate group intact. In addition, the importance of the N sulfate for FGF-1 and FGF-2 binding was determined by the lack of competition for the totally de-sulfated heparin compared to the 2, 6-de N sulfated heparin. It was also shown that there is a variation in the degree of binding between the 2, 6-de N sulfated with FGF-1 and FGF-2.

The interactions of FGF-1 and FGF-2 with heparin oligosaccharides is enhanced as length increases, since longer heparin oligosaccharides were better competitors than the shorter ones. This would be expected because for longer oligosaccharides the number of available binding sites will increase, offering more opportunities for docking and rebinding events and leading to stronger binding of FGF-1 and FGF-2. This observation was previously reported by other researchers (Wu *et al.*, 2003; Zhang *et al.*, 2009). Heparin oligosaccharide of the size 6-mer and longer provided a high degree of binding with FGF-1. This result is in agreement with Kreuger et al (1999), who suggested that the 5-7 heparin monosaccharide units are needed for FGF-1 binding. However, Wu et al (2003) anticipated that a 4-mer is enough for binding; the type of assays used in each report and the way that saccharides were prepared could explain the variations in the observed results.

In previous binding studies on HS sulfation selectivity for FGF-1 and FGF-2 it was shown that FGF-1 requires the 6-O, 2-O and N sulfates, whilst FGF-2 needs only the 2-O and N sulfation for their interaction with HS/ heparin (Turnbull *et al.*, 1992; Guimond *et al.*, 1993; Walker *et al.*, 1994; Ishihara, 1994; Kreuger *et al.*, 1999; Kreuger *et al.*, 2001). In this study, the 6-de-sulfated 6-mer was able to bind FGF-1. This was unexpected, as most previous interaction studies have proposed that there is a need for the 6-O sulfate for FGF-1 binding. However, the interaction was clearly not as strong as with the heparin 6-mer, and furthermore, various lengths of oligosaccharides from the 2-de-sulfated, NA and 2, 6-de-sulfated were unable to interact with FGF-1. These data emphasize the necessity for the 2-O sulfate of the IdoA2S and the N-sulfate of the glucosamine for the HS binding to FGF-1. The FGF-2 interaction with the modified heparin oligosaccharides validated what has been proposed previously with regard to size requirements as 4-mer or larger saccharides were able to interact with FGF-2 (Delehedde *et al.*, 2002a). In addition, the necessity for the 2-O sulfate for the interaction was confirmed, and the 6-de sulfated oligosaccharides showed less inhibitory action than for FGF-1 (Guimond *et al.*, 1993; Ishihara, 1994; Walker *et al.*, 1994; Kreuger *et al.*, 1999; Kreuger *et al.*, 2001). This could be explained by the fact that oligosaccharides generated by SEC may encounter a degree of heterogeneity, which could affect the FGF-2 because it is more sensitive to the sulfates.

The investigations of the HS-FGF interaction have always used heparin or chemically modified heparins as an HS proxy. However, heparin is more homogeneous and highly sulfated compared to HS, and it lacks the domain structure. This means that when using heparin the NA and NA/NS domains of the HS are ignored, and the highly sulfated domain (NS) are the focus of study. The modified heparins were used to address the basic sulfation requirements. Despite that, heparin and the chemically modified heparin oligosaccharides have helped in determining the size and sulfation required for the interaction with FGF-1 and FGF-2, and set the scene for the more diverse structure and more biologically relevant HS saccharides to be studied. In addition, heparin studies provided valuable information about the assay requirements in term of the amount of saccharides and proteins, which are difficult to carry out with the HS saccharides, as they are difficult to purify in large quantities (see Chapter 3).

Tissue HS extracted from porcine mucosal intestinal is a rich source in the highly complex saccharides with different combinations of N and O sulfation (Walker *et al.*, 1994; Guimond and Turnbull, 1999). In this study, SEC generated 6-mer and 8-mer PMHS saccharides, which were separated according to their sulfate content using SAX-HPLC; the result was libraries of 20 and 32 fractions respectively of structurally diverse oligosaccharides (see Chapter 3). A selected number of the SAX-HPLC fractions were screened for binding with FGF-1 and FGF-2. These two particular sizes (6 and 8-mer) were selected according to data from the heparin and modified heparin studies and from what have been established in the literature. The strategy for the selection was to choose fractions across the gradient (and thus with low, medium and high sulfate content), to provide different structures with diverse sulfate content for screening. In this report, the structurally diverse HS oligosaccharides displayed different abilities to bind to FGF-1 and FGF-2. From the binding data, it was evident that the profiles of interactions did not relate to general changes in the charge density and the extent of sulfation, suggesting that the 6-mer and 8-mer PMHS oligosaccharides may contain selective structural motifs responsible for their differential interactions with FGF-1 and FGF-2. The heparin 6-mer (fully sulfated) showed strongest binding with FGF-1. But, with the FGF-2 two of the fractions (R 6 and T 6) showed better binding than the 6-mer heparin. Interestingly, the 8-mer heparin showed higher binding with both FGF-1 and FGF-2 compared with the 8-mer PMHS SAX fractions.

It has been described that more than a hundred proteins interact with HS (Conard, 1998; Capila and Linhardt, 2002; Bishop *et al.*, 2007; Ori *et al.*, 2008). However, to date only a few of these interactions have been established as being functionally important. Therefore, the interaction studies have been followed by activity studies for the SAX-HPLC generated 8-mer HS. Pye et al (1998) and Guimond and Turnbull (1999) found that minimum size to activate or inhibit effectively in the FGF systems was a 10-mer. However, many researchers have found that smaller oligosaccharides than a 10-mer are also capable of promoting FGF-1 and FGF-2 signalling through FGFRs (Delehedde *et al.*, 2002a; Wu *et al.*, 2003; Ashikari-Hada *et al.*, 2004; Ashikari-Hada *et al.*, 2009). From the current binding data, it has been established that different 8-mer SAX fractions bind differentially to FGF-1 and FGF-2 (Figure 5.10).

The 8-mer PMHS fractions were selected rather than the 6-mer fractions as it has been suggested by many researchers, that a longer oligosaccharide is required for the interaction with both the FGF and the FGFR. The activities of the 8-mer PMHS fractions in the signalling system of FGF-1 or FGF-2 with FGFR1c were investigated using the BaF3 assay. This assay is well recognized for making systematic comparisons of FGFR isoforms responses and screening signalling activity with HS saccharides. In these cells, the activity responses of the FGFs are dependent on the addition of exogenous activating oligosaccharides or heparin (Venkataraman *et al.*, 1996; Guimond and Turnbull, 1999). Activity screening of selected SAX sub-fractions of the 8-mers showed that they had differing abilities to activate signalling by FGFR1c in response to FGF-1 or FGF-2.

The activity data showed that some fractions were strong activators of signalling via FGF-2 despite being weaker binders, whereas some fractions (such as the 8 M, 8 P fractions) were both strong binders and strong activators. With regard to FGF-1, the 8 M and 8 P fractions showed a higher degree of activity comparing to other saccharides. These results support the view reported by Pye et al, (2000), that the sulfate positions, rather than the simple sulfate content, plays a critical role in HS regulation of the FGFs signalling system.

It has been mentioned earlier that SAX-HPLC fractions were single peaks or clustered groups of 2-3 peaks (Chapter 3). Thus, a further purification step was added using the RPIP-HPLC, resulting in a 3-dimensional (3D) chromatography protocol using SEC, SAX and finally RPIP-HPLC. This 3D approach was useful in additional separation of selected multiple peaks, fractions such as 8 M and 8 S, from the SAX-HPLC profile (Figure 5.12). 8 M showed a high relative activity and 8 S a lower activity with FGF-2 and FGF-1, despite being less charged.

The structural sequences of the RPIP-HPLC generated sub-fractions (M1, M2, M3, S1 and S2) were established (see Appendix 4, Figure A 4.1) with the help of Dr. A Atrih, utilizing a combination of techniques such as tag labelling of oligosaccharides (Skidmore *et al.*, 2009), sequencing enzymes and ES-MS (manuscript in preparation).

Further work is required to establish the identity of the uronic acid residues. The 8 M 2 sub-fraction promoted FGF-2 signalling with the FGFR1c more than the other 8 M sub-fractions, (e.g. M 3, the predominant peak, was unable to promote FGF-2 signalling) and about 2-fold to the 8-mer heparin. The sequence for the 8 M 2 was established as ΔUA-GlcNS-UA2S-GlcNS-UA-GlcNAc-UA-GlcNS (Figure A 4.1); this sequence has no 6-O-sulfate, which challenges current dogma, based on the previous finding indicated that the position of a 6-O-sulfate group on glucosamine residues is essential for FGF-2 activation (Guimond *et al.*, 1993). The sequence the 8 S 2 (ΔUA2S-GlcNH-UA2S-GlcNS6S-UA-GlcNAc-UA2S-GlcNH) showed that it has more sulfate groups and has the 6-O-sulfate on the N sulfated glucosamine. Despite this it was a less potent activator for FGF-2 signalling than the M 2. In the FGF-1 signalling system, S 1 (ΔUA-GlcNS-UA-GlcNAc6S-UA2S-GlcNH-UA-GlcNAc6S), which lacks the GlcNS6S, was a slightly better activator than the S 2. This also again contrasts previous data on FGF-1 activation, which was shown to require the 6-O-sulfate of the IdoA2S-GlcNS (Kreuger *et al.*, 1999).

These findings provide support for the hypothesis that selective HS sequences vary significantly in their protein interactions and ability to activate biological activity, at least in the FGF-FGFR signalling system. Thus, variations in the sequences of HS structures expressed *in vivo* could provide a mechanism for regulation of protein function of HS-binding proteins.

6 General discussion and future directions

Oligosaccharides are essential for decoding HS structure-function: It has been established that HS binds to a high numbers of proteins (Capila and Linhardt, 2002; Bishop *et al.*, 2007; Ori *et al.*, 2008). The interactions with some of these proteins have been demonstrated to be functionally important (Guimond and Turnbull, 1999; Hussain *et al.*, 2006). Furthermore, researchers in the field are frequently adding more proteins to the list of those regulated by HS and different proteins require distinct HS structures (Turnbull *et al.*, 2001). The obvious example is the pentasaccharide sequence that interacts with high affinity with the anti-thrombin III protein, causing a conformational change and enhancing its interaction with thrombin, leading to inhibition of blood coagulation (Oscarsson *et al.*, 1989; Sabourin *et al.*, 1993). Although, this example seems to be unusually specific, most proteins are more relaxed in their requirements. Natural HS is known to be a long polysaccharide present on the surface of most cells and attached to carrier proteins forming HSPGs. HS is also recognized as being structurally complex and tissue-specific as there are many structures present in any tissue. The complexity of HS arises from the way it is biosynthesized, with a family of ~20 enzymes, which share the task of making HS; these enzymes do not act to completion and the biosynthesis is not template driven. Therefore, the product is HS with complex and diverse domain structures (Spillmann *et al.*, 1998). Thus, an important question is how does the diverse structure of HS relate to its functions? In order to answer this question robust and reliable tools and approaches are needed. As demonstrated here, both chemically modified heparins, and oligosaccharide libraries (derived from natural HS or modified heparins) are valuable tools for studying the potential selectivity or specificity of binding and activity of HS with different protein ligands. Although, oligosaccharides are eventually limited to how well they can be separated and sequenced if structure-function studies are to be conducted. A robust set of methods for preparing diverse saccharide types from various starting polysaccharides have been described.

Apart from the applications described in this thesis, and in other collaborative studies, these tools should prove invaluable for use in an increasing number of studies in the future. There is also a need to produce much larger libraries in order to undertake more detailed structure-activity studies, and to improve separation techniques, the methods described provide a basis for this. Examples could include a wider range of oligosaccharide size classes; different sources of tissue HS, and the use of recombinant enzymes (e.g. sulfotransferases) to diversify oligosaccharide structures (Liu *et al.*, 2010; Wang *et al.*, 2010).

Selective HS sulfation is a key to binary and ternary Slit and Robo complexes: Many studies have emphasized the role of HS in Slit and Robo signalling (Zhang *et al.*, 2001b; Piper *et al.*, 2006; Hohenester, 2008). In collaboration with the Hohenester lab (Imperial College, London) a ternary complex composed of Slit/ Robo/HS was proposed (Hussain *et al.*, 2006). However, the nature of this ternary complex is, as yet, unknown (Morlot *et al.*, 2007; Fukuhara *et al.*, 2008). Work presented in this thesis represented the first effort to unravel some of the structural characteristics involved in HS, Slit and Robo interactions and their biological importance.

Ship and Hsieh-Wilson (2007) described the need for 6-O and N-sulfates of the glucosamine of HS for binary complex formation with Slit (Shipp and Hsieh-Wilson, 2007). However, they did not report a role for the 2-O sulfated iduronic acid in mainly sulfated saccharides, which, as well as glycosidic linkages, provide important conformational flexibility for HS (Yates *et al.*, 1996; Powell *et al.*, 2004; Rudd *et al.*, 2010; Rudd and Yates, 2010). In contrast, the current more detailed investigations here have emphasized the need for the 6-O and N sulfates of the glucosamine, but also to some extent 2-O sulfated iduronic acid, for successful interactions with Slit. This finding is in agreement with Irie et al (2002), as they proposed that the 2-O as well as the 6-O sulfates are important in molecules that are involved in axon guidance, which is known to involve Slit (Irie *et al.*, 2002).

Furthermore, the recent structural data by Fukuhara et al (2008) have revealed that HS binding site on Slit and established that it flanks the Robo binding site in basic patches on the Slit D2. To fit in this conformational arrangement, the HS molecule must be flexible to allow access of the saccharides to their binding sites on the protein. These facts would be in accord with the need for the 2-O sulfates, in addition to the glycosidic linkage, which is one of this thesis finding.

The sulfate group requirement studies for Robo-HS interactions have not previously been extensively investigated. There are many types of Robo with different structural characteristics. Thus, this could be an important subject, similar to the interactions of FGF receptor with HS, which has been found to be critical in FGF function (Guimond and Turnbull, 1999). The present results have revealed that Robo binding involves the 6-O, and to a lesser extent the 2-O and N-sulfate groups, a pattern distinct from that for the Slit ligand. Simple electrostatic interactions were dismissed as being dominant for both Slit and Robo because over-sulfated heparin was a weaker binder than heparin. In addition, other GAGs such as CS-C failed to bind both proteins.

Furthermore, direct ELISA was used to learn about structural requirements in HS/ Slit/ Robo ternary complex formation. Loss of the N-sulfate from glucosamine caused a significant drop in the affinity of ternary complex interactions compared to adding heparin, whereas, the loss of 6-O sulfate of glucosamine or 2-O of the iduronic acid had much greater effects. However, when both the 2-O and 6-O sulfates were removed, promotion of ternary complex formation was abolished. This was also the case with over-sulfated heparin. Hence, it can be speculated from these data that 2-O and 6-O sulfates are equally important in ternary complex formation, whereas N-sulfates are less critical, and the interactions are not primarily due to simply electrostatic interactions. The data could be classed as ternary complex screening or "footprinting", because the polyvalent nature of the polysaccharides does not allow a detailed examination of structural selectivity, as discussed in section 4.3. It will be important to examine how the more highly complex variant HS saccharides may differentially influence Slit-Robo interactions. This could be achieved using the natural HS saccharide libraries generated in these studies.

So how is structure related to function in the Slit-Robo system? To answer this question, an activity assay was carried out of growth cone collapse assay in chick retinal neurons (Kapfhammer *et al.*, 2007). Adding Slit protein to the growth cone causes changes in the morphology of the growth cone from spread to collapsed, via signalling mediated by the Robo receptor. For Slit to perform this action endogenous HS is required, thus, removing HS will prevent Slit from functioning correctly. However, the addition of exogenous HS can restore Slit function.

Surprisingly, the results of this assay showed that removing one sulfate from HS had no influence on the rescue experiment. However, removing two or more sulfates significantly reduced the rescue activity of Slit. Interestingly, these findings were in agreement with the analytical SEC data on ternary complex formation, suggesting clearly that the mechanism by which HS influences Slit-Robo signalling is via altering ternary complex formation. It is tempting to speculate that the kinetics or stability of these complexes is crucial for signalling, and this provides a way for changes in HS structure to influence signalling *in vivo*. Spatial control of different HS structures may also provide a mechanism for HS to influence axon guidance, as suggested by Pratt and co-workers from studies on 2OST and 6OST1 knockout mice (Pratt *et al.*, 2006).

The effect of oligosaccharide size in Slit-Robo complex formation was examined because determination of the size required for complex formation is crucial in follow-up studies such as co-crystallography of the complexes. Hussain et al (2006) suggested that heparin 10-mer is smallest size able to induce Slit and Robo signalling. However, there had previously been no comprehensive study exploring the size requirement for the interactions of HS with Slit and Robo. One of the aims of generating heparin oligosaccharides was to study the minimum size of HS required for interactions with Slit/ Robo complex. Both Slit and Robo were found to demand no less than 8-mer oligosaccharides for binary complex formation with heparin, whereas 10-mer and larger oligosaccharides were capable of stronger binding. As mentioned before, Slit and Robo binding studies were performed by competition ELISA. It would be helpful in the future to use another interaction technique such as competition optical biosensors, or dual polarisation interferometry (DPI, which can also determine the geometry of complexes) and compare the data generated by both techniques to competition ELISA.

Furthermore, direct ELISA studies examining the ternary complex using heparin oligosaccharides found that 10-mer and larger oligosaccharides enhanced the ternary complex formation. In addition, in the analytical SEC there was a slight shift in the Slit-Robo complex peak observed with 10-mer heparin, but 12 and 14-mers showed a much clearer shift when mixed in a 1:1:1 molar ratio. This result was confirmed by SDS-PAGE. Testing of modified heparin oligosaccharides also underlined the need for two sulfates in HS to efficiently, promote ternary complex formation.

Importantly, these studies suggest that activity studies of HS oligosaccharides will need to be explored rather than simply modified heparin polysaccharide, and using Slit2 D2 instead of the Slit-2 condition medium might give a better understanding of the nature of the interactions. Oligosaccharides from analytical SEC experiments are mixtures, and there is a need to use an array of more pure oligosaccharides to add to enhance understanding of the molecular interactions.

These more pure oligosaccharides should, preferably originate from tissue HS rather than heparin, because the diversity of natural HS is more likely to reveal interesting structure-activity relationships. Nevertheless, it is important to be sure it comes from relevant tissues or areas of tissues. Such data will further the investigation of Slit-Robo-HS interactions, illuminating the complex relationship between HS and Slit-Robo, and the potential for selectivity in regulation of signalling responses. Thus, further work is necessary to comprehend fully the structure activity relationship. From the data presented here it is clear that the selectivity/ specificity of this system may not be as stringent as in the case of heparin/ ATIII, or indeed the FGF-FGFR system, and this is an emerging trend with a number of HS-binding proteins being studied. The Slit-Robo-HS biochemical and bioactivity data described in this thesis has provided some insight into the complex nature of these interactions and contributes new information on their structure-function relationships.

Structures with similar or identical size and sulfation content differ widely in their bioactivity in the FGF-FGFR signalling system: HS interactions with FGFs and FGFRs have been extensively studied owing to the importance of the FGF proteins and their activities, which are known to control many essential developmental processes (Rapraeger *et al.*, 1991; Yayon *et al.*, 1991). Appropriate cell activation by FGF is of major importance for many physiological events and altered FGF stimulation may result in pathological conditions; a better understanding of the factors involved is therefore needed.

The interactions of FGF-1 and FGF-2 with heparin derivatives or CS-C were examined in this study. Data showed that binding was not due to general electrostatic interactions because CS-C bearing two negative charges was unable to compete better than 2-O and 6-O de-sulfated heparins with N-sulfate groups intact. However, removal of all of the sulfates totally abolished binding. These facts emphasized the necessity of sulfated sequences in the interactions of FGF-1 and FGF-2 with HS. Loss of sulfation caused more dramatic changes in the case of FGF-2 compared to FGF-1.

Generation of HS/ heparins oligosaccharides in this project (Chapter 3) facilitated more in-depth studies of the FGF system and the involvement of HS structure, helping to further, decode HS structure-function relationships. As anticipated, longer heparin oligosaccharides were better binders to FGF-1 and FGF-2, probably due to enhanced binding and rebinding potential compared to shorter saccharides. All binding experiments of FGF-1 and FGF-2 with heparin derivatives and heparin oligosaccharides were performed by competition ELISA. Using additional assays such as optical biosensors could improve the interpretation of the data generated from competition ELISA by providing data on kinetics and actual affinity (K_d) measurements. Optical biosensor (IASys) was selected because it offers an instant readout of the interactions between the protein and saccharides. Although preliminary studies were inconclusive, this approach is clearly warranted in future studies, since the kinetics and affinities of the saccharide-protein interactions may be more closely related to biological activity than simple binding data.

Several hundred proteins have been found to bind heparin (Ori *et al.*, 2008). The interactions of some of these proteins have been found to be functionally relevant, and FGF-1 and FGF-2 are part of this group. In this study, functional screening showed that 8-mer SAX sub-fractions displayed differential activation of FGF-1 and FGF-2 signalling via FGFR1c (Figure 5.11), providing evidence for significant functional selectivity of HS saccharide structures in this signalling system. Interestingly, whilst they also differed in their binding characteristics for FGF1 and FGF2, the differences (at least in simple binding data) were not so clear-cut, and there was no simple direct correlation between extent of binding and functional activity.

Sequence analysis for some of these oligosaccharides identified as having identical size and similar sulfation levels showed that they in fact varied in their sulfation patterns (i.e. primary sequences; see Appendix 4). These data directly addresses the question posed earlier about selectivity/ specificity for HS structures, since there are clear differences in activity for these HS saccharides with divergent sequences in terms of FGF-FGFR signalling. Further studies are clearly required to explore this selectivity, looking in addition at the role of different FGF receptors, since previous studies indicated specificity for both FGF ligands and FGF receptors (Guimond and Turnbull, 1999).

A wider range of HS saccharides will need to be generated in order to investigate whether consensus primary sequences can be identified, or alternatively whether a range of different saccharide sequences may be functional, dependent perhaps on conformational isomerism as recently suggested (Rudd *et al.*, 2010; Rudd and Yates, 2010) in which appropriate sulfation patterns are displayed for interaction with cognate protein surfaces in FGF-FGFR complexes. Either way, further studies should enhance our understanding of structural selectivity in this system and aid understanding concerning how dynamic changes in HS structures *in vivo* may provide a unique mechanism for biological regulation.

7 References

Abdel-Rahman, W. M.; Kalinina, J.; Shoman, S.; Eissa, S.; Ollikainen, M.; Elomaa, O.; Eliseenkova, A. V.; Butzow, R.; Mohammadi, M. and Peltomaki, P. (2008) Somatic FGF9 mutations in colorectal and endometrial carcinomas associated with membranous beta-catenin. *Hum Mutat,* 29, 390-7.

Abramsson, A.; Kurup, S.; Busse, M.; Yamada, S.; Lindblom, P.; Schallmeiner, E.; Stenzel, D.; Sauvaget, D.; Ledin, J.; Ringvall, M.; Landegren, U.; Kjellen, L.; Bondjers, G.; Li, J. P.; Lindahl, U.; Spillmann, D.; Betsholtz, C. and Gerhardt, H. (2007) Defective N-sulfation of heparan sulfate proteoglycans limits PDGF-BB binding and pericyte recruitment in vascular development. *Genes Dev,* 21, 316-31.

Adam, R. M.; Eaton, S. H.; Estrada, C.; Nimgaonkar, A.; Shih, S. C.; Smith, L. E.; Kohane, I. S.; Bagli, D. and Freeman, M. R. (2004) Mechanical stretch is a highly selective regulator of gene expression in human bladder smooth muscle cells. *Physiol Genomics,* 20, 36-44.

Adam, R. M.; Roth, J. A.; Cheng, H. L.; Rice, D. C.; Khoury, J.; Bauer, S. B.; Peters, C. A. and Freeman, M. R. (2003) Signaling through PI3K/Akt mediates stretch and PDGF-BB-dependent DNA synthesis in bladder smooth muscle cells. *J Urol,* 169, 2388-93.

Ai, X.; Do, A. T.; Kusche-Gullberg, M.; Lindahl, U.; Lu, K. and Emerson, C. P., Jr. (2006) Substrate specificity and domain functions of extracellular heparan sulfate 6-O-endosulfatases, QSulf1 and QSulf2. *J Biol Chem,* 281, 4969-76.

Ai, X.; Do, A. T.; Lozynska, O.; Kusche-Gullberg, M.; Lindahl, U. and Emerson, C. P., Jr. (2003) QSulf1 remodels the 6-O sulfation states of cell surface heparan sulfate proteoglycans to promote Wnt signaling. *J Cell Biol,* 162, 341-51.

Ai, X.; Kitazawa, T.; Do, A. T.; Kusche-Gullberg, M.; Labosky, P. A. and Emerson, C. P., Jr. (2007) SULF1 and SULF2 regulate heparan sulfate-mediated GDNF signaling for esophageal innervation. *Development,* 134, 3327-38.

Aikawa, J. and Esko, J. D. (1999) Molecular cloning and expression of a third member of the heparan sulfate/heparin GlcNAc N-deacetylase/ N-sulfotransferase family. *J Biol Chem,* 274, 2690-5.

Aikawa, J.; Grobe, K.; Tsujimoto, M. and Esko, J. D. (2001) Multiple isozymes of heparan sulfate/heparin GlcNAc N-deacetylase/GlcN N-sulfotransferase. Structure and activity of the fourth member, NDST4. *J Biol Chem,* 276, 5876-82.

Alexopoulou, A. N.; Multhaupt, H. A. and Couchman, J. R. (2007) Syndecans in wound healing, inflammation and vascular biology. *Int J Biochem Cell Biol.* 39, 505-28.

Alfano, I.; Vora, P.; Mummery, R. S.; Mulloy, B. and Rider, C. C. (2007) The major determinant of the heparin binding of glial cell-line-derived neurotrophic factor is near the N-terminus and is dispensable for receptor binding. *Biochem J,* 404, 131-40.

Allen, B. L. and Rapraeger, A. C. (2003) Spatial and temporal expression of heparan sulfate in mouse development regulates FGF and FGF receptor assembly. *J Cell Biol,* 163, 637-48.

Andrews, W.; Barber, M.; Hernadez-Miranda, L. R.; Xian, J.; Rakic, S.; Sundaresan, V.; Rabbitts, T. H.; Pannell, R.; Rabbitts, P.; Thompson, H.; Erskine, L.; Murakami, F. and Parnavelas, J. G. (2008) The role of Slit-Robo signaling in the generation, migration and morphological differentiation of cortical interneurons. *Dev Biol,* 313, 648-58.

Angulo, J.; Hricovini, M.; Gairi, M.; Guerrini, M.; De Paz, J. L.; Ojeda, R.; Martin-Lomas, M. and Nieto, P. M. (2005) Dynamic properties of biologically active synthetic heparin-like hexasaccharides. *Glycobiology,* 15, 1008-15.

Arungundram, S.; Al-Mafraji, K.; Asong, J.; Leach, F. E., 3rd; Amster, I. J.; Venot, A.; Turnbull, J. E. and Boons, G. J. (2009) Modular synthesis of heparan sulfate oligosaccharides for structure-activity relationship studies. *J Am Chem Soc,* 131, 17394-405.

Asada, M.; Shinomiya, M.; Suzuki, M.; Honda, E.; Sugimoto, R.; Ikekita, M. and Imamura, T. (2009) Glycosaminoglycan affinity of the complete fibroblast growth factor family. *Biochim Biophys Acta,* 1790, 40-8.

Ashikari-Hada, S.; Habuchi, H.; Kariya, Y.; Itoh, N.; Reddi, A. H. and Kimata, K. (2004) Characterization of growth factor-binding structures in heparin/heparan sulfate using an octasaccharide library. *J Biol Chem,* 279, 12346-54.

Ashikari-Hada, S.; Habuchi, H.; Sugaya, N.; Kobayashi, T. and Kimata, K. (2009) Specific inhibition of FGF-2 signaling with 2-O-sulfated octasaccharides of heparan sulfate. *Glycobiology,* 19, 644-54.

Asundi, V. K.; Erdman, R.; Stahl, R. C. and Carey, D. J. (2003) Matrix metalloproteinase-dependent shedding of syndecan-3, a transmembrane heparan sulfate proteoglycan, in Schwann cells. *J Neurosci Res,* 73, 593-602.

Avci, F. Y.; Karst, N. A. and Linhardt, R. J. (2003) Synthetic oligosaccharides as heparin-mimetics displaying anticoagulant properties. *Curr Pharm Des,* 9, 2323-35.

Avivi, A.; Yayon, A. and Givol, D. (1993) A novel form of FGF receptor-3 using an alternative exon in the immunoglobulin domain III. *FEBS Lett,* 330, 249-52.

Ayotte, L. and Perlin, A. S. (1986) N.m.r. spectroscopic observations related to the function of sulfate groups in heparin. Calcium binding vs. biological activity. *Carbohydr Res,* 145, 267-77.

Baloh, R. H.; Enomoto, H.; Johnson, E. M., Jr. and Milbrandt, J. (2000) The GDNF family ligands and receptors - implications for neural development. *Curr Opin Neurobiol,* 10, 103-10.

Bame, K. J.; Zhang, L.; David, G. and Esko, J. D. (1994) Sulphated and undersulphated heparan sulphate proteoglycans in a Chinese hamster ovary cell mutant defective in N-sulphotransferase. *Biochem J,* 303 (Pt 1), 81-7.

Barnett, M. W.; Fisher, C. E.; Perona-Wright, G. and Davies, J. A. (2002) Signalling by glial cell line-derived neurotrophic factor (GDNF) requires heparan sulphate glycosaminoglycan. *J Cell Sci,* 115, 4495-503.

Barth, H.; Schnober, E. K.; Zhang, F.; Linhardt, R. J.; Depla, E.; Boson, B.; Cosset, F. L.; Patel, A. H.; Blum, H. E. and Baumert, T. F. (2006) Viral and cellular determinants of the hepatitis C virus envelope-heparan sulfate interaction. *J Virol,* 80, 10579-90.

Bashaw, G. J.; Kidd, T.; Murray, D.; Pawson, T. and Goodman, C. S. (2000) Repulsive axon guidance: Abelson and Enabled play opposing roles downstream of the roundabout receptor. *Cell,* 101, 703-15.

Bates, C. M. (2007) Role of fibroblast growth factor receptor signaling in kidney development. *Pediatr Nephrol,* 22, 343-9.

Beauvais, D. M.; Burbach, B. J. and Rapraeger, A. C. (2004) The syndecan-1 ectodomain regulates alphavbeta3 integrin activity in human mammary carcinoma cells. *J Cell Biol,* 167, 171-81.

Bedell, V. M.; Yeo, S. Y.; Park, K. W.; Chung, J.; Seth, P.; Shivalingappa, V.; Zhao, J.; Obara, T.; Sukhatme, V. P.; Drummond, I. A.; Li, D. Y. and Ramchandran, R. (2005) roundabout4 is essential for angiogenesis in vivo. *Proc Natl Acad Sci U S A,* 102, 6373-8.

Beenken, A. and Mohammadi, M. (2009) The FGF family: biology, pathophysiology and therapy. *Nat Rev Drug Discov,* 8, 235-53.

Belford, D. A.; Hendry, I. A. and Parish, C. R. (1992) Ability of different chemically modified heparins to potentiate the biological activity of heparin-binding growth factor 1: lack of correlation with growth factor binding. *Biochemistry,* 31, 6498-503.

Belford, D. A.; Hendry, I. A. and Parish, C. R. (1993) Investigation of the ability of several naturally occurring and synthetic polyanions to bind to and potentiate the biological activity of acidic fibroblast growth factor. *J Cell Physiol,* 157, 184-9.

Bernfield, M.; Gotte, M.; Park, P. W.; Reizes, O.; Fitzgerald, M. L.; Lincecum, J. and Zako, M. (1999) Functions of cell surface heparan sulfate proteoglycans. *Annu Rev Biochem,* 68, 729-77.

Bezakova, G. and Ruegg, M. A. (2003) New insights into the roles of agrin. *Nat Rev Mol Cell Biol,* 4, 295-308.

Bhakta, S.; Bartes, A.; Bowman, K. G.; Kao, W. M.; Polsky, I.; Lee, J. K.; Cook, B. N.; Bruehl, R. E.; Rosen, S. D.; Bertozzi, C. R. and Hemmerich, S. (2000) Sulfation of N-acetylglucosamine by chondroitin 6-sulfotransferase 2 (GST-5). *J Biol Chem,* 275, 40226-34.

Bishop, J. R.; Schuksz, M. and Esko, J. D. (2007) Heparan sulphate proteoglycans fine-tune mammalian physiology. *Nature,* 446, 1030-7.

Bjork, I.; Nordling, K. and Olson, S. T. (1993) Immunologic evidence for insertion of the reactive-bond loop of antithrombin into the A beta-sheet of the inhibitor during trapping of target proteinases. *Biochemistry,* 32, 6501-5.

Bohmer, L. H.; Pitout, M. J.; Steyn, P. L. and Visser, L. (1990) Purification and characterization of a novel heparinase. *J Biol Chem,* 265, 13609-17.

Boilly, B.; Vercoutter-Edouart, A. S.; Hondermarck, H.; Nurcombe, V. and Le Bourhis, X. (2000) FGF signals for cell proliferation and migration through different pathways. *Cytokine Growth Factor Rev,* 11, 295-302.

Boltje, T. J.; Buskas, T. and Boons, G. J. (2009) Opportunities and challenges in synthetic oligosaccharide and glycoconjugate research. *Nat Chem,* 1, 611-622.

Bonneh-Barkay, D.; Shlissel, M.; Berman, B.; Shaoul, E.; Admon, A.; Vlodavsky, I.; Carey, D. J.; Asundi, V. K.; Reich-Slotky, R. and Ron, D. (1997) Identification of glypican as a dual modulator of the biological activity of fibroblast growth factors. *J Biol Chem,* 272, 12415-21.

Bourin, M. C. and Lindahl, U. (1993) Glycosaminoglycans and the regulation of blood coagulation. *Biochem J,* 289 (Pt 2), 313-30.

Bulow, H. E. and Hobert, O. (2004) Differential sulfations and epimerization define heparan sulfate specificity in nervous system development. *Neuron,* 41, 723-36.

Bulow, H. E.; Tjoe, N.; Townley, R. A.; Didiano, D.; Van Kuppevelt, T. H. and Hobert, O. (2008) Extracellular sugar modifications provide instructive and cell-specific information for axon-guidance choices. *Curr Biol,* 18, 1978-85.

Burkart, M. D.; Izumi, M.; Chapman, E.; Lin, C. H. and Wong, C. H. (2000) Regeneration of PAPS for the enzymatic synthesis of sulfated oligosaccharides. *J Org Chem,* 65, 5565-74.

Bussolino, F.; Di Renzo, M. F.; Ziche, M.; Bocchietto, E.; Olivero, M.; Naldini, L.; Gaudino, G.; Tamagnone, L.; Coffer, A. and Comoglio, P. M. (1992) Hepatocyte growth factor is a potent angiogenic factor which stimulates endothelial cell motility and growth. *J Cell Biol,* 119, 629-41.

Cai, W. and Chen, X. (2008) Multimodality molecular imaging of tumor angiogenesis. *J Nucl Med,* 49 Suppl 2, 113S-28S.

Campbell, P.; Hannesson, H. H.; Sandback, D.; Roden, L.; Lindahl, U. and Li, J. P. (1994) Biosynthesis of heparin/heparan sulfate. Purification of the D-glucuronyl C-5 epimerase from bovine liver. *J Biol Chem,* 269, 26953-8.

Capila, I. and Linhardt, R. J. (2002) Heparin-protein interactions. *Angew Chem Int Ed Engl,* 41, 391-412.

Capila, I.; Vandernoot, V. A.; Mealy, T. R.; Seaton, B. A. and Linhardt, R. J. (1999) Interaction of heparin with annexin V. *FEBS Lett,* 446, 327-30.

Cardin, A. D. and Weintraub, H. J. (1989) Molecular modeling of protein-glycosaminoglycan interactions. *Arteriosclerosis,* 9, 21-32.

Carmeliet, G.; Hauman, R.; Dom, R.; David, G.; Fryns, J. P.; Van Den Berghe, H. and Cassiman, J. J. (1990) Growth properties and in vitro life span of Alzheimer disease and Down syndrome fibroblasts. A blind study. *Mech Ageing Dev,* 53, 17-33.

Cepko, C. (2000) Giving in to the blues. *Nat Genet,* 24, 99-100.

Chan, P.; Mill, S.; Mulloy, B.; Kakkar, V. and Demoliou-Mason, C. (1992) Heparin inhibition of human vascular smooth muscle cell hyperplasia. *Int Angiol,* 11, 261-7.

Chen, C. L.; Huang, S. S. and Huang, J. S. (2006) Cellular heparan sulfate negatively modulates transforming growth factor-beta1 (TGF-beta1) responsiveness in epithelial cells. *J Biol Chem,* 281, 11506-14.

Chen, J.; Avci, F. Y.; Munoz, E. M.; Mcdowell, L. M.; Chen, M.; Pedersen, L. C.; Zhang, L.; Linhardt, R. J. and Liu, J. (2005) Enzymatic redesigning of biologically active heparan sulfate. *J Biol Chem,* 280, 42817-25.

Chen, J.; Jones, C. L. and Liu, J. (2007) Using an enzymatic combinatorial approach to identify anticoagulant heparan sulfate structures. *Chem Biol,* 14, 986-93.

Chen, Z.; Jing, Y.; Song, B.; Han, Y. and Chu, Y. (2009) Chemically modified heparin inhibits in vitro L-selectin-mediated human ovarian carcinoma cell adhesion. *Int J Gynecol Cancer,* 19, 540-6.

Chikazu, D.; Hakeda, Y.; Ogata, N.; Nemoto, K.; Itabashi, A.; Takato, T.; Kumegawa, M.; Nakamura, K. and Kawaguchi, H. (2000) Fibroblast growth factor (FGF)-2 directly stimulates mature osteoclast function through activation of FGF receptor 1 and p42/p44 MAP kinase. *J Biol Chem,* 275, 31444-50.

Chilton, J. K. (2006) Molecular mechanisms of axon guidance. *Dev Biol,* 292, 13-24.

Choay, J.; Petitou, M.; Lormeau, J. C.; Sinay, P.; Casu, B. and Gatti, G. (1983) Structure-activity relationship in heparin: a synthetic pentasaccharide with high affinity for antithrombin III and eliciting high anti-factor Xa activity. *Biochem Biophys Res Commun,* 116, 492-9.

Clamp, A.; Blackhall, F. H.; Henrioud, A.; Jayson, G. C.; Javaherian, K.; Esko, J.; Gallagher, J. T. and Merry, C. L. (2006) The morphogenic properties of oligomeric endostatin are dependent on cell surface heparan sulfate. *J Biol Chem,* 281, 14813-22.

Cochran, S.; Li, C. P. and Ferro, V. (2009) A surface plasmon resonance-based solution affinity assay for heparan sulfate-binding proteins. *Glycoconj J,* 26, 577-87.

Colliec-Jouault, S.; Shworak, N. W.; Liu, J.; De Agostini, A. I. and Rosenberg, R. D. (1994) Characterization of a cell mutant specifically defective in the synthesis of anticoagulantly active heparan sulfate. *J Biol Chem,* 269, 24953-8.

Conard, H. E. (1998) Heparin-binding proteins *Academic Press, ISBN 0-12-186060-4.*

Coombe, D. R. and Kett, W. C. (2005) Heparan sulfate-protein interactions: therapeutic potential through structure-function insights. *Cell Mol Life Sci,* 62, 410-24.

Cooper, M. A. (2002) Optical biosensors in drug discovery. *Nat Rev Drug Discov,* 1, 515-28.

Copeland, R.; Balasubramaniam, A.; Tiwari, V.; Zhang, F.; Bridges, A.; Linhardt, R. J.; Shukla, D. and Liu, J. (2008) Using a 3-O-sulfated heparin octasaccharide to inhibit the entry of herpes simplex virus type 1. *Biochemistry,* 47, 5774-83.

Couchman, J. R.; Chen, L. and Woods, A. (2001) Syndecans and cell adhesion. *Int Rev Cytol,* 207, 113-50.

Crawford, B. E.; Garner, O. B.; Bishop, J. R.; Zhang, D. Y.; Bush, K. T.; Nigam, S. K. and Esko, J. D. (2010) Loss of the heparan sulfate sulfotransferase, Ndst1, in mammary epithelial cells selectively blocks lobuloalveolar development in mice. *PLoS One,* 5, e10691.

Casu, B. (1990) Heparin structure. *Haemostasis,* 20 Suppl 1, 62-73.

Dailey, L.; Ambrosetti, D.; Mansukhani, A. and Basilico, C. (2005) Mechanisms underlying differential responses to FGF signaling. *Cytokine Growth Factor Rev,* 16, 233-47.

De Agostini, A. (2006) An unexpected role for anticoagulant heparan sulfate proteoglycans in reproduction. *Swiss Med Wkly,* 136, 583-90.

De Agostini, A. I.; Dong, J. C.; De Vantery Arrighi, C.; Ramus, M. A.; Dentand-Quadri, I.; Thalmann, S.; Ventura, P.; Ibecheole, V.; Monge, F.; Fischer, A. M.; Hajmohammadi, S.; Shworak, N. W.; Zhang, L.; Zhang, Z. and Linhardt, R. J. (2008) Human follicular fluid heparan sulfate contains abundant 3-O-sulfated chains with anticoagulant activity. *J Biol Chem,* 283, 28115-24.

Deepa, S. S.; Umehara, Y.; Higashiyama, S.; Itoh, N. and Sugahara, K. (2002) Specific molecular interactions of oversulfated chondroitin sulfate E with various heparin-binding growth factors. Implications as a physiological binding partner in the brain and other tissues. *J Biol Chem,* 277, 43707-16.

Delehedde, M.; Lyon, M.; Gallagher, J. T.; Rudland, P. S. and Fernig, D. G. (2002a) Fibroblast growth factor-2 binds to small heparin-derived oligosaccharides and stimulates a sustained phosphorylation of p42/44 mitogen-activated protein kinase and proliferation of rat mammary fibroblasts. *Biochem J,* 366, 235-44.

Delehedde, M.; Lyon, M.; Vidyasagar, R.; Mcdonnell, T. J. and Fernig, D. G. (2002b) Hepatocyte growth factor/scatter factor binds to small heparin-derived oligosaccharides and stimulates the proliferation of human HaCaT keratinocytes. *J Biol Chem,* 277, 12456-62.

Dell, A. and Morris, H. R. (2001) Glycoprotein structure determination by mass spectrometry. *Science,* 291, 2351-6.

Deng, C. X.; Wynshaw-Boris, A.; Shen, M. M.; Daugherty, C.; Ornitz, D. M. and Leder, P. (1994) Murine FGFR-1 is required for early postimplantation growth and axial organization. *Genes Dev,* 8, 3045-57.

Deng, F.; Hu, J.; Xiong, J. and Du, Y. (1993) Solid-state NMR studies of 1H spin diffusion in adsorbed organic molecules. *Solid State Nucl Magn Reson,* 2, 97-103.

Dickson, B. J. and Gilestro, G. F. (2006) Regulation of commissural axon pathfinding by slit and its Robo receptors. *Annu Rev Cell Dev Biol,* 22, 651-75.

Digabriele, A. D.; Lax, I.; Chen, D. I.; Svahn, C. M.; Jaye, M.; Schlessinger, J. and Hendrickson, W. A. (1998) Structure of a heparin-linked biologically active dimer of fibroblast growth factor. *Nature,* 393, 812-7.

Dinis Da Gama, A. (2008) [The unknown history of heparin's discovery]. *Rev Port Cir Cardiotorac Vasc,* 15, 25-30.

Doherty, P. and Walsh, F. S. (1996) CAM-FGF receptor interactions: a model for axonal growth. *Mol Cell Neurosci,* 8, 99-111.

Drummond, K. J.; Yates, E. A. and Turnbull, J. E. (2001) Electrophoretic sequencing of heparin/heparan sulfate oligosaccharides using a highly sensitive fluorescent end label. *Proteomics,* 1, 304-10.

Edge, A. S. and Spiro, R. G. (1990) Characterization of novel sequences containing 3-O-sulfated glucosamine in glomerular basement membrane heparan sulfate and localization of sulfated disaccharides to a peripheral domain. *J Biol Chem,* 265, 15874-81.

Esko, J. D. and Selleck, S. B. (2002) Order out of chaos: assembly of ligand binding sites in heparan sulfate. *Annu Rev Biochem,* 71, 435-71.

Essner, J. J.; Chen, E. and Ekker, S. C. (2006) Syndecan-2. *Int J Biochem Cell Biol,* 38, 152-6.

Eswarakumar, V. P.; Lax, I. and Schlessinger, J. (2005) Cellular signaling by fibroblast growth factor receptors. *Cytokine Growth Factor Rev,* 16, 139-49.

Evanko, S. P.; Tammi, M. I.; Tammi, R. H. and Wight, T. N. (2007) Hyaluronan-dependent pericellular matrix. *Adv Drug Deliv Rev,* 59, 1351-65.

Faham, S.; Hileman, R. E.; Fromm, J. R.; Linhardt, R. J. and Rees, D. C. (1996) Heparin structure and interactions with basic fibroblast growth factor. *Science,* 271, 1116-20.

Fernandis, A. Z. and Ganju, R. K. (2001) Slit: a roadblock for chemotaxis. *Sci STKE,* 2001, pe1.

Fernig, D. G. and Gallagher, J. T. (1994) Fibroblast growth factors and their receptors: an information network controlling tissue growth, morphogenesis and repair. *Prog Growth Factor Res,* 5, 353-77.

Ferro, D. R.; Provasoli, A.; Ragazzi, M.; Casu, B.; Torri, G.; Bossennec, V.; Perly, B.; Sinay, P.; Petitou, M. and Choay, J. (1990) Conformer populations of L-iduronic acid residues in glycosaminoglycan sequences. *Carbohydr Res,* 195, 157-67.

Feyzi, E.; Lustig, F.; Fager, G.; Spillmann, D.; Lindahl, U. and Salmivirta, M. (1997a) Characterization of heparin and heparan sulfate domains binding to the long splice variant of platelet-derived growth factor A chain. *J Biol Chem,* 272, 5518-24.

Feyzi, E.; Trybala, E.; Bergstrom, T.; Lindahl, U. and Spillmann, D. (1997b) Structural requirement of heparan sulfate for interaction with herpes simplex virus type 1 virions and isolated glycoprotein C. *J Biol Chem,* 272, 24850-7.

Fisher, C. E.; Michael, L.; Barnett, M. W. and Davies, J. A. (2001) Erk MAP kinase regulates branching morphogenesis in the developing mouse kidney. *Development,* 128, 4329-38.

Forsberg, E.; Pejler, G.; Ringvall, M.; Lunderius, C.; Tomasini-Johansson, B.; Kusche-Gullberg, M.; Eriksson, I.; Ledin, J.; Hellman, L. and Kjellen, L. (1999) Abnormal mast cells in mice deficient in a heparin-synthesizing enzyme. *Nature,* 400, 773-6.

Fransson, L. A.; Belting, M.; Cheng, F.; Jonsson, M.; Mani, K. and Sandgren, S. (2004) Novel aspects of glypican glycobiology. *Cell Mol Life Sci,* 61, 1016-24.

Fritz, T. A.; Gabb, M. M.; Wei, G. and Esko, J. D. (1994) Two N-acetylglucosaminyltransferases catalyze the biosynthesis of heparan sulfate. *J Biol Chem,* 269, 28809-14.

Fromm, J. R.; Hileman, R. E.; Caldwell, E. E.; Weiler, J. M. and Linhardt, R. J. (1995) Differences in the interaction of heparin with arginine and lysine and the importance of these basic amino acids in the binding of heparin to acidic fibroblast growth factor. *Arch Biochem Biophys,* 323, 279-87.

Fromm, J. R.; Hileman, R. E.; Weiler, J. M. and Linhardt, R. J. (1997) Interaction of fibroblast growth factor-1 and related peptides with heparan sulfate and its oligosaccharides. *Arch Biochem Biophys,* 346, 252-62.

Fukuhara, N.; Howitt, J. A.; Hussain, S. A. and Hohenester, E. (2008) Structural and functional analysis of slit and heparin binding to immunoglobulin-like domains 1 and 2 of Drosophila Robo. *J Biol Chem,* 283, 16226-34.

Funderburgh, J. L. (2000) Keratan sulfate: structure, biosynthesis, and function. *Glycobiology,* 10, 951-8.

Gallagher, J. T. (2001) Heparan sulfate: growth control with a restricted sequence menu. *J Clin Invest,* 108, 357-61.

Gallagher, J. T. (2006) Multiprotein signalling complexes: regional assembly on heparan sulphate. *Biochem Soc Trans,* 34, 438-41.

Gallagher, J. T. and Walker, A. (1985) Molecular distinctions between heparan sulphate and heparin. Analysis of sulphation patterns indicates that heparan sulphate and heparin are separate families of N-sulphated polysaccharides. *Biochem J,* 230, 665-74.

Gallo, R.; Kim, C.; Kokenyesi, R.; Adzick, N. S. and Bernfield, M. (1996) Syndecans-1 and -4 are induced during wound repair of neonatal but not fetal skin. *J Invest Dermatol,* 107, 676-83.

Garg, H. G.; Linhardt, R. and Charles, H. (2005) *Chemistry and Biology of Heparin and Heparan sulfate,* Oxford, UK, ELSEVIER Ltd.

Goetz, R.; Beenken, A.; Ibrahimi, O. A.; Kalinina, J.; Olsen, S. K.; Eliseenkova, A. V.; Xu, C.; Neubert, T. A.; Zhang, F.; Linhardt, R. J.; Yu, X.; White, K. E.; Inagaki, T.; Kliewer, S. A.; Yamamoto, M.; Kurosu, H.; Ogawa, Y.; Kuro-O, M.; Lanske, B.; Razzaque, M. S. and Mohammadi, M. (2007) Molecular insights into the klotho-dependent, endocrine mode of action of fibroblast growth factor 19 subfamily members. *Mol Cell Biol,* 27, 3417-28.

Goetz, R.; Dover, K.; Laezza, F.; Shtraizent, N.; Huang, X.; Tchetchik, D.; Eliseenkova, A. V.; Xu, C. F.; Neubert, T. A.; Ornitz, D. M.; Goldfarb, M. and Mohammadi, M. (2009) Crystal structure of a fibroblast growth factor homologous factor (FHF) defines a conserved surface on FHFs for binding and modulation of voltage-gated sodium channels. *J Biol Chem,* 284, 17883-96.

Goger, B.; Halden, Y.; Rek, A.; Mosl, R.; Pye, D.; Gallagher, J. and Kungl, A. J. (2002) Different affinities of glycosaminoglycan oligosaccharides for monomeric and dimeric interleukin-8: a model for chemokine regulation at inflammatory sites. *Biochemistry,* 41, 1640-6.

Gong, F.; Jemth, P.; Escobar Galvis, M. L.; Vlodavsky, I.; Horner, A.; Lindahl, U. and Li, J. P. (2003) Processing of macromolecular heparin by heparanase. *J Biol Chem,* 278, 35152-8.

Gonzalez-Martinez, D.; Kim, S. H.; Hu, Y.; Guimond, S.; Schofield, J.; Winyard, P.; Vannelli, G. B.; Turnbull, J. and Bouloux, P. M. (2004) Anosmin-1 modulates fibroblast growth factor receptor 1 signaling in human gonadotropin-releasing hormone olfactory neuroblasts through a heparan sulfate-dependent mechanism. *J Neurosci,* 24, 10384-92.

Goodger, S. J.; Robinson, C. J.; Murphy, K. J.; Gasiunas, N.; Harmer, N. J.; Blundell, T. L.; Pye, D. A. and Gallagher, J. T. (2008) Evidence that heparin saccharides promote FGF2 mitogenesis through two distinct mechanisms. *J Biol Chem,* 283, 13001-8.

Gould, S. E.; Upholt, W. B. and Kosher, R. A. (1992) Syndecan 3: a member of the syndecan family of membrane-intercalated proteoglycans that is expressed in high amounts at the onset of chicken limb cartilage differentiation. *Proc Natl Acad Sci U S A,* 89, 3271-5.

Grant, D.; Long, W. F.; Moffat, C. F. and Williamson, F. B. (1989) Infrared spectroscopy of chemically modified heparins. *Biochem J,* 261, 1035-8.

Grieshammer, U.; Le, M.; Plump, A. S.; Wang, F.; Tessier-Lavigne, M. and Martin, G. R. (2004) SLIT2-mediated ROBO2 signaling restricts kidney induction to a single site. *Dev Cell,* 6, 709-17.

Grobe, K. and Esko, J. D. (2002) Regulated translation of heparan sulfate N-acetylglucosamine N-deacetylase/n-sulfotransferase isozymes by structured 5'-untranslated regions and internal ribosome entry sites. *J Biol Chem,* 277, 30699-706.

Groth, C. and Lardelli, M. (2002) The structure and function of vertebrate fibroblast growth factor receptor 1. *Int J Dev Biol,* 46, 393-400.

Groth, C.; Nornes, S.; Mccarty, R.; Tamme, R. and Lardelli, M. (2002) Identification of a second presenilin gene in zebrafish with similarity to the human Alzheimer's disease gene presenilin2. *Dev Genes Evol,* 212, 486-90.

Guerrini, M.; Beccati, D.; Shriver, Z.; Naggi, A.; Viswanathan, K.; Bisio, A.; Capila, I.; Lansing, J. C.; Guglieri, S.; Fraser, B.; Al-Hakim, A.; Gunay, N. S.; Zhang, Z.; Robinson, L.; Buhse, L.; Nasr, M.; Woodcock, J.; Langer, R.; Venkataraman, G.; Linhardt, R. J.; Casu, B.; Torri, G. and Sasisekharan, R. (2008a) Oversulfated chondroitin sulfate is a contaminant in heparin associated with adverse clinical events. *Nat Biotechnol,* 26, 669-75.

Guerrini, M.; Guglieri, S.; Beccati, D.; Torri, G.; Viskov, C. and Mourier, P. (2006) Conformational transitions induced in heparin octasaccharides by binding with antithrombin III. *Biochem J,* 399, 191-8.

Guerrini, M.; Guglieri, S.; Casu, B.; Torri, G.; Mourier, P.; Boudier, C. and Viskov, C. (2008b) Antithrombin-binding octasaccharides and role of extensions of the active pentasaccharide sequence in the specificity and strength of interaction. Evidence for very high affinity induced by an unusual glucuronic acid residue. *J Biol Chem,* 283, 26662-75.

Guglieri, S.; Hricovini, M.; Raman, R.; Polito, L.; Torri, G.; Casu, B.; Sasisekharan, R. and Guerrini, M. (2008) Minimum FGF2 Binding Structural Requirements of Heparin and Heparan Sulfate Oligosaccharides As Determined by NMR Spectroscopy (dagger). *Biochemistry.*

Guimond, S.; Maccarana, M.; Olwin, B. B.; Lindahl, U. and Rapraeger, A. C. (1993) Activating and inhibitory heparin sequences for FGF-2 (basic FGF). Distinct requirements for FGF-1, FGF-2, and FGF-4. *J Biol Chem,* 268, 23906-14.

Guimond, S. E.; Puvirajesinghe, T. M.; Skidmore, M. A.; Kalus, I.; Dierks, T.; Yates, E. A. and Turnbull, J. E. (2009a) Rapid purification and high sensitivity analysis of heparan sulfate from cells and tissues: toward glycomics profiling. *J Biol Chem,* 284, 25714-22.

Guimond, S. E.; Rudd, T. R.; Skidmore, M. A.; Ori, A.; Gaudesi, D.; Cosentino, C.; Guerrini, M.; Edge, R.; Collison, D.; Mcinnes, E.; Torri, G.; Turnbull, J. E.; Fernig, D. G. and Yates, E. A. (2009b) Cations modulate polysaccharide structure to determine FGF-FGFR signaling: a comparison of signaling and inhibitory polysaccharide interactions with FGF-1 in solution. *Biochemistry,* 48, 4772-9.

Guimond, S. E. and Turnbull, J. E. (1999) Fibroblast growth factor receptor signalling is dictated by specific heparan sulphate saccharides. *Curr Biol,* 9, 1343-6.

Guimond, S. E.; Turnbull, J. E. and Yates, E. A. (2006) Engineered bio-active polysaccharides from heparin. *Macromol Biosci,* 6, 681-6.

Gunay, N. S.; Tadano-Aritomi, K.; Toida, T.; Ishizuka, I. and Linhardt, R. J. (2003) Evaluation of counterions for electrospray ionization mass spectral analysis of a highly sulfated carbohydrate, sucrose octasulfate. *Anal Chem,* 75, 3226-31.

Guo, Y. C. and Conrad, H. E. (1989) The disaccharide composition of heparins and heparan sulfates. *Anal Biochem,* 176, 96-104.

Habuchi, H.; Nagai, N.; Sugaya, N.; Atsumi, F.; Stevens, R. L. and Kimata, K. (2007) Mice deficient in heparan sulfate 6-O-sulfotransferase-1 exhibit defective heparan sulfate biosynthesis, abnormal placentation, and late embryonic lethality. *J Biol Chem,* 282, 15578-88.

Habuchi, H.; Tanaka, M.; Habuchi, O.; Yoshida, K.; Suzuki, H.; Ban, K. and Kimata, K. (2000) The occurrence of three isoforms of heparan sulfate 6-O-sulfotransferase having different specificities for hexuronic acid adjacent to the targeted N-sulfoglucosamine. *J Biol Chem,* 275, 2859-68.

Hagner-Mcwhirter, A.; Li, J. P.; Oscarson, S. and Lindahl, U. (2004) Irreversible glucuronyl C5-epimerization in the biosynthesis of heparan sulfate. *J Biol Chem,* 279, 14631-8.

Hagner-Mcwhirter, A.; Lindahl, U. and Li, J. (2000) Biosynthesis of heparin/heparan sulphate: mechanism of epimerization of glucuronyl C-5. *Biochem J,* 347 Pt 1, 69-75.

Hamel, D. J.; Sielaff, I.; Proudfoot, A. E. and Handel, T. M. (2009) Chapter 4. Interactions of chemokines with glycosaminoglycans. *Methods Enzymol,* 461, 71-102.

Handel, T. M.; Johnson, Z.; Rodrigues, D. H.; Dos Santos, A. C.; Cirillo, R.; Muzio, V.; Riva, S.; Mack, M.; Deruaz, M.; Borlat, F.; Vitte, P. A.; Wells, T. N.; Teixeira, M. M. and Proudfoot, A. E. (2008) An engineered monomer of CCL2 has anti-inflammatory properties emphasizing the importance of oligomerization for chemokine activity in vivo. *J Leukoc Biol,* 84, 1101-8.

Handler, M.; Yurchenco, P. D. and Iozzo, R. V. (1997) Developmental expression of perlecan during murine embryogenesis. *Dev Dyn,* 210, 130-45.

Hao, J. C.; Yu, T. W.; Fujisawa, K.; Culotti, J. G.; Gengyo-Ando, K.; Mitani, S.; Moulder, G.; Barstead, R.; Tessier-Lavigne, M. and Bargmann, C. I. (2001) C. elegans slit acts in midline, dorsal-ventral, and anterior-posterior guidance via the SAX-3/Robo receptor. *Neuron,* 32, 25-38.

Harmer, N. J.; Pellegrini, L.; Chirgadze, D.; Fernandez-Recio, J. and Blundell, T. L. (2004) The crystal structure of fibroblast growth factor (FGF) 19 reveals novel features of the FGF family and offers a structural basis for its unusual receptor affinity. *Biochemistry,* 43, 629-40.

Heldin, C. H. and Westermark, B. (1990) Signal transduction by the receptors for platelet-derived growth factor. *J Cell Sci,* 96 (Pt 2), 193-6.

Henriksen, J.; Roepstorff, P. and Ringborg, L. H. (2006) Ion-pairing reversed-phased chromatography/mass spectrometry of heparin. *Carbohydr Res,* 341, 382-7.

Higashiyama, S.; Abraham, J. A. and Klagsbrun, M. (1993) Heparin-binding EGF-*like growth factor stimulation* of smooth muscle cell migration: dependence on interactions with cell surface heparan sulfate. *J Cell Biol, 122, 933-40.*

Hileman, R. E.; Fromm, J. R.; Weiler, J. M. and Linhardt, R. J. (1998a) Glycosaminoglycan-protein interactions: definition of consensus sites in glycosaminoglycan binding proteins. *Bioessays,* 20, 156-67.

Hileman, R. E.; Jennings, R. N. and Linhardt, R. J. (1998b) Thermodynamic analysis of the heparin interaction with a basic cyclic peptide using isothermal titration calorimetry. *Biochemistry,* 37, 15231-7.

Hoch, W.; Campanelli, J. T. and Scheller, R. H. (1994) Agrin-induced clustering of acetylcholine receptors: a cytoskeletal link. *J Cell Biol,* 126, 1-4.

Hohenester, E. (2008) Structural insight into Slit-Robo signalling. *Biochem Soc Trans,* 36, 251-6.

Holmborn, K.; Ledin, J.; Smeds, E.; Eriksson, I.; Kusche-Gullberg, M. and Kjellen, L. (2004) Heparan sulfate synthesized by mouse embryonic stem cells deficient in NDST1 and NDST2 is 6-O-sulfated but contains no N-sulfate groups. *J Biol Chem,* 279, 42355-8.

Houssaint, E.; Blanquet, P. R.; Champion-Arnaud, P.; Gesnel, M. C.; Torriglia, A.; Courtois, Y. and Breathnach, R. (1990) Related fibroblast growth factor receptor genes exist in the human genome. *Proc Natl Acad Sci U S A,* 87, 8180-4.

Howitt, J. A.; Clout, N. J. and Hohenester, E. (2004) Binding site for Robo receptors revealed by dissection of the leucine-rich repeat region of Slit. *Embo J,* 23, 4406-12.

Hricovini, M.; Guerrini, M.; Torri, G. and Casu, B. (1997) Motional properties of E. coli polysaccharide K5 in aqueous solution analyzed by NMR relaxation measurements. *Carbohydr Res,* 300, 69-76.

Hricovini, M.; Guerrini, M.; Torri, G.; Piani, S. and Ungarelli, F. (1995) Conformational analysis of heparin epoxide in aqueous solution. An NMR relaxation study. *Carbohydr Res,* 277, 11-23.

Hu, Y.; Guimond, S. E.; Travers, P.; Cadman, S.; Hohenester, E.; Turnbull, J. E.; Kim, S. H. and Bouloux, P. M. (2009) Novel mechanisms of fibroblast growth factor receptor 1 regulation by extracellular matrix protein anosmin-1. *J Biol Chem,* 284, 29905-20.

Huminiecki, L.; Gorn, M.; Suchting, S.; Poulsom, R. and Bicknell, R. (2002) Magic roundabout is a new member of the roundabout receptor family that is endothelial specific and expressed at sites of active angiogenesis. *Genomics,* 79, 547-52.

Hussain, S. A.; Piper, M.; Fukuhara, N.; Strochlic, L.; Cho, G.; Howitt, J. A.; Ahmed, Y.; Powell, A. K.; Turnbull, J. E.; Holt, C. E. and Hohenester, E. (2006) A molecular mechanism for the heparan sulfate dependence of slit-robo signaling. *J Biol Chem,* 281, 39693-8.

Hutson, L. D.; Jurynec, M. J.; Yeo, S. Y.; Okamoto, H. and Chien, C. B. (2003) Two divergent slit1 genes in zebrafish. *Dev Dyn,* 228, 358-69.

Inatani, M.; Irie, F.; Plump, A. S.; Tessier-Lavigne, M. and Yamaguchi, Y. (2003) Mammalian brain morphogenesis and midline axon guidance require heparan sulfate. *Science,* 302, 1044-6.

Iozzo, R. V. (2005) Basement membrane proteoglycans: from cellar to ceiling. *Nat Rev Mol Cell Biol,* 6, 646-56.

Irie, A.; Yates, E. A.; Turnbull, J. E. and Holt, C. E. (2002) Specific heparan sulfate structures involved in retinal axon targeting. *Development,* 129, 61-70.

Ishihara, M. (1994) Structural requirements in heparin for binding and activation of FGF-1 and FGF-4 are different from that for FGF-2. *Glycobiology,* 4, 817-24.

Ishihara, M.; Tyrrell, D. J.; Stauber, G. B.; Brown, S.; Cousens, L. S. and Stack, R. J. (1993) Preparation of affinity-fractionated, heparin-derived oligosaccharides and their effects on selected biological activities mediated by basic fibroblast growth factor. *J Biol Chem,* 268, 4675-83.

Itoh, A.; Miyabayashi, T.; Ohno, M. and Sakano, S. (1998) Cloning and expressions of three mammalian homologues of Drosophila slit suggest possible roles for Slit in the formation and maintenance of the nervous system. *Brain Res Mol Brain Res,* 62, 175-86.

Itoh, N. and Konishi, M. (2007) The zebrafish fgf family. *Zebrafish,* 4, 179-86.

Itoh, N. and Ornitz, D. M. (2004) Evolution of the Fgf and Fgfr gene families. *Trends Genet,* 20, 563-9.

Ivins, J. K.; Litwack, E. D.; Kumbasar, A.; Stipp, C. S. and Lander, A. D. (1997) Cerebroglycan, a developmentally regulated cell-surface heparan sulfate proteoglycan, is expressed on developing axons and growth cones. *Dev Biol,* 184, 320-32.

Jacobsson, I.; Lindahl, U.; Jensen, J. W.; Roden, L.; Prihar, H. and Feingold, D. S. (1984) Biosynthesis of heparin. Substrate specificity of heparosan N-sulfate D-glucuronosyl 5-epimerase. *J Biol Chem,* 259, 1056-63.

Jairajpuri, M. A.; Lu, A.; Desai, U.; Olson, S. T.; Bjork, I. and Bock, S. C. (2003) Antithrombin III phenylalanines 122 and 121 contribute to its high affinity for heparin and its conformational activation. *J Biol Chem,* 278, 15941-50.

Jaseja, M.; Rej, R.; Francois, S. and Perlin, A. S. (1989) Novel regio- and stereoselective modifications of heparin in alkaline solution. Nuclear magnetic resonance spectroscopic evidence. *can. J. Chem.* , 67,, 1449-1456.

Jastrebova, N.; Vanwildemeersch, M.; Rapraeger, A. C.; Gimenez-Gallego, G.; Lindahl, U. and Spillmann, D. (2006) Heparan sulfate-related oligosaccharides in ternary complex formation with fibroblast growth factors 1 and 2 and their receptors. *J Biol Chem,* 281, 26884-92.

Jemth, P.; Kreuger, J.; Kusche-Gullberg, M.; Sturiale, L.; Gimenez-Gallego, G. and Lindahl, U. (2002) Biosynthetic oligosaccharide libraries for identification of protein-binding heparan sulfate motifs. Exploring the structural diversity by screening for fibroblast growth factor (FGF)1 and FGF2 binding. *J Biol Chem,* 277, 30567-73.

Jeong, J.; Han, I.; Lim, Y.; Kim, J.; Park, I.; Woods, A.; Couchman, J. R. and Oh, E. S. (2001) Rat embryo fibroblasts require both the cell-binding and the heparin-binding domains of fibronectin for survival. *Biochem J,* 356, 531-7.

Johnson, D. E. and Williams, L. T. (1993) Structural and functional diversity in the FGF receptor multigene family. *Adv Cancer Res,* 60, 1-41.

Johnson, Z.; Kosco-Vilbois, M. H.; Herren, S.; Cirillo, R.; Muzio, V.; Zaratin, P.; Carbonatto, M.; Mack, M.; Smailbegovic, A.; Rose, M.; Lever, R.; Page, C.; Wells, T. N. and Proudfoot, A. E. (2004) Interference with heparin binding and oligomerization creates a novel anti-inflammatory strategy targeting the chemokine system. *J Immunol,* 173, 5776-85.

Jorpes, J. E. (1959) Heparin: a mucopolysaccharide and an active antithrombotic drug. *Circulation,* 19, 87-91.

Juhasz, P. and Biemann, K. (1994) Mass spectrometric molecular-weight determination of highly acidic compounds of biological significance via their complexes with basic polypeptides. *Proc Natl Acad Sci U S A,* 91, 4333-7.

Juhasz, P. and Biemann, K. (1995) Utility of non-covalent complexes in the matrix-assisted laser desorption ionization mass spectrometry of heparin-derived oligosaccharides. *Carbohydr Res,* 270, 131-47.

Kaidonis, X.; Liaw, W. C.; Roberts, A. D.; Ly, M.; Anson, D. and Byers, S. (2010) Gene silencing of EXTL2 and EXTL3 as a substrate deprivation therapy for heparan sulphate storing mucopolysaccharidoses. *Eur J Hum Genet,* 18, 194-9.

Kaksonen, M.; Pavlov, I.; Voikar, V.; Lauri, S. E.; Hienola, A.; Riekki, R.; Lakso, M.; Taira, T. and Rauvala, H. (2002) Syndecan-3-deficient mice exhibit enhanced LTP and impaired hippocampus-dependent memory. *Mol Cell Neurosci,* 21, 158-72.

Kamimura, K.; Koyama, T.; Habuchi, H.; Ueda, R.; Masu, M.; Kimata, K. and Nakato, H. (2006) Specific and flexible roles of heparan sulfate modifications in Drosophila FGF signaling. *J Cell Biol,* 174, 773-8.

Kan, M.; Wang, F.; Xu, J.; Crabb, J. W.; Hou, J. and Mckeehan, W. L. (1993) An essential heparin-binding domain in the fibroblast growth factor receptor kinase. *Science,* 259, 1918-21.

Kan, M.; Wu, X.; Wang, F. and Mckeehan, W. L. (1999) Specificity for fibroblast growth factors determined by heparan sulfate in a binary complex with the receptor kinase. *J Biol Chem,* 274, 15947-52.

Kapfhammer, J. P.; Xu, H. and Raper, J. A. (2007) The detection and quantification of growth cone collapsing activities. *Nat Protoc,* 2, 2005-11.

Kariya, Y.; Kyogashima, M.; Suzuki, K.; Isomura, T.; Sakamoto, T.; Horie, K.; Ishihara, M.; Takano, R.; Kamei, K. and Hara, S. (2000) Preparation of completely 6-O-desulfated heparin and its ability to enhance activity of basic fibroblast growth factor. *J Biol Chem,* 275, 25949-58.

Karst, N. A.; Islam, T. F. and Linhardt, R. J. (2003) Sulfo-protected hexosamine monosaccharides: potentially versatile building blocks for glycosaminoglycan synthesis. *Org Lett,* 5, 4839-42.

Karst, N. A. and Linhardt, R. J. (2003) Recent chemical and enzymatic approaches to the synthesis of glycosaminoglycan oligosaccharides. *Curr Med Chem,* 10, 1993-2031.

Kato, M.; Wang, H.; Bernfield, M.; Gallagher, J. T. and Turnbull, J. E. (1994) Cell surface syndecan-1 on distinct cell types differs in fine structure and ligand binding of its heparan sulfate chains. *J Biol Chem,* 269, 18881-90.

Katz, M.; Amit, I. and Yarden, Y. (2007) Regulation of MAPKs by growth factors and receptor tyrosine kinases. *Biochim Biophys Acta,* 1773, 1161-76.

Keleman, K.; Rajagopalan, S.; Cleppien, D.; Teis, D.; Paiha, K.; Huber, L. A.; Technau, G. M. and Dickson, B. J. (2002) Comm sorts robo to control axon guidance at the Drosophila midline. *Cell,* 110, 415-27.

Kett, W. C.; Osmond, R. I.; Moe, L.; Skett, S. E.; Kinnear, B. F. and Coombe, D. R. (2003) Avidin is a heparin-binding protein. Affinity, specificity and structural analysis. *Biochim Biophys Acta,* 1620, 225-34.

Kim, B. T.; Kitagawa, H.; Tamura, J.; Saito, T.; Kusche-Gullberg, M.; Lindahl, U. and Sugahara, K. (2001) Human tumor suppressor EXT gene family members EXTL1 and EXTL3 encode alpha 1,4- N-acetylglucosaminyltransferases that likely are involved in heparan sulfate/ heparin biosynthesis. *Proc Natl Acad Sci U S A,* 98, 7176-81.

Kim, S. H.; Hu, Y.; Cadman, S. and Bouloux, P. (2008) Diversity in fibroblast growth factor receptor 1 regulation: learning from the investigation of Kallmann syndrome. *J Neuroendocrinol,* 20, 141-63.

Kiselyov, V. V.; Soroka, V.; Berezin, V. and Bock, E. (2005) Structural biology of NCAM homophilic binding and activation of FGFR. *J Neurochem,* 94, 1169-79.

Kjellen, L. (2003) Glucosaminyl N-deacetylase/N-sulphotransferases in heparan sulphate biosynthesis and biology. *Biochem Soc Trans,* 31, 340-2.

Kjellen, L. and Lindahl, U. (1991) Proteoglycans: structures and interactions. *Annu Rev Biochem,* 60, 443-75.

Knox, S. M. and Whitelock, J. M. (2006) Perlecan: how does one molecule do so many things? *Cell Mol Life Sci,* 63, 2435-45.

Kobayashi, M.; Sugumaran, G.; Liu, J.; Shworak, N. W.; Silbert, J. E. and Rosenberg, R. D. (1999) Molecular cloning and characterization of a human uronyl 2-sulfotransferase that sulfates iduronyl and glucuronyl residues in dermatan/chondroitin sulfate. *J Biol Chem,* 274, 10474-80.

Kobayashi, S.; Morimoto, K.; Shimizu, T.; Takahashi, M.; Kurosawa, H. and Shirasawa, T. (2000) Association of EXT1 and EXT2, hereditary multiple exostoses gene products, in Golgi apparatus. *Biochem Biophys Res Commun,* 268, 860-7.

Kobe, B. and Kajava, A. V. (2001) The leucine-rich repeat as a protein recognition motif. *Curr Opin Struct Biol,* 11, 725-32.

Kochoyan, A.; Poulsen, F. M.; Berezin, V.; Bock, E. and Kiselyov, V. V. (2008) Structural basis for the activation of FGFR by NCAM. *Protein Sci,* 17, 1698-705.

Koenig, A.; Norgard-Sumnicht, K.; Linhardt, R. and Varki, A. (1998) Differential interactions of heparin and heparan sulfate glycosaminoglycans with the selectins. Implications for the use of unfractionated and low molecular weight heparins as therapeutic agents. *J Clin Invest,* 101, 877-89.

Kolset, S. O.; Prydz, K. and Pejler, G. (2004) Intracellular proteoglycans. *Biochem J,* 379, 217-27.

Kolset, S. O. and Tveit, H. (2008) Serglycin--structure and biology. *Cell Mol Life Sci,* 65, 1073-85.

Konig, S. and Leary, J. A. (1998) Evidence for linkage position determination in cobalt coordinated pentasaccharides using ion trap mass spectrometry. *J Am Soc Mass Spectrom,* 9, 1125-34.

Koshida, S.; Suda, Y.; Sobel, M.; Ormsby, J. and Kusumoto, S. (1999) Synthesis of heparin partial structures and their binding activities to platelets. *Bioorg Med Chem Lett,* 9, 3127-32.

Kovensky, J.; Duchaussoy, P.; Bono, F.; Salmivirta, M.; Sizun, P.; Herbert, J. M.; Petitou, M. and Sinay, P. (1999) A synthetic heparan sulfate pentasaccharide, exclusively containing L-iduronic acid, displays higher affinity for FGF-2 than its D-glucuronic acid-containing isomers. *Bioorg Med Chem,* 7, 1567-80.

Koziel, L.; Kunath, M.; Kelly, O. G. and Vortkamp, A. (2004) Ext1-dependent heparan sulfate regulates the range of Ihh signaling during endochondral ossification. *Dev Cell,* 6, 801-13.

Kreuger, J.; Jemth, P.; Sanders-Lindberg, E.; Eliahu, L.; Ron, D.; Basilico, C.; Salmivirta, M. and Lindahl, U. (2005) Fibroblast growth factors share binding sites in heparan sulphate. *Biochem J,* 389, 145-50.

Kreuger, J.; Lindahl, U. and Jemth, P. (2003) Nitrocellulose filter binding to assess binding of glycosaminoglycans to proteins. *Methods Enzymol,* 363, 327-39.

Kreuger, J.; Matsumoto, T.; Vanwildemeersch, M.; Sasaki, T.; Timpl, R.; Claesson-Welsh, L.; Spillmann, D. and Lindahl, U. (2002) Role of heparan sulfate domain organization in endostatin inhibition of endothelial cell function. *Embo J,* 21, 6303-11.

Kreuger, J.; Prydz, K.; Pettersson, R. F.; Lindahl, U. and Salmivirta, M. (1999) Characterization of fibroblast growth factor 1 binding heparan sulfate domain. *Glycobiology,* 9, 723-9.

Kreuger, J.; Salmivirta, M.; Sturiale, L.; Gimenez-Gallego, G. and Lindahl, U. (2001) Sequence analysis of heparan sulfate epitopes with graded affinities for fibroblast growth factors 1 and 2. *J Biol Chem,* 276, 30744-52.

Kreuger, J.; Spillmann, D.; Li, J. P. and Lindahl, U. (2006) Interactions between heparan sulfate and proteins: the concept of specificity. *J Cell Biol,* 174, 323-7.

Kroger, S. and Schroder, J. E. (2002) Agrin in the developing CNS: new roles for a synapse organizer. *News Physiol Sci,* 17, 207-12.

Kuberan, B.; Beeler, D. L.; Lech, M.; Wu, Z. L. and Rosenberg, R. D. (2003) Chemoenzymatic synthesis of classical and non-classical anticoagulant heparan sulfate polysaccharides. *J Biol Chem,* 278, 52613-21.

Kuberan, B.; Lech, M.; Zhang, L.; Wu, Z. L.; Beeler, D. L. and Rosenberg, R. D. (2002) Analysis of heparan sulfate oligosaccharides with ion pair-reverse phase capillary high performance liquid chromatography-microelectrospray ionization time-of-flight mass spectrometry. *J Am Chem Soc,* 124, 8707-18.

Kuschert, G. S.; Coulin, F.; Power, C. A.; Proudfoot, A. E.; Hubbard, R. E.; Hoogewerf, A. J. and Wells, T. N. (1999) Glycosaminoglycans interact selectively with chemokines and modulate receptor binding and cellular responses. *Biochemistry,* 38, 12959-68.

Laguri, C.; Sadir, R.; Rueda, P.; Baleux, F.; Gans, P.; Arenzana-Seisdedos, F. and Lortat-Jacob, H. (2007) The novel CXCL12gamma isoform encodes an unstructured cationic domain which regulates bioactivity and interaction with both glycosaminoglycans and CXCR4. *PLoS One,* 2, e1110.

Lamanna, W. C.; Frese, M. A.; Balleininger, M. and Dierks, T. (2008) Sulf loss influences N-, 2-O-, and 6-O-sulfation of multiple heparan sulfate proteoglycans and modulates fibroblast growth factor signaling. *J Biol Chem,* 283, 27724-35.

Lamanna, W. C.; Kalus, I.; Padva, M.; Baldwin, R. J.; Merry, C. L. and Dierks, T. (2007) The heparanome--the enigma of encoding and decoding heparan sulfate sulfation. *J Biotechnol,* 129, 290-307.

Larnkjaer, A.; Hansen, S. H. and Ostergaard, P. B. (1995) Isolation and characterization of hexasaccharides derived from heparin. Analysis by HPLC and elucidation of structure by 1H NMR. *Carbohydr Res,* 266, 37-52.

Lau, E. K.; Paavola, C. D.; Johnson, Z.; Gaudry, J. P.; Geretti, E.; Borlat, F.; Kungl, A. J.; Proudfoot, A. E. and Handel, T. M. (2004) Identification of the glycosaminoglycan binding site of the CC chemokine, MCP-1: implications for structure and function in vivo. *J Biol Chem,* 279, 22294-305.

Ledin, J.; Staatz, W.; Li, J. P.; Gotte, M.; Selleck, S.; Kjellen, L. and Spillmann, D. (2004) Heparan sulfate structure in mice with genetically modified heparan sulfate production. *J Biol Chem,* 279, 42732-41.

Lee, M. K. and Lander, A. D. (1991) Analysis of affinity and structural selectivity in the binding of proteins to glycosaminoglycans: development of a sensitive electrophoretic approach. *Proc Natl Acad Sci U S A,* 88, 2768-72.

Li, J.; Hagner-Mcwhirter, A.; Kjellen, L.; Palgi, J.; Jalkanen, M. and Lindahl, U. (1997) Biosynthesis of heparin/heparan sulfate. cDNA cloning and expression of D-glucuronyl C5-epimerase from bovine lung. *J Biol Chem,* 272, 28158-63.

Li, W.; Johnson, D. J.; Esmon, C. T. and Huntington, J. A. (2004) Structure of the antithrombin-thrombin-heparin ternary complex reveals the antithrombotic mechanism of heparin. *Nat Struct Mol Biol,* 11, 857-62.

Lin, X. (2004) Functions of heparan sulfate proteoglycans in cell signaling during development. *Development,* 131, 6009-21.

Lind, T.; Tufaro, F.; Mccormick, C.; Lindahl, U. and Lidholt, K. (1998) The putative tumor suppressors EXT1 and EXT2 are glycosyltransferases required for the biosynthesis of heparan sulfate. *J Biol Chem,* 273, 26265-8.

Lindahl, B.; Eriksson, L. and Lindahl, U. (1995) Structure of heparan sulphate from human brain, with special regard to Alzheimer's disease. *Biochem J,* 306 (Pt 1), 177-84.

Lindahl, U.; Kusche-Gullberg, M. and Kjellen, L. (1998) Regulated diversity of heparan sulfate. *J Biol Chem,* 273, 24979-82.

Lindahl, U. and Li, J. P. (2009) Interactions between heparan sulfate and proteins-design and functional implications. *Int Rev Cell Mol Biol,* 276, 105-59.

Lindahl, U.; Lidholt, K.; Spillmann, D. and Kjellen, L. (1994) More to "heparin" than anticoagulation. *Thromb Res,* 75, 1-32.

Linhardt, R. J. (2003) 2003 Claude S. Hudson Award address in carbohydrate chemistry. Heparin: structure and activity. *J Med Chem,* 46, 2551-64.

Linhardt, R. J.; Gu, K. N.; Loganathan, D. and Carter, S. R. (1989) Analysis of glycosaminoglycan-derived oligosaccharides using reversed-phase ion-pairing and ion-exchange chromatography with suppressed conductivity detection. *Anal Biochem,* 181, 288-96.

Linhardt, R. J.; Rice, K. G.; Kim, Y. S.; Lohse, D. L.; Wang, H. M. and Loganathan, D. (1988) Mapping and quantification of the major oligosaccharide components of heparin. *Biochem J,* 254, 781-7.

Linhardt, R. J.; Rice, K. G.; Merchant, Z. M.; Kim, Y. S. and Lohse, D. L. (1986) Structure and activity of a unique heparin-derived hexasaccharide. *J Biol Chem,* 261, 14448-54.

Linhardt, R. J.; Turnbull, J. E.; Wang, H. M.; Loganathan, D. and Gallagher, J. T. (1990) Examination of the substrate specificity of heparin and heparan sulfate lyases. *Biochemistry,* 29, 2611-7.

Little, M.; Rumballe, B.; Georgas, K.; Yamada, T. and Teasdale, R. D. (2002) Conserved modularity and potential for alternate splicing in mouse and human Slit genes. *Int J Dev Biol,* 46, 385-91.

Litwack, E. D.; Ivins, J. K.; Kumbasar, A.; Paine-Saunders, S.; Stipp, C. S. and Lander, A. D. (1998) Expression of the heparan sulfate proteoglycan glypican-1 in the developing rodent. *Dev Dyn,* 211, 72-87.

Liu, J.; Shriver, Z.; Blaiklock, P.; Yoshida, K.; Sasisekharan, R. and Rosenberg, R. D. (1999) Heparan sulfate D-glucosaminyl 3-O-sulfotransferase-3A sulfates N-unsubstituted glucosamine residues. *J Biol Chem,* 274, 38155-62.

Liu, R.; Xu, Y.; Chen, M.; Weiwer, M.; Zhou, X.; Bridges, A. S.; Deangelis, P. L.; Zhang, Q.; Linhardt, R. J. and Liu, J. (2010) Chemoenzymatic design of heparan sulfate oligosaccharides. *J Biol Chem.*

Liu, Z. and Perlin, A. S. (1992) Adverse effects of alkali and acid on the anticoagulant potency of heparin, evaluated with methyl 2-deoxy-2-sulfamino-alpha-D-glucopyranoside 3-sulfate as a model compound. *Carbohydr Res,* 228, 29-36.

Lohman, G. J. and Seeberger, P. H. (2004) A stereochemical surprise at the late stage of the synthesis of fully N-differentiated heparin oligosaccharides containing amino, acetamido, and N-sulfonate groups. *J Org Chem,* 69, 4081-93.

Loo, B. M.; Kreuger, J.; Jalkanen, M.; Lindahl, U. and Salmivirta, M. (2001) Binding of heparin/heparan sulfate to fibroblast growth factor receptor 4. *J Biol Chem,* 276, 16868-76.

Lortat-Jacob, H. (2009) The molecular basis and functional implications of chemokine interactions with heparan sulphate. *Curr Opin Struct Biol,* 19, 543-8.

Lortat-Jacob, H.; Turnbull, J. E. and Grimaud, J. A. (1995) Molecular organization of the interferon gamma-binding domain in heparan sulphate. *Biochem J,* 310 (Pt 2), 497-505.

Lyon, M.; Deakin, J. A. and Gallagher, J. T. (1994) Liver heparan sulfate structure. A novel molecular design. *J Biol Chem,* 269, 11208-15.

Lyon, M.; Deakin, J. A.; Lietha, D.; Gherardi, E. and Gallagher, J. T. (2004) The interactions of hepatocyte growth factor/scatter factor and its NK1 and NK2 variants with glycosaminoglycans using a modified gel mobility shift assay. Elucidation of the minimal size of binding and activatory oligosaccharides. *J Biol Chem,* 279, 43560-7.

Lyon, M. and Gallagher, J. T. (1994) Hepatocyte growth factor/scatter factor: a heparan sulphate-binding pleiotropic growth factor. *Biochem Soc Trans,* 22, 365-70.

Lyon, M.; Rushton, G. and Gallagher, J. T. (1997) The interaction of the transforming growth factor-betas with heparin/heparan sulfate is isoform-specific. *J Biol Chem,* 272, 18000-6.

Mabie, P. C.; Mehler, M. F.; Marmur, R.; Papavasiliou, A.; Song, Q. and Kessler, J. A. (1997) Bone morphogenetic proteins induce astroglial differentiation of oligodendroglial-astroglial progenitor cells. *J Neurosci,* 17, 4112-20.

Maccarana, M.; Casu, B. and Lindahl, U. (1993) Minimal sequence in heparin/heparan sulfate required for binding of basic fibroblast growth factor. *J Biol Chem,* 268, 23898-905.

Maccarana, M.; Sakura, Y.; Tawada, A.; Yoshida, K. and Lindahl, U. (1996) Domain structure of heparan sulfates from bovine organs. *J Biol Chem,* 271, 17804-10.

Mach, H.; Volkin, D. B.; Burke, C. J.; Middaugh, C. R.; Linhardt, R. J.; Fromm, J. R.; Loganathan, D. and Mattsson, L. (1993) Nature of the interaction of heparin with acidic fibroblast growth factor. *Biochemistry,* 32, 5480-9.

Mahley, R. W. and Ji, Z. S. (1999) Remnant lipoprotein metabolism: key pathways involving cell-surface heparan sulfate proteoglycans and apolipoprotein E. *J Lipid Res,* 40, 1-16.

Mahoney, D. J.; Whittle, J. D.; Milner, C. M.; Clark, S. J.; Mulloy, B.; Buttle, D. J.; Jones, G. C.; Day, A. J. and Short, R. D. (2004) A method for the non-covalent immobilization of heparin to surfaces. *Anal Biochem,* 330, 123-9.

Marcum, J. A. and Rosenberg, R. D. (1987) Anticoagulantly active heparan sulfate proteoglycan and the vascular endothelium. *Semin Thromb Hemost,* 13, 464-74.

Margalit, H.; Fischer, N. and Ben-Sasson, S. A. (1993) Comparative analysis of structurally defined heparin binding sequences reveals a distinct spatial distribution of basic residues. *J Biol Chem,* 268, 19228-31.

Marneros, A. G. and Olsen, B. R. (2005) Physiological role of collagen XVIII and endostatin. *Faseb J,* 19, 716-28.

Mason, I. (2007) Initiation to end point: the multiple roles of fibroblast growth factors in neural development. *Nat Rev Neurosci,* 8, 583-96.

Mccaffrey, T. A.; Falcone, D. J.; Brayton, C. F.; Agarwal, L. A.; Welt, F. G. and Weksler, B. B. (1989) Transforming growth factor-beta activity is potentiated by heparin via dissociation of the transforming growth factor-beta/alpha 2-macroglobulin inactive complex. *J Cell Biol,* 109, 441-8.

Mccarthy, T. L.; Centrella, M. and Canalis, E. (1989) Effects of fibroblast growth factors on deoxyribonucleic acid and collagen synthesis in rat parietal bone cells. *Endocrinology,* 125, 2118-26.

Mcquade, K. J.; Beauvais, D. M.; Burbach, B. J. and Rapraeger, A. C. (2006) Syndecan-1 regulates alphavbeta5 integrin activity in B82L fibroblasts. *J Cell Sci,* 119, 2445-56.

Mei, C.; Mao, Z.; Shen, X.; Wang, W.; Dai, B.; Tang, B.; Wu, Y.; Cao, Y.; Zhang, S.; Zhao, H. and Sun, T. (2005) Role of keratinocyte growth factor in the pathogenesis of autosomal dominant polycystic kidney disease. *Nephrol Dial Transplant,* 20, 2368-75.

Merry, C. L.; Bullock, S. L.; Swan, D. C.; Backen, A. C.; Lyon, M.; Beddington, R. S.; Wilson, V. A. and Gallagher, J. T. (2001) The molecular phenotype of heparan sulfate in the Hs2st-/- mutant mouse. *J Biol Chem,* 276, 35429-34.

Merry, C. L.; Lyon, M.; Deakin, J. A.; Hopwood, J. J. and Gallagher, J. T. (1999) Highly sensitive sequencing of the sulfated domains of heparan sulfate. *J Biol Chem,* 274, 18455-62.

Meyers, E. N.; Lewandoski, M. and Martin, G. R. (1998) An Fgf8 mutant allelic series generated by Cre- and Flp-mediated recombination. *Nat Genet,* 18, 136-41.

Mitsi, M.; Forsten-Williams, K.; Gopalakrishnan, M. and Nugent, M. A. (2008) A catalytic role of heparin within the extracellular matrix. *J Biol Chem,* 283, 34796-807.

Mobli, M.; Nilsson, M. and Almond, A. (2008) The structural plasticity of heparan sulfate NA-domains and hence their role in mediating multivalent interactions is confirmed by high-accuracy (15)N-NMR relaxation studies. *Glycoconj J,* 25, 401-14.

Mongiat, M.; Taylor, K.; Otto, J.; Aho, S.; Uitto, J.; Whitelock, J. M. and Iozzo, R. V. (2000) The protein core of the proteoglycan perlecan binds specifically to fibroblast growth factor-7. *J Biol Chem,* 275, 7095-100.

Morlot, C.; Thielens, N. M.; Ravelli, R. B.; Hemrika, W.; Romijn, R. A.; Gros, P.; Cusack, S. and Mccarthy, A. A. (2007) Structural insights into the Slit-Robo complex. *Proc Natl Acad Sci U S A,* 104, 14923-8.

Mourier, P. A. and Viskov, C. (2004) Chromatographic analysis and sequencing approach of heparin oligosaccharides using cetyltrimethylammonium dynamically coated stationary phases. *Anal Biochem,* 332, 299-313.

Mulloy, B. and Forster, M. J. (2000) Conformation and dynamics of heparin and heparan sulfate. *Glycobiology,* 10, 1147-56.

Mulloy, B.; Forster, M. J.; Jones, C. and Davies, D. B. (1993) N.m.r. and molecular-modelling studies of the solution conformation of heparin. *Biochem J,* 293 (Pt 3), 849-58.

Murakami, M.; Elfenbein, A. and Simons, M. (2008) Non-canonical fibroblast growth factor signalling in angiogenesis. *Cardiovasc Res,* 78, 223-31.

Murphy, K. J.; Mclay, N. and Pye, D. A. (2008) Structural studies of heparan sulfate hexasaccharides: new insights into iduronate conformational behavior. *J Am Chem Soc,* 130, 12435-44.

Murphy, K. J.; Merry, C. L.; Lyon, M.; Thompson, J. E.; Roberts, I. S. and Gallagher, J. T. (2004) A new model for the domain structure of heparan sulfate based on the novel specificity of K5 lyase. *J Biol Chem,* 279, 27239-45.

Naggar, E. F.; Costello, C. E. and Zaia, J. (2004) Competing fragmentation processes in tandem mass spectra of heparin-like glycosaminoglycans. *J Am Soc Mass Spectrom,* 15, 1534-44.

Najjam, S.; Gibbs, R. V.; Gordon, M. Y. and Rider, C. C. (1997) The binding of interleukin 2 to heparin revealed by a novel ELISA method. *Biochem Soc Trans,* 25, 3S.

Naka, D.; Ishii, T.; Shimomura, T.; Hishida, T. and Hara, H. (1993) Heparin modulates the receptor-binding and mitogenic activity of hepatocyte growth factor on hepatocytes. *Exp Cell Res,* 209, 317-24.

Nakato, H. and Kimata, K. (2002) Heparan sulfate fine structure and specificity of proteoglycan functions. *Biochim Biophys Acta,* 1573, 312-8.

Neilson, K. M. and Friesel, R. (1996) Ligand-independent activation of fibroblast growth factor receptors by point mutations in the extracellular, transmembrane, and kinase domains. *J Biol Chem,* 271, 25049-57.

Neufeld, G. and Gospodarowicz, D. (1985) The identification and partial characterization of the fibroblast growth factor receptor of baby hamster kidney cells. *J Biol Chem,* 260, 13860-8.

Nguyen-Ba-Charvet, K. T.; Plump, A. S.; Tessier-Lavigne, M. and Chedotal, A. (2002) Slit1 and slit2 proteins control the development of the lateral olfactory tract. *J Neurosci,* 22, 5473-80.

Nguyen Ba-Charvet, K. T.; Brose, K.; Ma, L.; Wang, K. H.; Marillat, V.; Sotelo, C.; Tessier-Lavigne, M. and Chedotal, A. (2001) Diversity and specificity of actions of Slit2 proteolytic fragments in axon guidance. *J Neurosci,* 21, 4281-9.

Niclou, S. P.; Jia, L. and Raper, J. A. (2000) Slit2 is a repellent for retinal ganglion cell axons. *J Neurosci,* 20, 4962-74.

Norgard-Sumnicht, K. and Varki, A. (1995) Endothelial heparan sulfate proteoglycans that bind to L-selectin have glucosamine residues with unsubstituted amino groups. *J Biol Chem,* 270, 12012-24.

Noti, C.; De Paz, J. L.; Polito, L. and Seeberger, P. H. (2006) Preparation and use of microarrays containing synthetic heparin oligosaccharides for the rapid analysis of heparin-protein interactions. *Chemistry,* 12, 8664-86.

Noti, C. and Seeberger, P. H. (2005) Chemical approaches to define the structure-activity relationship of heparin-like glycosaminoglycans. *Chem Biol,* 12, 731-56.

Olson, S. T. and Bjork, I. (1992) Role of protein conformational changes, surface approximation and protein cofactors in heparin-accelerated antithrombin-proteinase reactions. *Adv Exp Med Biol,* 313, 155-65.

Orgueira, H. A.; Bartolozzi, A.; Schell, P.; Litjens, R. E.; Palmacci, E. R. and Seeberger, P. H. (2003) Modular synthesis of heparin oligosaccharides. *Chemistry,* 9, 140-69.

Ori, A.; Wilkinson, M. C. and Fernig, D. G. (2008) The heparanome and regulation of cell function: structures, functions and challenges. *Front Biosci,* 13, 4309-38.

Ornitz, D. M. (2000) FGFs, heparan sulfate and FGFRs: complex interactions essential for development. *Bioessays,* 22, 108-12.

Ornitz, D. M.; Herr, A. B.; Nilsson, M.; Westman, J.; Svahn, C. M. and Waksman, G. (1995) FGF binding and FGF receptor activation by synthetic heparan-derived di- and trisaccharides. *Science,* 268, 432-6.

Ornitz, D. M. and Itoh, N. (2001) Fibroblast growth factors. *Genome Biol,* 2, REVIEWS3005.

Ornitz, D. M.; Xu, J.; Colvin, J. S.; Mcewen, D. G.; Macarthur, C. A.; Coulier, F.; Gao, G. and Goldfarb, M. (1996) Receptor specificity of the fibroblast growth factor family. *J Biol Chem,* 271, 15292-7.

Ornitz, D. M.; Yayon, A.; Flanagan, J. G.; Svahn, C. M.; Levi, E. and Leder, P. (1992) Heparin is required for cell-free binding of basic fibroblast growth factor to a soluble receptor and for mitogenesis in whole cells. *Mol Cell Biol,* 12, 240-7.

Oscarsson, L. G.; Pejler, G. and Lindahl, U. (1989) Location of the antithrombin-binding sequence in the heparin chain. *J Biol Chem,* 264, 296-304.

Osmond, R. I.; Kett, W. C.; Skett, S. E. and Coombe, D. R. (2002) Protein-heparin interactions measured by BIAcore 2000 are affected by the method of heparin immobilization. *Anal Biochem,* 310, 199-207.

Ostrovsky, O.; Berman, B.; Gallagher, J.; Mulloy, B.; Fernig, D. G.; Delehedde, M. and Ron, D. (2002) Differential effects of heparin saccharides on the formation of specific fibroblast growth factor (FGF) and FGF receptor complexes. *J Biol Chem,* 277, 2444-53.

Palladino, M. A.; Morris, R. E.; Starnes, H. F. and Levinson, A. D. (1990) The transforming growth factor-betas. A new family of immunoregulatory molecules. *Ann N Y Acad Sci,* 593, 181-7.

Pallerla, S. R.; Lawrence, R.; Lewejohann, L.; Pan, Y.; Fischer, T.; Schlomann, U.; Zhang, X.; Esko, J. D. and Grobe, K. (2008) Altered heparan sulfate structure in mice with deleted NDST3 gene function. *J Biol Chem,* 283, 16885-94.

Pantoliano, M. W.; Horlick, R. A.; Springer, B. A.; Van Dyk, D. E.; Tobery, T.; Wetmore, D. R.; Lear, J. D.; Nahapetian, A. T.; Bradley, J. D. and Sisk, W. P. (1994) Multivalent ligand-receptor binding interactions in the fibroblast growth factor system produce a cooperative growth factor and heparin mechanism for receptor dimerization. *Biochemistry,* 33, 10229-48.

Partanen, A. M.; Alaluusua, S.; Miettinen, P. J.; Thesleff, I.; Tuomisto, J.; Pohjanvirta, R. and Lukinmaa, P. L. (1998) Epidermal growth factor receptor as a mediator of developmental toxicity of dioxin in mouse embryonic teeth. *Lab Invest,* 78, 1473-81.

Patey, S. J.; Edwards, E. A.; Yates, E. A. and Turnbull, J. E. (2006) Heparin derivatives as inhibitors of BACE-1, the Alzheimer's beta-secretase, with reduced activity against factor Xa and other proteases. *J Med Chem,* 49, 6129-32.

Pawson, T. (1995) Protein modules and signalling networks. *Nature,* 373, 573-80.

Pellegrini, L.; Burke, D. F.; Von Delft, F.; Mulloy, B. and Blundell, T. L. (2000) Crystal structure of fibroblast growth factor receptor ectodomain bound to ligand and heparin. *Nature,* 407, 1029-34.

Peterson, S.; Frick, A. and Liu, J. (2009) Design of biologically active heparan sulfate and heparin using an enzyme-based approach. *Nat Prod Rep,* 26, 610-27.

Petitou, M. (2003) [From heparin to synthetic antithrombotic oligosaccharides]. *Bull Acad Natl Med,* 187, 47-56; discussion 56-7.

Petitou, M.; Duchaussoy, P.; Lederman, I.; Choay, J.; Sinay, P.; Jacquinet, J. C. and Torri, G. (1986) Synthesis of heparin fragments. A chemical synthesis of the pentasaccharide O-(2-deoxy-2-sulfamido-6-O-sulfo-alpha-D-glucopyranosyl)-(1-4)-O-(beta-D-glucopyranosyluronic acid)-(1-4)-O-(2-deoxy-2-sulfamido-3,6-di-O-sulfo-alpha-D-glu copyranosyl)-(1-4)-O-(2-O-sulfo-alpha-L-idopyranosyluronic acid)-(1-4)-2-deoxy-2-sulfamido-6-O-sulfo-D-glucopyranose decasodium salt, a heparin fragment having high affinity for antithrombin III. *Carbohydr Res,* 147, 221-36.

Petitou, M.; Herault, J. P.; Bernat, A.; Driguez, P. A.; Duchaussoy, P.; Lormeau, J. C. and Herbert, J. M. (1999) [New antithrombotic oligosaccharides]. *Ann Pharm Fr,* 57, 232-9.

Petitou, M.; Imberty, A.; Duchaussoy, P.; Driguez, P. A.; Ceccato, M. L.; Gourvenec, F.; Sizun, P.; Herault, J. P.; Perez, S. and Herbert, J. M. (2001) Experimental proof for the structure of a thrombin-inhibiting heparin molecule. *Chemistry,* 7, 858-73.

Petitou, M. and Van Boeckel, C. A. (1992) Chemical synthesis of heparin fragments and analogues. *Fortschr Chem Org Naturst,* 60, 143-210.

Petitou, M. and Van Boeckel, C. A. (2004) A synthetic antithrombin III binding pentasaccharide is now a drug! What comes next? *Angew Chem Int Ed Engl,* 43, 3118-33.

Pinhal, M. A.; Smith, B.; Olson, S.; Aikawa, J.; Kimata, K. and Esko, J. D. (2001) Enzyme interactions in heparan sulfate biosynthesis: uronosyl 5-epimerase and 2-O-sulfotransferase interact in vivo. *Proc Natl Acad Sci U S A,* 98, 12984-9.

Piper, M.; Anderson, R.; Dwivedy, A.; Weinl, C.; Van Horck, F.; Leung, K. M.; Cogill, E. and Holt, C. (2006) Signaling mechanisms underlying Slit2-induced collapse of Xenopus retinal growth cones. *Neuron,* 49, 215-28.

Piper, M.; Georgas, K.; Yamada, T. and Little, M. (2000) Expression of the vertebrate Slit gene family and their putative receptors, the Robo genes, in the developing murine kidney. *Mech Dev,* 94, 213-7.

Polat, T. and Wong, C. H. (2007) Anomeric reactivity-based one-pot synthesis of heparin-like oligosaccharides. *J Am Chem Soc,* 129, 12795-800.

Ponighaus, C.; Ambrosius, M.; Casanova, J. C.; Prante, C.; Kuhn, J.; Esko, J. D.; Kleesiek, K. and Gotting, C. (2007) Human xylosyltransferase II is involved in the biosynthesis of the uniform tetrasaccharide linkage region in chondroitin sulfate and heparan sulfate proteoglycans. *J Biol Chem,* 282, 5201-6.

Popplewell, J.; Freeman, N.; Carrington, S.; Ronan, G.; Mcdonnell, C. and Ford, R. C. (2005) Quantification of the effects of melittin on liposome structure. *Biochem Soc Trans,* 33, 931-3.

Popplewell, J. F.; Swann, M. J.; Ahmed, Y.; Turnbull, J. E. and Fernig, D. G. (2009) Fabrication of carbohydrate surfaces by using nonderivatised oligosaccharides, and their application to measuring the assembly of sugar-protein complexes. *Chembiochem,* 10, 1218-26.

Powell, A. K.; Ahmed, Y. A.; Yates, E. A. and Turnbull, J. E. (2010) Generating heparan sulfate saccharide libraries for glycomics applications. *Nat Protoc,* 5, 821-33.

Powell, A. K.; Fernig, D. G. and Turnbull, J. E. (2002) Fibroblast growth factor receptors 1 and 2 interact differently with heparin/heparan sulfate. Implications for dynamic assembly of a ternary signaling complex. *J Biol Chem,* 277, 28554-63.

Powell, A. K.; Yates, E. A.; Fernig, D. G. and Turnbull, J. E. (2004) Interactions of heparin/heparan sulfate with proteins: appraisal of structural factors and experimental approaches. *Glycobiology,* 14, 17R-30R.

Powell, A. K.; Zhi, Z. L. and Turnbull, J. E. (2009) Saccharide microarrays for high-throughput interrogation of glycan-protein binding interactions. *Methods Mol Biol,* 534, 313-29.

Powers, C. J.; Mcleskey, S. W. and Wellstein, A. (2000) Fibroblast growth factors, their receptors and signaling. *Endocr Relat Cancer,* 7, 165-97.

Pratt, T.; Conway, C. D.; Tian, N. M.; Price, D. J. and Mason, J. O. (2006) Heparan sulphation patterns generated by specific heparan sulfotransferase enzymes direct distinct aspects of retinal axon guidance at the optic chiasm. *J Neurosci,* 26, 6911-23.

Presto, J.; Thuveson, M.; Carlsson, P.; Busse, M.; Wilen, M.; Eriksson, I.; Kusche-Gullberg, M. and Kjellen, L. (2008) Heparan sulfate biosynthesis enzymes EXT1 and EXT2 affect NDST1 expression and heparan sulfate sulfation. *Proc Natl Acad Sci U S A,* 105, 4751-6.

Princivalle, M.; Hasan, S.; Hosseini, G. and De Agostini, A. I. (2001) Anticoagulant heparan sulfate proteoglycans expression in the rat ovary peaks in preovulatory granulosa cells. *Glycobiology,* 11, 183-94.

Pye, D. A. and Gallagher, J. T. (1999) Monomer complexes of basic fibroblast growth factor and heparan sulfate oligosaccharides are the minimal functional unit for cell activation. *J Biol Chem,* 274, 13456-61.

Pye, D. A.; Vives, R. R.; Hyde, P. and Gallagher, J. T. (2000) Regulation of FGF-1 mitogenic activity by heparan sulfate oligosaccharides is dependent on specific structural features: differential requirements for the modulation of FGF-1 and FGF-2. *Glycobiology,* 10, 1183-92.

Pye, D. A.; Vives, R. R.; Turnbull, J. E.; Hyde, P. and Gallagher, J. T. (1998) Heparan sulfate oligosaccharides require 6-O-sulfation for promotion of basic fibroblast growth factor mitogenic activity. *J Biol Chem,* 273, 22936-42.

Raab, G. and Klagsbrun, M. (1997) Heparin-binding EGF-like growth factor. *Biochim Biophys Acta,* 1333, F179-99.

Rabenstein, D. L. (2002) Heparin and heparan sulfate: structure and function. *Nat Prod Rep,* 19, 312-31.

Rabenstein, D. L.; Robert, J. M. and Peng, J. (1995) Multinuclear magnetic resonance studies of the interaction of inorganic cations with heparin. *Carbohydr Res,* 278, 239-56.

Rademacher, T. W.; Parekh, R. B. and Dwek, R. A. (1988) Glycobiology. *Annu Rev Biochem,* 57, 785-838.

Rahmoune, H.; Chen, H. L.; Gallagher, J. T.; Rudland, P. S. and Fernig, D. G. (1998) Interaction of heparan sulfate from mammary cells with acidic fibroblast growth factor (FGF) and basic FGF. Regulation of the activity of basic FGF by high and low affinity binding sites in heparan sulfate. *J Biol Chem,* 273, 7303-10.

Rajagopalan, S.; Vivancos, V.; Nicolas, E. and Dickson, B. J. (2000) Selecting a longitudinal pathway: Robo receptors specify the lateral position of axons in the Drosophila CNS. *Cell,* 103, 1033-45.

Raper, J. A. and Kapfhammer, J. P. (1990) The enrichment of a neuronal growth cone collapsing activity from embryonic chick brain. *Neuron,* 4, 21-9.

Rapraeger, A. C.; Guimond, S.; Krufka, A. and Olwin, B. B. (1994) Regulation by heparan sulfate in fibroblast growth factor signaling. *Methods Enzymol,* 245, 219-40.

Rapraeger, A. C.; Krufka, A. and Olwin, B. B. (1991) Requirement of heparan sulfate for bFGF-mediated fibroblast growth and myoblast differentiation. *Science,* 252, 1705-8.

Rapraeger, A. C. and Ott, V. L. (1998) Molecular interactions of the syndecan core proteins. *Curr Opin Cell Biol,* 10, 620-8.

Reizes, O.; Lincecum, J.; Wang, Z.; Goldberger, O.; Huang, L.; Kaksonen, M.; Ahima, R.; Hinkes, M. T.; Barsh, G. S.; Rauvala, H. and Bernfield, M. (2001) Transgenic expression of syndecan-1 uncovers a physiological control of feeding behavior by syndecan-3. *Cell,* 106, 105-16.

Rhiner, C.; Gysi, S.; Frohli, E.; Hengartner, M. O. and Hajnal, A. (2005) Syndecan regulates cell migration and axon guidance in C. elegans. *Development,* 132, 4621-33.

Rickard, S. M.; Mummery, R. S.; Mulloy, B. and Rider, C. C. (2003) The binding of human glial cell line-derived neurotrophic factor to heparin and heparan sulfate: importance of 2-O-sulfate groups and effect on its interaction with its receptor, GFRalpha1. *Glycobiology,* 13, 419-26.

Rider, C. C. (2003) Interaction between glial-cell-line-derived neurotrophic factor (GDNF) and 2-O-sulphated heparin-related glycosaminoglycans. *Biochem Soc Trans,* 31, 337-9.

Rider, C. C. (2006) Heparin/heparan sulphate binding in the TGF-beta cytokine superfamily. *Biochem Soc Trans,* 34, 458-60.

Robinson, C. J.; Harmer, N. J.; Goodger, S. J.; Blundell, T. L. and Gallagher, J. T. (2005) Cooperative dimerization of fibroblast growth factor 1 (FGF1) upon a single heparin saccharide may drive the formation of 2:2:1 FGF1.FGFR2c.heparin ternary complexes. *J Biol Chem,* 280, 42274-82.

Robinson, C. J.; Mulloy, B.; Gallagher, J. T. and Stringer, S. E. (2006) VEGF165-binding sites within heparan sulfate encompass two highly sulfated domains and can be liberated by K5 lyase. *J Biol Chem,* 281, 1731-40.

Robinson, M. L. (2006) An essential role for FGF receptor signaling in lens development. *Semin Cell Dev Biol,* 17, 726-40.

Ronca, F.; Andersen, J. S.; Paech, V. and Margolis, R. U. (2001) Characterization of Slit protein interactions with glypican-1. *J Biol Chem,* 276, 29141-7.

Rudd, T. R.; Guimond, S. E.; Skidmore, M. A.; Duchesne, L.; Guerrini, M.; Torri, G.; Cosentino, C.; Brown, A.; Clarke, D. T.; Turnbull, J. E.; Fernig, D. G. and Yates, E. A. (2007) Influence of substitution pattern and cation binding on conformation and activity in heparin derivatives. *Glycobiology,* 17, 983-93.

Rudd, T. R.; Skidmore, M. A.; Guimond, S. E.; Guerrini, M.; Cosentino, C.; Edge, R.; Brown, A.; Clarke, D. T.; Torri, G.; Turnbull, J. E.; Nichols, R. J.; Fernig, D. G. and Yates, E. A. (2008) Site-specific interactions of copper(II) ions with heparin revealed with complementary (SRCD, NMR, FTIR and EPR) spectroscopic techniques. *Carbohydr Res,* 343, 2184-93.

Rudd, T. R.; Uniewicz, K. A.; Ori, A.; Guimond, S. E.; Skidmore, M. A.; Gaudesi, D.; Xu, R.; Turnbull, J. E.; Guerrini, M.; Torri, G.; Siligardi, G.; Wilkinson, M. C.; Fernig, D. G. and Yates, E. A. (2010) Comparable stabilisation, structural changes and activities can be induced in FGF by a variety of HS and non-GAG analogues: implications for sequence-activity relationships. *Org Biomol Chem.*

Rudd, T. R. and Yates, E. A. (2010) Conformational degeneracy restricts the effective information content of heparan sulfate. *Molecular BioSystems,* 2010 Vol.6.

Ruhrberg, C. (2003) Growing and shaping the vascular tree: multiple roles for VEGF. *Bioessays,* 25, 1052-60.

Saad, O. M.; Ebel, H.; Uchimura, K.; Rosen, S. D.; Bertozzi, C. R. and Leary, J. A. (2005) Compositional profiling of heparin/heparan sulfate using mass spectrometry: assay for specificity of a novel extracellular human endosulfatase. *Glycobiology,* 15, 818-26.

Saad, O. M. and Leary, J. A. (2004) Delineating mechanisms of dissociation for isomeric heparin disaccharides using isotope labeling and ion trap tandem mass spectrometry. *J Am Soc Mass Spectrom,* 15, 1274-86.

Saad, O. M. and Leary, J. A. (2005) Heparin sequencing using enzymatic digestion and ESI-MSn with HOST: a heparin/HS oligosaccharide sequencing tool. *Anal Chem,* 77, 5902-11.

Sabourin, C. L.; Kusewitt, D. F.; Applegate, L. A.; Budge, C. L. and Ley, R. D. (1993) Expression of fibroblast growth factors in ultraviolet radiation-induced corneal tumors and corneal tumor cell lines from Monodelphis domestica. *Mol Carcinog,* 7, 197-205.

Safaiyan, F.; Lindahl, U. and Salmivirta, M. (2000) Structural diversity of N-sulfated heparan sulfate domains: distinct modes of glucuronyl C5 epimerization, iduronic acid 2-O-sulfation, and glucosamine 6-O-sulfation. *Biochemistry,* 39, 10823-30.

Sakaguchi, K. (1992) Acidic fibroblast growth factor autocrine system as a mediator of calcium-regulated parathyroid cell growth. *J Biol Chem,* 267, 24554-62.

Salmivirta, M.; Lidholt, K. and Lindahl, U. (1996) Heparan sulfate: a piece of information. *Faseb J,* 10, 1270-9.

Sasaki, T.; Larsson, H.; Kreuger, J.; Salmivirta, M.; Claesson-Welsh, L.; Lindahl, U.; Hohenester, E. and Timpl, R. (1999) Structural basis and potential role of heparin/heparan sulfate binding to the angiogenesis inhibitor endostatin. *Embo J,* 18, 6240-8.

Schlessinger, J.; Plotnikov, A. N.; Ibrahimi, O. A.; Eliseenkova, A. V.; Yeh, B. K.; Yayon, A.; Linhardt, R. J. and Mohammadi, M. (2000) Crystal structure of a ternary FGF-FGFR-heparin complex reveals a dual role for heparin in FGFR binding and dimerization. *Mol Cell,* 6, 743-50.

Schuck, P. (1997) Use of surface plasmon resonance to probe the equilibrium and dynamic aspects of interactions between biological macromolecules. *Annu Rev Biophys Biomol Struct,* 26, 541-66.

Seeger, M.; Tear, G.; Ferres-Marco, D. and Goodman, C. S. (1993) Mutations affecting growth cone guidance in Drosophila: genes necessary for guidance toward or away from the midline. *Neuron,* 10, 409-26.

Shaklee, P. N. and Conrad, H. E. (1984) Hydrazinolysis of heparin and other glycosaminoglycans. *Biochem J,* 217, 187-97.

Shaklee, P. N. and Conrad, H. E. (1986) The disaccharides formed by deaminative cleavage of N-deacetylated glycosaminoglycans. *Biochem J,* 235, 225-36.

Shaklee, P. N.; Glaser, J. H. and Conrad, H. E. (1985) A sulfatase specific for glucuronic acid 2-sulfate residues in glycosaminoglycans. *J Biol Chem,* 260, 9146-9.

Shipp, E. L. and Hsieh-Wilson, L. C. (2007) Profiling the sulfation specificities of glycosaminoglycan interactions with growth factors and chemotactic proteins using microarrays. *Chem Biol,* 14, 195-208.

Shively, J. E. and Conrad, H. E. (1976) Formation of anhydrosugars in the chemical depolymerization of heparin. *Biochemistry,* 15, 3932-42.

Shriver, Z.; Raman, *R.; Venkataraman,* G.; Drummond, K.; Turnbull, J.; Toida, T.; Linhardt, R.; Biemann, K. and Sasisekharan, *R. (2000) Sequencing of 3-O* sulfate containing heparin decasaccharides with a partial antithrombin *III* binding site. *Proc Natl Acad Sci U S A,* 97, 10359-64.

Shukla, D.; Liu, J.; Blaiklock, P.; Shworak, N. W.; Bai, X.; Esko, J. D.; Cohen, G. H.; Eisenberg, R. J.; Rosenberg, R. D. and Spear, P. G. (1999) A novel role for 3-O-sulfated heparan sulfate in herpes simplex virus 1 entry. *Cell,* 99, 13-22.

Shworak, N. W.; Liu, J.; Petros, L. M.; Zhang, L.; Kobayashi, M.; Copeland, N. G.; Jenkins, N. A. and Rosenberg, R. D. (1999) Multiple isoforms of heparan sulfate D-glucosaminyl 3-O-sulfotransferase. Isolation, characterization, and expression of human cdnas and identification of distinct genomic loci. *J Biol Chem,* 274, 5170-84.

Simpson, J. H.; Kidd, T.; Bland, K. S. and Goodman, C. S. (2000) Short-range and long-range guidance by slit and its Robo receptors. Robo and Robo2 play distinct roles in midline guidance. *Neuron,* 28, 753-66.

Skidmore, M.; Atrih, A.; Yates, E. and Turnbull, J. E. (2009) Labelling heparan sulphate saccharides with chromophore, fluorescence and mass tags for HPLC and MS separations. *Methods Mol Biol,* 534, 157-69.

Skidmore, M. A.; Dumax-Vorzet, A. F.; Guimond, S. E.; Rudd, T. R.; Edwards, E. A.; Turnbull, J. E.; Craig, A. G. and Yates, E. A. (2008) Disruption of rosetting in Plasmodium falciparum malaria with chemically modified heparin and low molecular weight derivatives possessing reduced anticoagulant and other serine protease inhibition activities. *J Med Chem,* 51, 1453-8.

Sleeman, M.; Fraser, J.; Mcdonald, M.; Yuan, S.; White, D.; Grandison, P.; Kumble, K.; Watson, J. D. and Murison, J. G. (2001) Identification of a new fibroblast growth factor receptor, FGFR5. *Gene,* 271, 171-82.

Sobel, M.; Soler, D. F.; Kermode, J. C. and Harris, R. B. (1992) Localization and characterization of a heparin binding domain peptide of human von Willebrand factor. *J Biol Chem,* 267, 8857-62.

Song, H. K.; Lee, S. H. and Goetinck, P. F. (2004) FGF-2 signaling is sufficient to induce dermal condensations during feather development. *Dev Dyn,* 231, 741-9.

Spillmann, D. and Lindahl, U. (1994) Glycosaminoglycan-protein interactions: a question of specificity. *Current Opinion in Structural Biology,* 4, 677-682.

Spillmann, D.; Witt, D. and Lindahl, U. (1998) Defining the interleukin-8-binding domain of heparan sulfate. *J Biol Chem,* 273, 15487-93.

Springer, B. A.; Pantoliano, M. W.; Barbera, F. A.; Gunyuzlu, P. L.; Thompson, L. D.; Herblin, W. F.; Rosenfeld, S. A. and Book, G. W. (1994) Identification and concerted function of two receptor binding surfaces on basic fibroblast growth factor required for mitogenesis. *J Biol Chem,* 269, 26879-84.

Steigemann, P.; Molitor, A.; Fellert, S.; Jackle, H. and Vorbruggen, G. (2004) Heparan sulfate proteoglycan syndecan promotes axonal and myotube guidance by slit/robo signaling. *Curr Biol,* 14, 225-30.

Stepp, M. A.; Gibson, H. E.; Gala, P. H.; Iglesia, D. D.; Pajoohesh-Ganji, A.; Pal-Ghosh, S.; Brown, M.; Aquino, C.; Schwartz, A. M.; Goldberger, O.; Hinkes, M. T. and Bernfield, M. (2002) Defects in keratinocyte activation during wound healing in the syndecan-1-deficient mouse. *J Cell Sci, 115, 4517-31.*

Strader, A. D.; Reizes, O.; Woods, S. C.; Benoit, S. C. and Seeley, R. J. (2004) Mice lacking the syndecan-3 gene are resistant to diet-induced obesity. *J Clin Invest,* 114, 1354-60.

Stringer, S. E.; Forster, M. J.; Mulloy, B.; Bishop, C. R.; Graham, G. J. and Gallagher, J. T. (2002) Characterization of the binding site on heparan sulfate for macrophage inflammatory protein 1alpha. *Blood,* 100, 1543-50.

Stringer, S. E.; Mayer-Proschel, M.; Kalyani, A.; Rao, M. and Gallagher, J. T. (1999) Heparin is a unique marker of progenitors in the glial cell lineage. *J Biol Chem,* 274, 25455-60.

Suchting, S.; Heal, P.; Tahtis, K.; Stewart, L. M. and Bicknell, R. (2005) Soluble Robo4 receptor inhibits in vivo angiogenesis and endothelial cell migration. *Faseb J,* 19, 121-3.

Suda, Y.; Mori, K.; Bird, K.; Marques, D.; Ormsby, J.; Tanaka, S.; Koshida, S.; Nakamura, M.; Kusumoto, S. and Sobel, M. (1999) A novel crosslinking reagent and its application for the detection and isolation of heparin-binding protein(s) on the platelet surface. *J Biochem,* 125, 1011-5.

Sugahara, K.; Mikami, T.; Uyama, T.; Mizuguchi, S.; Nomura, K. and Kitagawa, H. (2003) Recent advances in the structural biology of chondroitin sulfate and dermatan sulfate. *Curr Opin Struct Biol,* 13, 612-20.

Suyama, K.; Shapiro, I.; Guttman, M. and Hazan, R. B. (2002) A signaling pathway leading to metastasis is controlled by N-cadherin and the FGF receptor. *Cancer Cell,* 2, 301-14.

Swann, M. J.; Peel, L. L.; Carrington, S. and Freeman, N. J. (2004) Dual-polarization interferometry: an analytical technique to measure changes in protein structure in real time, to determine the stoichiometry of binding events, and to differentiate between specific and nonspecific interactions. *Anal Biochem,* 329, 190-8.

Takahashi, I.; Noguchi, N.; Nata, K.; Yamada, S.; Kaneiwa, T.; Mizumoto, S.; Ikeda, T.; Sugihara, K.; Asano, M.; Yoshikawa, T.; Yamauchi, A.; Shervani, N. J.; Uruno, A.; Kato, I.; Unno, M.; Sugahara, K.; Takasawa, S.; Okamoto, H. and Sugawara, A. (2009) Important role of heparan sulfate in postnatal islet growth and insulin secretion. *Biochem Biophys Res Commun,* 383, 113-8.

Tanno, T.; Takenaka, S. and Tsuyama, S. (2004) Expression and function of Slit1alpha, a novel alternative splicing product for slit1. *J Biochem,* 136, 575-81.

Tekin, M.; Hismi, B. O.; Fitoz, S.; Ozdag, H.; Cengiz, F. B.; Sirmaci, A.; Aslan, I.; Inceoglu, B.; Yuksel-Konuk, E. B.; Yilmaz, S. T.; Yasun, O. and Akar, N. (2007) Homozygous mutations in fibroblast growth factor 3 are associated with a new form of syndromic deafness characterized by inner ear agenesis, microtia, and microdontia. *Am J Hum Genet,* 80, 338-44.

Ten Dam, G. B.; Van De Westerlo, E. M.; Smetsers, T. F.; Willemse, M.; Van Muijen, G. N.; Merry, C. L.; Gallagher, J. T.; Kim, Y. S. and Van Kuppevelt, T. H. (2004) Detection of 2-O-sulfated iduronate and N-acetylglucosamine units in heparan sulfate by an antibody selected against acharan sulfate (IdoA2S-GlcNAc)n. *J Biol Chem,* 279, 38346-52.

Terry, C. J.; Popplewell, J. F.; Swann, M. J.; Freeman, N. J. and Fernig, D. G. (2006) Characterisation of membrane mimetics on a dual polarisation interferometer. *Biosens Bioelectron,* 22, 627-32.

Tessier-Lavigne, M. and Goodman, C. S. (1996) The molecular biology of axon guidance. *Science,* 274, 1123-33.

Thanawiroon, C.; Rice, K. G.; Toida, T. and Linhardt, R. J. (2004) Liquid chromatography/mass spectrometry sequencing approach for highly sulfated heparin-derived oligosaccharides. *J Biol Chem,* 279, 2608-15.

Thomas, G.; Clayton, A.; Thomas, J.; Davies, M. and Steadman, R. (2003) Structural and functional changes in heparan sulfate proteoglycan expression associated with the myofibroblastic phenotype. *Am J Pathol,* 162, 977-89.

Thompson, H.; Andrews, W.; Parnavelas, J. G. and Erskine, L. (2009) Robo2 is required for Slit-mediated intraretinal axon guidance. *Dev Biol,* 335, 418-26.

Thompson, L. D.; Pantoliano, M. W. and Springer, B. A. (1994a) Energetic characterization of the basic fibroblast growth factor-heparin interaction: identification of the heparin binding domain. *Biochemistry,* 33, 3831-40.

Thompson, S. A.; Higashiyama, S.; Wood, K.; Pollitt, N. S.; Damm, D.; Mcenroe, G.; Garrick, B.; Ashton, N.; Lau, K.; Hancock, N. and Et Al. (1994b) Characterization of sequences within heparin-binding EGF-like growth factor that mediate interaction with heparin. *J Biol Chem,* 269, 2541-9.

Thompson, S. M.; Fernig, D. G.; Jesudason, E. C.; Losty, P. D.; Van De Westerlo, E. M.; Van Kuppevelt, T. H. and Turnbull, J. E. (2009) Heparan sulfate phage display antibodies identify distinct epitopes with complex binding characteristics: insights into protein binding specificities. *J Biol Chem,* 284, 35621-31.

Tissot, B.; Ceroni, A.; Powell, A. K.; Morris, H. R.; Yates, E. A.; Turnbull, J. E.; Gallagher, J. T.; Dell, A. and Haslam, S. M. (2008) Software Tool for the Structural Determination of Glycosaminoglycans by Mass Spectrometry. *Anal Chem.*

Tissot, B.; Gasiunas, N.; Powell, A. K.; Ahmed, Y.; Zhi, Z. L.; Haslam, S. M.; Morris, H. R.; Turnbull, J. E.; Gallagher, J. T. and Dell, A. (2007) Towards GAG glycomics: analysis of highly sulfated heparins by MALDI-TOF mass spectrometry. *Glycobiology,* 17, 972-82.

Tiwari, V.; Clement, C.; Duncan, M. B.; Chen, J.; Liu, J. and Shukla, D. (2004) A role for 3-O-sulfated heparan sulfate in cell fusion induced by herpes simplex virus type 1. *J Gen Virol,* 85, 805-9.

Trueb, B.; Zhuang, L.; Taeschler, S. and Wiedemann, M. (2003) Characterization of FGFRL1, a novel fibroblast growth factor (FGF) receptor preferentially expressed in skeletal tissues. *J Biol Chem,* 278, 33857-65.

Tseng, K.; Hedrick, J. L. and Lebrilla, C. B. (1999) Catalog-library approach for the rapid and sensitive structural elucidation of oligosaccharides. *Anal Chem,* 71, 3747-54.

Turnbull, J.; Powell, A. and Guimond, S. (2001) Heparan sulfate: decoding a dynamic multifunctional cell regulator. *Trends Cell Biol,* 11, 75-82.

Turnbull, J. E.; Fernig, D. G.; Ke, Y.; Wilkinson, M. C. and Gallagher, J. T. (1992) Identification of the basic fibroblast growth factor binding sequence in fibroblast heparan sulfate. *J Biol Chem,* 267, 10337-41.

Turnbull, J. E. and Field, R. A. (2007) Emerging glycomics technologies. *Nat Chem Biol,* 3, 74-7.

Turnbull, J. E. and Gallagher, J. T. (1988) Oligosaccharide mapping of heparan sulphate by polyacrylamide-gradient-gel electrophoresis and electrotransfer to nylon membrane. *Biochem J,* 251, 597-608.

Turnbull, J. E. and Gallagher, J. T. (1990) Molecular organization of heparan sulphate from human skin fibroblasts. *Biochem J,* 265, 715-24.

Turnbull, J. E. and Gallagher, J. T. (1991) Distribution of iduronate 2-sulphate residues in heparan sulphate. Evidence for an ordered polymeric structure. *Biochem J,* 273 (Pt 3), 553-9.

Turnbull, J. E.; Hopwood, J. J. and Gallagher, J. T. (1999) A strategy for rapid sequencing of heparan sulfate and heparin saccharides. *Proc Natl Acad Sci U S A,* 96, 2698-703.

Umemori, H.; Linhoff, M. W.; Ornitz, D. M. and Sanes, J. R. (2004) FGF22 and its close relatives are presynaptic organizing molecules in the mammalian brain. *Cell,* 118, 257-70.

Uniewicz, K. A. and Fernig, D. G. (2008) Neuropilins: a versatile partner of extracellular molecules that regulate development and disease. *Front Biosci,* 13, 4339-60.

Uniewicz, K. A.; Ori, A.; Xu, R.; Ahmed, Y.; Wilkinson, M. C.; Fernig, D. G. and Yates, E. A. (2010) Differential Scanning Fluorimetry Measurement of Protein Stability Changes upon Binding to Glycosaminoglycans: A Screening Test for Binding Specificity. *Anal Chem.*

Van Den Born, J.; Gunnarsson, K.; Bakker, M. A.; Kjellen, L.; Kusche-Gullberg, M.; Maccarana, M.; Berden, J. H. and Lindahl, U. (1995) Presence of N-unsubstituted glucosamine units in native heparan sulfate revealed by a monoclonal antibody. *J Biol Chem,* 270, 31303-9.

Van Kuppevelt, T. H.; Dennissen, M. A.; Van Venrooij, W. J.; Hoet, R. M. and Veerkamp, J. H. (1998) Generation and application of type-specific anti-heparan sulfate antibodies using phage display technology. Further evidence for heparan sulfate heterogeneity in the kidney. *J Biol Chem,* 273, 12960-6.

Van Swieten, J. C.; Brusse, E.; De Graaf, B. M.; Krieger, E.; Van De Graaf, R.; De Koning, I.; Maat-Kievit, A.; Leegwater, P.; Dooijes, D.; Oostra, B. A. and Heutink, P. (2003) A mutation in the fibroblast growth factor 14 gene is associated with autosomal dominant cerebellar ataxia [corrected]. *Am J Hum Genet,* 72, 191-9.

Van Zoelen, E. J. (1989) Receptor-ligand interaction: a new method for determining binding parameters without a priori assumptions on non-specific binding. *Biochem J,* 262, 549-56.

Vanpouille, C.; Deligny, A.; Delehedde, M.; Denys, A.; Melchior, A.; Lienard, X.; Lyon, M.; Mazurier, J.; Fernig, D. G. and Allain, F. (2007) The heparin/heparan sulfate sequence that interacts with cyclophilin B contains a 3-O-sulfated N-unsubstituted glucosamine residue. *J Biol Chem,* 282, 24416-29.

Vargesson, N.; Luria, V.; Messina, I.; Erskine, L. and Laufer, E. (2001) Expression patterns of Slit and Robo family members during vertebrate limb development. *Mech Dev,* 106, 175-80.

Varki, A.; Cummings, R. D.; Esko, J. D.; Freeze, H. H.; Stanley, P.; Bertozzi, C. R.; Hart, G. W. and Marth, J. D. (2009) *Essentials of Glycobiology,* New York., Cold spring Harbor Laboratory Press.

Venkataraman, G.; Sasisekharan, V.; Herr, A. B.; Ornitz, D. M.; Waksman, G.; Cooney, C. L.; Langer, R. and Sasisekharan, R. (1996) Preferential self-association of basic fibroblast growth factor is stabilized by heparin during receptor dimerization and activation. *Proc Natl Acad Sci U S A,* 93, 845-50.

Venkataraman, G.; Shriver, Z.; Raman, R. and Sasisekharan, R. (1999) Sequencing complex polysaccharides. *Science,* 286, 537-42.

Vives, R. R.; Goodger, S. and Pye, D. A. (2001) Combined strong anion-exchange HPLC and PAGE approach for the purification of heparan sulphate oligosaccharides. *Biochem J,* 354, 141-7.

Vorup-Jensen, T.; Chi, L.; Gjelstrup, L. C.; Jensen, U. B.; Jewett, C. A.; Xie, C.; Shimaoka, M.; Linhardt, R. J. and Springer, T. A. (2007) Binding between the integrin alphaXbeta2 (CD11c/CD18) and heparin. *J Biol Chem,* 282, 30869-77.

Walker, A.; Turnbull, J. E. and Gallagher, J. T. (1994) Specific heparan sulfate saccharides mediate the activity of basic fibroblast growth factor. *J Biol Chem,* 269, 931-5.

Wang, K. H.; Brose, K.; Arnott, D.; Kidd, T.; Goodman, C. S.; Henzel, W. and Tessier-Lavigne, M. (1999) Biochemical purification of a mammalian slit protein as a positive regulator of sensory axon elongation and branching. *Cell,* 96, 771-84.

Wang, Y.; Ye, X. S. and Zhang, L. H. (2007) Oligosaccharide assembly by one-pot multi-step strategy. *Org Biomol Chem,* 5, 2189-200.

Wang, Z.; Xu, Y.; Yang, B.; Tiruchinapally, G.; Sun, B.; Liu, R.; Dulaney, S.; Liu, J. and Huang, X. (2010) Preactivation-based, one-pot combinatorial synthesis of heparin-like hexasaccharides for the analysis of heparin-protein interactions. *Chemistry,* 16, 8365-75.

Warda, M.; Toida, T.; Zhang, F.; Sun, P.; Munoz, E.; Xie, J. and Linhardt, R. J. (2006) Isolation and characterization of heparan sulfate from various murine tissues. *Glycoconj J,* 23, 555-63.

Watson, D. J.; Lander, A. D. and Selkoe, D. J. (1997) Heparin-binding properties of the amyloidogenic peptides Abeta and amylin. Dependence on aggregation state and inhibition by Congo red. *J Biol Chem,* 272, 31617-24.

Wei, M.; Tai, G.; Gao, Y.; Li, N.; Huang, B.; Zhou, Y.; Hao, S. and Zeng, X. (2004) Modified heparin inhibits P-selectin-mediated cell adhesion of human colon carcinoma cells to immobilized platelets under dynamic flow conditions. *J Biol Chem,* 279, 29202-10.

Werner, S. and Grose, R. (2003) Regulation of wound healing by growth factors and cytokines. *Physiol Rev,* 83, 835-70.

Westermark, B.; Claesson-Welsh, L. and Heldin, C. H. (1990) Structural and functional aspects of platelet-derived growth factor and its receptors. *Ciba Found Symp,* 150, 6-14; discussion 14-22.

Westling, C. and Lindahl, U. (2002) Location of N-unsubstituted glucosamine residues in heparan sulfate. *J Biol Chem,* 277, 49247-55.

Whitford, K. L.; Marillat, V.; Stein, E.; Goodman, C. S.; Tessier-Lavigne, M.; Chedotal, A. and Ghosh, A. (2002) Regulation of cortical dendrite development by Slit-Robo interactions. *Neuron,* 33, 47-61.

Wilkie, A. O. (2005) Bad bones, absent smell, selfish testes: the pleiotropic consequences of human FGF receptor mutations. *Cytokine Growth Factor Rev,* 16, 187-203.

Wong, P. and Burgess, W. H. (1998) FGF2-Heparin co-crystal complex-assisted design of mutants FGF1 and FGF7 with predictable heparin affinities. *J Biol Chem,* 273, 18617-22.

Wu, X.; Kan, M.; Wang, F.; Jin, C.; Yu, C. and Mckeehan, W. L. (2001) A rare premalignant prostate tumor epithelial cell syndecan-1 forms a fibroblast growth factor-binding complex with progression-promoting ectopic fibroblast growth factor receptor 1. *Cancer Res,* 61, 5295-302.

Wu, Z. L.; Zhang, L.; Yabe, T.; Kuberan, B.; Beeler, D. L.; Love, A. and Rosenberg, R. D. (2003) The involvement of heparan sulfate (HS) in FGF1/HS/FGFR1 signaling complex. *J Biol Chem,* 278, 17121-9.

Xian, J.; Clark, K. J.; Fordham, R.; Pannell, R.; Rabbitts, T. H. and Rabbitts, P. H. (2001) Inadequate lung development and bronchial hyperplasia in mice with a targeted deletion in the Dutt1/Robo1 gene. *Proc Natl Acad Sci U S A,* 98, 15062-6.

Xie, B.; Tassi, E.; Swift, M. R.; Mcdonnell, K.; Bowden, E. T.; Wang, S.; Ueda, Y.; Tomita, Y.; Riegel, A. T. and Wellstein, A. (2006) Identification of the fibroblast growth factor (FGF)-interacting domain in a secreted FGF-binding protein by phage display. *J Biol Chem,* 281, 1137-44.

Xu, D.; Moon, A. F.; Song, D.; Pedersen, L. C. and Liu, J. (2008) Engineering sulfotransferases to modify heparan sulfate. *Nat Chem Biol,* 4, 200-2.

Xu, D.; Tiwari, V.; Xia, G.; Clement, C.; Shukla, D. and Liu, J. (2005) Characterization of heparan sulphate 3-O-sulphotransferase isoform 6 and its role in assisting the entry of herpes simplex virus type 1. *Biochem J,* 385, 451-9.

Xu, X.; Weinstein, M.; Li, C.; Naski, M.; Cohen, R. I.; Ornitz, D. M.; Leder, P. and Deng, C. (1998) Fibroblast growth factor receptor 2 (FGFR2)-mediated reciprocal regulation loop between FGF8 and FGF10 is essential for limb induction. *Development,* 125, 753-65.

Yamada, S.; Sakamoto, K.; Tsuda, H.; Yoshida, K.; Sugiura, M. and Sugahara, K. (1999) Structural studies of octasaccharides derived from the low-sulfated repeating disaccharide region and octasaccharide serines derived from the protein linkage region of porcine intestinal heparin. *Biochemistry,* 38, 838-47.

Yamashita, T.; Konishi, M.; Miyake, A.; Inui, K. and Itoh, N. (2002) Fibroblast growth factor (FGF)-23 inhibits renal phosphate reabsorption by activation of the mitogen-activated protein kinase pathway. *J Biol Chem,* 277, 28265-70.

Yang, Y. J.; Zhang, Y. L.; Li, X.; Dan, H. L.; Lai, Z. S.; Wang, J. D.; Wang, Q. Y.; Cui, H. H.; Sun, Y. and Wang, Y. D. (2003) Contribution of eIF-4E inhibition to the expression and activity of heparanase in human colon adenocarcinoma cell line: LS-174T. *World J Gastroenterol,* 9, 1707-12.

Yates, E. A.; Guimond, S. E. and Turnbull, J. E. (2004) Highly diverse heparan sulfate analogue libraries: providing access to expanded areas of sequence space for bioactivity screening. *J Med Chem,* 47, 277-80.

Yates, E. A.; Jones, M. O.; Clarke, C. E.; Powell, A. K.; Johnson, S. R.; Porch, A.; Edwards, P. P. and Turnbull, J. E. (2003) Microwave-enhanced reaction of carbohydrates with amino-derivatised labels and glass surfaces. *J. Mater. Chem.,* 13, 2061-2063.

Yates, E. A.; Mackie, W. and Lamba, D. (1995) The crystal and molecular structure of 2-sulfamino-2-deoxy-alpha-D-glucopyranose sodium salt.2H2O (glucosamine 2-sulfate). *Int J Biol Macromol,* 17, 219-26.

Yates, E. A.; Santini, F.; Guerrini, M.; Naggi, A.; Torri, G. and Casu, B. (1996) 1H and 13C NMR spectral assignments of the major sequences of twelve systematically modified heparin derivatives. *Carbohydr Res,* 294, 15-27.

Yates, E. A.; Terry, C. J.; Rees, C.; Rudd, T. R.; Duchesne, L.; Skidmore, M. A.; Levy, R.; Thanh, N. T.; Nichols, R. J.; Clarke, D. T. and Fernig, D. G. (2006) Protein-GAG interactions: new surface-based techniques, spectroscopies and nanotechnology probes. *Biochem Soc Trans,* 34, 427-30.

Yayon, A.; Klagsbrun, M.; Esko, J. D.; Leder, P. and Ornitz, D. M. (1991) Cell surface, heparin-like molecules are required for binding of basic fibroblast growth factor to its high affinity receptor. *Cell,* 64, 841-8.

Yee, K. T.; Simon, H. H.; Tessier-Lavigne, M. and O'leary, D. M. (1999) Extension of long leading processes and neuronal migration in the mammalian brain directed by the chemoattractant netrin-1. *Neuron,* 24, 607-22.

Young, H. M.; Anderson, R. B. and Anderson, C. R. (2004) Guidance cues involved in the development of the peripheral autonomic nervous system. *Auton Neurosci,* 112, 1-14.

Yu, X.; Ibrahimi, O. A.; Goetz, R.; Zhang, F.; Davis, S. I.; Garringer, H. J.; Linhardt, R. J.; Ornitz, D. M.; Mohammadi, M. and White, K. E. (2005) Analysis of the biochemical mechanisms for the endocrine actions of fibroblast growth factor-23. *Endocrinology,* 146, 4647-56.

Yuan, W.; Zhou, L.; Chen, J. H.; Wu, J. Y.; Rao, Y. and Ornitz, D. M. (1999) The mouse SLIT family: secreted ligands for ROBO expressed in patterns that suggest a role in morphogenesis and axon guidance. *Dev Biol,* 212, 290-306.

Yuguchi, Y.; Kominato, R.; Ban, T.; Urakawa, H.; Kajiwara, K.; Takano, R.; Kamei, K. and Hara, S. (2005) Structural observation of complexes of FGF-2 and regioselectively desulfated heparin in aqueous solutions. *Int J Biol Macromol,* 35, 19-25.

Yunmbam, M. K. and Wellstein, A. (2001) The bacterial polysaccharide tecogalan blocks growth of breast cancer cells in vivo. *Oncol Rep,* 8, 161-4.

Zaia, J. (2009) On-line separations combined with MS for analysis of glycosaminoglycans. *Mass Spectrom Rev,* 28, 254-72.

Zak, B. M.; Crawford, B. E. and Esko, J. D. (2002) Hereditary multiple exostoses and heparan sulfate polymerization. *Biochim Biophys Acta,* 1573, 346-55.

Zamora, P. O.; Tsang, R.; Pena, L. A.; Osaki, S. and Som, P. (2002) Local delivery of basic fibroblast growth factor (bFGF) using adsorbed silyl-heparin, benzyl-bis(dimethylsilylmethyl)oxycarbamoyl-heparin. *Bioconjug Chem,* 13, 920-6.

Zhang, F.; Zhang, Z.; Lin, X.; Beenken, A.; Eliseenkova, A. V.; Mohammadi, M. and Linhardt, R. J. (2009) Compositional analysis of heparin/heparan sulfate interacting with fibroblast growth factor.fibroblast growth factor receptor complexes. *Biochemistry,* 48, 8379-86.

Zhang, L.; Lawrence, R.; Frazier, B. A. and Esko, J. D. (2006) CHO glycosylation mutants: proteoglycans. *Methods Enzymol,* 416, 205-21.

Zhang, L.; Rice, A. B.; Adler, K.; Sannes, P.; Martin, L.; Gladwell, W.; Koo, J. S.; Gray, T. E. and Bonner, J. C. (2001a) Vanadium stimulates human bronchial epithelial cells to produce heparin-binding epidermal growth factor-like growth factor: a mitogen for lung fibroblasts. *Am J Respir Cell Mol Biol,* 24, 123-31.

Zhang, Z.; Coomans, C. and David, G. (2001b) Membrane heparan sulfate proteoglycan-supported FGF2-FGFR1 signaling: evidence in support of the "cooperative end structures" model. *J Biol Chem,* 276, 41921-9.

Zhang, Z.; Mccallum, S. A.; Xie, J.; Nieto, L.; Corzana, F.; Jimenez-Barbero, J.; Chen, M.; Liu, J. and Linhardt, R. J. (2008) Solution structures of chemoenzymatically synthesized heparin and its precursors. *J Am Chem Soc,* 130, 12998-3007.

Zhao, H.; Liu, H.; Chen, Y.; Xin, X.; Li, J.; Hou, Y.; Zhang, Z.; Zhang, X.; Xie, C.; Geng, M. and Ding, J. (2006) Oligomannurarate sulfate, a novel heparanase inhibitor simultaneously targeting basic fibroblast growth factor, combats tumor angiogenesis and metastasis. *Cancer Res,* 66, 8779-87.

Zhi, Z. L.; Laurent, N.; Powell, A. K.; Karamanska, R.; Fais, M.; Voglmeir, J.; Wright, A.; Blackburn, J. M.; Crocker, P. R.; Russell, D. A.; Flitsch, S.; Field, R. A. and Turnbull, J. E. (2008) A versatile gold surface approach for fabrication and interrogation of glycoarrays. *Chembiochem,* 9, 1568-75.

Zhi, Z. L.; Powell, A. K. and Turnbull, J. E. (2006) Fabrication of carbohydrate microarrays on gold surfaces: direct attachment of nonderivatized oligosaccharides to hydrazide-modified self-assembled monolayers. *Anal Chem,* 78, 4786-93.

Zhu, H.; Ramnarayan, K.; Menzel, P.; Miao, Y.; Zheng, J. and Mong, S. (1998) Identification of two new hydrophobic residues on basic fibroblast growth factor important for fibroblast growth factor receptor binding. *Protein Eng,* 11, 937-40.

Zimmermann, M.; Gardoni, F. and Di Luca, M. (2005) Molecular rationale for the pharmacological treatment of Alzheimer's disease. *Drugs Aging,* 22 Suppl 1, 27-37.

Zmojdzian, M.; Da Ponte, J. P. and Jagla, K. (2008) Cellular components and signals required for the cardiac outflow tract assembly in Drosophila. *Proc Natl Acad Sci U S A,* 105, 2475-80.

Zuck, B.; Goepfert, C.; Nedlin-Chittka, A.; Sohrt, K.; Voigt, K. D. and Knabbe, C. (1992) Regulation of fibroblast growth factor-like protein(s) in the androgen-responsive human prostate carcinoma cell line LNCaP. *J Steroid Biochem Mol Biol,* 41, 659-63.

Zugmaier, G.; Favoni, R.; Jaeger, R.; Rosen, N. and Knabbe, C. (1999) Polysulfated heparinoids selectively inactivate heparin-binding angiogenesis factors. Ann N Y Acad Sci, 886, 243-8.

Appendices

Appendix 1: Mass spectrometry data

2-mer

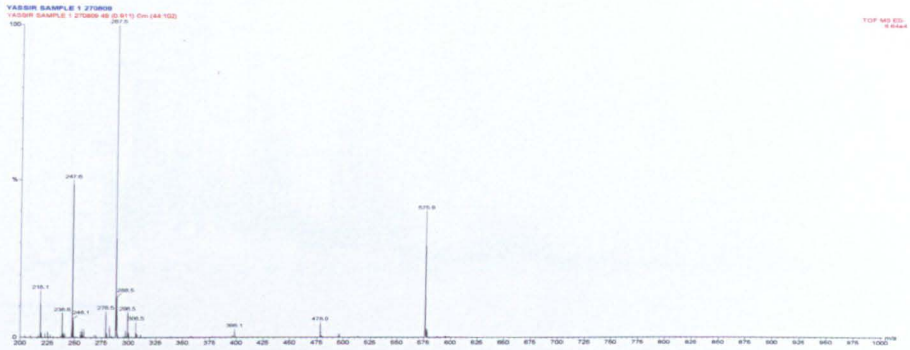

4-mer

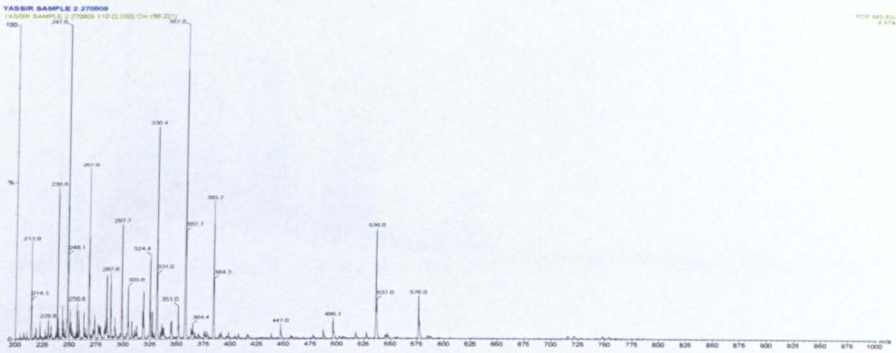

6-mer

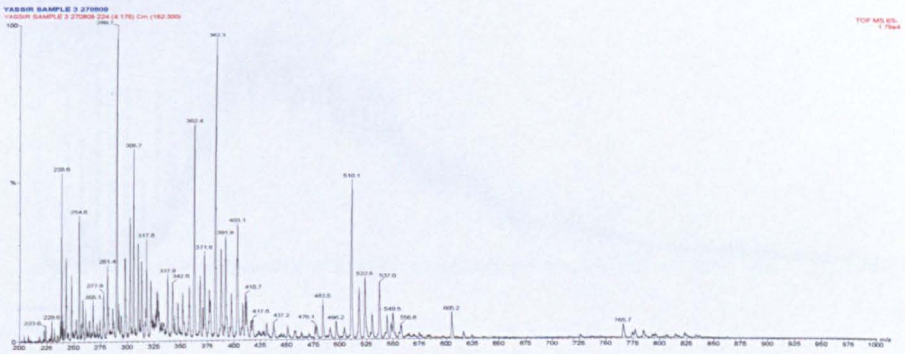

8-mer

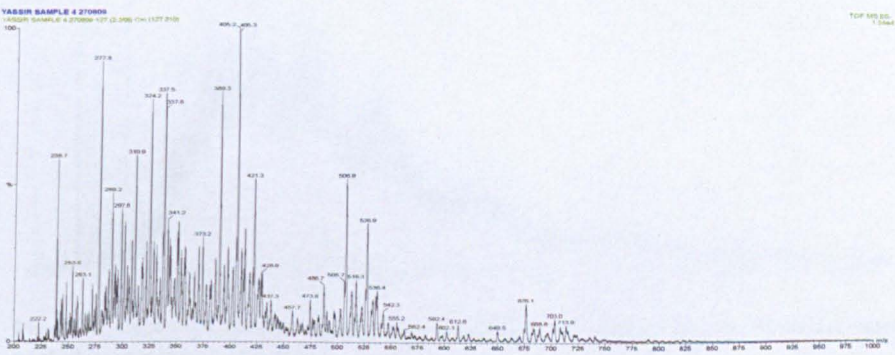

10-mer

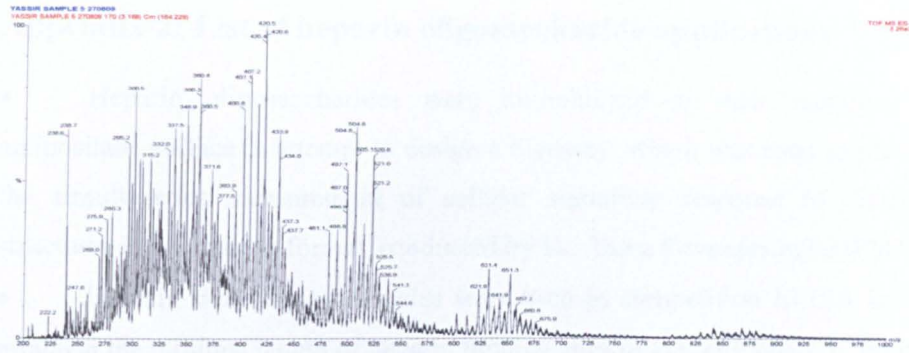

12-mer

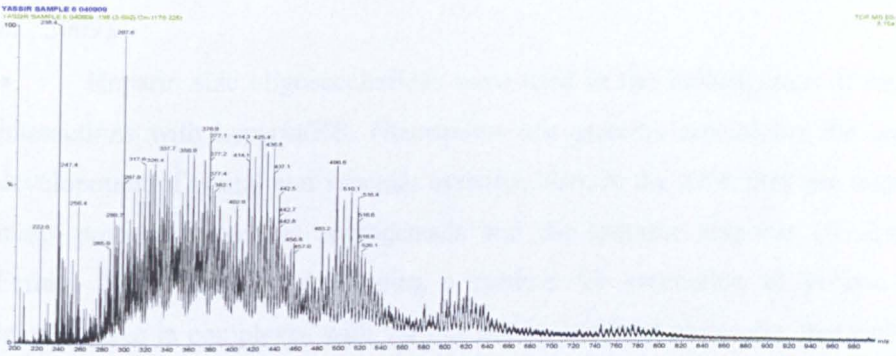

14-mer

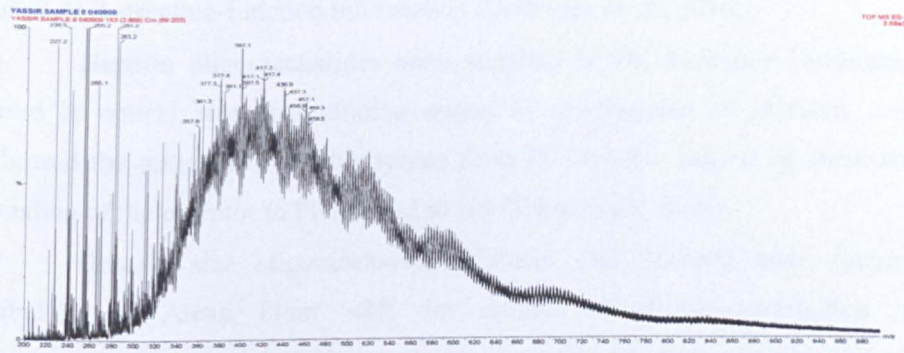

16-mer

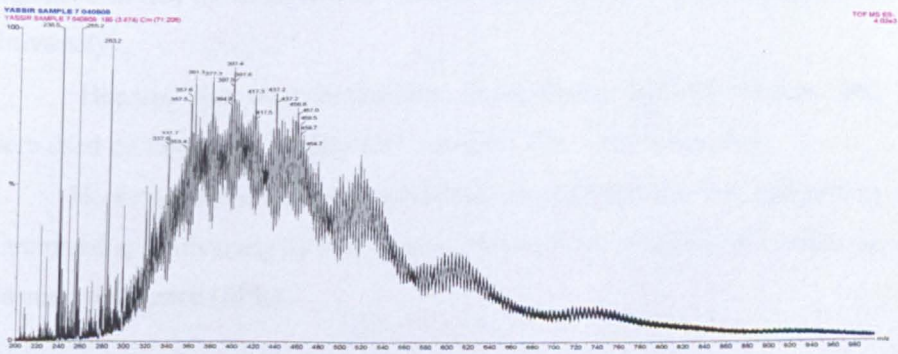

Figure A.1 ESI-MS spectra of SEC generated heparin oligosaccharide fractions obtained by partial heparinase I digestion.

Appendix-2: List of heparin oligosaccharide applications

- Heparin oligosaccharides were immobilized at their reducing end to aminosilane surface in attempt to design a bioassay, which was used as platform for the simultaneous measurement of cellular signalling response to different HS structures in microarray format, conducted by Dr. Tania Puvirajesinghe (PhD thesis).
- Heparin size oligosaccharides were used in competition ELISA in order to establish the minimal length of heparin binding sites of HS antibodies. (Thompson *et al.*, 2009).
- Heparin size oligosaccharides were used in the investigation of neuropilins interactions with heparin/HS. Neuropilins are proteins crucial for the embryonic development of neural and vascular systems; also, in the adult they are important in many processes, such as angiogenesis and the immune response (Uniewicz and Fernig, 2008). Also in developing a method for estimation of protein melting temperatures in complexes with various heparin-derived molecules that can provide important structure-function information (Uniewicz *et al.*, 2010).
- Heparin oligosaccharides were supplied to Dr. Laurence Duchesne, to be used in optical biosensor binding assays in continuation of previous study that showed the removal of the N-glycans from FGFR1-IIIc caused an increase in the binding of the receptor to FGF-2 and to HS (Yates *et al.*, 2006).
- Heparin size oligosaccharides (12-mer and 20-mer) were fluorescently labelled by Alexa Fluor 488, for uptake of fluorescent-labelled heparin oligosaccharides by Zebrafish in collaboration with Dr. Sally Stringer (Manchester University).
- Heparin size oligosaccharides, fluorescently labelled 12-mer, and 20-mer were used on functional studies on *C. elegans.* Dr. Tarja Kinnunen
- Heparin 14-mer enzyme generated oligosaccharide was utilized by Dr. R. Karamanska, (University of East Anglia, Norwich) in HS-proteins studies on surface plasmon resonance (SPR).

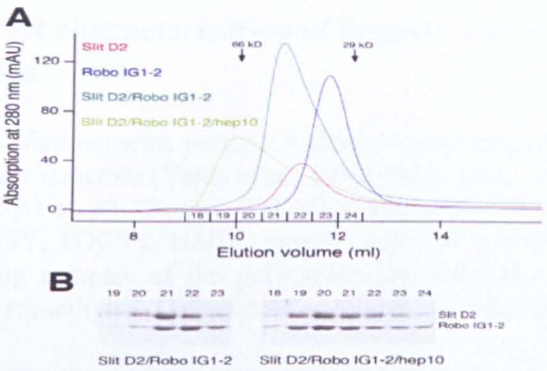

Figure A2.1 SEC analysis of a minimal ternary Slit-Robo-heparin complex. *A*, gel filtration chromatograms of isolated *Drosophila* Slit D2 and Robo IG1–2, a 1:1 mixture of the two proteins, and a 1:1:1 mixture of the two proteins with a heparin-derived decasaccharide (*hep10*). The elution volumes of two globular molecular mass standards are indicated by *vertical arrows* (albumin, 66 kDa; carbonic anhydrase, 29 kDa). The void volume of the column is 8.0 ml. The fractions collected for SDS-PAGE analysis are indicated. *B*, Coomassie Blue-stained SDS-PAGE gel of the peak fractions indicated in *A*. The fraction numbers are shown at the *top*. This figure is reproduced from (Hussain *et al.*, 2006).

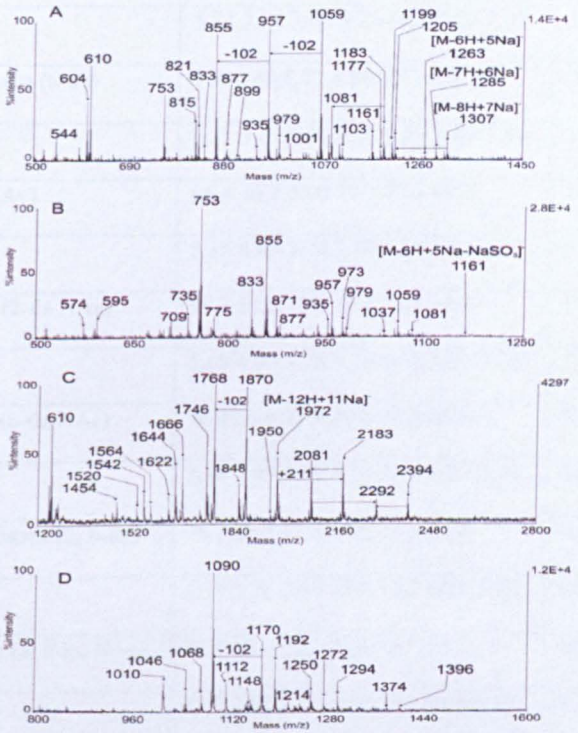

Figure A2.2 MALDI-TOF MS spectra of representative dp4 and dp6 heparin-derived fractions. (A) Spectrum of the dp4 fraction acquired using ImCHCA as matrix. (B) Spectrum of the dp4 fraction acquired using norharmane as matrix. (C) Spectrum of the dp6 fraction acquired using ImCHCA as matrix. Dashed arrows represent the loss of 102 mu corresponding to the replacement of a NaSO3 group by a proton and dotted arrows represent the matrix adducts observed with the highest sulfated species (+211 mu). (D) Spectrum of the dp6 fraction acquired using norharmane as matrix. This figure is reproduced from (Tissot *et al.*, 2007)

Appendix-3: NMR characterisation of heparin and chemically modified heparins

The chemically modified heparins polysaccharides were characterized by ^{1}H and ^{13}C NMR to confirm their structure (Yates *et al.*, 1996; Patey *et al.*, 2006). NMR spectra were recorded in D_2O at 40 °C on a 400 MHz instrument. Assignment was by a combination of COSY, TOCSY, HMBC two-dimensional spectra. ^{13}C spectra were recorded on 150 mg samples of the polysaccharide. Chemical shift values were recorded relative to trimethylsilyl propionate as reference standard at 40 °C.

	Glucosamine	**Iduronate**
Polysaccharide	**A-1 A-2 A-3 A-4 A-5 A-6**	**I-1 I-2 I-3 I-4 I-5**
Porcine mucosal heparin (PMH)	99.5 60.7 72.5 78.8 72.0 69.2	102.1 78.9 72.1 79.0 72.3
	5.42 3.31 3.69 3.79 4.05 4.30-4.42	5.23 4.37 4.22 4.14 4.82
2-de-O-sulfate heparin (2-de)	98.1 60.3 72.4 80.1 71.5 68.7	104.6 71.1 70.4 77.2 71.2
	5.34 3.24 3.65 3.71 4.02 4.36 4.23	5.04 3.78 4.12 4.08 4.84
6-de-O-sulfate heparin (6-de)	100.0 60.8 72.4 80.5 73.8 62.6	102.0 77.6 70.7 78.7 71.4
	5.31 3.27 3.71 3.70 3.89 3.86-3.88	5.26 4.35 4.25 4.06 4.84
N-acetyl heparin (NAc)	96.6 56.2 73.0 79.3 72.3 69.6	102.2 76.8 67.3 74.2 70.8
	5.15 4.03 3.76 3.78 4.04 4.31-4.37	5.20 4.37 4.31 4.08 4.91
2-de-O-sulfate NAc (2-de NAc)	97.1 56.2 72.5 79.6 71.8 68.8	104.6 72.0 71.4 77.0 71.9
	5.18 4.00 3.78 3.79 4.08 4.37-4.26	5.01 3.75 3.42 4.10 4.78
6-de-O-sulfate NAc (6-de NAc)	96.8 56.6 72.9 80.6 74.2 62.9	102.3 76.6 67.1 74.1 70.6
	5.14 4.03 3.79 3.76 3.91 3.87-3.92	5.26 4.37 4.28 4.07 4.91
2, 6-de-O-sulfate heparin (2, 6-de)	98.2 60.5 72.5 80.2 73.5 62.4	104.3 72.2 71.5 77.8 72.2
	5.39 3.26 3.67 3.72 3.87 3.84-3.88	4.95 3.74 4.11 4.08 4.77
2, 6-de-Osulfate NAc (2, 6-de NAc)	97.1 56.2 72.3 79.6 73.7 62.3	104.3 72.5 72.2 77.3 72.6
	5.18 3.97 3.76 3.74 3.89 3.85-3.88	4.92 3.69 3.89 4.07 4.73

The ^{1}H chemical shift values quoted for position-6 of glucosamine residues (A-6) are intervals. Signals from the carbonyl group of iduronate and acetyl CH_3 groups of *N*-acetylated glucosamine derivatives are not shown.

Table A3.1 of the chemical shift values for ^{1}H and ^{13}C NMR heparin and chemically modified heparins polysaccharides

Appendix-4: Screening 8-mer library + Mass-tag/ES-MS sequencing

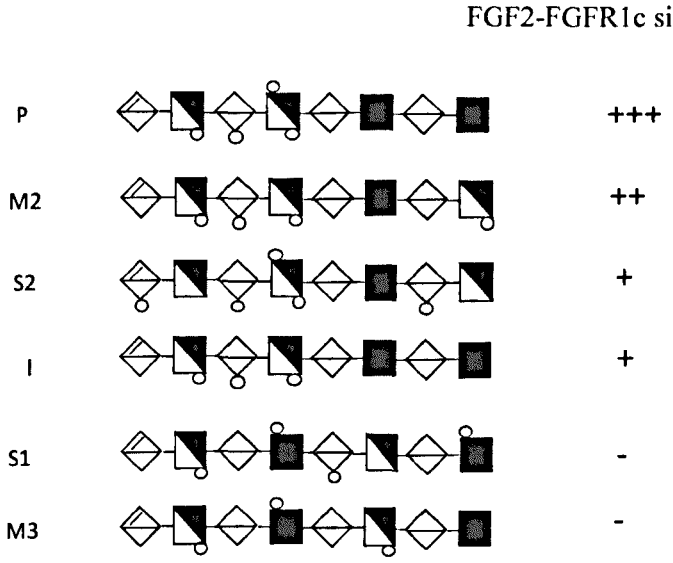

Figure A4.1 Structural analysis of 8-mer sub-fractions using lyase, hydrolase and sulfatase enzymes, in addition to SAX-HPLC, IPRP-HPLC and ES-MS.

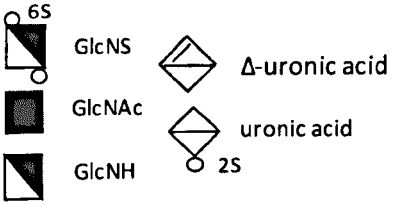

Appendix 5: List of outputs

Publications:

Turnbull, J. E.; Miller, R. L.; **Ahmed, Y.**; Puvirajesinghe, T. M. and Guimond, S. E. (2010) Glycomics profiling of heparan sulfate structure and activity. *Methods Enzymol,* 480, 65-85.

Uniewicz, K. A.; Ori, A.; Xu, R.; **Ahmed, Y.**; Wilkinson, M. C.; Fernig, D. G. and Yates, E. A. (2010) Differential Scanning Fluorimetry Measurement of Protein Stability Changes upon Binding to Glycosaminoglycans: A Screening Test for Binding Specificity. *Anal Chem.*

Powell, A. K.; **Ahmed, Y. A.**; Yates, E. A. and Turnbull, J. E. (2010) Generating heparan sulfate saccharide libraries for glycomics applications. *Nat Protoc,* 5, 821-33.

Popplewell, J. F.; Swann, M. J.; **Ahmed, Y.**; Turnbull, J. E. and Fernig, D. G. (2009) Fabrication of carbohydrate surfaces by using nonderivatised oligosaccharides, and their application to measuring the assembly of sugar-protein complexes. *Chembiochem,* 10, 1218-26.

Tissot, B.; Gasiunas, N.; Powell, A. K.; **Ahmed, Y.**; Zhi, Z. L.; Haslam, S. M.; Morris, H. R.; Turnbull, J. E.; Gallagher, J. T. and Dell, A. (2007) Towards GAG glycomics: analysis of highly sulfated heparins by MALDI-TOF mass spectrometry. *Glycobiology,* 17, 972-82.

In preparation:

Ahmed, Y.; Powell, A. K.; Yates, E. A., Moss, D. J.; Hussain, S. A.; Hohenester, E. and Turnbull, J. E. Selective effects of chemically modified heparins on promotion of Slit-Robo ternary complex formation and biological activity (In preparation for *J Biol. Chem.*).

Atrih, A.; **Ahmed, Y.;** Powell, A. K. and Turnbull, J. E. Improved Separation and Mass Spectrometry Analysis of Bioactive Heparan Sulfate Saccharides (In preparation for *J. Biol. Chem*).